Summary Report of Research on Permanent Ground Anchor Walls, Volume III: Model-Scale Wall Tests and Ground Anchor Tests

PUBLICATION NO. FHWA-RD-98-067

SEPTEMBER 1998

U.S. Department of Transportation
Federal Highway Administration

Research and Development
Turner-Fairbank Highway Research Center
6300 Georgetown Pike
McLean, VA 22101-2296

FOREWORD

This report is part of a four-volume series which summarizes a comprehensive study on permanent ground anchor walls. Volume I (FHWA-RD-98-065) discusses current practice and limiting equilibrium analyses. Volume II (FHWA-RD-98-066) presents results of full-scale wall tests and a soil-structure interaction model. Volume III (FHWA-RD-98-067) covers model-scale wall tests and ground anchor tests. Volume IV (FHWA-RD-98-068) summarizes the first three volumes and presents conclusions and recommendations.

Charles J. Nemmers, P.E.
Office of Engineering
Research and Development

NOTICE

Technical Report Documentation Page

1. Report No.	2. Government Accession No.	3. Recipient's Catalog No.
FHWA-RD-98-067		

4. Title and Subtitle	5. Report Date
SUMMARY REPORT OF RESEARCH ON PERMANENT GROUND ANCHOR WALLS, VOLUME III: MODEL-SCALE WALL TESTS AND GROUND ANCHOR TESTS	September 1998
	6. Performing Organization Code

7. Author(s)	8. Performing Organization Report No.
Mueller, C.G., Long, J.H., Weatherby, D.E., Cording, E.J., Powers III, W.F., and Briaud, J.-L.	

9. Performing Organization Name and Address	10. Work Unit No. (TRAIS)
Schnabel Foundation Company 45240 Business Court, Suite 250 Sterling, Virginia 20166	3E3B0139
	11. Contract or Grant No. DTFH61-89-C-00038

12. Sponsoring Agency Name and Address	13. Type of Report and Period Covered
U.S. Department of Transportation Federal Highway Administration, Research and Development 6300 Georgetown Pike McLean, Virginia 22101-2296	Final Report September 1989–November 1997
	14. Sponsoring Agency Code

15. Supplemental Notes

FHWA Contracting Officer's Technical Representative (COTR): Albert F. DiMillio, HNR-10
FHWA Technical Consultant: Richard S. Cheney, HNG-31

16. Abstract

Research directed toward improving the design and construction of permanent ground anchor walls is presented. The research focused on tiedback soldier beam walls for highway applications. These walls are generally less than 25 ft high, and they are supported by one or two rows of permanent ground anchors.

This volume is part of a four-volume report summarizing the research. It presents the results of research on four model-scale soldier beam and lagging walls constructed in medium-dense sand, and the results of tests performed on 10 hollow-stem-augered ground anchors installed in fine-grained soil. Bending moments, axial loads, earth pressures, and wall and ground movements for model walls with different soldier beam stiffnesses and one or two levels of anchors are presented. Load tests and long-term monitoring resutls for the ground anchors are included. Measured strains in the ground anchor tendons and the anchor grout for six anchors are presented. Recommendations regarding apparent earth pressures, control of ground movements, ground anchor design and installation, and ground anchor testing are made.

This volume is the third in a series. The other three volumes are entitled:

FHWA-RD-98-065	Volume I	Current Practice and Limiting Equilibrium Analyses
FHWA-RD-98-066	Volume II	Full-scale Wall Tests and a Soil-structure Interaction Model
FHWA-RD-98-068	Volume IV	Conclusions and Recommendations

In addition, a manual and computer program were developed that incorporate research results. They are entitled:

FHWA-RD-97-130	Design Manual for Permanent Ground Anchor Walls
FHWA-RD-98-093	TB Wall — Anchored Wall Design and Analysis Program for Personal Computers

17. Key Words	18. Distribution Statement
Ground anchor walls, tiebacks, ground anchors, anchors, retaining walls, apparent earth pressure, earth pressures, wall deformations, ground movements, model tests.	No restrictions. This document is available to the public through the National Technical Information Service, Springfield, Virginia 22161.

19. Security Classif. (of this report)	20. Security Classif. (of this page)	21. No. of Pages	22. Price
Unclassified	Unclassified		

SI* (MODERN METRIC) CONVERSION FACTORS

APPROXIMATE CONVERSIONS TO SI UNITS

Symbol	When You Know	Multiply By	To Find	Symbol
	LENGTH			
in	inches	25.4	millimeters	mm
ft	feet	0.305	meters	m
yd	yards	0.914	meters	m
mi	miles	1.61	kilometers	km
	AREA			
in^2	square inches	645.2	square millimeters	mm^2
ft^2	square feet	0.093	square meters	m^2
yd^2	square yards	0.836	square meters	m^2
ac	acres	0.405	hectares	ha
mi^2	square miles	2.59	square kilometers	km^2
	VOLUME			
fl oz	fluid ounces	29.57	milliliters	ml
gal	gallons	3.785	liters	l
ft^3	cubic feet	0.028	cubic meters	m^3
yd^3	cubic yards	0.765	cubic meters	m^3
NOTE: Volumes greater than 1000 l shall be shown in m^3.				
	MASS			
oz	ounces	28.35	grams	g
lb	pounds	0.454	kilograms	kg
T	short tons (2000 lb)	0.907	megagrams	Mg
	TEMPERATURE (exact)			
°F	Fahrenheit temperature	5(F-32)/9 or (F-32)/1.8	Celcius temperature	°C
	ILLUMINATION			
fc	foot-candles	10.76	lux	l
fl	foot-Lamberts	3.426	candela/m^2	cd/m^2
	FORCE and PRESSURE or STRESS			
lbf	poundforce	4.45	newtons	N
psi	poundforce per square inch	6.89	kilopascals	kPa

APPROXIMATE CONVERSIONS FROM SI UNITS

Symbol	When You Know	Multiply By	To Find	Symbol
	LENGTH			
mm	millimeters	0.039	inches	in
m	meters	3.28	feet	ft
m	meters	1.09	yards	yd
km	kilometers	0.621	miles	mi
	AREA			
mm^2	square millimeters	0.0016	square inches	in^2
m^2	square meters	10.764	square feet	ft^2
m^2	square meters	1.195	square yards	ac
ha	hectares	2.47	acres	mi^2
km^2	square kilometers	0.386	square miles	
	VOLUME			
ml	milliliters	0.034	fluid ounces	fl oz
l	liters	0.264	gallons	gal
m^3	cubic meters	35.71	cubic feet	ft^3
m^3	cubic meters	1.307	cubic yards	yd^3
	MASS			
g	grams	0.035	ounces	oz
kg	kilograms	2.202	pounds	lb
Mg	megagrams	1.103	short tons (2000 lb)	T
	TEMPERATURE (exact)			
°C	Celcius temperature	1.8C + 32	Fahrenheit temperature	°F
	ILLUMINATION			
lx	lux	0.0929	foot-candles	fc
cd/m^2	candela/m^2	0.2919	foot-Lamberts	fl
	FORCE and PRESSURE or STRESS			
N	newtons	0.225	poundforce	lbf
kPa	kilopascals	0.145	poundforce per square inch	psi

* SI is the symbol for the International System of Units. Appropriate rounding should be made to comply with Section 4 of ASTM E380.

(Revised August 1992)

TABLE OF CONTENTS

TABLE OF CONTENTS
(continued)

TABLE OF CONTENTS
(continued)

LIST OF FIGURES

LIST OF FIGURES
(continued)

LIST OF FIGURES
(continued)

LIST OF FIGURES
(continued)

LIST OF FIGURES
(continued)

LIST OF FIGURES
(continued)

LIST OF FIGURES
(continued)

LIST OF TABLES

LIST OF ABBREVIATIONS AND SYMBOLS

A	=	Cross-sectional area of an anchor tendon
A_p	=	Cross-sectional area of model soldier beam at the tip
b	=	Soldier beam width
D	=	Toe depth
d_s	=	Ground anchor diameter
E	=	Young's modulus for steel
EI	=	Wall stiffness
E_s	=	Secant modulus for soil
H	=	Depth of excavation at design grade, height of wall
H^*	=	Effective height of retained soil required to yield the observed thrust
h	=	Depth of the excavation
h	=	Position of the lower level of anchors on the wall
I	=	Anchor inclination
I	=	Moment of inertia of soldier beam
K_a	=	Coefficient of active earth pressure
K_o	=	Coefficient of passive earth pressure
k	=	Spring constant for an elastic soil spring
L	=	Unsupported span length
L_e	=	Effective elastic length of an anchor tendon
L_1	=	Depth to the upper ground anchor
L_2	=	Depth to the lower ground anchor
l_a	=	Anchor bond length

LIST OF ABBREVIATIONS AND SYMBOLS
(continued)

L_{bulge}	=	Length of a wall between two supports and subjected to bending deformations
L_{cant}	=	Length of a wall above the upper support and subject to bending deformations
M_{max}	=	Maximum bending moment
n	=	Empirical coefficient in an equation to describe the shape of the settlement trough behind the wall
P_b	=	Thrust at the base of a wall, the difference between the total lateral earth load and the horizontal component of the model anchor
Q_{down}	=	Downdrag load
Q_{end}	=	Mobilized end bearing resistance
Q_{skin}	=	Mobilized skin friction resistance
Q_{total}	=	Maximum axial resistance of a soldier beam
s_u	=	Undrained shear strength of a soil
TAMU	=	Texas A&M University
T_1	=	Upper ground anchor load
T_2	=	Second-tier ground anchor load
T_u	=	Ultimate capacity of a ground anchor
T_v	=	Vertical component of anchor force
V_L	=	Volume of lateral wall movement
V_V	=	Volume of ground surface settlement
y_L	=	Maximum lateral wall movement
y_{bulge}	=	Bulging deformation of a wall
y_{cant}	=	Cantilever deformation of a wall

LIST OF ABBREVIATIONS AND SYMBOLS
(continued)

y_{max}	=	Maximum ground surface settlement
y_{rot}	=	Lateral movement of a wall resulting from rotation
y_{trans}	=	Lateral movement of a wall resulting from translation
y_V	=	Maximum ground surface settlement
α	=	Adhesion factor for determining anchor adhesion with respect to undrained shear strength
ΔH	=	Depth of the cut
δ_v	=	Soldier beam settlement
$\mu\epsilon$	=	Microstrains (10^{-6})
ϕ	=	Angle of internal friction
ϕ_{avail}	=	Available friction angle
ϕ_{mob}	=	Mobilized friction angle
Θ	=	Rotation angle of a wall resulting from settlement

CHAPTER 1
INTRODUCTION

This volume is part of a four-volume report summarizing research done to improve the design of permanent ground anchor walls for highway applications. It presents the results of research performed on four, large-scale, model walls, and the results of research performed on 10 hollow-stem-auger ground anchors constructed in a fine-grained soil. The chapters in Volume III include the following:

- Chapter 2 describes the construction of the model-scale walls, and presents axial loads, bending moments, wall and ground movements, and anchor loads for each stage of construction. Results are presented for walls with different soldier beam stiffnesses and one or two levels of anchors.
- Chapter 3 discusses wall and ground movements for the model-scale walls, and relates their movements to observations made on selected case histories. Sources of wall movements are identified and their relative importance are discussed. The effect of soldier beam settlement on walls with steeply inclined ground anchors is described.
- Chapter 4 describes the development of lateral earth pressures on the soldier beam in the model walls and discusses the changes that occur with wall deformations and wall stiffness. Results show that apparent earth pressure diagrams should be used to design walls supported by one row of ground anchors.
- Chapter 5 presents the results of load tests performed on instrumented and non-instrumented hollow-stem-augered ground anchors in a fine-grained soil. Results from long-term load monitoring observations are presented. Strain distributions in the tendon and the anchor grout are presented. Recommendations for improving the load-carrying capacity and creep behavior of large-diameter ground anchors are made.

The other three volumes of the research report are entitled:

Volume I	Current Practice and Limiting Equilibrium Analysis (Long, et al., 1998)
Volume II	Full-scale Wall Tests and a Soil-structure Interaction Model (Weatherby, et al., 1998)
Volume IV	Conclusions and Recommendations (Weatherby, 1998)

The four volumes address the major elements of permanent ground anchor wall design and provide guidance and recommendations to be used in the development of a design procedure presented in a separate manual. Some research finds were incorporated in a computer code developed for the design or analysis of permanent ground anchor walls. The manual is entitled *Design Manual for Permanent Ground Anchor Walls* (Weatherby, 1997) and the computer program is named *TB WALL - Anchored Wall Design and Analysis Program for Personal Computers* (Urzua and Weatherby, 1998).

Recommendations and findings presented in this report are intended to apply to permanent ground anchor walls for highway applications. They were not developed for temporary earth support systems, but many of the principles apply to both permanent and temporary construction.

CHAPTER 2
MODEL-SCALE WALL STUDY

2.1 INTRODUCTION

Four model-scale soldier beam and lagging walls supported by anchors were constructed in sand using the large-scale model test facility at the University of Illinois. The model-scale walls were used to examine the following aspects of anchored wall behavior:

- Sources of wall and ground movement.
- Development of lateral earth pressures.
- Axial load transfer.

In this chapter, the behavior of the four model-scale tests is summarized. Wall and ground movements, lateral earth pressures, and axial loads observed during construction of Model Test 4 are used to define the basic mechanics of anchored wall response. Brief descriptions of observations made during construction of Model Tests 1, 2, and 3 are provided to highlight differences in behavior associated with various aspects of design and construction. A brief description of the walls, test variables, instrumentation, and construction procedures is also provided. More detailed discussion of the model-scale testing program and results may be found in Chapters 3 and 4 of this report.

2.2 MODEL-SCALE TESTING PROGRAM

2.2.1 Description of the Tests

Four large-scale model anchored walls were constructed in this study. The walls consisted of soldier beams and lagging, supported by one or two levels of anchors. Each wall had a completed height at design grade of 6.25 ft, with 1.25 ft of toe penetration below grade. Wall geometry and structural characteristics were scaled to provide a load and deformation response consistent with full-scale walls supported by one or two levels of anchors. A photograph of a completed model-scale wall is provided in Figure 1. Figure 2 shows a section through the model wall.

The model walls were constructed inside the large-scale model test facility at the University of Illinois. The facility includes a rigid-walled test chamber (16×14 ft in plan and 10 ft in depth), conveyors and buckets for deposition of sand into the test chamber, a data acquisition system, and a 5-ton cone penetrometer. The soil used inside the test chamber was a dry, fine to medium, uniform sand (SP). The sand was deposited to a medium-dense condition (Dr = 45 to 55 percent). Dry sand was used to simplify material handling, and to provide a drained

soil response. Use of a medium-dense sand reduced concerns for scale effects associated with non-linear shear strength and volume change behavior.

Model soldier beams consisted of structural steel tubing with a rectangular cross-section (Figure 3). Nine soldier beams were used in each test and these were spaced on 2-ft centers. The flanges of the soldier beams were covered with an adhesive-backed grit paper to provide surface roughness characteristics consistent with full-scale soldier beams. Beam tips in Model Test 1 were open (low end bearing capacity), while in the remaining tests, soldier beam tips were fitted with an enlarged bearing plate (high end bearing capacity). Steel plate, 0.125 in thick, was used to simulate the 3-in thick hardwood boards used in field construction (Figure 4). Small-diameter steel bars were used to model the ground anchors. The steel bars were rigidly connected to a reaction frame inside the test chamber and to a wale at the wall (Figure 5). Fixing the bars to the back wall of the chamber eliminated components of wall deformation associated with mass movements behind the anchors, or load redistribution in the anchorage zone.

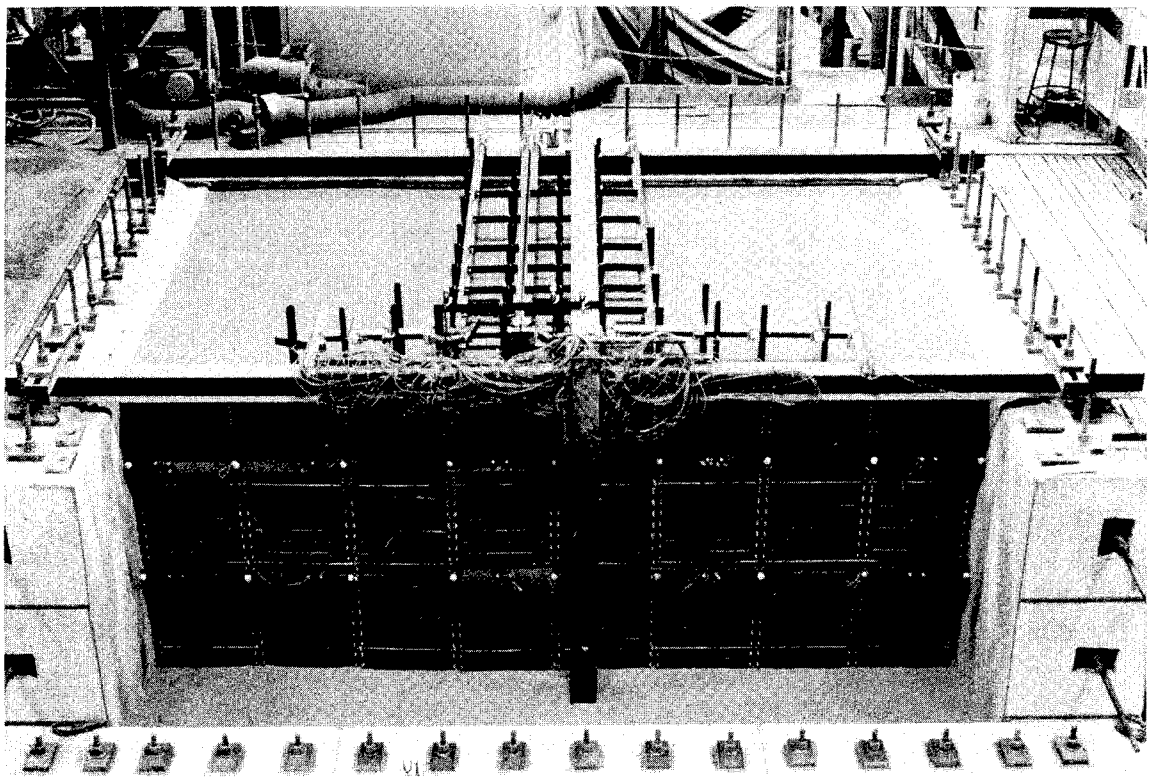

FIGURE 1
Photograph of Completed Model Wall Supported by Two Levels of Anchors

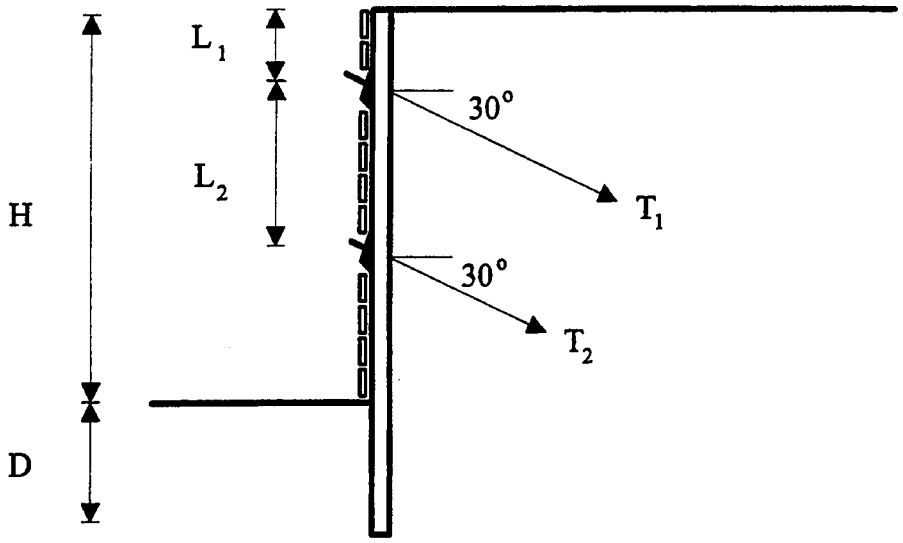

TEST	*H* (ft)	*D* (ft)	L_1 (ft)	L_2 (ft)	T_1 (lb)	T_2 (lb)	*I* (in^4)	A_p (in^2)	*b* (in)	Failure Mode
1	6.25	1.25	2.25	n/a	3300	n/a	0.958	1.38	4.0	(1)
2	6.25	1.25	2.25	n/a	3300	n/a	0.337	24.00	2.5	(2), (1)
3	6.25	1.25	1.50	2.5	1750	1750	0.337	24.00	2.5	(2), (1)
4	6.25	1.25	2.25	2.5	1750	1750	0.096	2400	2.5	(2), (1)

I = Moment of inertial of soldier beam
A_p = Cross-sectional area of beam at tip
b = Soldier beam width

(1) Over-excavation of toe
(2) Ground anchor loads reduced

FIGURE 2
Section View of a Test Wall and Summary of the Model-scale Testing Program

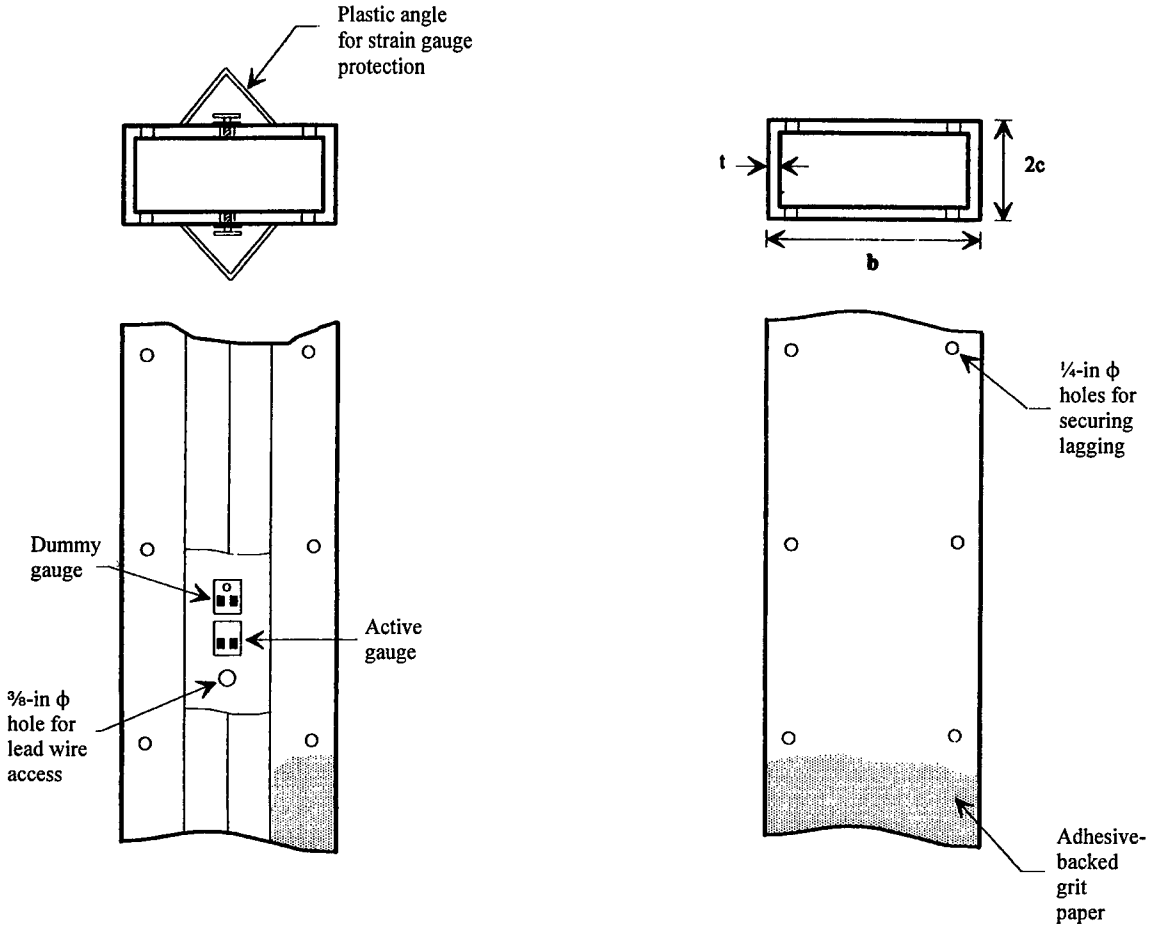

a) Instrumented soldier pile

b) Uninstrumented soldier pile

TEST	t (in)	c (in)	b (in)
1	0.120	2.00	4.0
2	0.125	0.75	2.5
3	0.125	0.75	2.5
4	0.083	0.50	2.5

FIGURE 3
Soldier Beams Used in Model Tests

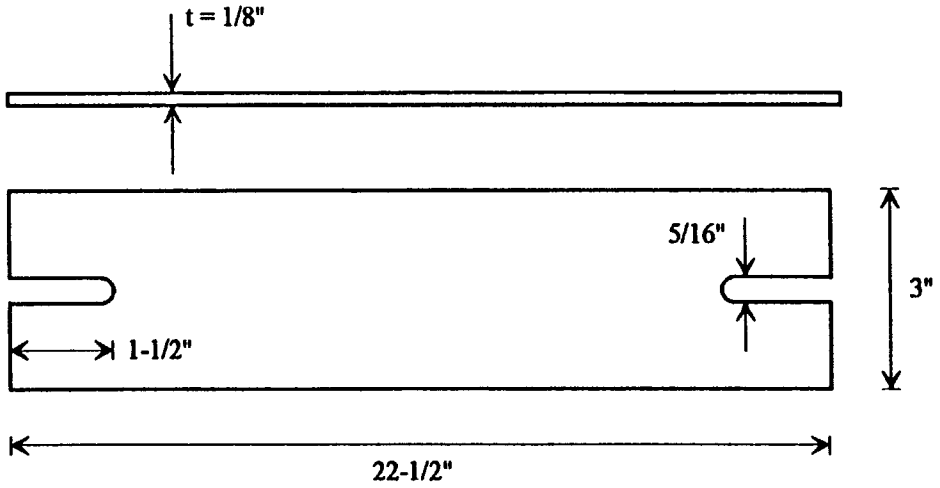

FIGURE 4
Steel Plate Used in Model Tests to Simulate Lagging

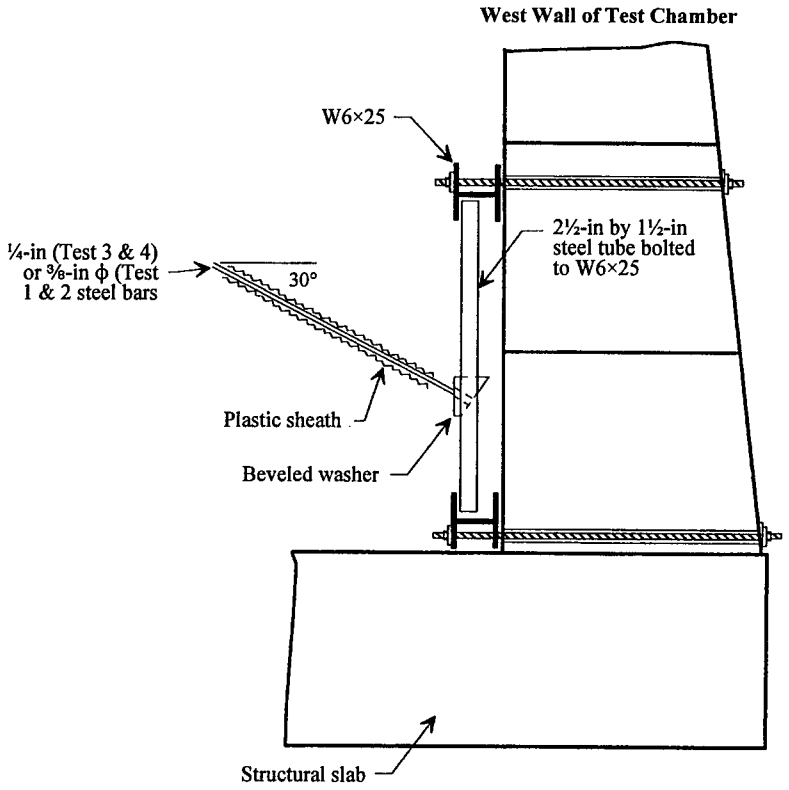

a) Connection of model anchors to reaction frame inside test chamber

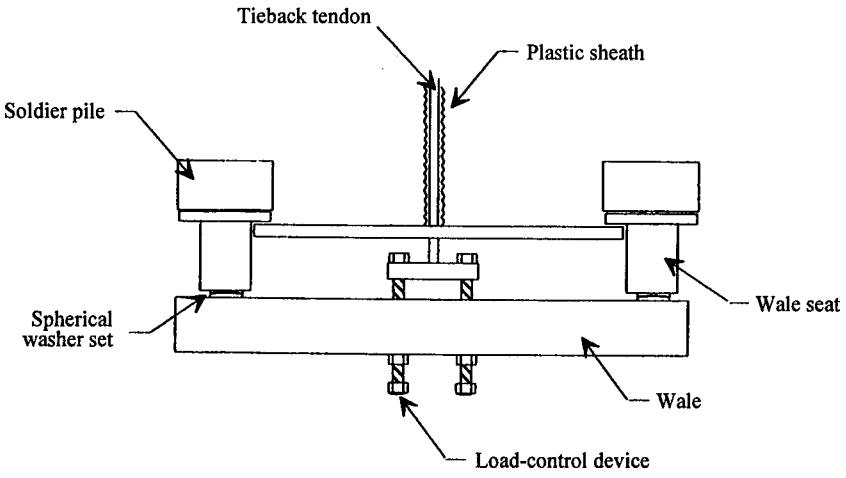

b) Connection of model anchors to load-control device and wale at the wall

FIGURE 5
Model Anchor Connections

2.2.2 Test Variables

Variables of the model-scale testing program included:

- Number of anchor levels.
- Relative soil/wall stiffness.
- Axial load-carrying capacity.
- Mode of failure.

The number of anchor levels and their spacing along the wall were selected as representative of full-scale walls with a completed height of between 25 and 30 ft. The significance of relative soil/wall stiffness in controlling certain components of wall deformation has been examined by O'Rourke and Cording (1974). Relative soil/wall stiffness in the model tests was varied approximately one order of magnitude, so that a full range of behavior could be studied. Ending bearing capacities of the soldier beams were varied so that the significance of soldier beam settlements for vertical load transfer and lateral wall movements could be assessed. In Model Test 1, soldier beam dimensions provided an end bearing capacity that was significantly less than the vertical component of anchor force. In Model Tests 2, 3, and 4, the beams were fitted with an enlarged bearing plate to provide end bearing capacity greater than the vertical component of ground anchor force. Failure modes at the end of construction included unloading of ground anchors and over-excavation in front of the embedded length of the wall. The model testing program is summarized in Figure 2.

2.2.3 Instrumentation

Test measurements made during construction of the model walls included wall and ground movements, bending, and axial strains in two soldier beams, and ground anchor loads. Instrumentation was concentrated near the center of the walls to reduce concerns for boundary effects near the test chamber walls.

Ground surface settlements were measured using dial gauges (Figure 6) with a travel of 1.0-in and graduated in 0.001-in increments. Lateral and vertical ground movements in the sand mass were recorded using DC-DC LVDT's (Trans-Tek Model No. 244-0001). The gauges were placed inside protective PVC sleeves and secured with set screws. Extension rods were used to couple the DC-DC LVDT's to form horizontal and vertical multiple position extensometers. For a supply voltage of 5V, the sensitivity of the gauges should have permitted repeatable measurements to the nearest 0.001 in. In practice, however, the voltage output from the gauges was sporadic, and the estimated error in the measurements was ± 0.02 in.

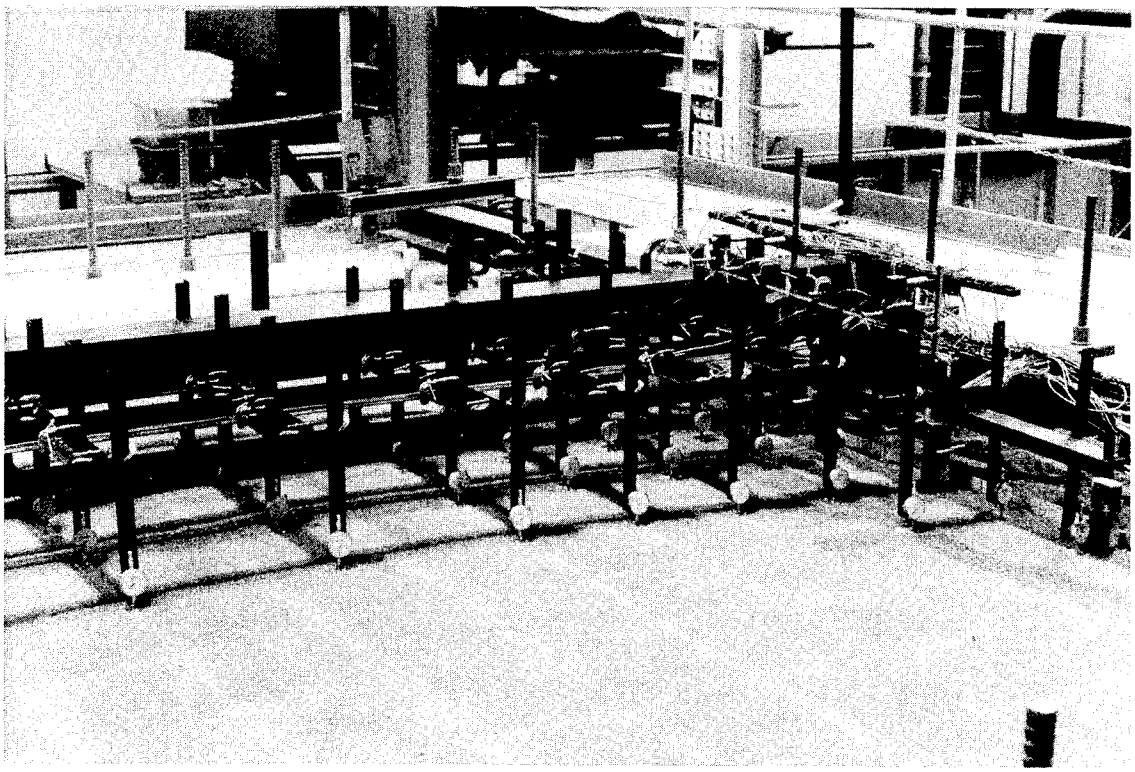

FIGURE 6
Dial Gauges to Measure Ground Surface Settlement Behind the Model Walls

Two soldier beams for each wall were equipped with bonded resistance type strain gauges (Measurements Group Inc., Model No. EA-06-250PD). Gauges were installed along the full length of the soldier beams typically at 6-in spacing, excluding the toe of the beams, where a 3-in spacing was used. Each gauge location consisted of two active gauges on the front and back flanges of the beams (Figure 7), with two dummy gauges to compensate for temperature variations and drift. The beams were calibrated for both bending and axial strains. The estimated accuracy of the strain measurements was ± 2 microstrains ($\pm 2\mu\epsilon$), which corresponds to about 50 in-lb. for bending moments and about 100 lb for axial load.

Ground anchor loads were measured using one pair of bonded resistance strain gauges placed near the head of each anchor. In addition to the strain gauges, extensometer rods were epoxied to the bars near their connection with the west wall of the model test facility. The extensometer rods provided a redundant measure of axial load in the ground anchors.

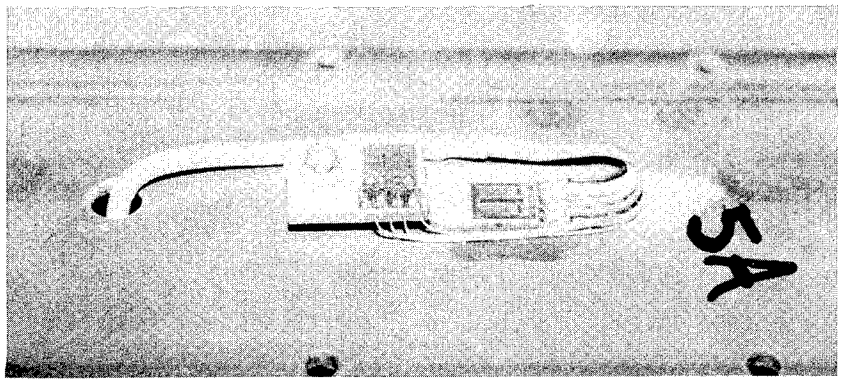

FIGURE 7
Bonded Resistance Type Strain Gauges Used to Measure Bending and Axial Strains of Soldier Beams

2.2.4 Construction

The first step in the construction process consisted of forming a sand sample inside the test chamber, which was accomplished by pluviation through air from concrete buckets hoisted into position with a crane. The relative density of the deposit was controlled by fixing the height of fall and mass rate of flow from the buckets. Cone penetration soundings were performed after formation of a sand sample to evaluate uniformity of the deposit and to estimate engineering properties.

To prevent damage to instrumentation, it was necessary to place some of the wall components during sand deposition. Once the level of sand reached the soldier beam tip elevation, the beams were spaced on 2-ft centers across the width of the model facility and temporarily secured to a wide flange beam (Figure 8). The clamps used to secure the soldier beams were removed once the sand reached the top of the model facility. Model ground anchors also were placed during sand deposition. The anchor rods were placed inside an extensible hose to isolate them from the sand mass and were secured to a reaction frame along the west wall of the model facility (Figure 8). The ground anchors were temporarily connected to wales (Figure 8), which were used to hold the ground anchors in position during sand raining. Once the level of sand reached the wale locations, the ground anchors were disconnected from the wale until later exposed by excavation. A geotextile fabric was placed between the soldier beams during sand deposition. The fabric prevented "running" of the sand during excavation required to install the model lagging, yet allowed a soil deformation condition consistent with field experience to develop below grade.

Once the sand reached the top of the model test facility, the surface was leveled by hand using a trowel, and dial gauges were placed to record ground surface settlements. Zeros were then recorded on all instruments. Excavation proceeded in small increments about equal to the depth and length of a single piece of model lagging. The geotextile fabric supported the sand

temporarily while model lagging was slipped over machine screws installed through the soldier beams and secured with coupler nuts. Any void that developed between the lagging board and geotextile fabric was promptly backfilled with a sand/glue mixture. All electronic instrumentation was read immediately prior to and following installation of a single lagging board. Dial gauges at the ground surface were read after completion of a complete row of lagging, corresponding to an excavation increment of about 3 in.

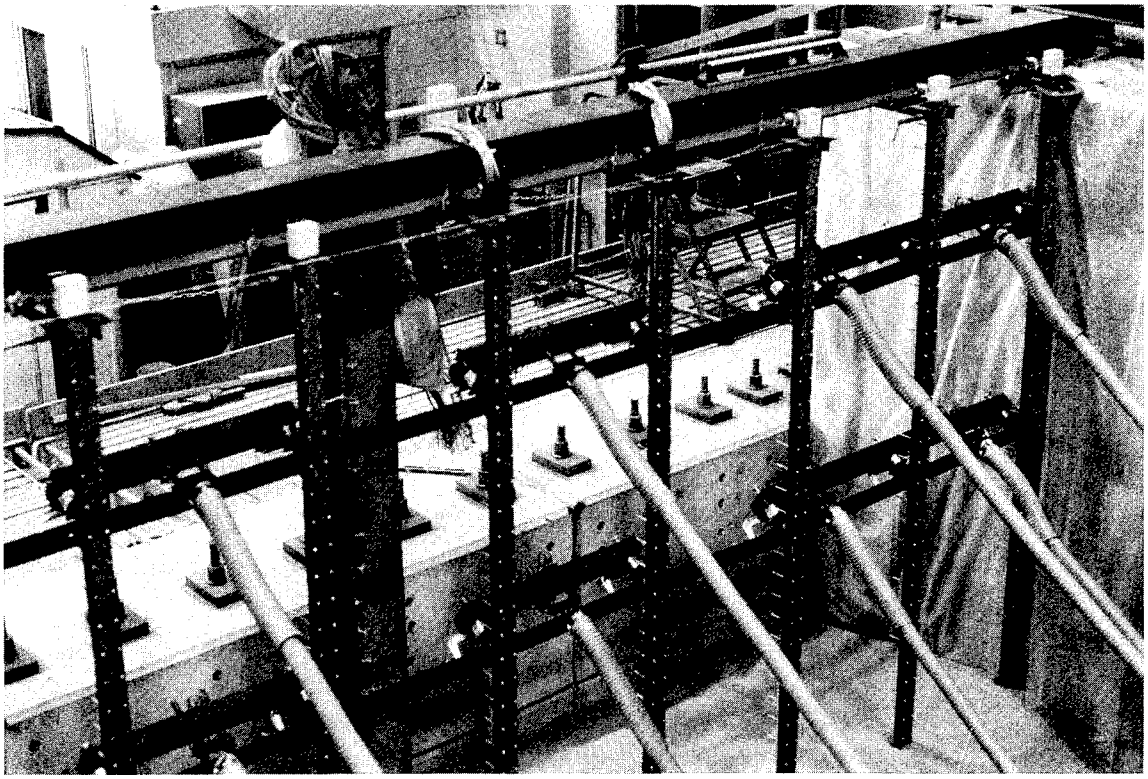

FIGURE 8
Intermediate Stage of Sand Deposition Showing Temporary Connection of Soldier Beams to Wide Flange Beam and Anchors to Load-control Device

Excavation continued in the manner described above until the anchor rods were exposed. A waler used to span adjacent beams was then connected to the ground anchors. Ground anchors were loaded using a device similar to a gear puller. Each anchor was loaded to approximately 120 percent of the design load. The loads were then decreased and locked-off at 75 percent of the design load. Design loads were computed assuming a trapezoidal earth pressure distribution with an intensity of $25H$ (H represents the depth of excavation at design grade). All electronic instrumentation and dial gauges were recorded with loads in the ground anchors at 120 and 75 percent of the design load.

After loading the first level of ground anchors, excavation and installation of lagging continued to the next level of ground anchors, or to design grade. After excavating to design grade, the

walls were brought to failure usually by some combination of anchor load reduction and over-excavation.

2.3 OBSERVED BEHAVIOR OF THE MODEL-SCALE WALLS

The behavior of the four model-scale walls is summarized for the following stages of construction:

1. Excavation to an anchor level.
2. Anchor stressing.
3. Excavation below an anchor level.

In addition, the behavior of the walls at large deformations, resulting from anchor unloading and over-excavation, is discussed.

Observations from Model Test 4 are used to illustrate the basic mechanics of anchor wall response. Brief summaries of Model Tests 1, 2 and 3, are provided to highlight differences in observed behavior associated with various aspects of design and construction.

2.3.1 Flexible Beam Supported by Two Levels of Ground Anchors (Test 4)

Model Test 4 was constructed using flexible soldier beams (I = 0.096 in^4) compared with the beams used in Model Test 1 (I = 0.958 in^4)and Model Tests 2 and 3 (I = 0.337 in^4). Soldier beam tips were fitted with an enlarged bearing area (A_p = 24 in^2) compared with Model Test 1 (A_p = 1.4 in^2) to increase end bearing capacity and reduce settlements. Model Test 4 was supported by two levels of ground anchors at depths of 18 and 48 in. Construction was completed in five relevant stages:

1. Excavation to the first ground anchor level (18 in).
2. Stressing of the upper ground anchor.
3. Excavation to the second ground anchor level (48 in).
4. Stressing of the second ground anchor.
5. Excavation to design grade (75 in).

The behavior of Model Test 4 was studied at large deformations by first unloading the lower ground anchors and then reducing loads in the upper anchors. The excavation was extended below design grade after reducing loads in the upper anchors.

2.3.1.1 Excavation to the Upper Ground Anchor

Installation and stressing of the upper ground anchor required excavation to a depth of about 18 in. Wall behavior during this stage of construction was consistent with a flexible canti-

lever, which develops support by mobilization of passive resistance along the embedded length of wall. Maximum lateral ground movements (~ 0.14 in) were observed at the top of the wall and decreased to small values about 1 ft below the excavation level (Figure 9). Lateral ground movements measured between soldier beams were generally consistent with the soldier beam displacements.

Maximum ground surface settlements (~ 0.07 to 0.12 in) were observed immediately adjacent to the wall and decreased to zero at a distance behind the wall of about $1.5\Delta H$ (where ΔH represents the depth of the cut). The variability of ground surface settlements at the wall probably reflects closure of small voids between the lagging and geotextile fabric. The geotextile fabric was placed between the soldier beams during deposition of sand inside the test chamber and was used to artificially provide "stand-up" time for placement of lagging during excavation. Lagging was placed flush with the beam flanges, which usually resulted in a void between the lagging and ground (geotextile fabric). Care was taken to fill voids prior to deepening the excavation, but some of the voids were probably not detected. It was not visually possible to estimate the amount of unfilled void space, but based on volume comparisons of lateral wall movements and ground surface settlements, the significance of void closure in the model tests was believed to have been small.

The maximum bending moment measured in the soldier beams was about 530 in-lb, and occurred at a depth of about 1 ft below the excavation level. The lateral earth pressure interpretation developed from measured bending strains indicated a parabolic distribution of active thrust on the upper part of the wall (Figure 10). The shape of the earth pressure distribution may reflect the sequence of excavation and installation of lagging. When excavating, the soil moved outward relative to the soldier beams and could have caused a redistribution of active thrust to stiffer, previously lagged, sections of the wall. The total active thrust on the wall was approximately consistent with a Coulomb solution for an angle of internal friction of 44° and mobilized wall friction of $2/3\phi$. An angle of internal friction of 44° is believed to represent an upper bound to the shear strength of the sand based on the measured constant volume friction angle ($\phi \approx 39°$) and the variation in secant friction angle with effective normal stress summarized by Terzaghi, et al., (1996). The earth pressure was greater than the Coulomb pressure near the top of the wall (assuming a triangular distribution) and decreased below the Coulomb pressure near the excavation level.

Axial strain measurements did not indicate development of a significant compressive force in the soldier beams with excavation to the first anchor level. Downward relative movement of the ground with respect to the wall was observed, however. Assuming mobilized wall friction of about $2/3\phi$, a maximum compressive force of 20 lb would be consistent with the interpreted distribution of active thrust on the upper part of the wall. A compressive force of 20 lb corresponds to about $1\mu\epsilon$ for the section properties of the beams used in Test 4. This value is less than the sensitivity of the gauges. It is probable that downdrag did develop during this stage of construction, but that the instrumentation was not sufficiently sensitive to detect the small strains.

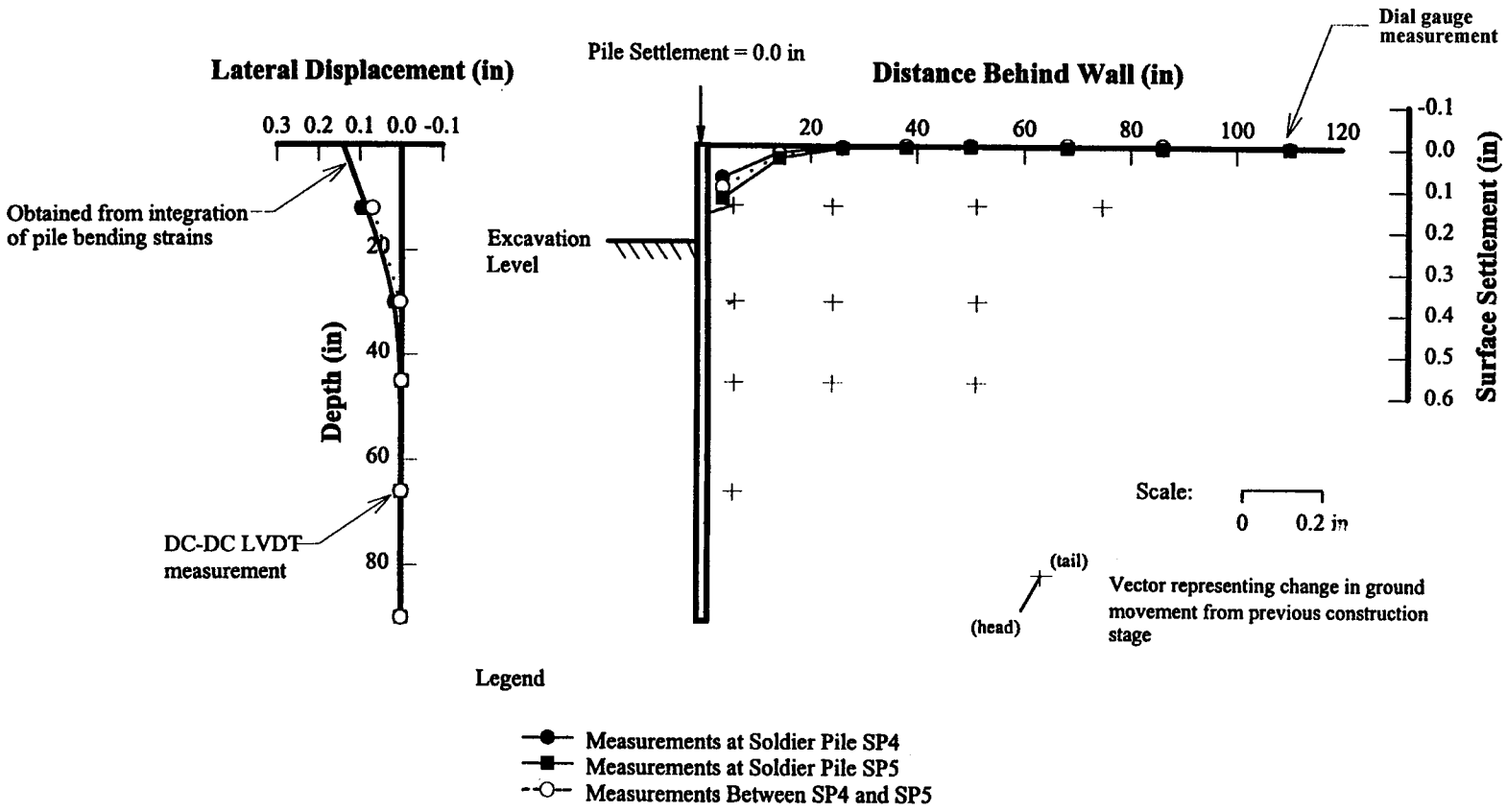

FIGURE 9
Wall and Ground Movements with Excavation to First Anchor — Model Test 4

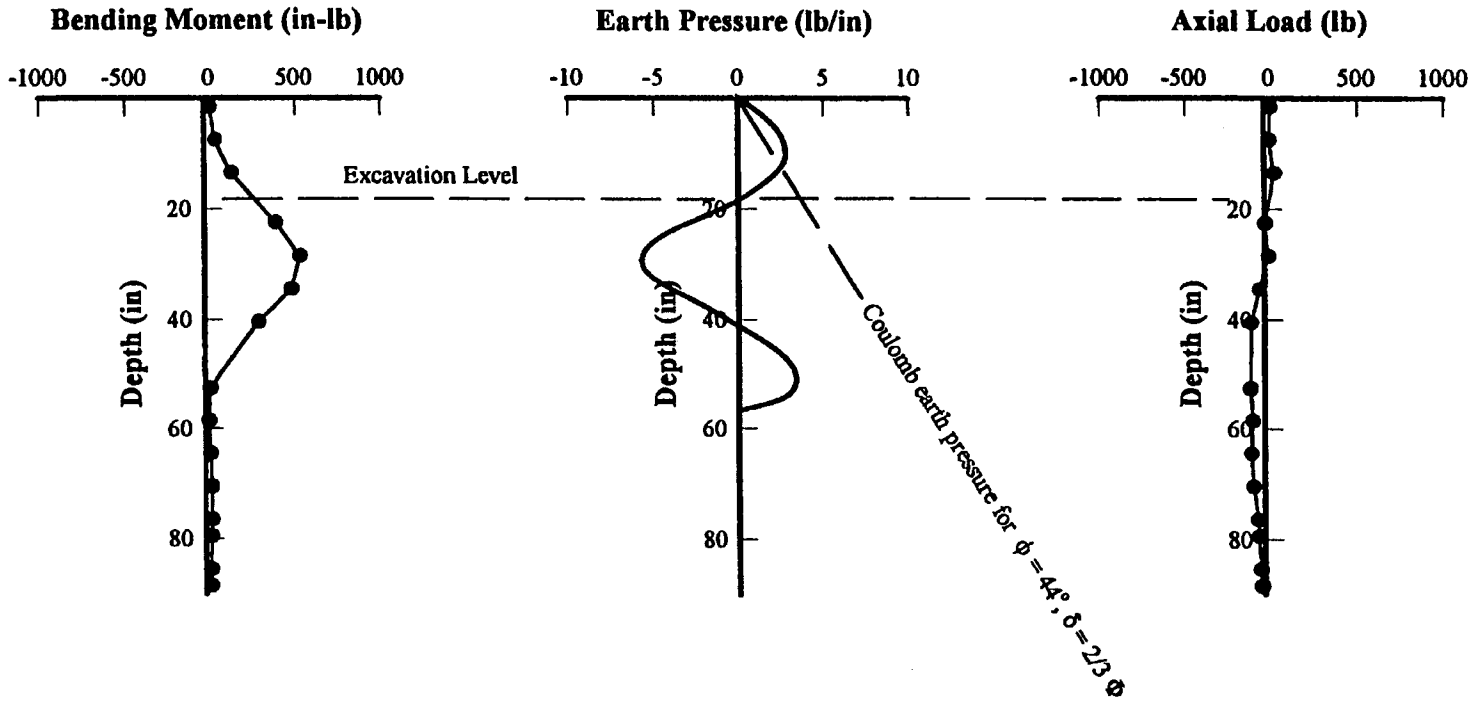

FIGURE 10
Bending Moments, Earth Pressures, and Axial Load with Excavation to First Anchor — Model Test 4, SP4

2.3.1.2 Stressing of the Upper Ground Anchors

Stressing of the upper ground anchors had the effect of pulling the soldier beams back into the retained soil (~ 0.07 in), as shown in Figure 11. The changes in soldier beam displacement were significant (~ 0.07 in) and in some of the model tests the beams were pulled back beyond the initial zero taken prior to excavation. Reducing ground anchor loads from 120 to 75 percent of the design load (DL) did not result in measurable outward soldier beam displacement. Ground anchor stressing did not have a significant effect on the ground movements between soldier beams (Figure 12).

Maximum observed bending stresses in the model tests developed at the anchor during prestressing. Maximum bending moments were estimated by extrapolation of "best-fit" curves to the test measurements and ranged from 2200 to 2400 in-lb when the anchor load was at 120 percent of the design load. With loads in the upper ground anchors at 75 percent of design, maximum bending moments between 1700 and 1800 in-lb were estimated. Anchor prestressing produced an approximately symmetric "bulb" of pressure at the anchor level (Figure 13). Maximum pressures at the upper anchor level were significantly greater than the at-rest stress, and approached the passive capacity of the wall (soldier beams and lagging) with anchor test loads equal to 120 percent of the design load.

Small downward movements (~ 0.005 in) of the soldier beams were sufficient to develop support for the vertical component of anchor force. The most significant feature of the axial load distribution in the soldier beams is the tensile force that developed immediately above the anchor level and the very small contribution to support from mobilized end bearing resistance (Figure 13). About one-third of the vertical component of force was supported above the anchor level. The balance of the vertical load was carried principally in skin friction below the level of the excavation. The model soldier beams were axially rigid, so that skin friction and end bearing resistance should have developed simultaneously. It is believed that compression of the beam tip bearing plates may have affected end bearing resistance during the initial stages of construction.

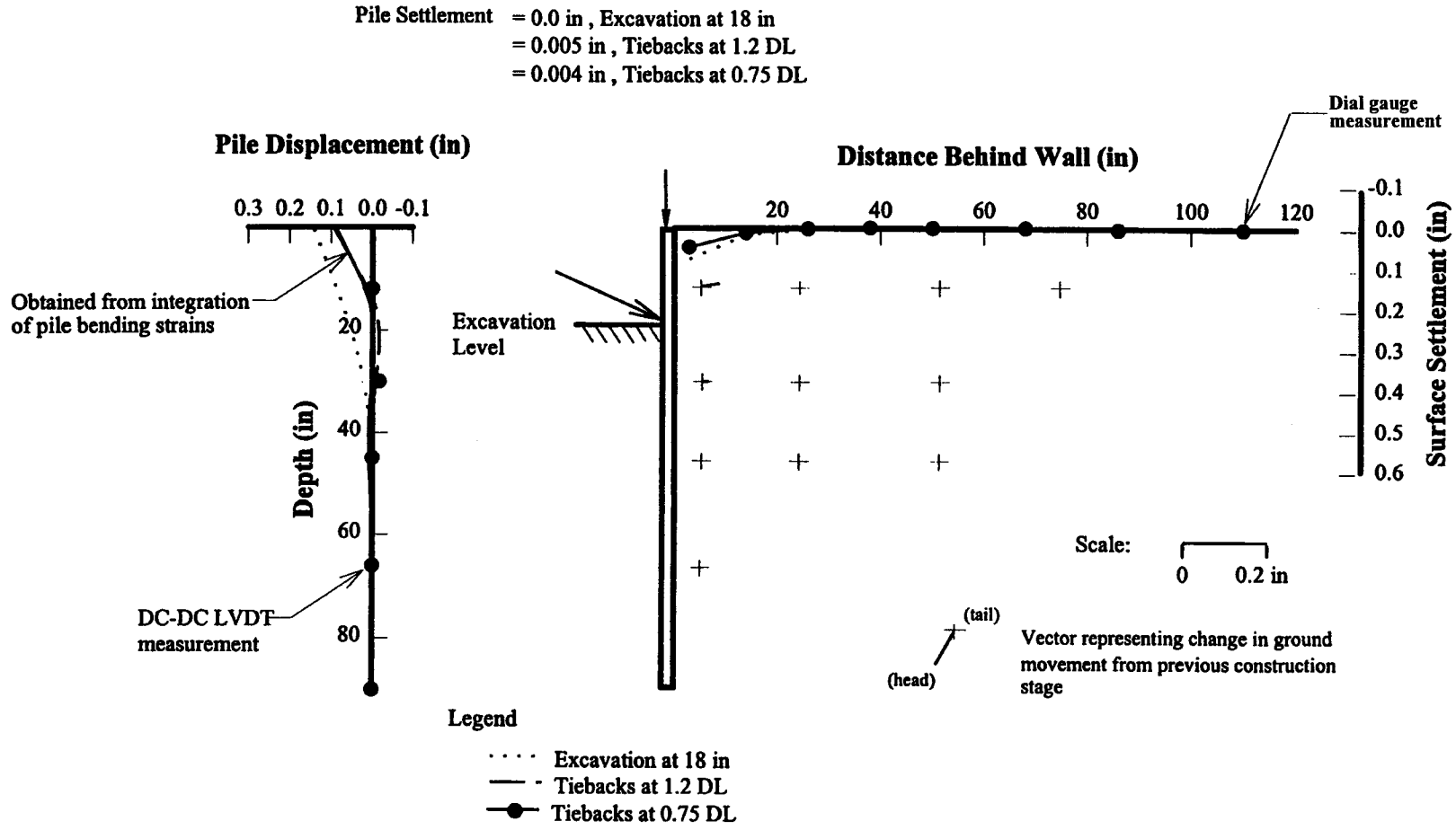

FIGURE 11
Wall and Ground Movements During Stressing of Upper Anchors — Model Test 4, SP4

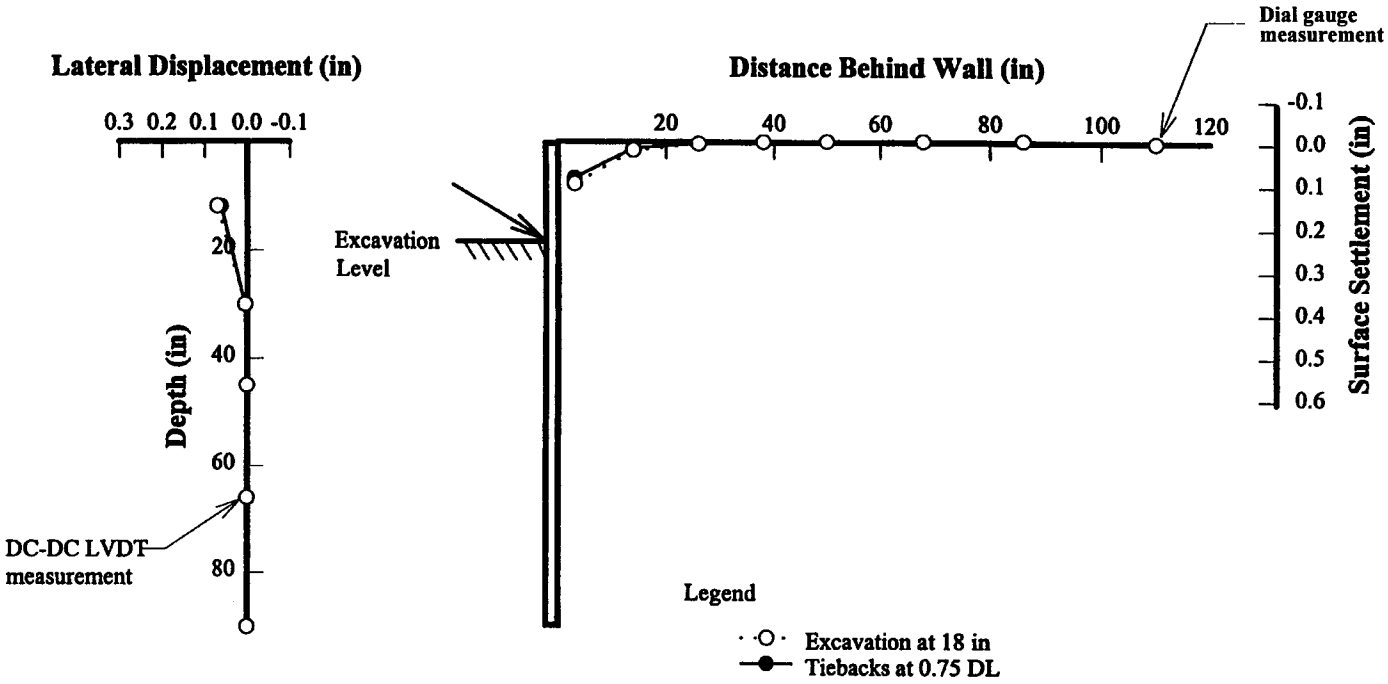

FIGURE 12
Ground Movements Between Soldier Beams During Stressing of Upper Anchors — Model Test 4

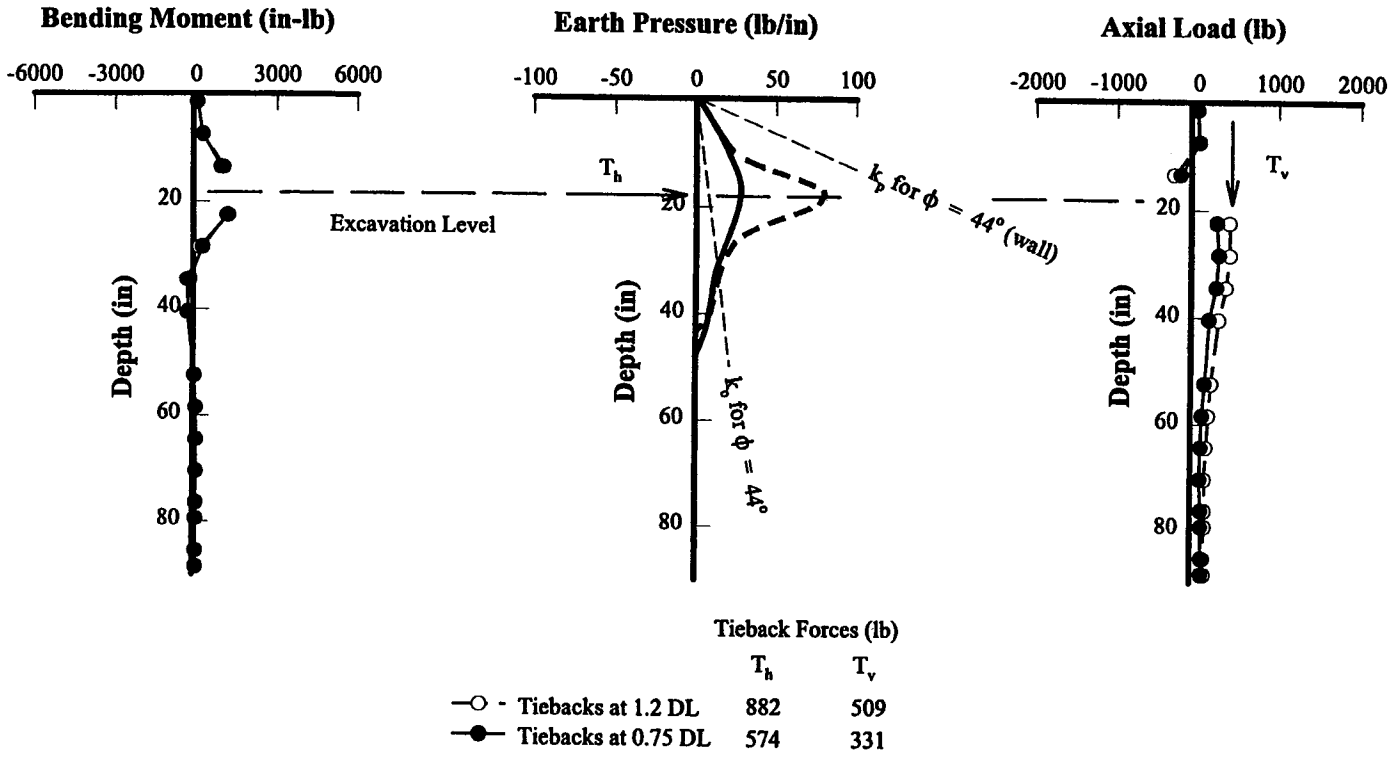

FIGURE 13
Bending Moments, Earth Pressures, and Axial Loads During Stressing of Upper Anchors — Model Test 4, SP4

2.3.1.3 Excavation Below the Upper Anchor

Excavation below the upper anchor resulted in lateral bulging of the wall below the anchor (Figure 14). Lateral bulging developed with the wall essentially fixed against displacement at the anchor level, and additional resistance to movement provided by the embedded length of the wall. Note that the distribution of bending strains in the embedded portion of the soldier beam (toe) was consistent with a fixed-earth support condition (Figure 15). A point of contra-flexure in the soldier beams was observed at a depth of about 1 ft below the excavation level. The maximum lateral bulge of the wall (~ 0.04 in) was observed near the excavation level, with about one-half of the volume of lateral displacement occurring below grade. The pattern of ground surface settlement was consistent with that which developed during the cantilever stage. Maximum ground surface settlements (~ 0.09 to 0.11 in) were observed at the wall and decreased to zero at a distance behind the wall about equal to the depth of the cut. Incremental lateral ground strains were maximum near the excavation level, while incremental vertical ground strains were maximum at the top of the wall.

Small changes in bending moments and lateral earth pressures were observed during excavation below the upper ground anchor (Figure 15). Estimated maximum bending moments at the ground anchor level were unchanged, while maximum negative bending moments in the span below the anchor increased from between 310 and 380 in-lb to between 490 and 550 in-lb Excavation below the upper anchor resulted in a decrease in lateral earth pressures along the unsupported span of the wall, and increases in pressure in the vicinity of the anchors and near the base of the wall. These observations are consistent with full-scale behavior of flexible, braced walls (Terzaghi, 1943) and model-scale behavior of anchored bulkheads (Rowe, 1952).

The most significant change in the distribution of forces on the wall for this stage of construction concerned axial loads (Figure 15). The retained soil moved downward relative to the wall, which resulted in an increase in axial load due to downdrag of between 120 and 190 lb/beam. The increase in vertical load on the wall was manifested by a decrease in tensile force in the soldier beam above the anchor level, and an increase in compressive force in the vicinity of the ground anchors. Note that the increase in vertical load on the wall resulted in significant increases in mobilized end bearing resistance, while the distribution of load supported in skin friction was essentially unchanged.

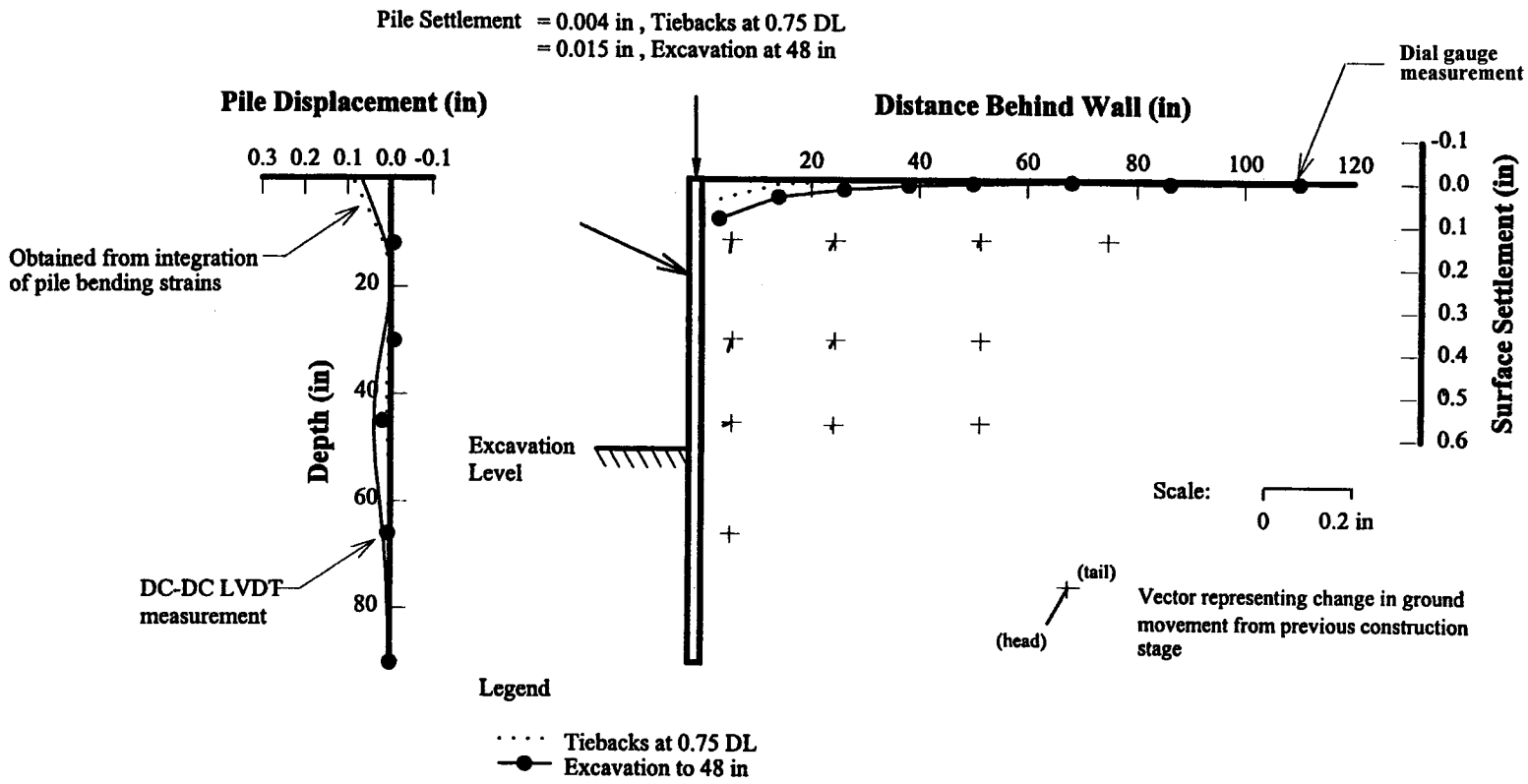

FIGURE 14
Wall and Ground Movements with Excavation at 48 In — Model Test 4, SP4

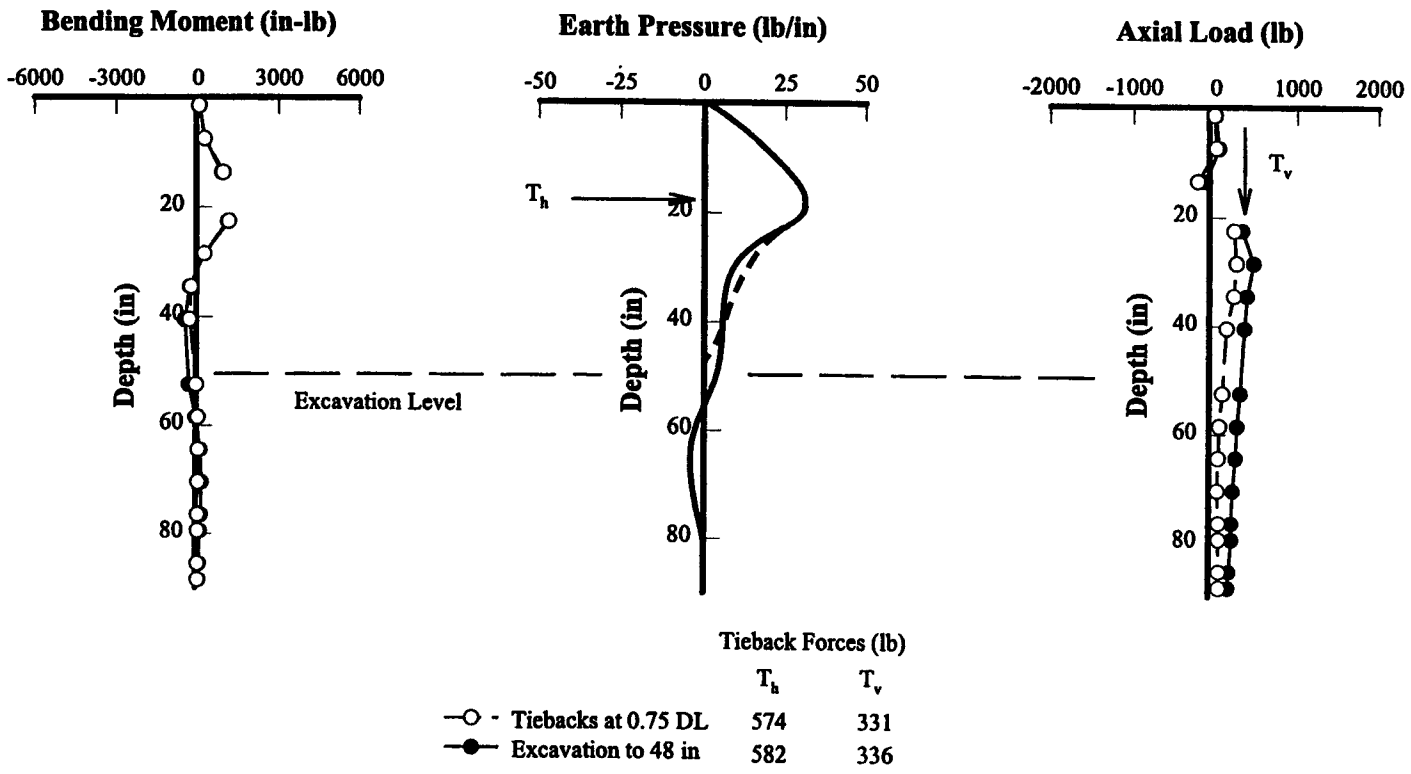

FIGURE 15
Bending Moments, Earth Pressures, and Axial Loads During Excavation to 48 In — Model Test 4, SP4

2.3.1.4 Stressing of the Lower Ground Anchors

The behavior of the wall during stressing of the lower anchors was similar to that which had been observed during stressing of the upper ones. The soldier beams were pulled back into the retained soil at the anchor level (~ 0.07 in), which effectively eliminated the bulging of the beams that had developed during excavation below the upper anchor (Figure 16). Only small changes in ground movements between soldier beams were observed (Figure 17), so that anchor prestressing caused only a "local effect" on wall deformations in the model tests.

Stressing of the lower ground anchors produced a similar pressure bulb to that which developed during stressing of the upper ground anchors (Figure 18). Downward movement of the soldier beams with respect to the soil developed during anchor prestressing. This relative displacement reduced the contribution to vertical load from downdrag, and facilitated significant load transfer above the excavation level. The total vertical force supported by the soldier beams was between 690 and 745 lb/beam, which compares with a vertical load introduced by anchor prestressing of about 636 lb/beam.

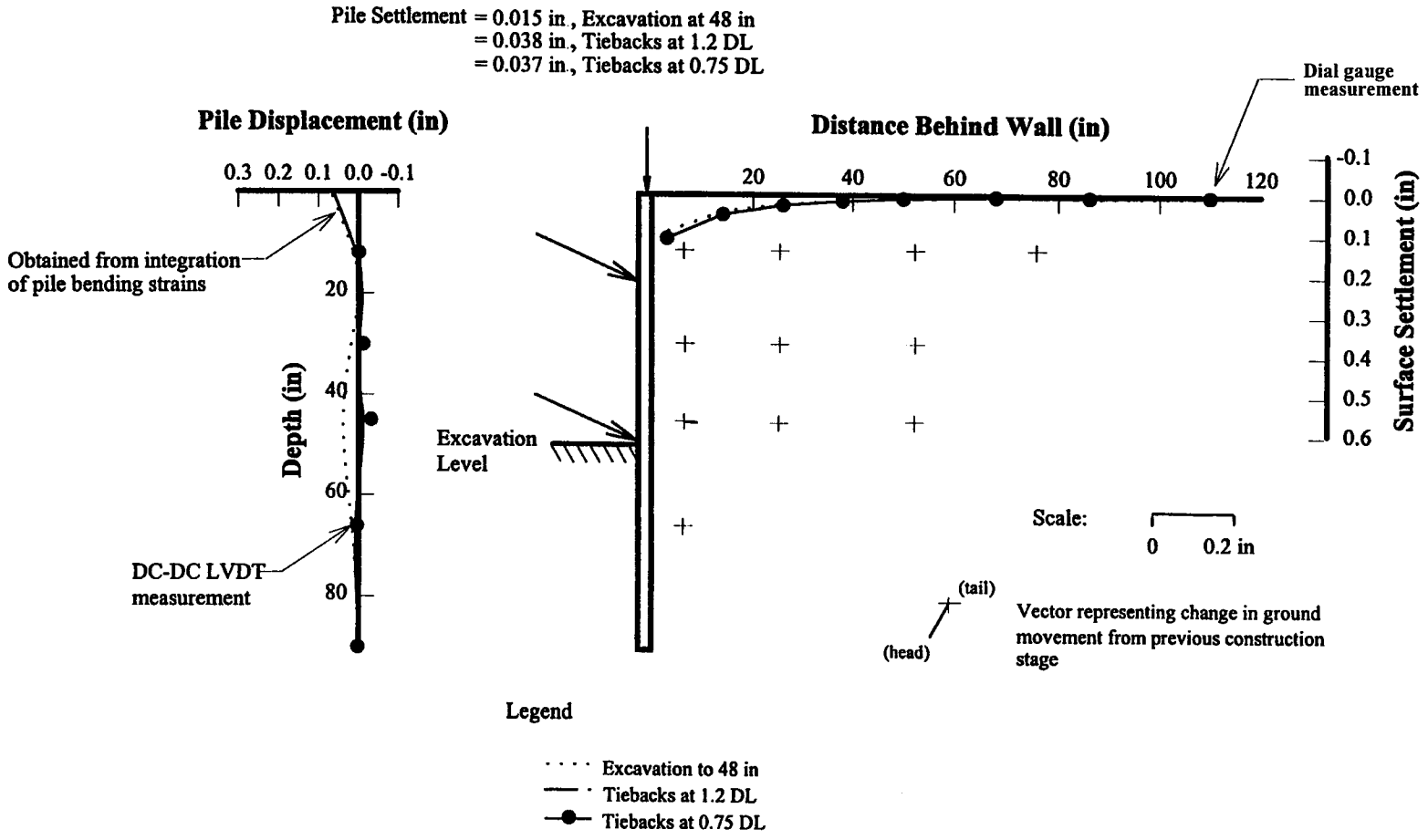

FIGURE 16
Wall and Ground Movement During Stressing of Second Level of Anchors — Model Test 4, SP4

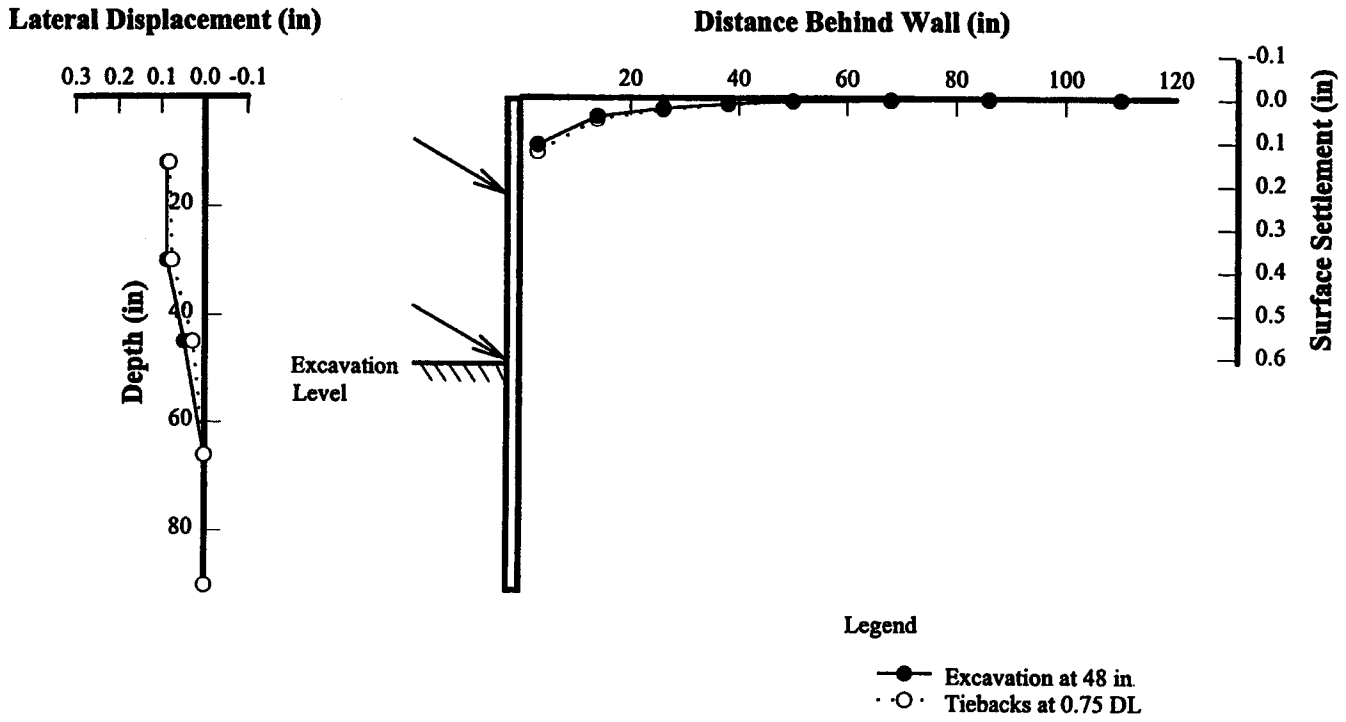

FIGURE 17
Ground Movements Between Soldier Beams During Stressing of Lower Anchors — Model Test 4

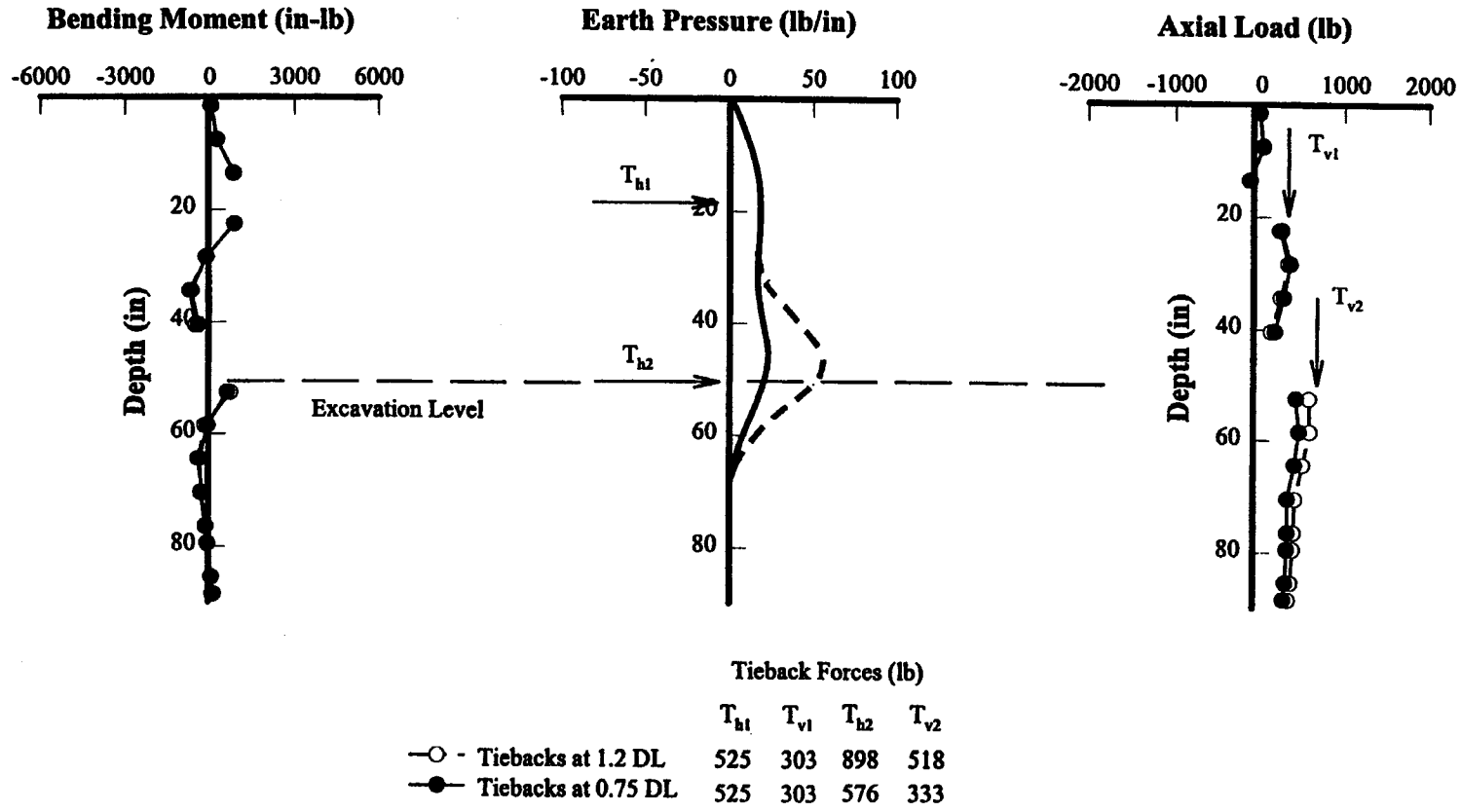

FIGURE 18
Bending Moments, Earth Pressures, and Axial Loads During Stressing of Second Level of Anchors — Model Test 4, SP4

2.3.1.5 Excavation to Design Grade

Two sources of wall movement were identified during excavation to design grade:

- Lateral bulging of the wall below the lower anchor.
- Outward rotation about the soldier beam toe (Figure 19).

Outward rotation of the wall about the toe coincided with increases in soldier beam settlements (~ 0.1 in). Increases in beam settlement resulted from progressive transfer of vertical load to the soldier beam tips. More load was transferred to the tips of the beams as a result of a reduction in skin friction above the excavation level and increased downdrag load.

Kinematically, soldier beam settlement permits outward translation of an anchored wall without change in anchor load (Hanna, 1968). In the model tests, the tendency for outward translation of the walls was resisted by mobilization of load along the embedded length of the soldier beams (passive resistance and beam tip shear) and increased anchor loads. The resistance provided by the anchors and beam toe resulted in a pattern of wall deformation that consisted principally of outward rotation (Figure 20). The observed model wall response can be represented by wall translation, consistent with Hanna's (1968) observations, and a rotation of the wall about the lower anchor level required to restore the beam tip to a near zero deformation condition. Thus, outward rotation of the model walls can be geometrically expressed in terms of soldier beam settlement, δ_v, anchor inclination, i, and the position of the lower level of anchors on the wall, h. Wall rotation observed in the model tests was in close agreement with the geometric relationship (Figure 21).

Ground surface settlements at the end of construction were maximum at the wall (~ 0.22 in), and measurable (~ 0.003 in) at a distance behind the wall about equal to $1.5H$ (where H represents the depth of the cut at design grade). The volume of ground surface settlement was slightly greater than the volume of lateral movement at the wall, which probably reflects ground losses from sources other than wall movements. The model sand was medium-dense and slightly dilative at the low stress levels associated with the test chamber. It is likely that ground movements behind the wall were influenced by void closure between the lagging and geotextile fabric in all four tests.

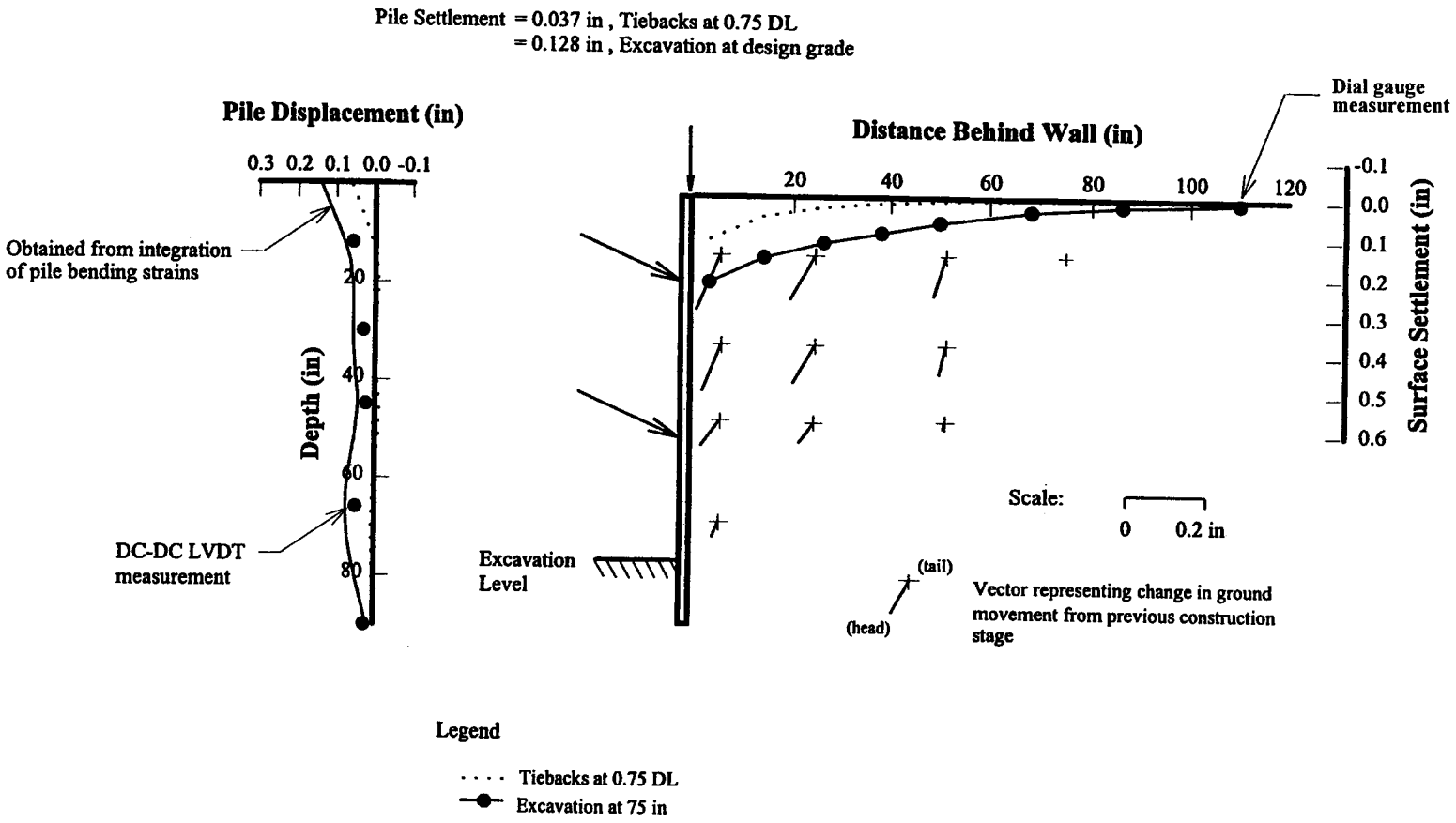

FIGURE 19
Wall and Ground Movement with Excavation at Design Grade — Model Test 4, SP4

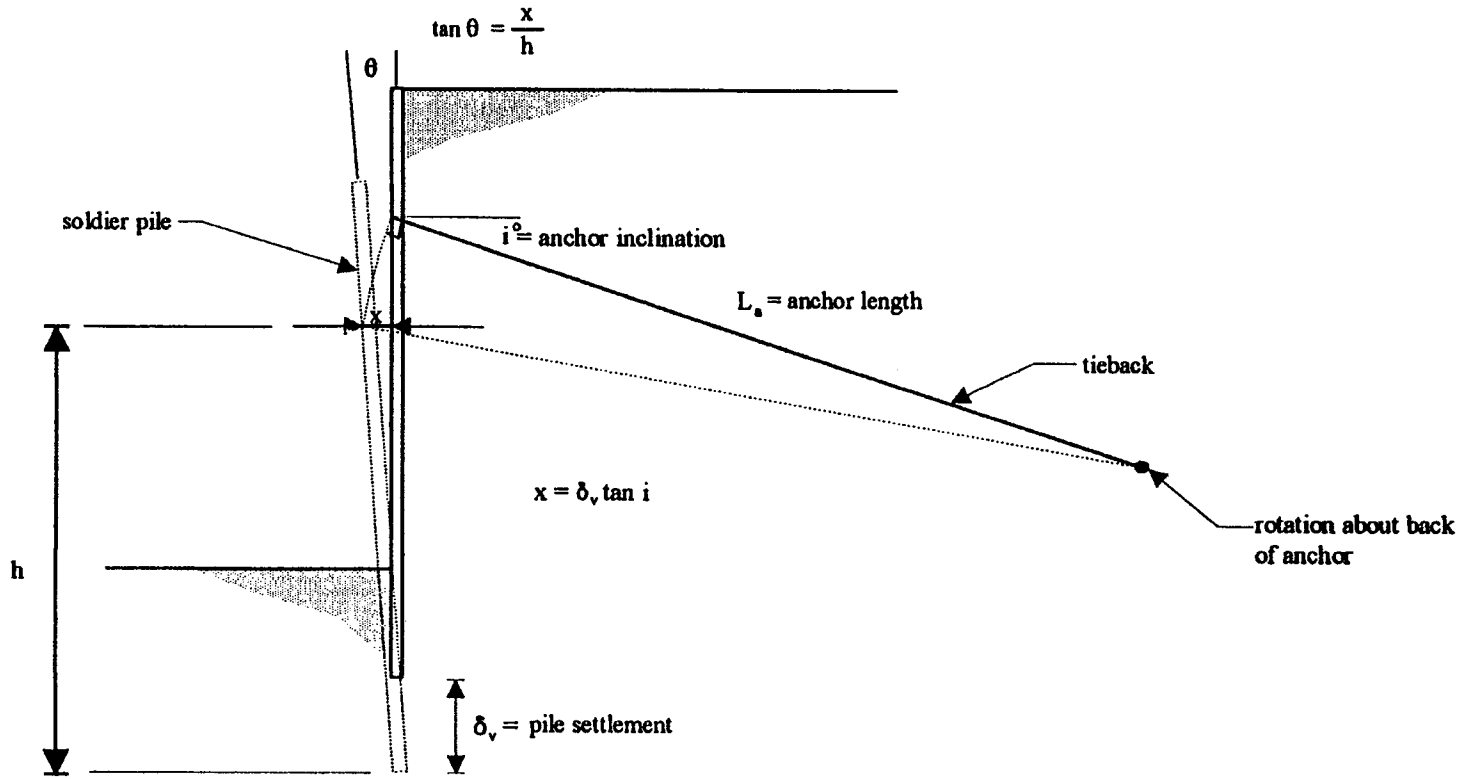

FIGURE 20
Relationship Between Soldier Beam Settlement and Wall Rotation Observed in the Model Tests

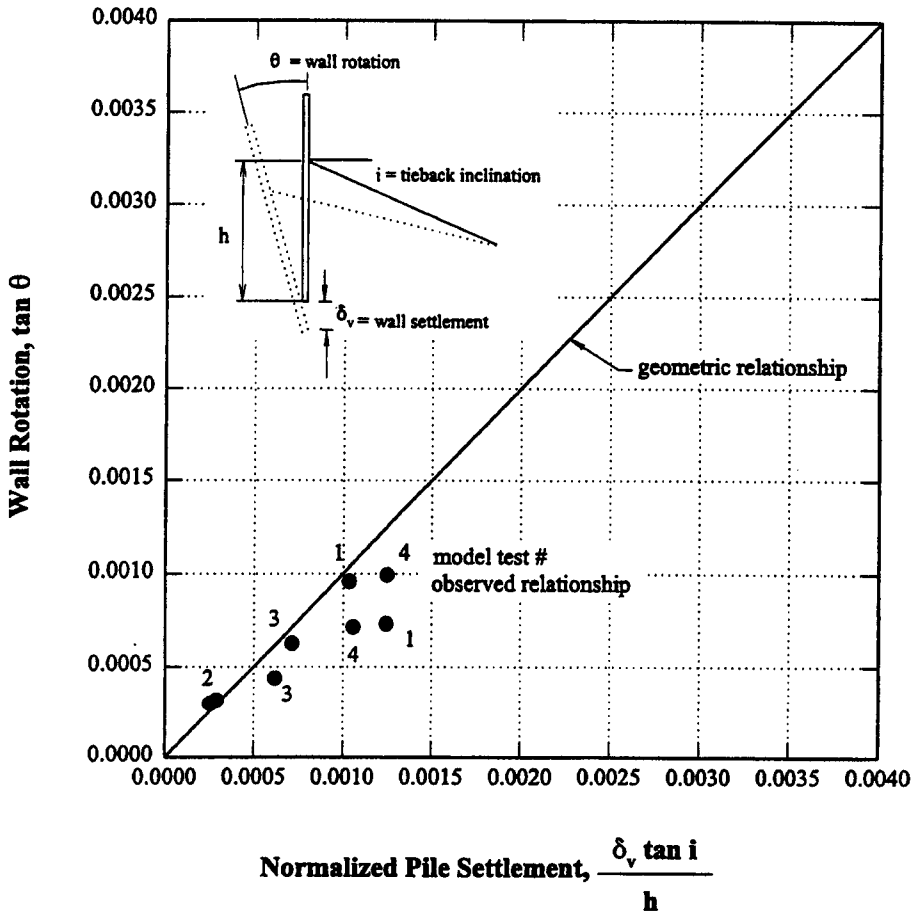

FIGURE 21
Relationship Between Soldier Beam Settlement and Wall Rotation in Model Tests

Maximum positive bending moments were observed at the anchor levels and ranged from about 1400 to 1500 in-lb. Maximum negative bending moments (~800 in-lb) were observed in the span between the lower anchor level and design grade. Despite the significant outward rotation of the wall that developed during excavation below the lower anchor, the lateral earth pressure interpretation developed from measured bending strains still showed the pronounced effect of anchor prestressing (Figure 22). In fact, lateral earth pressures increased in the vicinity of the ground anchors during excavation to design grade. Small increases in active thrust near the base of the excavation were balanced by mobilization of passive resistance along the toe and beam tip shear. Toe reactions below the excavation were between 75 and 80 lb/beam. For comparison, the computed required reaction in the toe was about 190 lb/beam. The final earth pressure distribution was generally consistent with the trapezoidal loading diagram assumed in design, but was more pronounced at the anchor locations and decreased in the span between the upper and lower anchors and the span below the lower anchor.

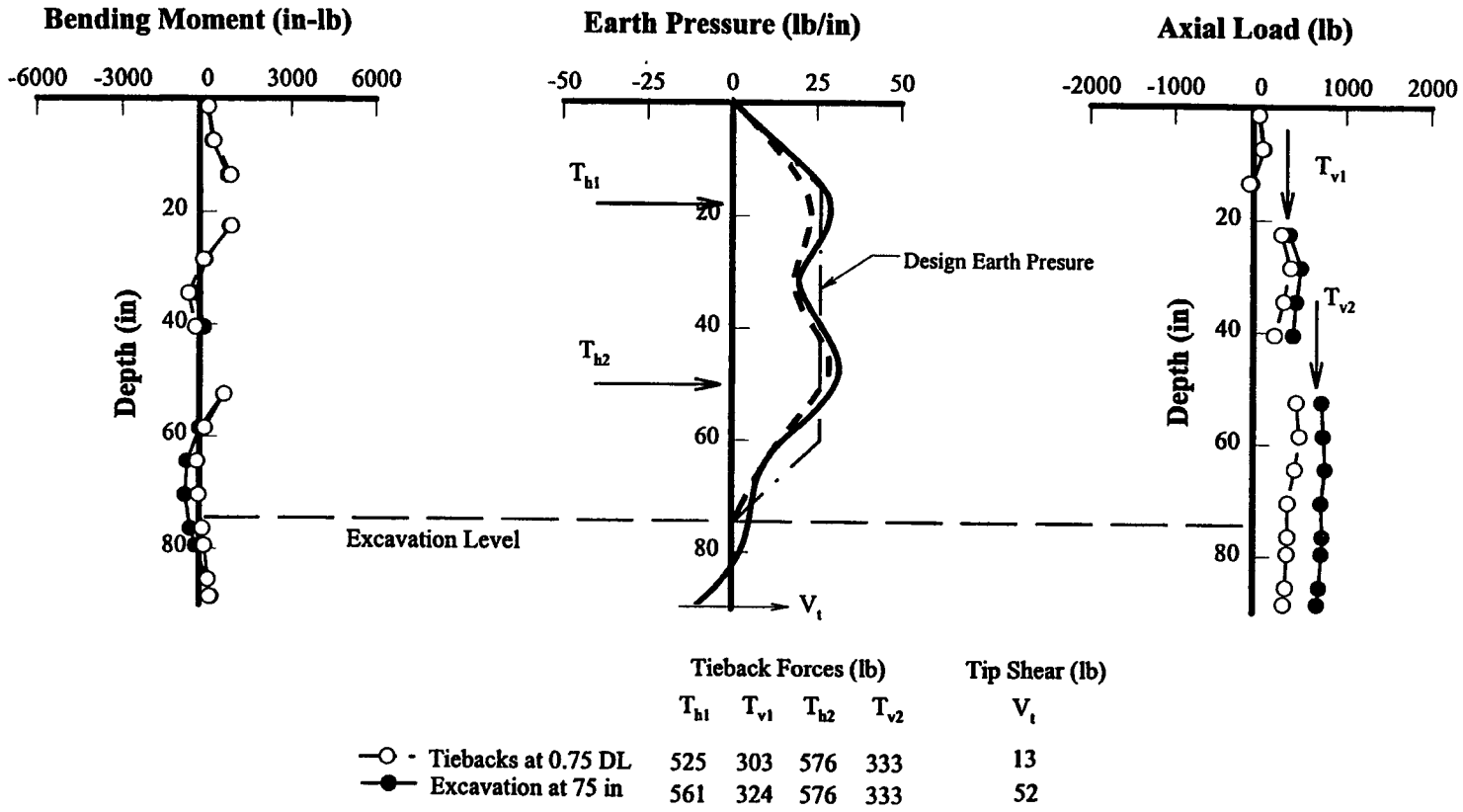

	Tieback Forces (lb)				Tip Shear (lb)
	T_{h1}	T_{v1}	T_{h2}	T_{v2}	V_t
○ - Tiebacks at 0.75 DL	525	303	576	333	13
● Excavation at 75 in	561	324	576	333	52

FIGURE 22
Bending Moments, Earth Pressures, and Axial Loads with Excavation at 75 In — Model Test 4, SP4

During excavation below the lower ground anchors, relative downward movements of the ground with respect to the wall developed. This resulted in reduced carrying capacity for the vertical component of anchor force above the excavation level and increased the total vertical load on the wall. With the excavation at design grade, the total vertical force on the wall was between 830 and 930 lb/beam. This compares with a vertical component of anchor force of about 660 lb/beam. Thus, between 170 and 270 lb of the observed axial load could be attributed to downdrag. At design grade, between 640 and 690 lb of axial load was carried in end bearing, with the balance of the vertical force supported by skin friction, principally between the upper and lower ground anchors.

2.3.1.6 Unloading Lower Ground Anchors

Each of the lower ground anchors was simultaneously unloaded in small decrements (~ 50 lb) after reaching design grade. Approximately 1330 lb of load was removed from the anchor at the instrumented test section of the wall, which corresponds to a horizontal component of force about 290 lb/ft of wall. Once the load was removed, the ground anchors were disconnected from the load-control device and wales, so that during subsequent construction activities the lower ground anchors would not constrain the wall against deformations.

The changes in wall and ground movements that occurred during anchor unloading are summarized in Figure 23. Significant changes in the patterns of wall and ground movements were observed. The wall bulged outward approximately 0.4 in below the upper anchor, which compares with a maximum lateral bulge of about 0.04 in with the excavation at design grade. Thus, increasing the unsupported span (distance between an anchor and the excavation level) by a factor of about two, produced an order of magnitude increase in bulging deformations. This illustrates the importance of wall span for controlling certain components of wall deformation.

Ground surface settlements immediately adjacent to the wall did not change during anchor unloading. Development of deep-seated lateral ground strains, however, resulted in increases in ground surface settlement further behind the wall. Deep-seated bulging produced a broader surface settlement trough than had been observed with previous construction stages. The maximum ground surface settlement was observed at a distance of about $0.25H$ (where H represents the depth of the cut) behind the wall.

Unloading the lower ground anchors also resulted in significant changes in the distribution of bending stresses and lateral earth pressures (Figure 24). A reversal in curvature was observed at the lower anchor level, with a maximum negative moment below the upper anchor of about 1950 in-lb. This compares with a maximum negative moment of about 800 in-lb with the excavation at design grade. Unloading the lower level of anchors reduced the pressure bulb in the vicinity of the support. There was no evidence of anchor prestress at the lower anchor level after unloading was completed. Loads in the upper ground anchors increased about 455 lb, corresponding to a horizontal component of force of about 100 lb/ft of wall. In addition, the reaction provided by the toe of the wall (passive resistance and beam tip shear) increased about 50 lb/ft of wall.

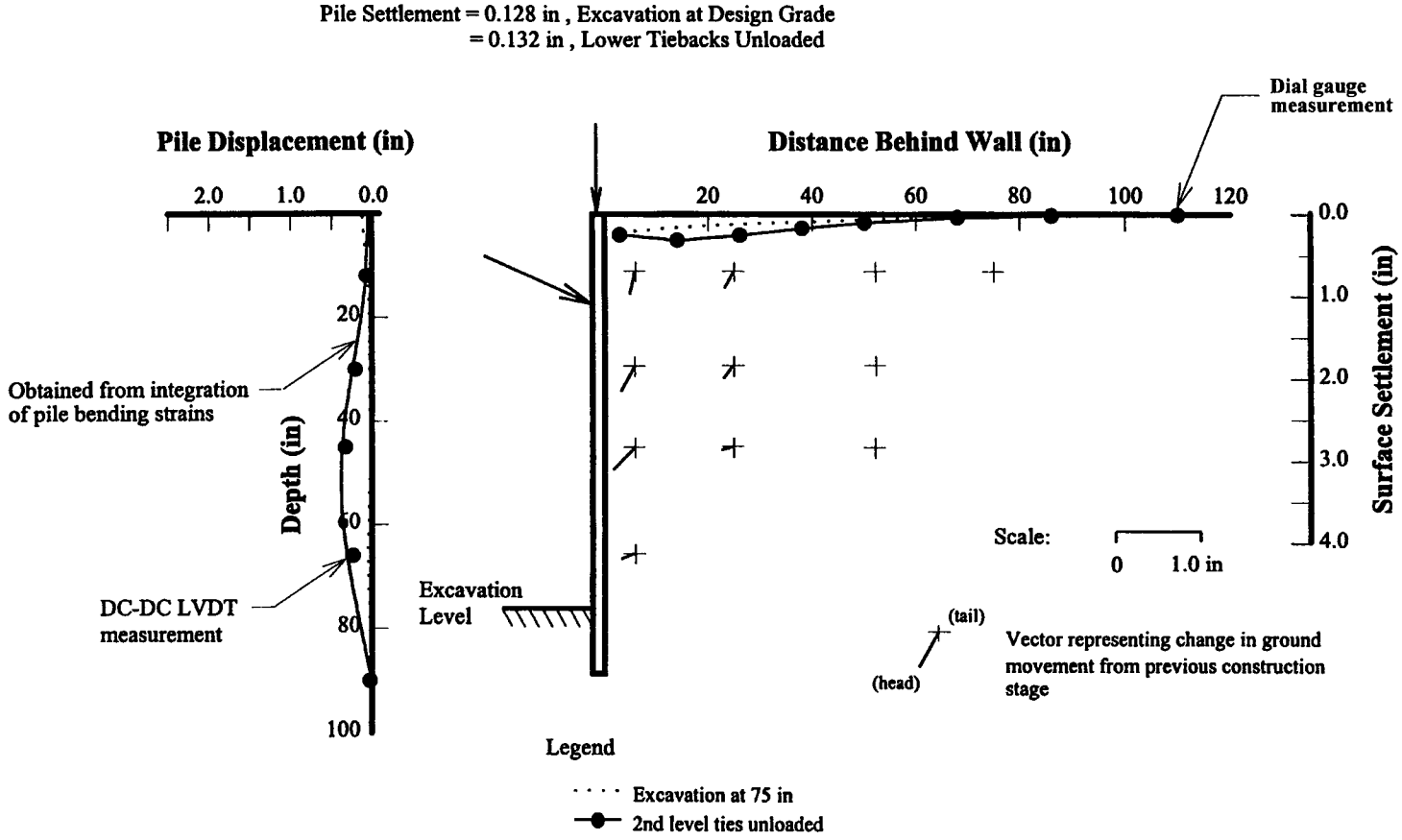

FIGURE 23
Wall and Ground Movement After Unloading Second Level of Anchors — Model Test 4, SP4

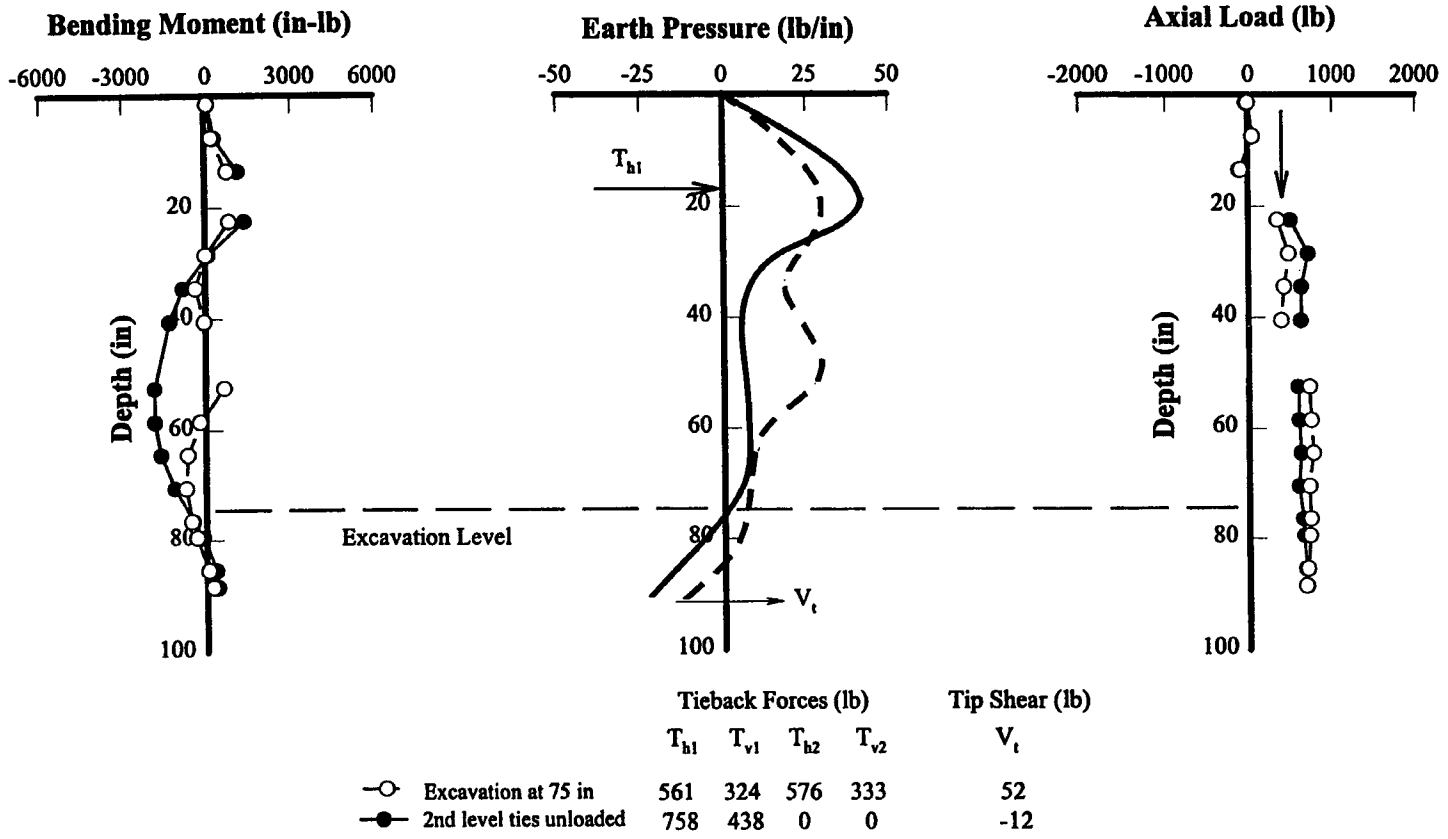

	Tieback Forces (lb)				Tip Shear (lb)
	T_{h1}	T_{v1}	T_{h2}	T_{v2}	V_t
Excavation at 75 in	561	324	576	333	52
2nd level ties unloaded	758	438	0	0	-12

FIGURE 24
Bending Moments, Earth Pressures, and Axial Loads After Unloading Second Level of Anchors — Model Test 4, SP4

2.3.1.7 Reducing Loads in Upper Ground Anchors

After unloading the lower ground anchors, loads in the upper ground anchors were reduced from about 1750 to 1200 lb at the instrumented test section. Ground anchors were simultaneously unloaded in about 50-lb decrements until further load reduction could not be achieved. This condition was assumed to correspond to a limit state of stress. The total lateral thrust supported by the wall was about 370 lb/ft of wall, which includes the horizontal component of anchor force, mobilized lateral toe resistance, and beam tip shear. The vertical component of load associated with downdrag was about 170 lb/ft of wall. Using a trial wedge analysis, this distribution of forces on the wall corresponds to a mobilized angle of internal friction of about 45°.

Reducing loads in the upper ground anchors resulted in outward rotation of the wall about the toe, with small increases in bulging deformations in the span below the upper ground anchors. The maximum lateral displacement of the wall measured about 0.75 in (Figure 25). The maximum ground surface settlement was about 0.68 in at a distance behind the wall of about $0.25H$. Despite the increased contribution to lateral wall deformations from outward rotation about the toe, the surface settlement trough maintained the distinctive "bowl" shape that had developed during unloading of the lower ground anchors.

The maximum positive bending moment at the upper anchor level decreased from about 2500 to 1300 in-lb. during anchor unloading. The maximum negative moment in the span below the upper anchor increased from about 1950 to 3000 in-lb. Although a limit condition was assumed to have developed through anchor unloading, the earth pressure distribution still displayed the influence of anchor prestressing (Figure 26). It was not possible to develop a triangular distribution of pressure in any of the four model tests.

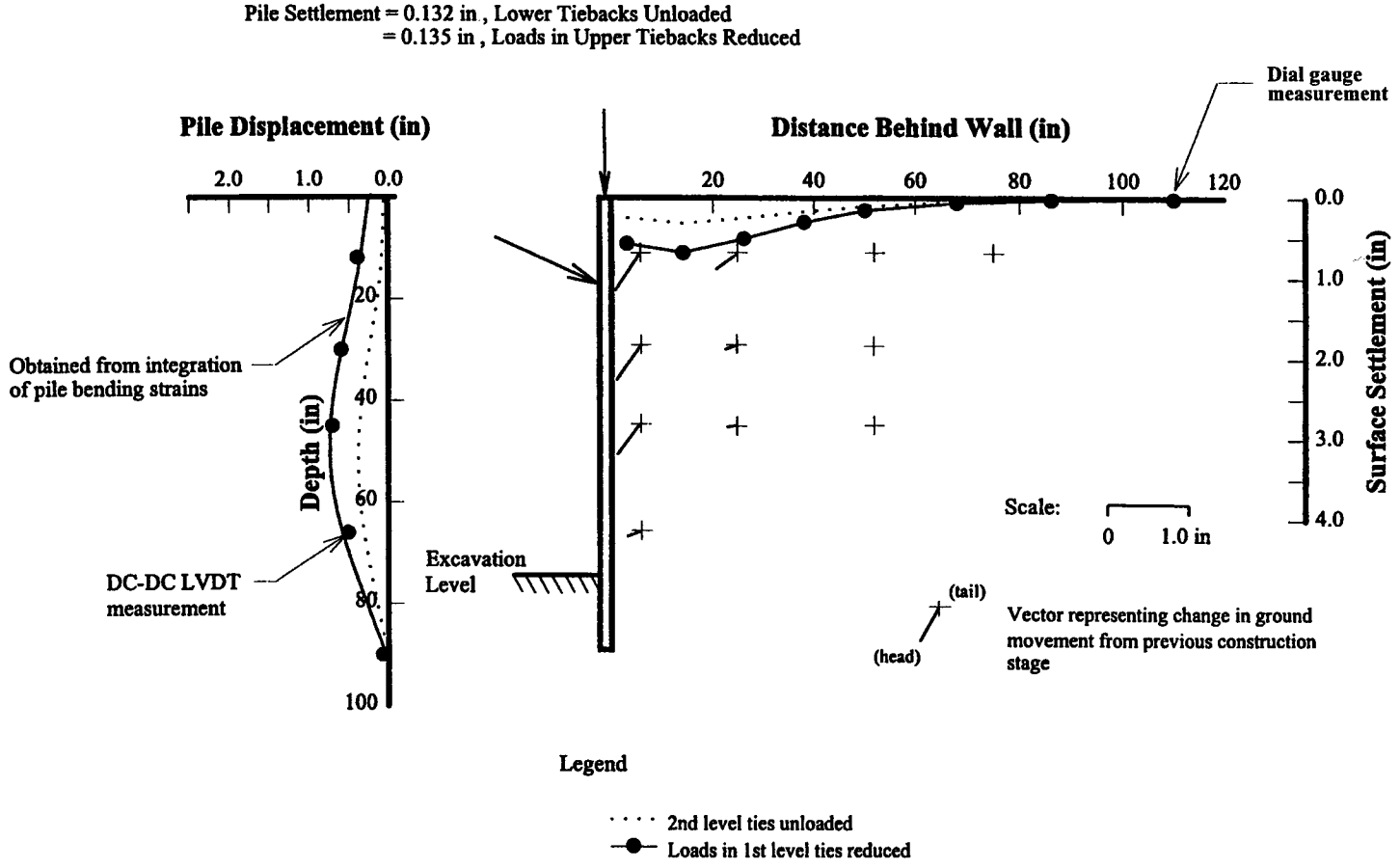

FIGURE 25
Wall and Ground Movements After Reducing Loads in Upper Anchors — Model Test 4, SP4

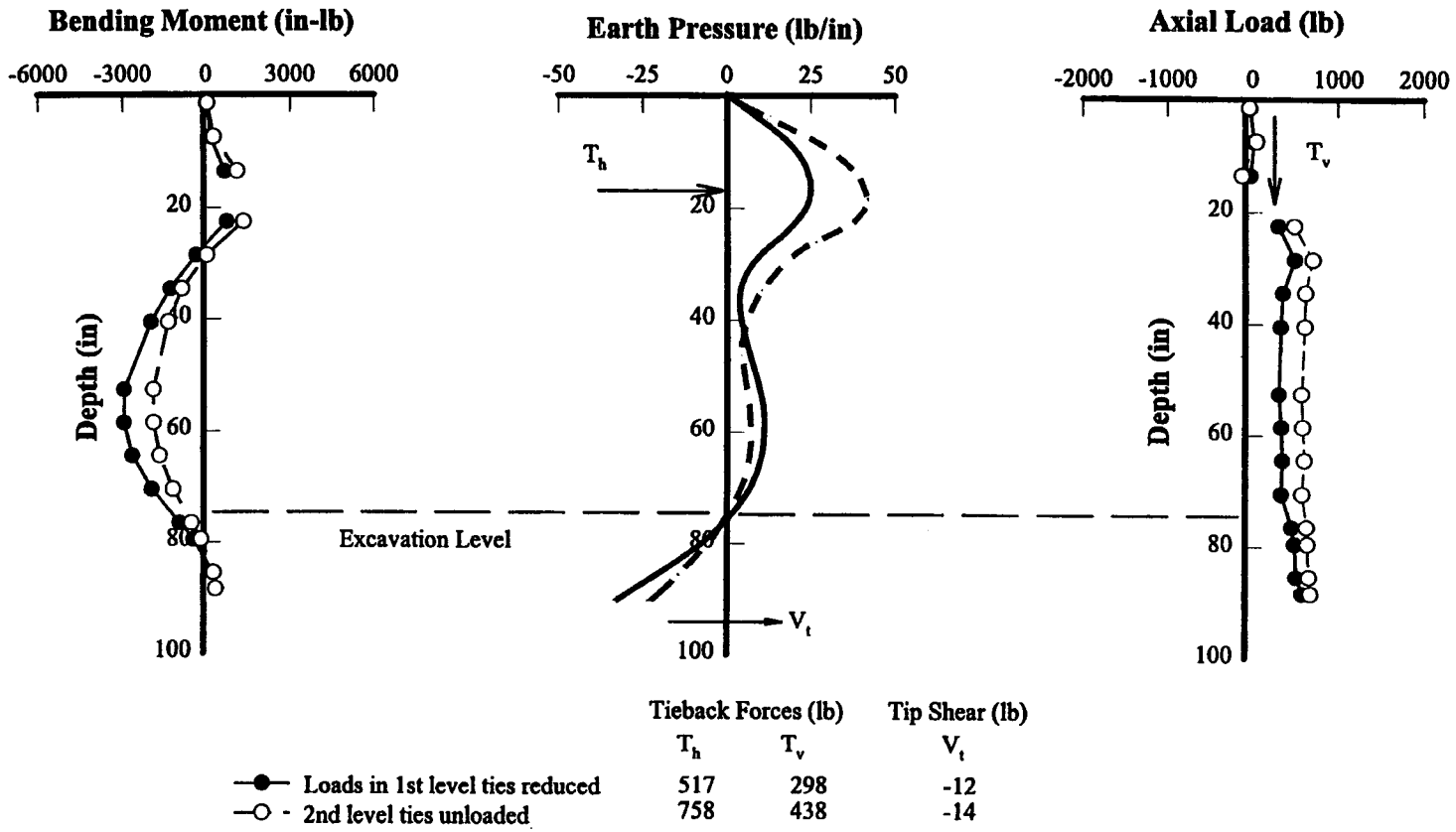

FIGURE 26
Bending Moments, Earth Pressures, and Axial Loads After Reducing Loads in Upper Anchors — Model Test 4, SP4

2.3.1.8 Over-excavation

The excavation was extended to a depth of 81 in after reducing loads in the upper ground anchors. The effect of removing lateral and vertical support from the beam toe on wall and ground deformations is shown in Figure 27. The wall rotated about the upper ground anchor level, with the top of the beams moving back into the retained soil and the bottom of the beams moving outward into the excavation. The maximum lateral movement of the wall was about 1.4 in and occurred near the excavation level. Outward displacement of the wall at the soldier beam tips was about 0.4 in.

Lateral earth pressures on the upper part of the wall increased as the soldier beams rotated back into the retained soil. In addition, significant increases in earth pressure near the base of the wall were observed (Figure 28). The increase in pressure near the base of the wall was balanced by a corresponding increase in passive lateral toe resistance and beam tip shear. The total lateral resistance of the toe was about 330 lb/beam, which represents about one-third of the total lateral thrust supported by the wall.

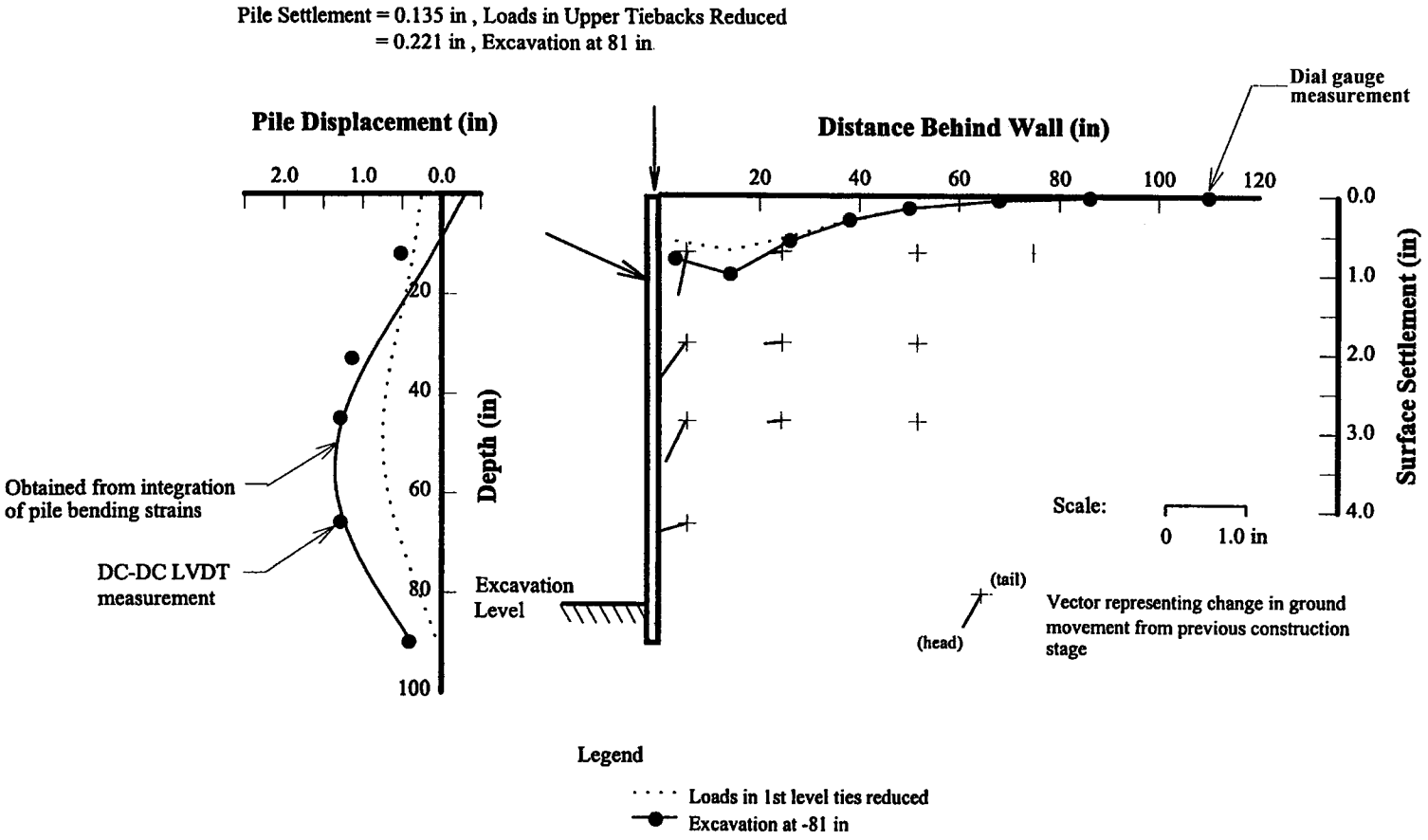

FIGURE 27
Wall and Ground Movement with Excavation at 81 In — Model Test 4, SP4

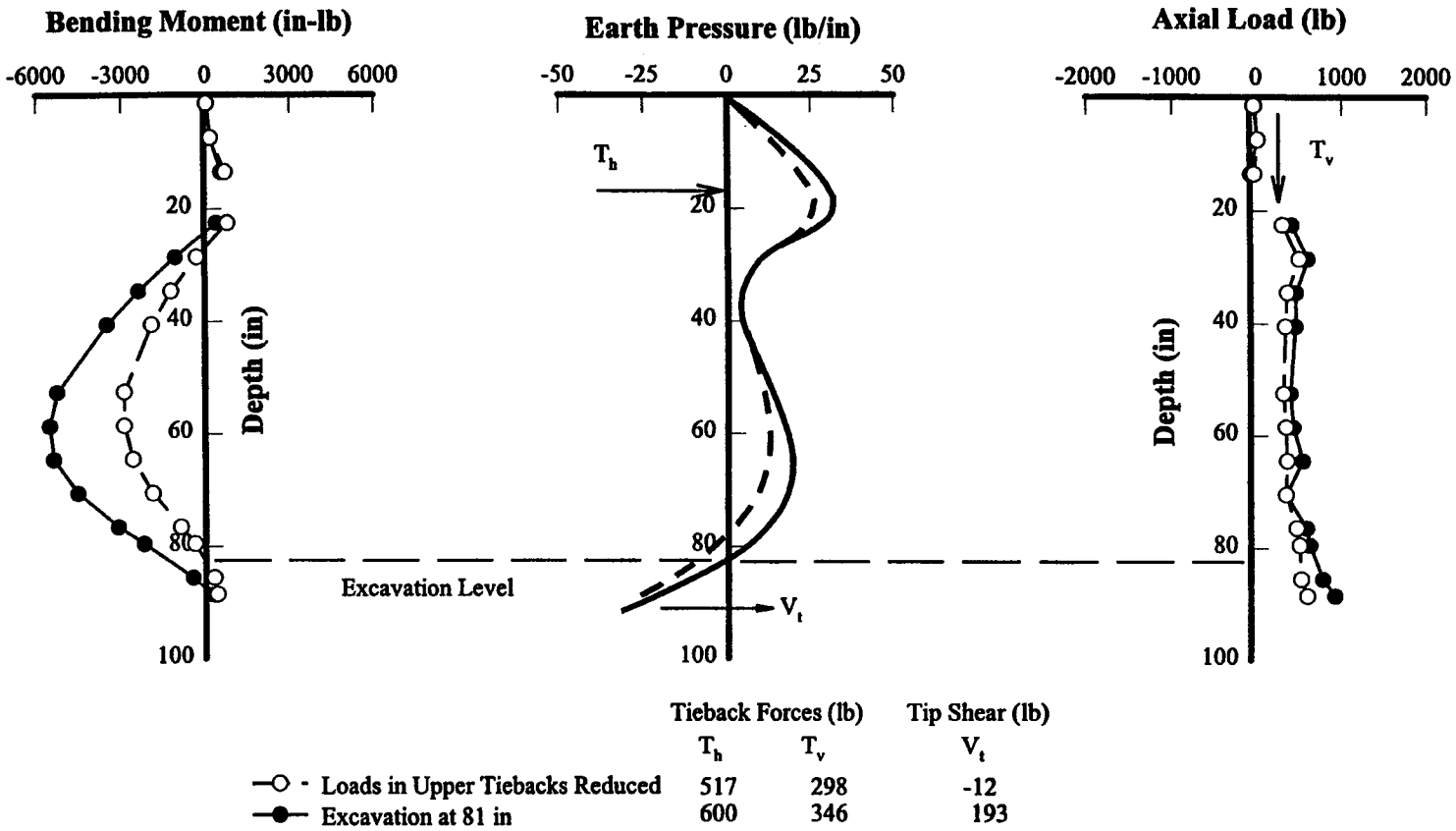

FIGURE 28
Bending Moments, Earth Pressures, and Axial Loads with Excavation at 81 In — Model Test 4, SP4

2.3.2 Stiff Beam Supported by a Single Level of Ground Anchors (Test 1)

Model Test 1 was supported by a single level of ground anchors at a depth of about 27 in ($0.36H$). Section properties of the model beams ($I = 0.958$ in^4) were selected to provide a relative soil/wall stiffness consistent with the driven beam test section supported by a single level of ground anchors at Texas A&M (Chung and Briaud, 1993). The soldier beams in Test 1 had a total available axial capacity (end bearing and skin friction) that was less than the vertical component of anchor force. Failure was induced by extending the excavation below design grade.

2.3.2.1 Excavation to Design Grade

The behavior of Model Test 1 differed in several important respects from the other model tests:

- Comparatively large beam settlements developed as the excavation approached design grade.
- Ground movements were more strongly influenced by void closure between the lagging and geotextile fabric.
- Mobilized end bearing resistance was small.
- One ground anchor failed to develop 120 percent of the design load or to maintain the lock-off load.

Wall and ground movements that developed during construction of Test 1 are summarized in Figure 29. The maximum lateral movement of the wall was about 0.1 in and included contributions from bending (cantilever type movements and lateral bulging) and outward rotation due to beam settlement. Large increases (~ 0.14 in) in beam settlement, associated with mobilization of ultimate end bearing resistance, were observed during excavation from a depth of 48 in to design grade (75 in). Between 0.07 and 0.09 in of the observed lateral wall movement could be attributed to soldier beam settlement.

Large ground surface settlements (~ 0.46 in) developed in Test 1. Ground surface settlements were maximum at the wall and decreased to small values (~ 0.01 in) at a distance behind the wall of about $1.5H$. The volume of ground surface settlement was about 1.5 times the volume of lateral movement at the wall. Volumes of lateral movement at the wall were estimated from measured soldier beam displacements, but excluded the movements of the beams back into the retained soil that developed during anchor prestressing. It is believed that the comparatively large volumes of ground surface settlement that developed in Test 1 were due to significant void closure between the lagging and geotextile fabric. In the other model tests, the volume of ground surface settlement was only one to 1.2 times larger than the volume of lateral movement at the wall.

The distribution of forces on the wall for the final construction stage is summarized in Figure 30. The estimated maximum positive bending moments were observed at the anchor level and measured about 4500 in-lb. Maximum negative bending moments were observed in the span below the anchor and measured about 2000 in-lb. The lateral earth pressure interpretation developed from measured bending strains was influenced by decreases in the anchor forces (~ 250 lb/beam). Although the earth pressure distribution showed the pronounced effect of anchor prestressing after lock-off, subsequent decreases in the anchor forces resulted in a flattening of the earth pressure distribution in the vicinity of the anchor and comparatively large increases in pressure near the base of the wall. The total reaction developed below the base of the excavation (lateral toe resistance and beam tip shear) was about 100 lb/beam, which was less than one-third of the computed required reaction. Mobilized shear at the beam tip was small in this test (~ 5 lb), which is consistent with the small bearing area of the beams used in Test 1.

Despite development of large soldier beam settlements, relative downward movements of the ground with respect to the wall were observed during excavation below the ground anchors. This resulted in an increase in the axial load supported by the wall due to downdrag of between 260 and 340 lb. Comparatively small end bearing resistance was mobilized in Test 1 (~120 to 200 lb). The most significant feature of the axial load distribution was the mobilization of skin friction (~590 lb) along the toe of the soldier beams.

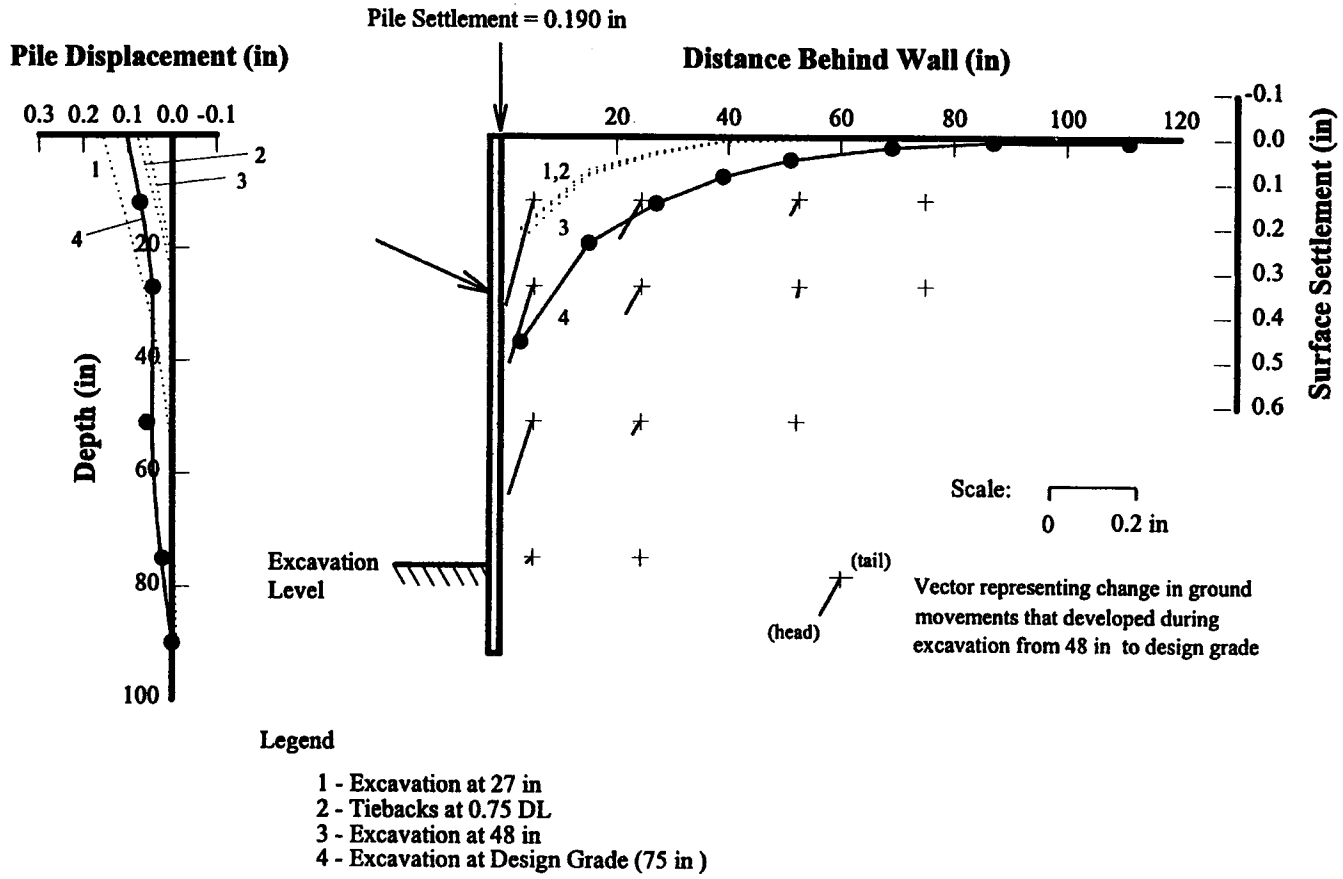

Legend

1 - Excavation at 27 in
2 - Tiebacks at 0.75 DL
3 - Excavation at 48 in
4 - Excavation at Design Grade (75 in)

FIGURE 29
Summary of Wall and Ground Movements During Construction — Model Test 1, SP4

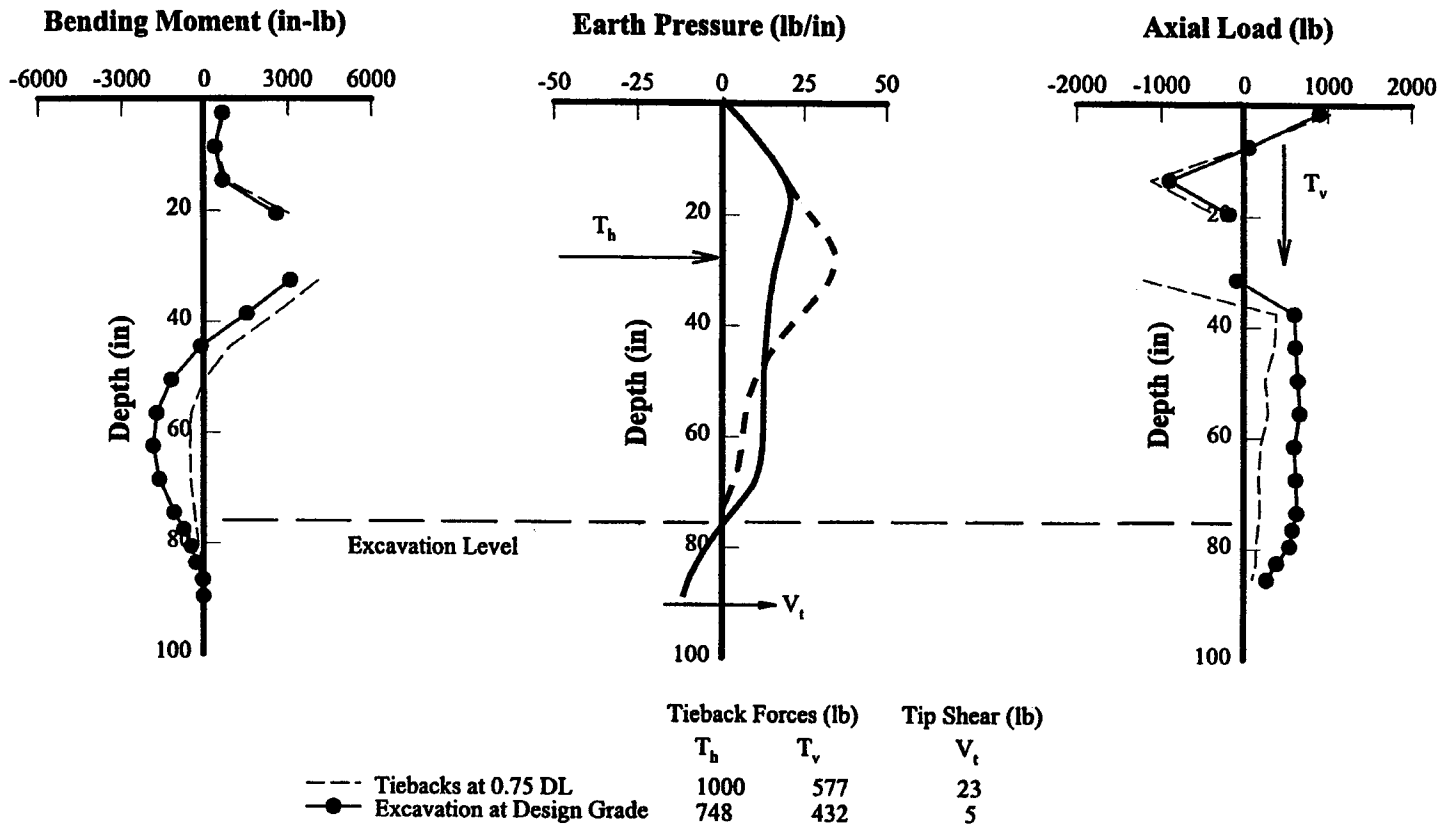

FIGURE 30
Bending Moments, Lateral Earth Pressures, and Axial Loads with Excavation at Design Grade — Model Test 1, SP4

2.3.2.2 Over-excavation

The excavation depth in Test 1 was extended to 84 in after reaching design grade (75 in), so that the behavior of the wall at large deformations could be studied. As shown in Figure 31, increasing the depth of excavation by 9 in resulted in significant increase (~ 2 in) in soldier beam settlement, downdrag, and mobilized end bearing resistance (Figure 32). The wall translated into the excavation about 1.2 in, which is consistent in magnitude with the observed soldier beam settlements. The observed pattern of wall displacement was probably influenced by slip of the anchors at their connections with the reaction frame inside the test chamber and reduced soldier beam toe penetration.

Despite the large increase in wall displacements with additional excavation, the total lateral thrust supported by the wall was about the same as with the excavation at design grade (420 versus 450 lb/beam). There was a decrease in pressure in the vicinity of the anchors and an increase in pressure near the base of the wall, so that the resulting earth pressure distribution was more triangular (Figure 32). Significant increases in lateral toe resistance and beam tip shear developed during this stage of construction. Approximately 184 lb/beam of lateral toe resistance and beam tip shear developed, which corresponds to about 40 percent of the total lateral thrust supported by the wall. In the model tests, development of significant lateral resistance of the toe was coincident with large wall and ground movements.

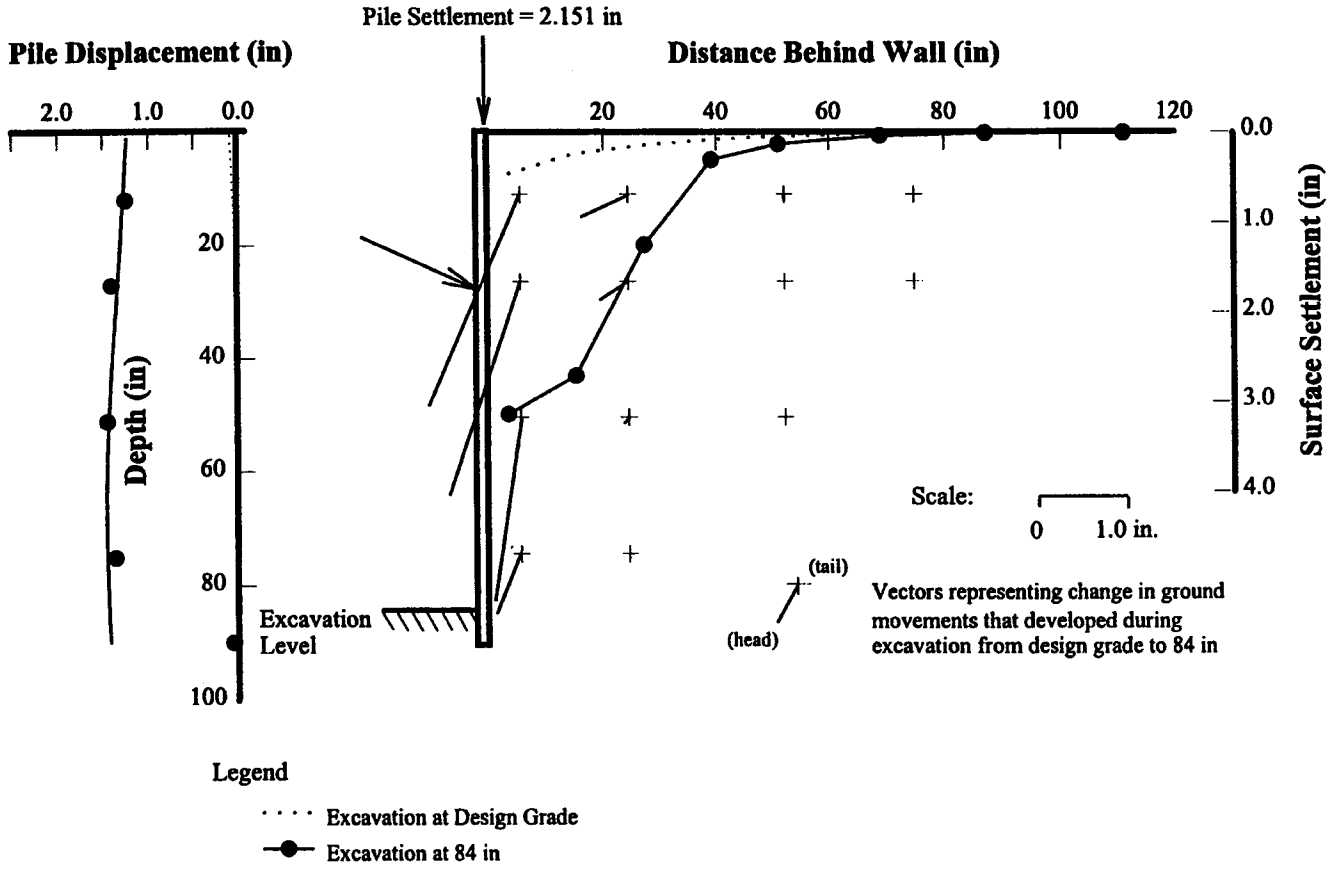

FIGURE 31
Wall and Ground Movements with Excavation at 84 In — Model Test 1, SP4

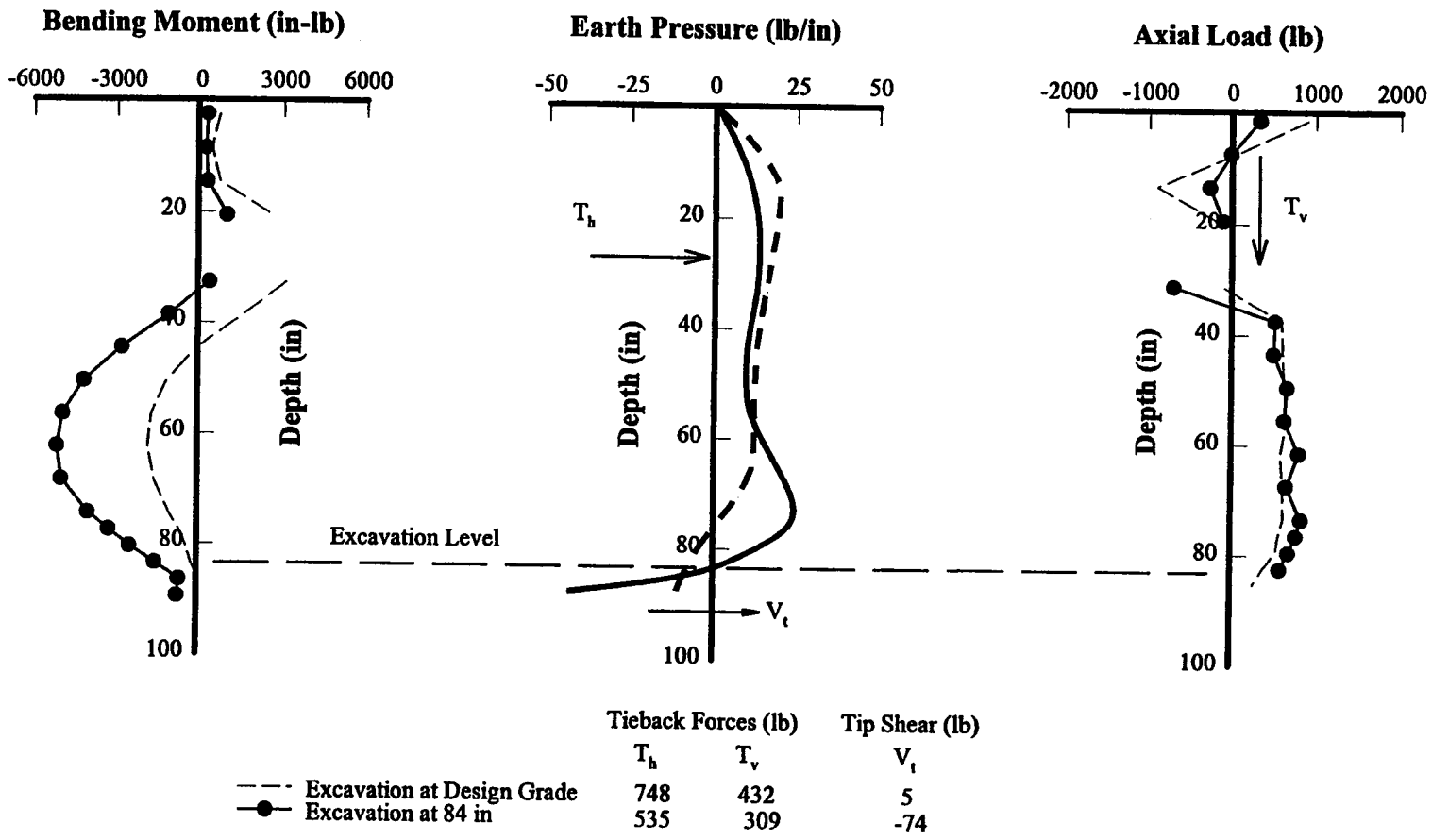

FIGURE 32
Bending Moments, Lateral Earth Pressures, and Axial Loads with Excavation at 84 In — Model Test 1, SP4

2.3.3 Flexible Beam Supported by Single Level of Ground Anchors (Test 2)

Model Test 2 was supported by a single level of ground anchors at a depth of about 27 in. Section properties of the model beams ($I = 0.337$ in^4) were selected to provide a more flexible wall system than used in Test 1 ($I = 0.958$ in^4), so that the influence of relative soil/wall stiffness on bending components of deformation and lateral earth pressures could be compared for walls of similar geometry.

The influence of large beam settlements and significant decreases in anchor loads on the behavior of Test 1 resulted in several modifications for Test 2. Specifically, the beam tip bearing area was increased ($A_p = 24$ in^2) to provide increased axial capacity and stiffness. In addition, modifications of the anchor reaction frame were made to prevent reductions in anchor loads.

Construction of Test 2 was accomplished in three stages:

1. Excavation to the first anchor level (cantilever stage).
2. Prestressing of the ground anchors.
3. Excavation below the ground anchors to design grade.

Loads in the ground anchors were reduced after reaching design grade. The ground anchors were simultaneously unloaded in small decrements (~ 50 lb) until further load reduction could not be accomplished, which was assumed to correspond to a limiting state of stress. After reducing anchor loads, the excavation was extended to a depth of about 86 in.

2.3.3.1 Excavation to Design Grade

Wall and ground movements that developed during excavation to design grade are summarized in Figure 33. Maximum lateral wall movements at the end of construction were observed at the top of the wall and ranged from about 0.18 to 0.2 in. Lateral wall movements developed both from bending (cantilever type movements and lateral bulging) and beam settlement. Outward rotation and translation associated with beam settlements were comparatively small, representing between 15 to 20 percent of the maximum lateral wall movements at the end of construction. Thus, use of an enlarged bearing area at the soldier beam tips was effective in increasing the axial stiffness of the beam/soil system. Maximum ground surface settlements (~ 0.31 in) developed at the wall and decreased to small (~ 0.005 in), but measurable values, at a distance behind the wall of about $1.5H$ (H represents the depth of the cut).

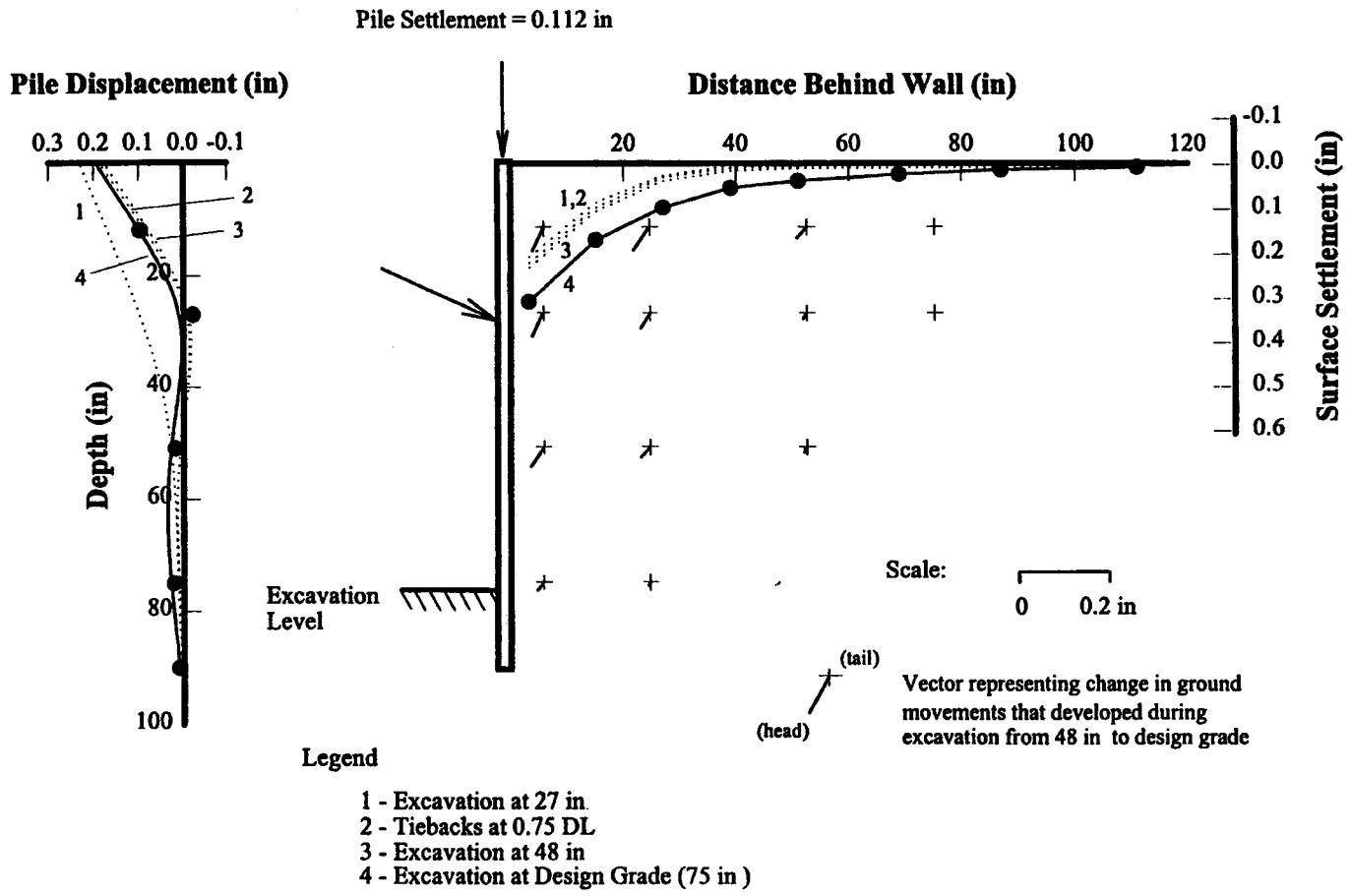

FIGURE 33
Summary of Wall and Ground Movements During Construction — Model Test 2, SP4

Maximum positive bending moments at the ground anchor level of about 7100 in-lb were estimated with the anchor loads at about 1.2 times the design loads. With anchor loads at 75 percent of design, maximum positive bending moments were about 5800 in-lb. The bending moment at the anchor level did not decrease in proportion to the reduction in anchor load as the anchor was locked-off. Maximum negative bending moments (~ 1400 to 1600 in-lb) were observed at about mid-span between the anchor level and design grade, and developed during excavation below the ground anchors. Compared with Model Test 1, only small changes in lateral earth pressures were observed following anchor prestressing. A pronounced pressure "bulb" was observed at the anchor level following prestressing (Figure 34). During excavation below the ground anchors, small decreases in pressure were observed in the span below the ground anchors, which resulted in small increases in pressure at the anchor level and near the bottom of the excavation. The reaction developed along the embedded length of the beam (lateral toe resistance and shear at the soldier beam tips) was about 60 to 70 lb/beam, or 20 percent of the computed required toe reaction.

The total vertical load supported by the soldier beams, with the excavation at design grade, ranged from about 900 to 1060 lb/beam. The vertical component of anchor force was about 630 lb, corresponding to an increase in axial load of between 270 and 430 lb/beam due to relative downward movement of the ground with respect to the soldier beams (~ 0.01 to 0.05 in). Although a small portion of the vertical load was carried in skin friction above the anchor level, most of the vertical load (~ 600 to 780 lb) was carried in end bearing, a consequence of the increased axial tip stiffness associated with use of an enlarged bearing plate.

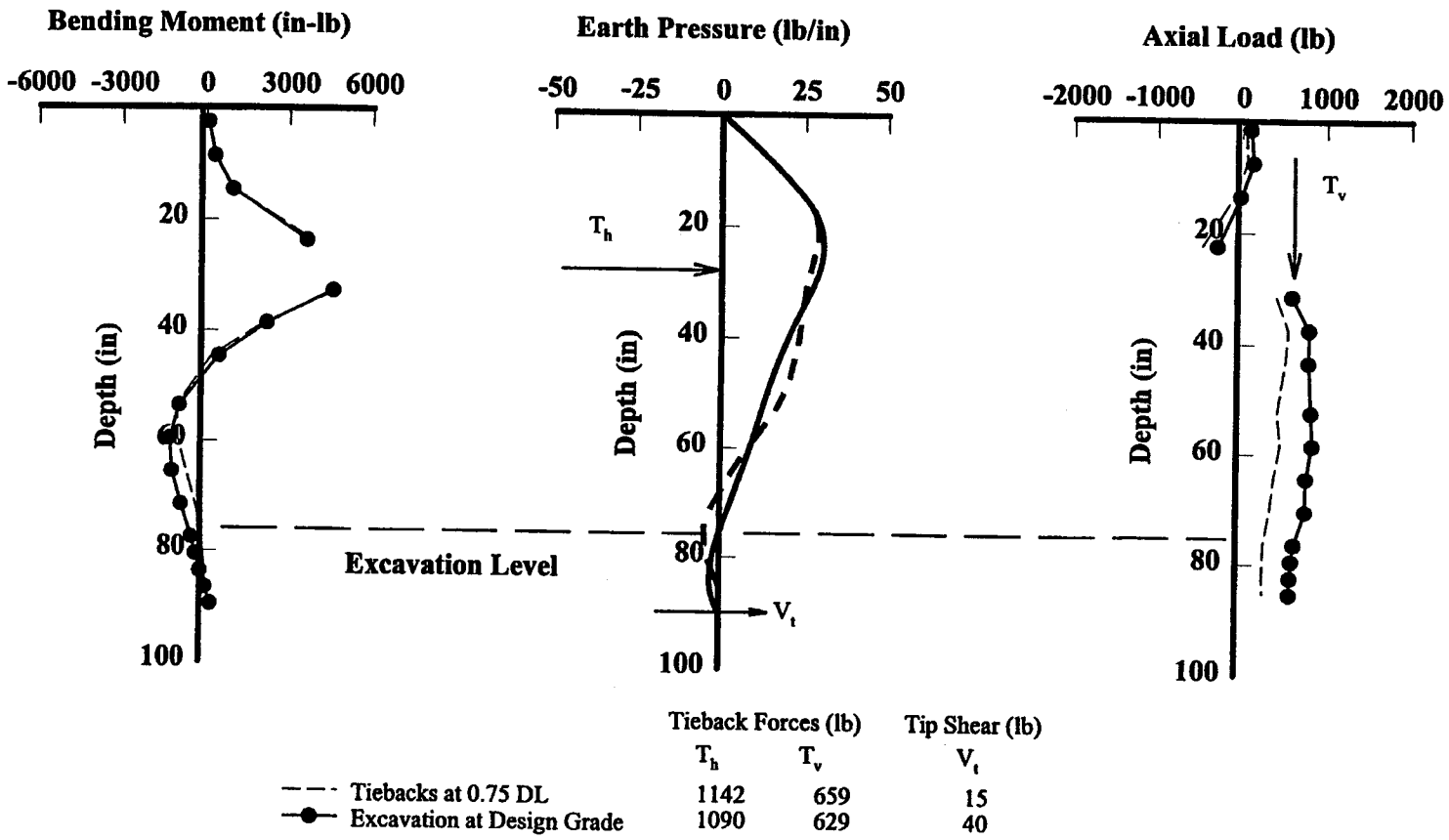

FIGURE 34
Bending Moments, Earth Pressures, and Axial Loads with Excavation at Design Grade — Model Test 2, SP4

2.3.3.2 Failure Modes

The behavior of Test 2 at large deformations was studied by reducing loads in the anchors and extending the excavation to a depth of about 85.5 in. Reducing loads in the upper ground anchors resulted in outward rotation of the wall about the toe (Figure 35). Maximum lateral wall movements increased from about 0.19 to 0.55 in, with corresponding increases in the volume of ground surface settlement. Small increases in soldier beam settlement (~ 0.02 in) were observed. Although the vertical component of the anchor force was decreased from 629 to 259 lb/beam, the total axial force supported by the soldier beams was essentially unchanged because of a corresponding increase in axial loads associated with downdrag (Figure 36).

Reducing load in the ground anchors resulted in a flattening of the earth pressure in the vicinity of the anchors, although the prestressing effect was still apparent. Significant increases in lateral toe resistance developed during unloading (~ 110 lb/beam), although a reversal in soldier beam curvature near the excavation level resulted in development of beam tip shear that was opposite in direction to the mobilized lateral toe resistance. The net reaction (lateral toe resistance and beam tip shear) provided by the embedded length of the soldier beams was about the same before and after reducing the ground anchor load.

Extending the excavation to a depth of about 86 in resulted in outward rotation of the wall about the toe (Figure 37). The magnitude and pattern of observed wall displacement was consistent with the small increases in soldier beam settlements (~ 0.08 in). Increases in settlement occurred due to relative downward movement of the ground with respect to the wall and increases in mobilized end bearing resistance. The increase in axial load associated with downdrag, and corresponding increase in mobilized end bearing resistance, was about 300 lb/beam.

Significant increases in ground anchor forces developed during excavation to a depth of 86 in, which were reflected by increases in lateral earth pressure in the vicinity of the anchors (Figure 38). Changes in earth pressure near the base of the wall were small. Although significant decreases in lateral toe resistance along the embedded length of the wall were observed, increases in beam tip shear also were observed, such that the net contributions from beam tip shear and lateral toe resistance were essentially unchanged by excavation to a depth of 86 in. Note by contrast with the previous stage of construction that the distribution of bending moments was consistent with a free earth support condition.

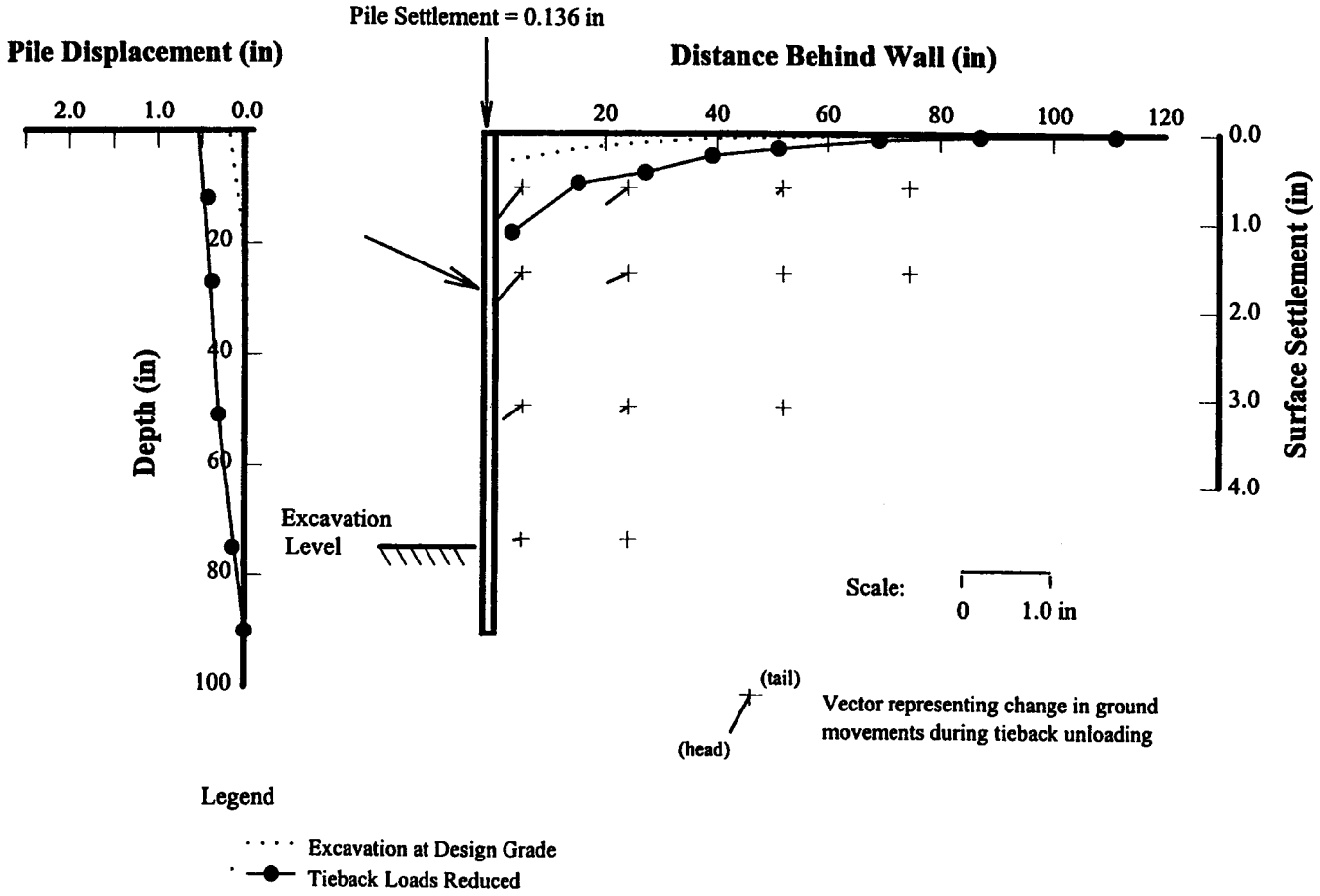

FIGURE 35
Wall and Ground Movements During Unloading of Anchors — Model Test 2, SP4

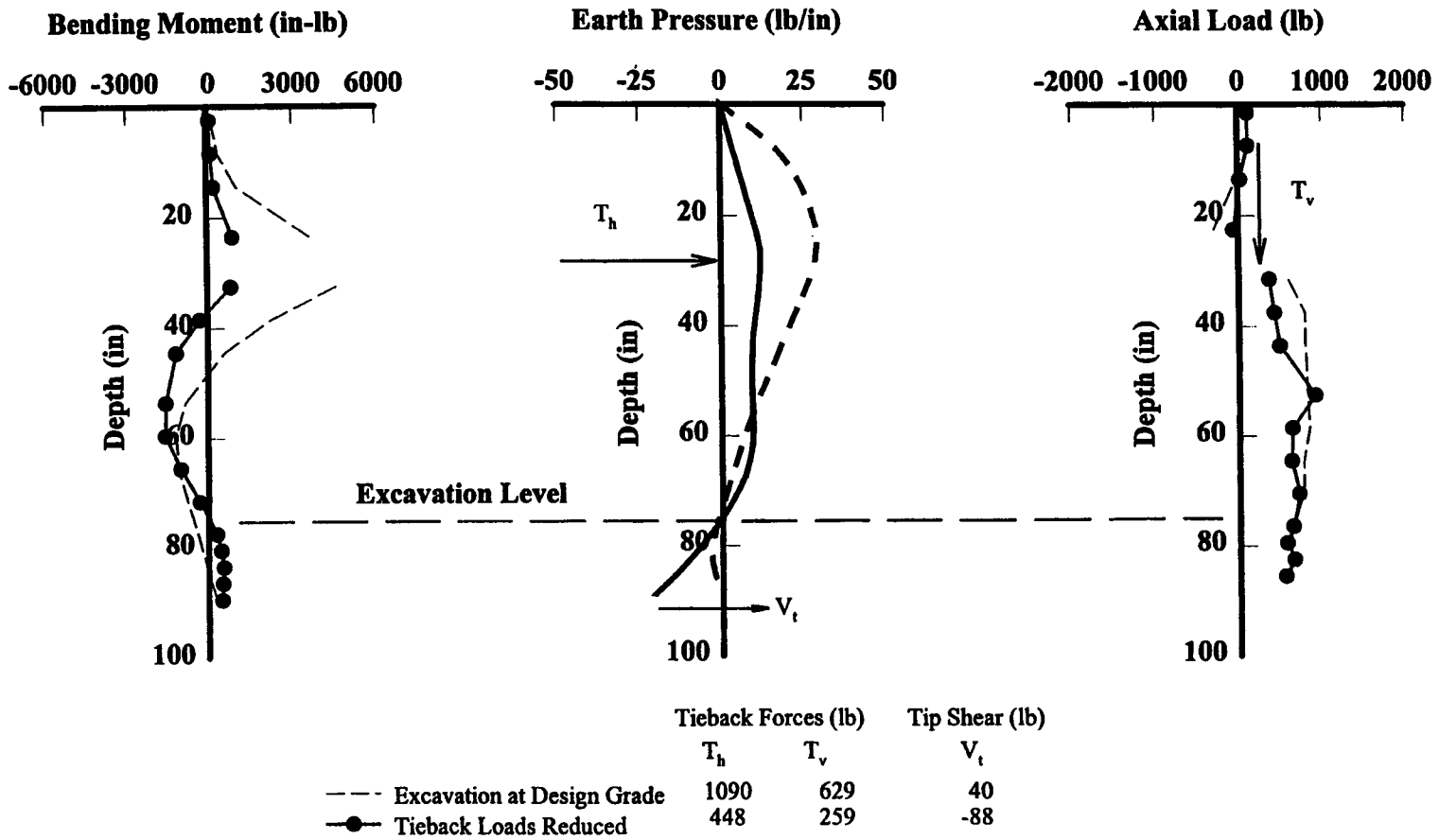

FIGURE 36
Bending Moments, Earth Pressures, and Axial Loads During Unloading Anchors — Model Test 2, SP4

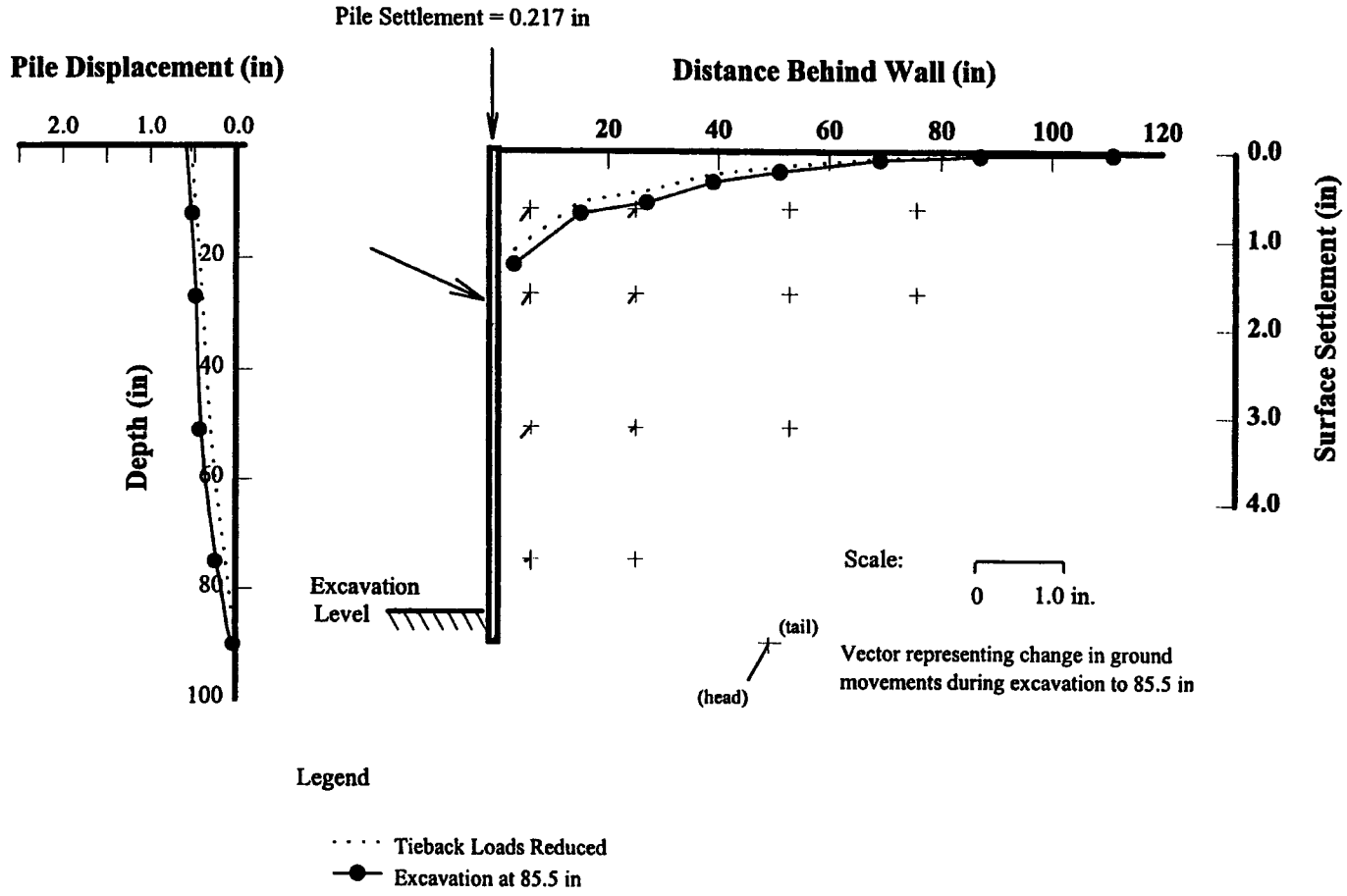

FIGURE 37
Wall and Ground Movements with Excavation at 85.5 In — Model Test 2, SP4

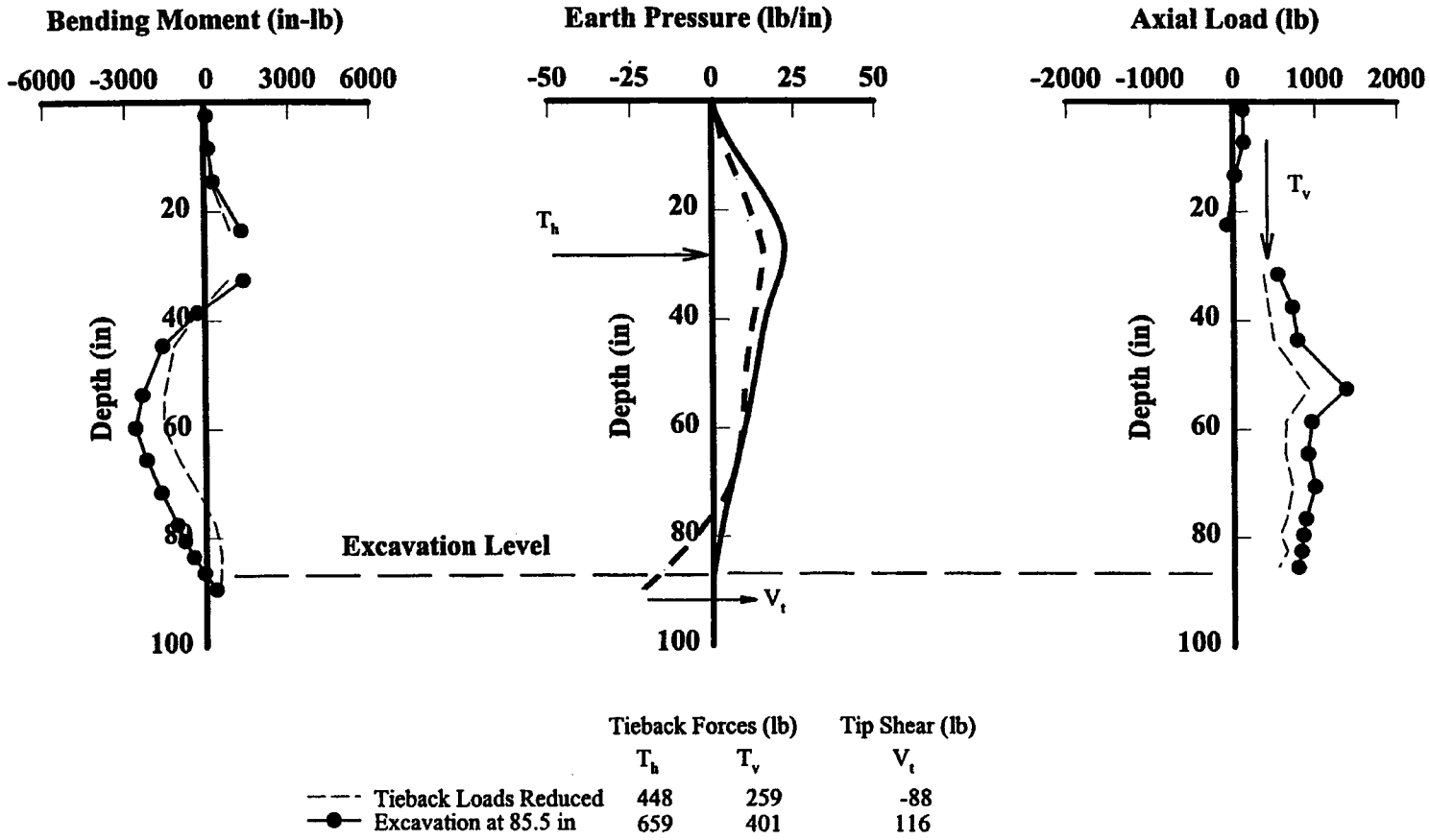

FIGURE 38
Bending Moments, Earth Pressures, and Axial Loads with Excavation at 85.5 In — Model Test 2, SP4

2.3.4 Stiff Beam Supported by Two Levels of Ground Anchors (Test 3)

Model Test No. 3 was constructed with a beam of the same stiffness ($I = 0.337$ in^4) as used in Model Test No. 2, but was supported by two levels of ground anchors at depths of 18 and 48 in. Soldier beam properties were selected to provide a relative soil/wall stiffness that was consistent with the driven beam section supported by two levels of ground anchors at Texas A&M (Chung and Briaud, 1993). Consistent with Tests 2 and 4, an enlarged bearing area was used at the beam tips.

Excavation to design grade was accomplished in five stages:

1. Excavation to the upper anchor level.
2. Prestress the upper ground anchors.
3. Excavation to the lower anchor level.
4. Prestress the lower ground anchors.
5. Excavation below the lower anchor to design grade.

After reaching design grade, the lower level of ground anchors was unloaded to examine load redistribution to the upper ground anchors and toe of the wall and corresponding wall deformations. The lower level of anchors was then reloaded, and the excavation extended approximately the full depth of the soldier beams (88.5 in).

2.3.4.1 Excavation to Design Grade

Wall and ground movements that developed during excavation to design grade are summarized in Figure 39. Maximum lateral wall movements were observed at the top of the wall and measured about 0.04 in. Although cantilever type displacement and lateral bulging did contribute to deformations of the wall, significant outward rotation developed during excavation below the lower level of ground anchors. Note that stressing of the upper and lower ground anchors had the effect of pulling the soldier beams back beyond the initial zero measurements taken prior to excavation. During excavation below the lower anchor, increases in beam settlement on the order of 0.04 to 0.05 in were observed. Beam settlements resulted in an increase in lateral movements at the top of the wall from 0.004 in to 0.04 in during the final stage of construction. Maximum ground surface settlements (~ 0.11 to 0.14 in) were observed at the wall and decreased to zero at a distance behind the wall of about $1.5H$.

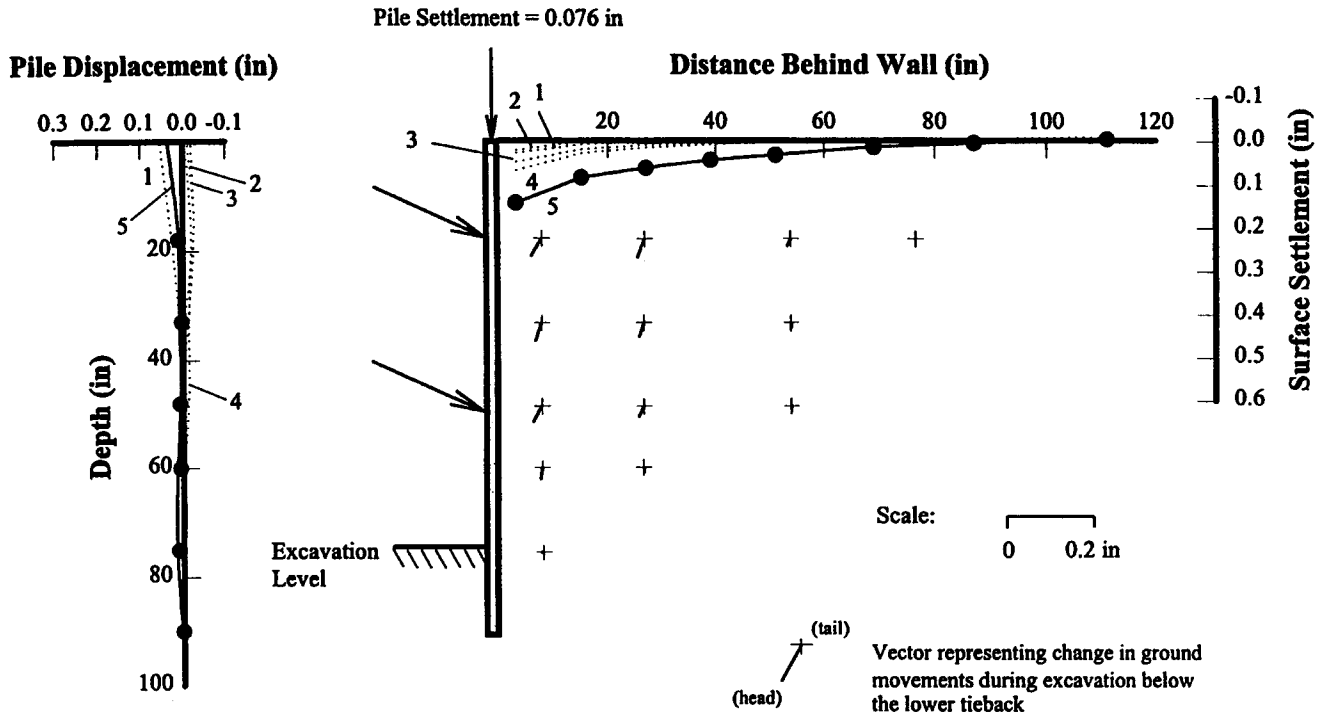

Legend

1 - Excavation to Upper Tieback Level (18 in)
2 - Upper Tiebacks at 0.75 DL
3 - Excavation to Lower Tieback Level (48 in)
4 - Lower Tiebacks at 0.75 DL
5 - Excavation at Design Grade (75 in)

FIGURE 39
Wall and Ground Movements with Excavation at Design Grade — Model Test 3, SP4

Maximum positive bending moments between 2400 and 2700 in-lb were estimated at the upper anchor level when the anchors were loaded to 120 percent of the design load. When the anchor loads were reduced and locked-off at 75 percent of design, maximum positive bending moments ranged from about 1800 to 2100 in-lb. As was the case with the other walls, the bending moments at the anchor did not decrease proportionally with the reduction of anchor loads. Maximum negative bending moments (~ 800 in-lb) developed in the span below the lower ground anchors when the excavation reached design grade. The earth pressure interpretation developed from measured bending strains shows the pronounced effect of anchor prestressing at each support level (Figure 40). Below the lower anchor level, the earth pressure decreases to a small value at the bottom of the cut. The mobilized toe reaction (lateral toe resistance and beam tip shear) ranged between 60 and 70 lb/beam, or about 20 percent of the computed required reaction below the base of the cut.

The total vertical load supported by the soldier beams at design grade ranged from about 860 to 1040 lb/beam. For comparison, the vertical component of anchor force at the end of construction was 651 lb/beam. During excavation below the upper and lower ground anchors, the ground moved downward relative to the wall. The observed increase in axial load above that introduced by anchor prestressing is consistent with relative downward movement of the ground with respect to the wall. Between 750 and 800 lb/beam of vertical load was supported by a combination of end bearing and skin friction below the level of the excavation.

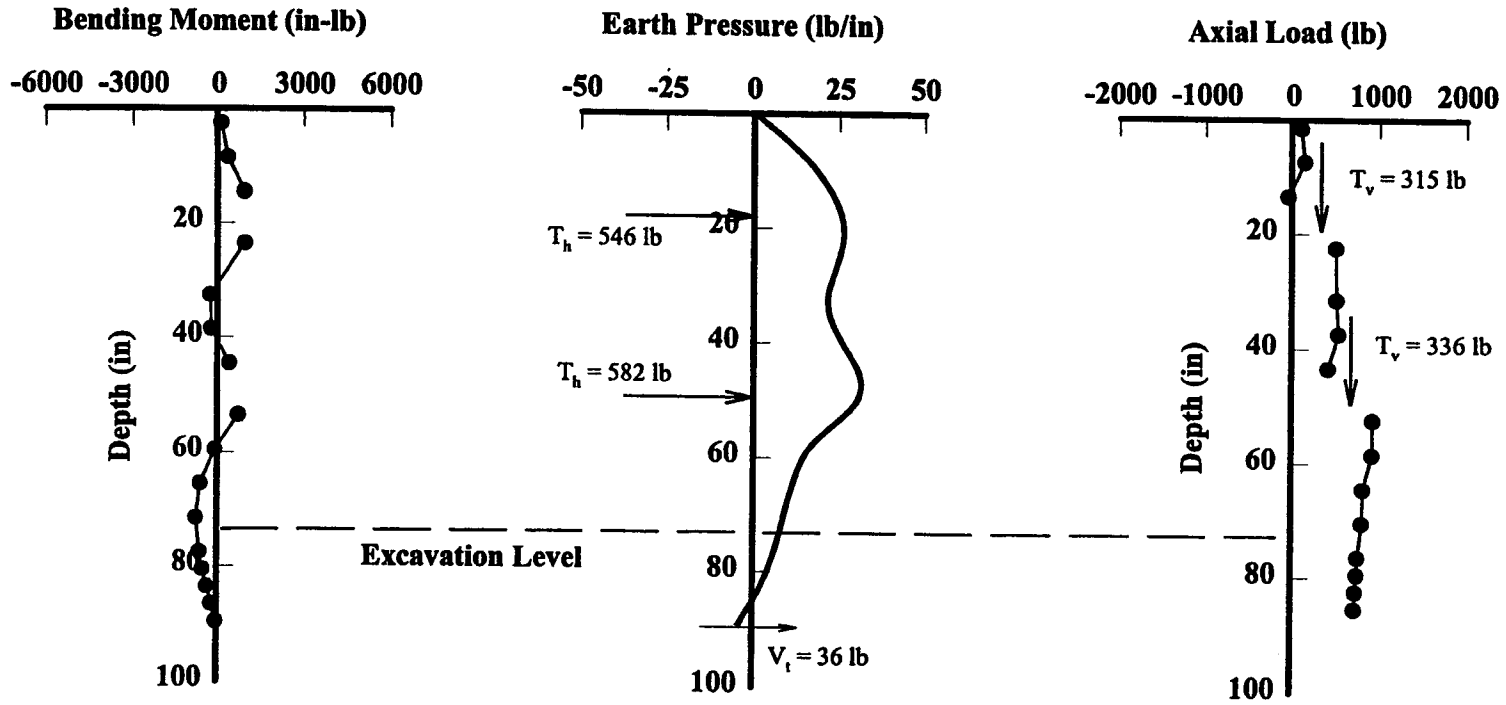

FIGURE 40
Bending Moments, Earth Pressures, and Axial Loads with Excavation at Design Grade — Model Test 3, SP4

2.3.4.2 Failure Modes

Unloading the lower level of ground anchors resulted in significant increases in bulging deformations below the upper anchor (Figure 41). At design grade, the maximum bulging deformation of the wall was about 0.013 in. Unloading the lower level of ground anchors effectively increased the unsupported span of the wall by a factor of two, which resulted in an order of magnitude increase (from 0.013 to 0.1 in) in bulging deformations. Maximum negative bending moments in the span increased from about 800 to 1800 in-lb (Figure 42). Thus, unloading the lower level of ground anchors showed the importance of wall span in controlling bending stresses and bulging deformations.

Unloading the lower level of ground anchors resulted in a redistribution of pressure to the upper ground anchors and toe of the wall. A total horizontal component of force of about 580 lb/beam was removed from the lower ground anchors. As shown in Figure 43, loads in the upper ground anchors increased from about 550 to 690 lb/beam. In addition, the reaction provided by the toe (mobilized lateral toe resistance and beam tip shear) increased from about 60 lb to 85 lb/beam. Although significant lateral toe resistance was mobilized during anchor unloading, a reversal in beam curvature occurred just below grade, resulting in beam tip shear that acted in an opposite direction to the mobilized lateral toe resistance.

Reloading the lower level of ground anchors resulted in only small changes in wall and ground movements (Figure 44). Reloading the lower anchors re-established the pressure concentration that had been observed during excavation to design grade in the vicinity of the lower anchors. The total mobilized lateral resistance along the toe (lateral toe resistance and beam tip shear) was unchanged.

Extending the excavation to a depth of 88.5 in resulted in significant increases in wall and ground movements (Figure 45). The lateral movement scale in Figure 45 is different from the scale in the earlier figures. Wall displacements developed as a rotational component of movement about the beam toe associated with increased beam settlements (~ 0.3 in). Displacements at the top of the wall increased from about 0.04 to 0.25 in. Maximum ground surface settlements increased from about 0.17 to 1.5 in. Changes in the distribution of lateral earth pressure and mobilized toe reaction were small (Figure 46). Large beam settlements facilitated a small reduction in the total vertical load supported by the wall, from about 1080 lb/beam after reloading the lower level of ground anchors, to 1000 lb/beam during excavation to 88.5 in. Furthermore, there was a decrease in skin friction and end bearing resistance in the toe (~ 200 lb), and an increase in mobilized skin friction (~ 100 lb) above the excavation level.

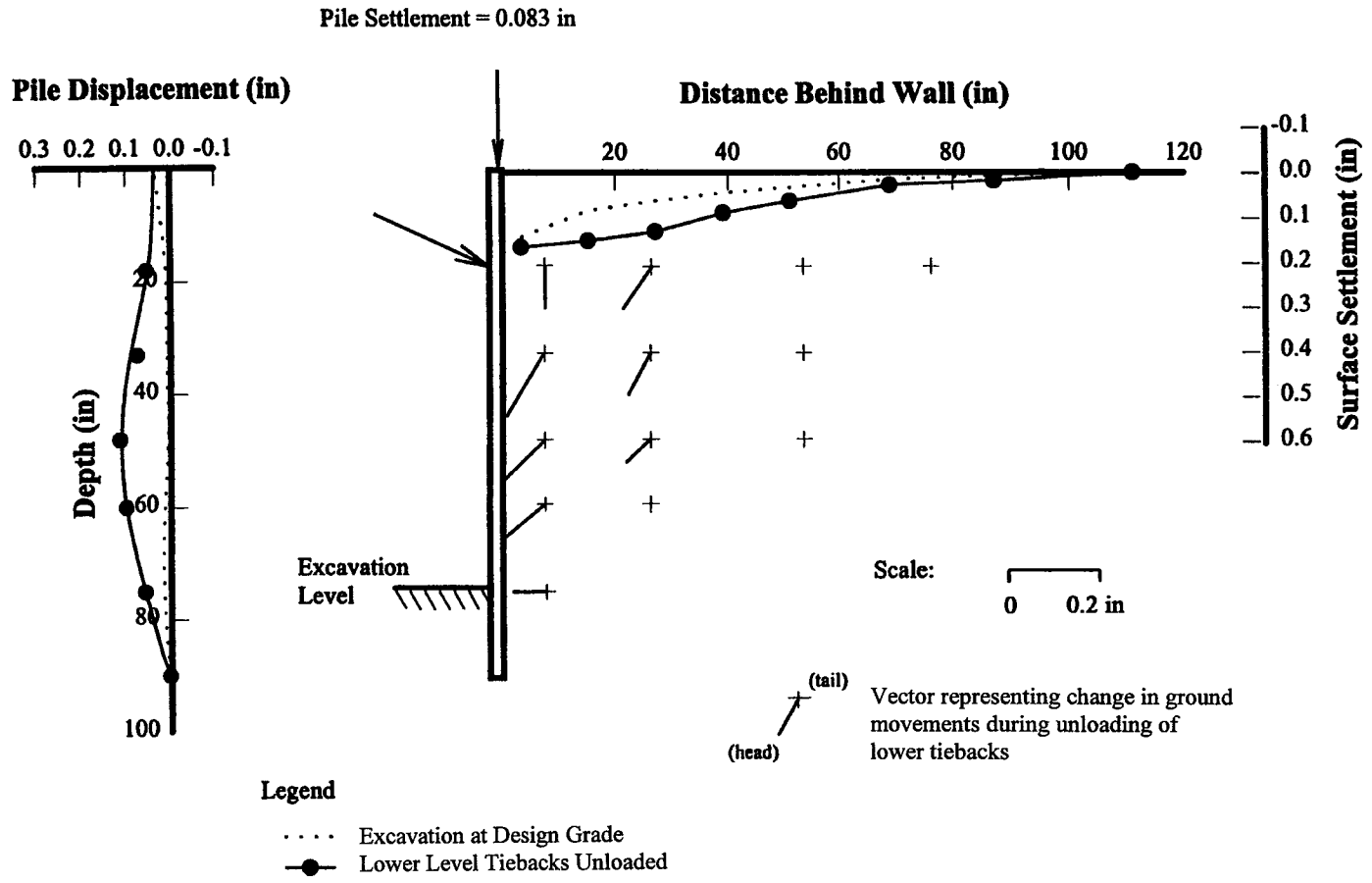

FIGURE 41
Wall and Ground Movements with Lower Level Anchors Unloaded — Model Test 3, SP4

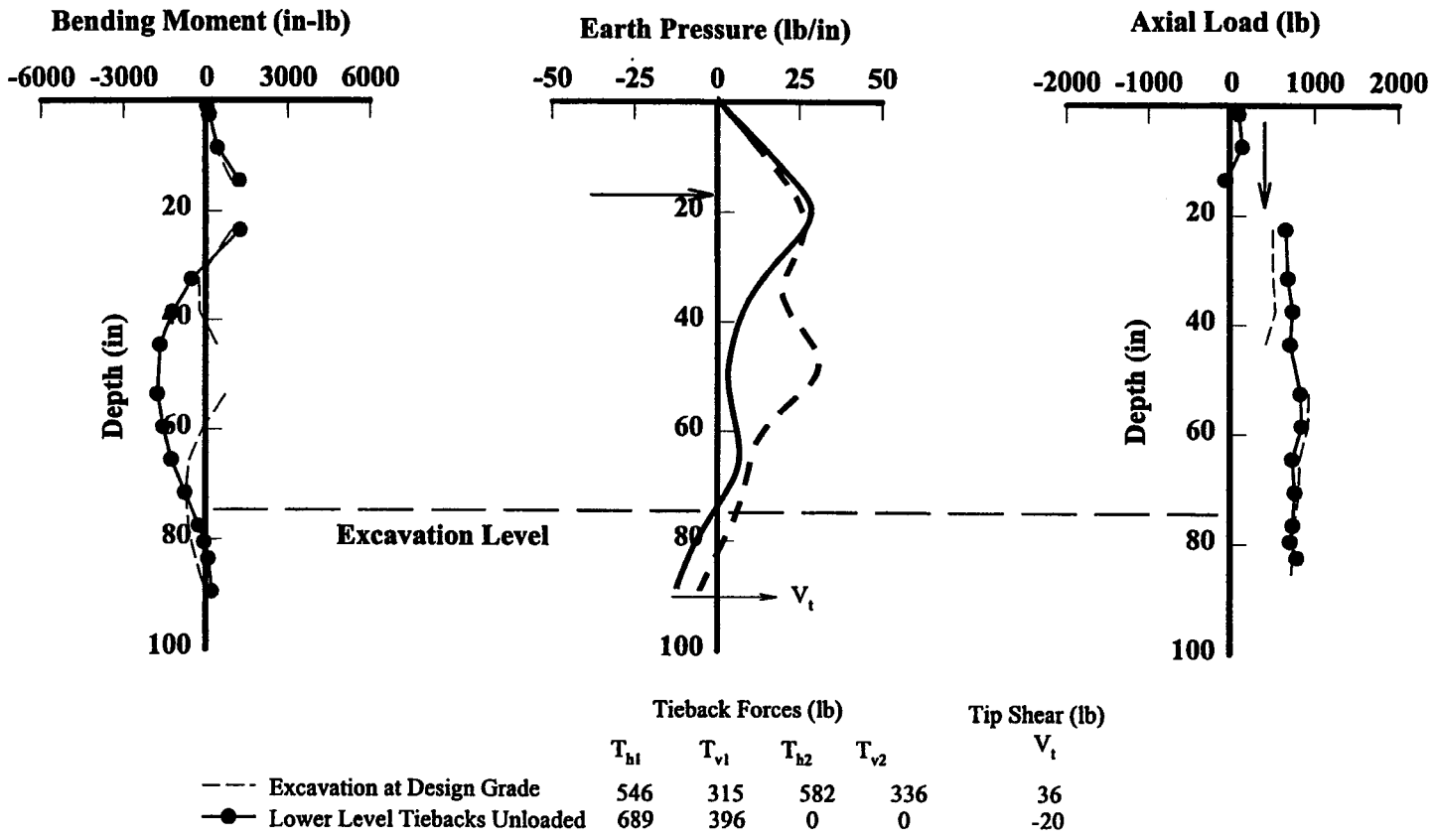

FIGURE 42
Bending Moments, Earth Pressures, and Axial Loads After Unloading Lower Anchors — Model Test 3, SP4

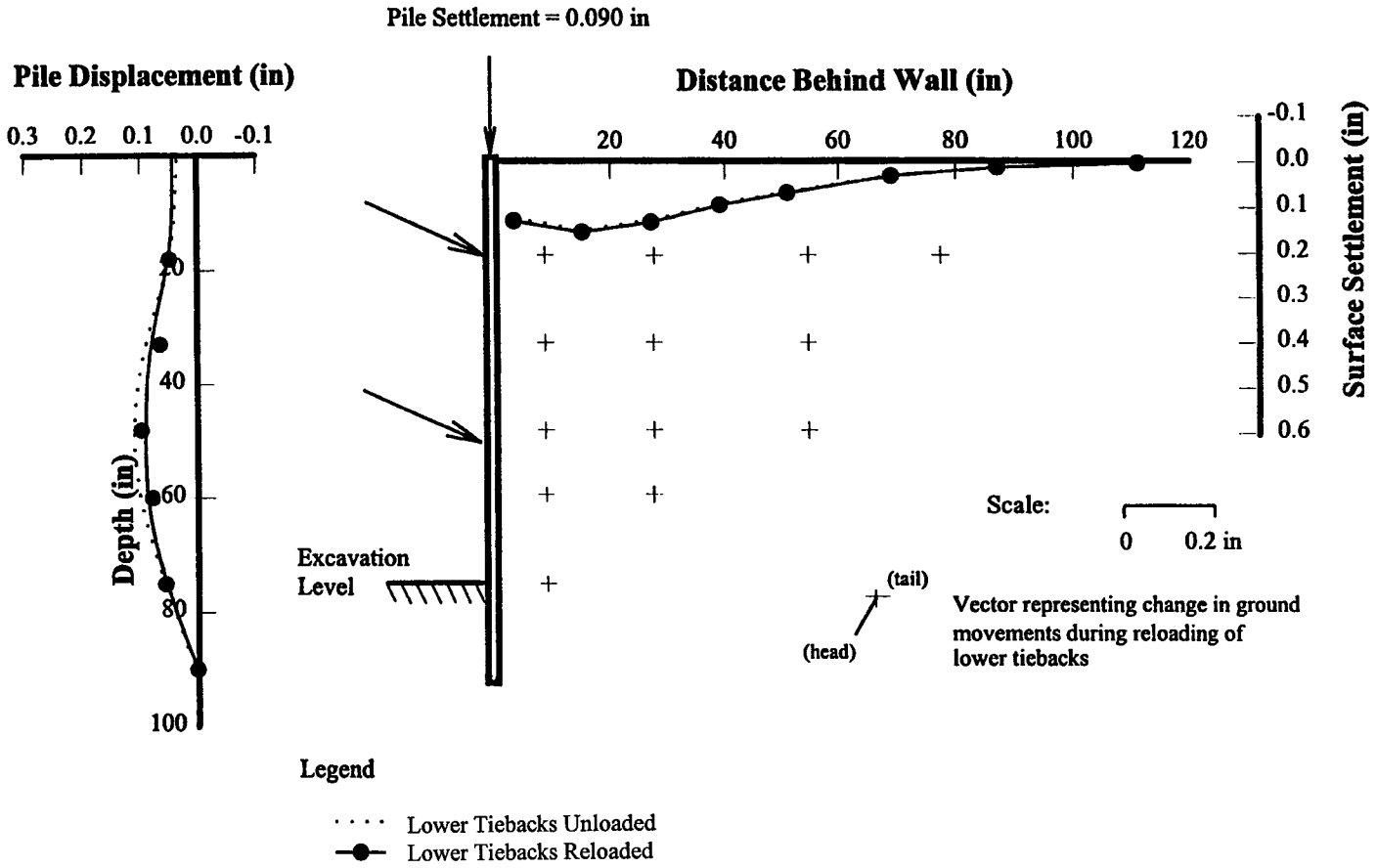

FIGURE 43
Wall and Ground Movements After Reloading Second Level of Anchors — Model Test 3, SP4

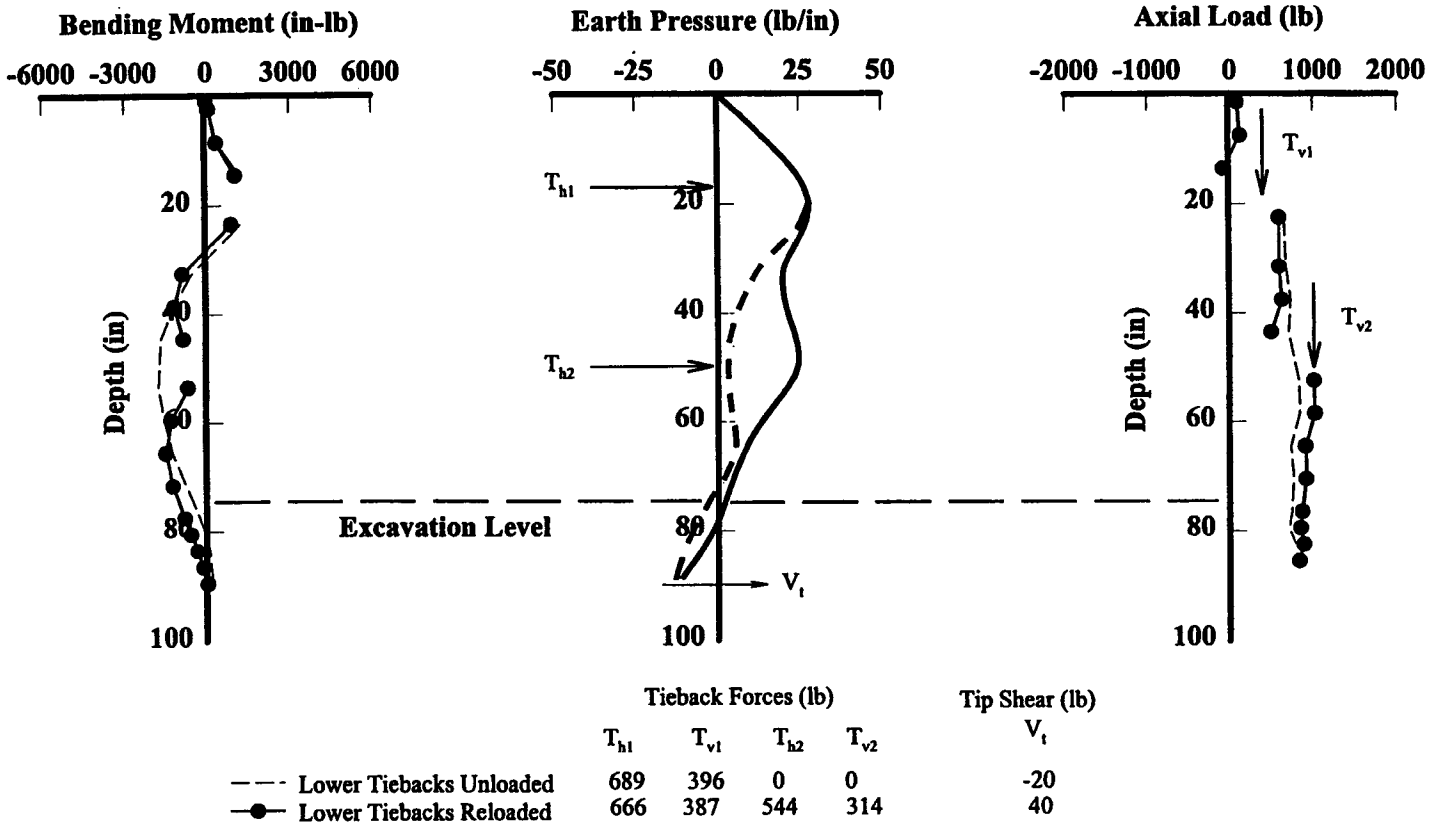

FIGURE 44
Bending Moments, Earth Pressures, and Axial Loads After Reloading Second Level of Anchors — Model Test 3, SP4

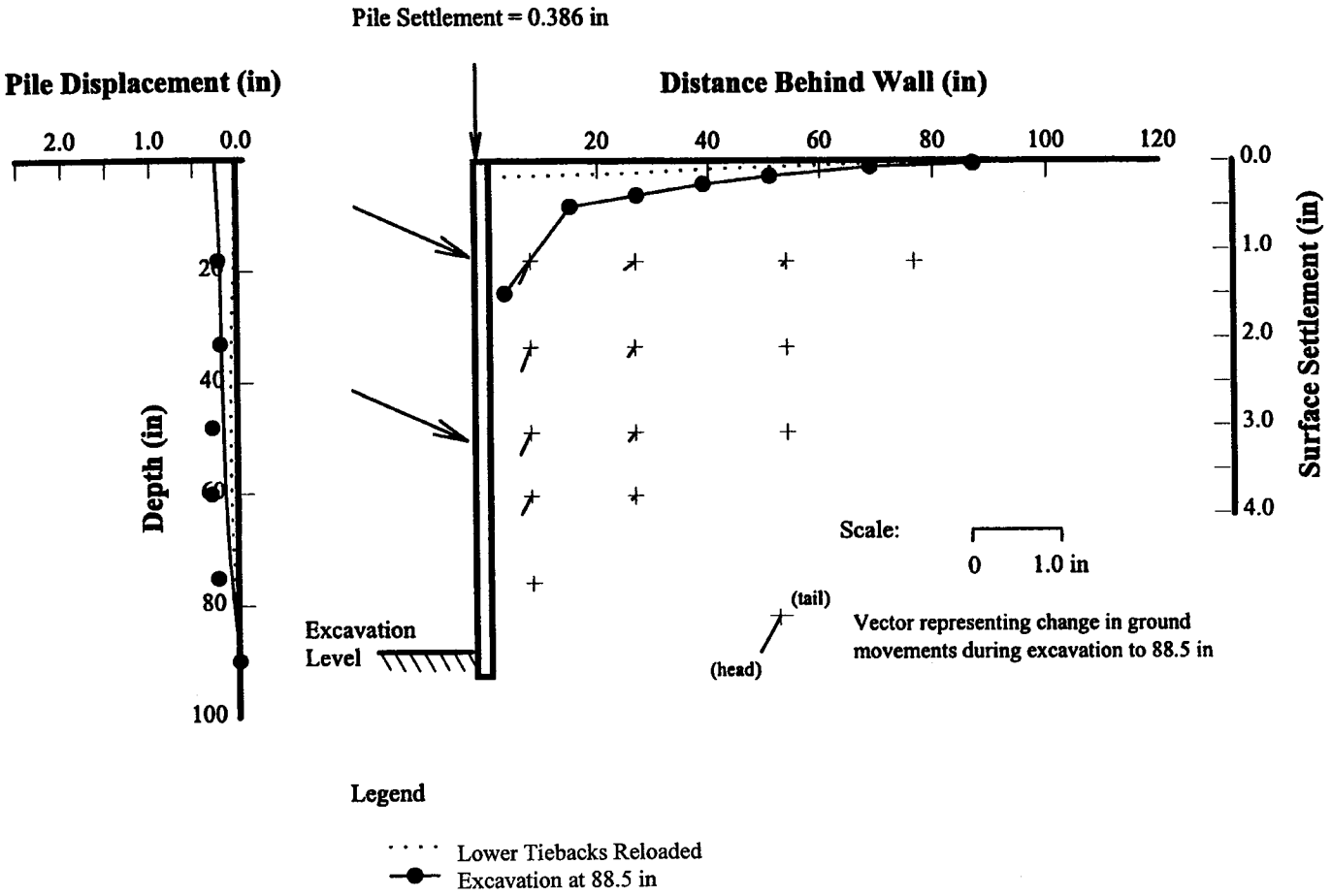

FIGURE 45
Wall and Ground Movements with Excavation at 88.5 In — Model Test 3, SP4

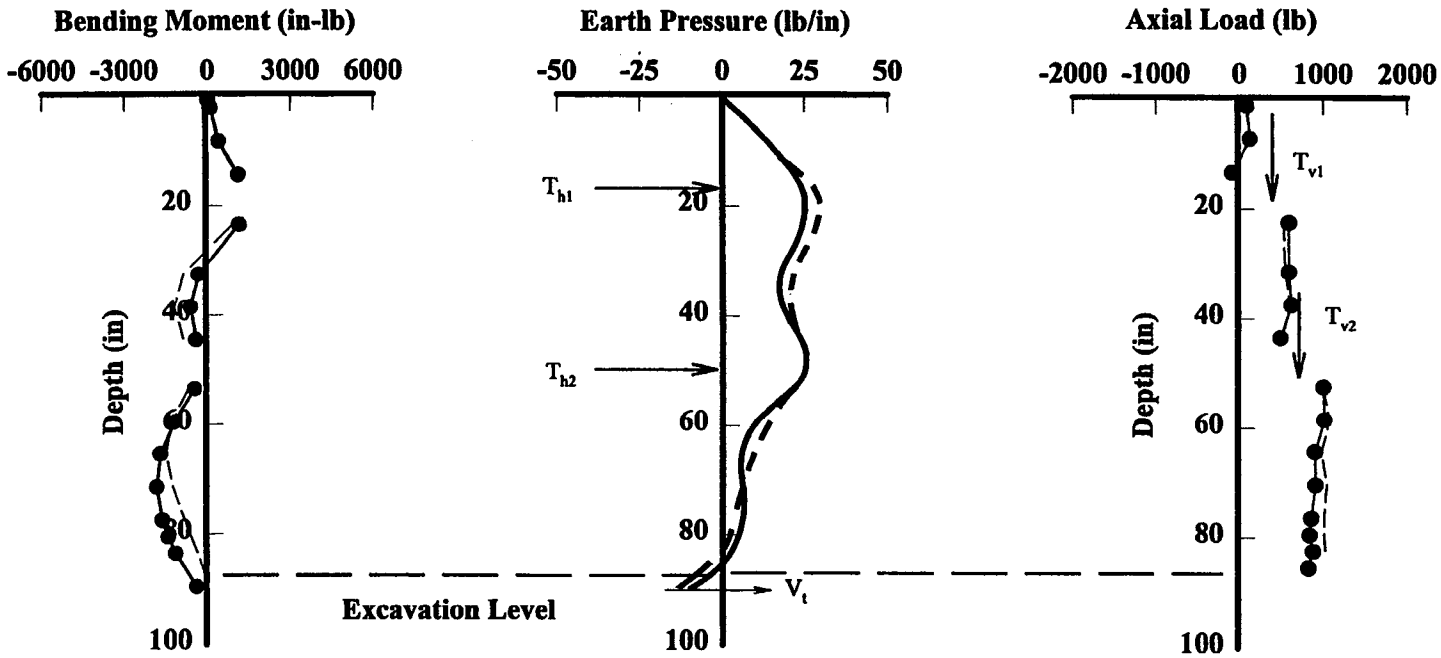

FIGURE 46
Bending Movements, Earth Pressures, and Axial Loads with Excavation at 88.5 In — Model Test 3, SP4

2.3.5 Summary

Four large-scale model anchor walls were constructed to examine their behavior. Measurements included wall and ground movements and bending and axial soldier beam strains. Measured bending strains and ground anchor loads were used to develop interpretations of lateral earth pressures. The walls were constructed using scaled structural components intended to provide a load and deformation response consistent with field experience. Realistic construction procedures were used. Thus, trends observed from the model testing program can be extended to practice and utilized in design.

Maximum lateral wall movements in the model tests ranged from about 0.05 in to 0.2 in with the excavation at design grade (Table 1), which corresponds to between 0.07 and 0.27 percent of the wall height. Two sources of wall movement were identified in the model tests: (1) bending of the wall during excavation to the first ground anchor level (cantilever-type movements) or excavation below an anchor (lateral bulging), and (2) outward translation or rotation of the wall about the toe associated with soldier beam settlements. The significance of cantilever-type movements and lateral bulging depended upon beam stiffness and the distance between anchor levels. In general, bulging deformations that developed during excavation below an anchor were small (Table 2). Both cantilever-type movements and wall rotations due to soldier beam settlement were significant in the model tests (Table 2) and ranged from about 30 to 100 percent of the maximum lateral movement of the model walls.

Maximum ground surface settlements in the model tests ranged from about 0.1 to 0.5 in, corresponding to between 0.13 and 0.67 percent of the wall height at the end of construction. Maximum ground surface settlements were observed at the walls and decreased to small, but measurable values, at a distance behind the wall of about 1.5 times the depth of the cut. In general, the volume of ground surface settlement was about equal to the volume of lateral movement at the wall. Ground surface settlements in Test 1 were influenced significantly by void closure between the model lagging and geotextile fabric.

Maximum bending stresses observed in the soldier beams occurred at the anchor levels during prestressing and ranged from about 4400 to 5500 in-lb with the excavation at design grade for walls supported by a single level of anchors, and from 1440 to 1610 in-lb with the excavation at design grade for walls supported by two levels of ground anchors (Table 3). For comparison, maximum bending moments estimated using the design pressure diagram were 5200 and 2200 in-lb for walls supported by one and two levels of anchors, respectively. Lateral earth pressures were conditioned principally by anchor prestressing, with only small changes in pressures during excavation below a support. Lateral support (beam tip shear and lateral toe resistance) provided by the soldier beam toes was small (Table 4) and ranged from about 20 to 40 percent of the calculated resistance.

Axial loads in the soldier beams developed from anchor prestressing and relative downward movement of the ground with respect to the walls during excavation below an anchor. The contribution to axial loads from downdrag ranged from about 170 to 430 lb/beam. In general,

vertical loads were carried by a combination of end bearing and skin friction below the excavation level, with only a small contribution from mobilized skin friction above the excavation level (Table 5).

TABLE 1
Summary of Maximum Wall and Ground Movements During Excavation to Design Grade

Test	Construction State	Maximum Lateral Movement (y_L) (in)		Maximum Ground Surface Settlement (y_V) (in)		Volume of Lateral Wall Movement (V_L) (in³/in)		Volume of Ground Surface Settlement (V_V) (in³/in)	
		Beam 4	Beam 5	Beam 4	Beam 5	Beam 4	Beam 5	Beam 4	Beam 5
1	Excavation to 27 in	0.16	0.19	0.21	0.22	3.70	4.95	3.35	3.68
	Anchors at 0.75 DL	0.08	0.09	0.20	0.23	0.82	1.45	3.10	3.82
	Excavation to 48 in	0.06	0.06	0.23	0.26	0.62	0.65	3.66	4.78
	Excavation at Design Grade	0.10	0.12	0.46	0.48	4.07	4.89	11.08	12.03
2	Excavation to 27 in	0.23	0.26	0.21	0.22	6.36	7.01	3.04	3.62
	Anchors at 0.75 DL	0.19	0.17	0.22	0.24	2.40	2.20	2.91	3.96
	Excavation to 48 in	0.18	0.16	0.23	0.24	2.24	1.80	4.36	4.58
	Excavation at Design Grade	0.20	0.18	0.31	0.31	3.92	3.54	6.52	8.06
3	Excavation to 18 in	0.05	0.05	0.03	0.04	1.23	1.28	0.32	0.44
	Upper Anchors at 0.75 DL	0.00	0.00	0.02	0.01	-0.70	-0.26	0.18	0.10
	Excavation to 48 in	0.01	0.01	0.05	0.02	-0.34	-0.34	0.78	0.56
	Lower Anchors at 0.75 DL	0.01	0.00	0.07	0.04	-0.66	-1.05	1.21	1.02
	Excavation at Design Grade	0.04	0.04	0.14	0.11	1.14	1.23	4.30	3.95
4	Excavation to 18 in	0.14	0.14	0.07	0.12	2.50	2.36	0.78	1.40
	Upper Anchors at 0.75 DL	0.09	0.07	0.04	0.07	0.82	0.48	0.47	0.92
	Excavation to 48 in	0.07	0.06	0.09	0.11	1.88	1.32	1.49	2.20
	Lower Anchors at 0.75 DL	0.06	0.06	0.11	0.13	0.33	0.86	1.69	2.49
	Excavation at Design Grade	0.14	0.14	0.22	0.22	5.68	5.90	7.92	6.79

TABLE 2
Contribution of Bending, Rotation, and Translation to Maximum Wall Movements with Excavation at Design Grade

Wall	Beam	Maximum Horizontal Displacement Y_{max} (in)	Cantilever Bending Displacement (% Y_{max})	Bulging Displacement (% Y_{max})	Rotational Displacement (% Y_{max})	Transitional Displacement (% Y_{max})
Model Test 1	4	0.10	36	18	64	0
	5	0.12	33	18	67	0
Model Test 2	4	0.20	95	15	1	4
	5	0.18	97	20	0	3
Model Test 3	4	0.04	61	35	39	0
	5	0.04	75	33	25	0
Model Test 4	4	0.14	52	29	32	16
	5	0.14	50	32	28	22

Notes: 1. Components of wall displacement expressed as a percentage of the maximum displacement observed at the end of construction.

2. Actual wall rotations due to beam settlement were greater than summarized in this table, since soldier beams were pulled back beyond the initial zero measurements during anchor prestressing.

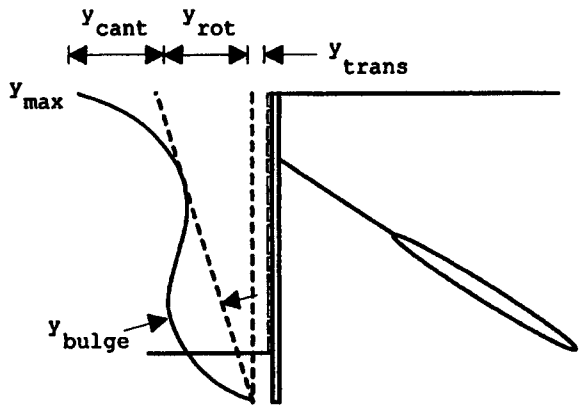

TABLE 3
Maximum Bending Moments Observed in Soldier Beams

Test	Construction State	Maximum Positive Moment, $M_{max}^{(+)}$ (in-lb)		Depth (in)		Maximum Negative Moment $M_{max}^{(-)}$ (in-lb)		Depth (in)	
		Beam 4	Beam 5	Beam 4	Beam 5	Beam 4	Beam 5	Beam 4	Beam 5
1	Excavation at 27 in	2390	2730	45	45	---	---	---	---
	Anchors at 0.75 DL	6040	6260	27	27	790	950	59	60
	Excavation at Design Grade	4420	4550	27	27	1920	2020	63	64
2	Excavation at 27 in	1320	1350	45	45	---	---	---	---
	Anchors at 1.2 DL	7140	7020	27	27	1200	1260	56	55
	Anchors at 0.75 DL	5890	5740	27	27	1160	1180	56	57
	Excavation at Design Grade	5420	5500	27	27	1420	1590	64	63
3	Excavation at 18 in	570	560	33	33	---	---	---	---
	Upper Anchors at 1.2 DL	2670	2390	18	18	680	590	41	40
	Upper Anchors at 0.75 DL	2060	1800	18	18	580	510	43	43
	Excavation at 48 in	1930	1780	18	18	830	760	46	48
	Lower Anchors at 1.2 DL	1940	2070	48	48	780	710	37	71
	Lower Anchors at 0.75 DL	1530	1400	18	48	640	590	36	72
	Excavation at Design Grade	1610	1470	18	18	800	810	74	72
4	Excavation at 18 in	530	530	29	29	---	---	---	---
	Upper Anchors at 1.2 DL	2200	2350	18	18	320	400	41	35
	Upper Anchors at 0.75 DL	1680	1790	18	18	310	380	41	41
	Excavation at 48 in	1660	1770	18	18	490	550	41	41
	Lower Anchors at 1.2 DL	1560	1610	48	48	730	680	35	35
	Lower Anchors at 0.75 DL	1505	1600	18	18	661	610	35	35
	Excavation at Design Grade	1440	1530	18	18	780	780	71	71

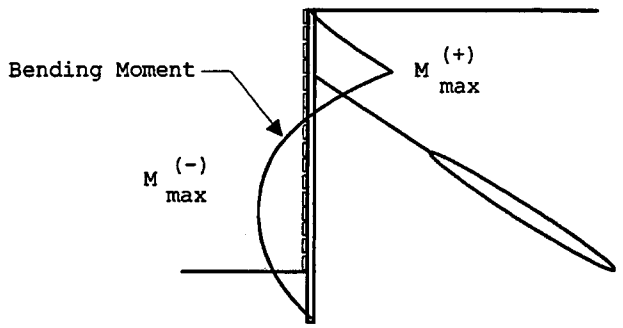

TABLE 4
Observed Lateral Resistance Below the Bottom of the Excavation at Design Grade

Model Test	Soldier Beam No.	Lateral Toe Resistance (lb)	Beam Tip Shear (lb)	Sum (lb)	Percent of Computed Total Lateral Resistance (%)
1	4	101	5	106	29
	5	120	0	120	33
2	4	24	40	64	18
	5	32	38	70	19
3	4	17	36	53	28
	5	35	30	65	34
4	4	22	52	74	39
	5	68	12	80	42

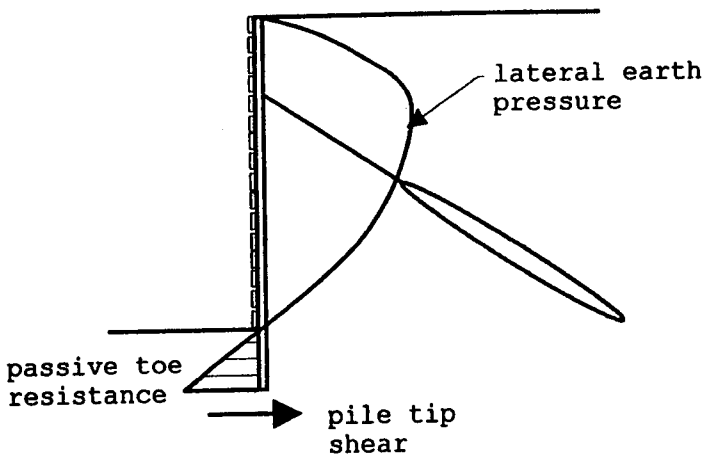

TABLE 5
Distribution of Axial Load in Soldier Beams with Excavation at Design Grade

Test	T_v (lb)	Q_{total} (lb)		Q_{end} (lb)		Q_{skin} (lb)		Q_{down} (lb)	
		Beam 4	Beam 5	Beam 4	Beam 5	Beam 4	Beam 5	Beam 4	Beam 5
1	452	714	789	121	201	593	588	262	337
2	629	899	1060	602	786	297	274	270	431
3	651	1040	858	717	698	323	141	389	207
4	657	934	829	641	687	293	142	277	172

T_v = Vertical component of anchor force

Q_{total} = Maximum axial load

Q_{end} = Mobilized end bearing

Q_{skin} = Mobilized skin friction

Q_{down} = Downdrag load

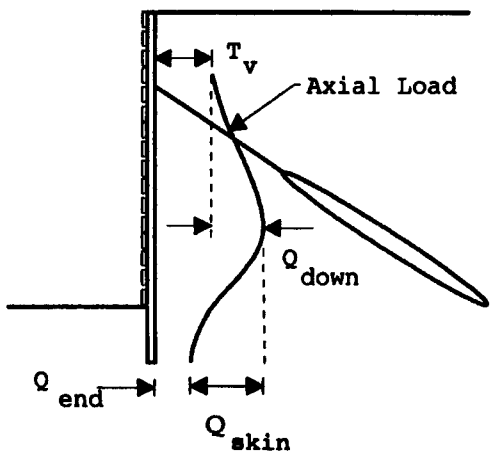

CHAPTER 3
WALL AND GROUND MOVEMENTS

3.1 INTRODUCTION

Anchored walls are frequently used in dense urban areas where control of ground movements is important to minimize damage to adjacent structures or utilities. Thus, prediction of ground movements before construction can be an important part of wall design. Where ground movement control is critical, wall stiffness, anchor preload, and anchor lengths may be controlled by deformation considerations versus limiting stress or capacity requirements.

Prediction of ground movements generated by construction is usually based on experience. Often predictions of anchored wall response are unsatisfactory due to difficulties in extrapolating experience to different sites, a general lack of understanding concerning sources of movements, and an inability to quantify construction effects on ground deformations.

In this chapter, sources of movements that develop during anchored wall construction are evaluated. Model test observations are used to define the basic mechanics of anchored wall response. Field case histories are used to supplement the model test observations and to provide a practical perspective for the significance of various components of wall deformations. The relationship between movements of the wall and the distribution of ground movements behind the wall is discussed for a range of ground conditions. The end product of this chapter is an improved ability to predict and control the deformation response of anchored walls.

3.2 PATTERNS OF MOVEMENT

Anchored walls are constructed in stages (Figure 47), each of which contributes to observed patterns of wall movement in a characteristic manner. Figures 48 through 54 summarize typical patterns of wall movement observed during construction of the model tests. Wall displacements were determined from integration of soldier beam bending strains, using measured beam rotation and translation to evaluate constants of integration. Lateral ground movements measured between soldier beams are shown, where required to clarify the deformation response of the walls. Lateral and vertical ground movements in mass were measured using a combination of dial gauges and DC-DC LVDT's connected in series to form multiple position extensometers. Wall and ground displacements have been normalized with respect to the maximum depth of excavation, H.

Model soldier beams and ground anchors were installed inside the test chamber during deposition of the sand. Thus, components of ground movement associated with these construction activities were not modeled. Model lagging was installed during excavation, however, and ground movements resulting from closure of voids between the back of the excavation and model lagging probably did develop. The significance of void closure on measured ground

movements was believed to be small based on volume comparisons of lateral wall movements and ground surface settlements. The significance of construction procedures on wall and ground response has been evaluated by O'Rourke (1981), Wong and Broms (1989), and Clough and O'Rourke (1990).

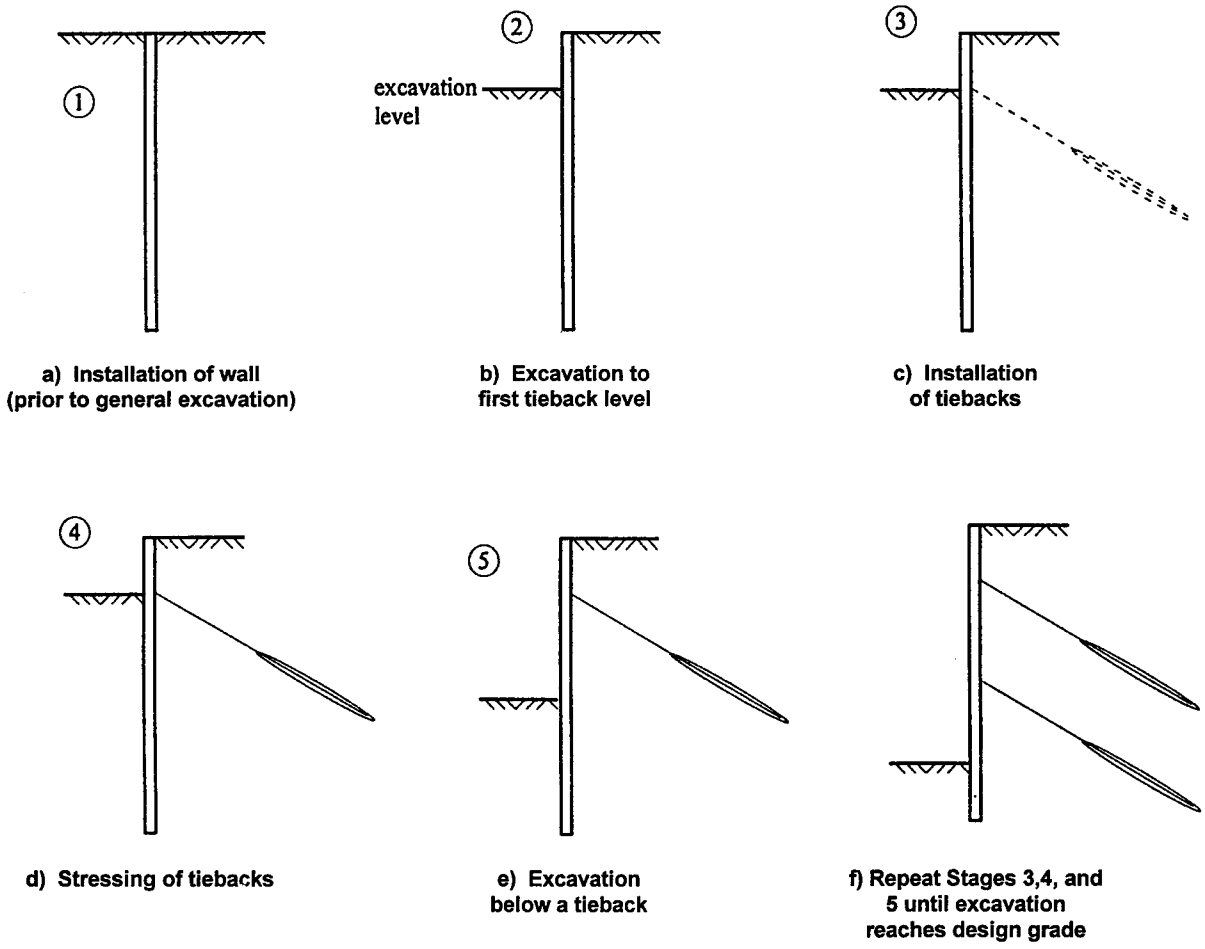

FIGURE 47
Stages of Anchored Wall Construction

3.2.1 Excavation to the First Ground Anchor Level (Cantilever Stage)

The model walls were unsupported above subgrade during excavation to the first ground anchor level and required development of passive resistance along the embedded length of the beams to balance active thrust on the upper part of the walls. Wall displacement patterns were consistent with a flexible cantilever (Figure 48) and could be described principally by bending of the beams below the excavation level. Maximum lateral displacements were observed at the top of the walls and ranged from about 0.07 to 0.34 percent of H. The significance of canti-

lever movements in the model tests was a function of wall stiffness and the depth of excavation. As shown in Figure 48, excavation from a depth of 0.24 to 0.36H resulted in an increase in maximum lateral wall movements by a factor of about four. Cantilever movements can represent a significant component of the maximum lateral wall movement observed at the end of construction (Table 6). The model tests illustrate the importance of minimizing the depth of excavation to the first ground anchor level where ground movements must be minimized.

Maximum ground surface settlements were observed at the wall and decreased to zero at a distance behind the wall of between 0.5 and 0.6H. The shape of the settlement trough in the model tests could be described by a Gaussian distribution given by

$$y = y_{max}\, e^{-\frac{nx}{h}} \qquad \ldots [3.1]$$

where y_{max} is the maximum ground surface settlement, x is the distance behind the wall, h represents the depth of the excavation, and n is an empirical coefficient that ranged between 2 and 2.5 for the cantilever excavation in the model tests. The patterns of observed ground movement are consistent with previous field (O'Rourke, 1974) and model-scale (Milligan, 1974) experience for cantilever-type wall movements.

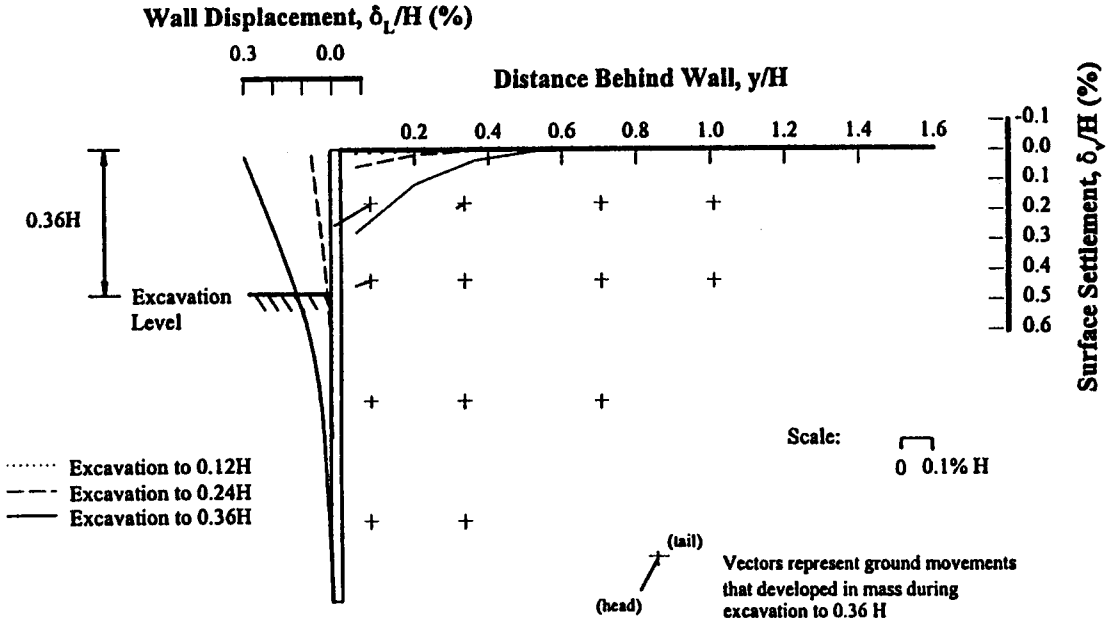

FIGURE 48
Patterns of Wall and Ground Movement During Excavation to the First Anchor Level

3.2.2 Stressing the Upper Ground Anchors

Anchors in the model studies were loaded similar to proof tests used in the field. Model ground anchors were initially loaded to about 120 percent of design and the loads subsequently decreased and locked-off at 75 percent of design. Anchor loads were computed on the basis of a trapezium of earth pressure with an intensity of $25H$. At lock-off loads, the ground anchors provided a total thrust on the wall that was about 1.6 times the Rankine active pressure for an assumed friction angle of 44°.

Stressing of the upper level of anchors had the effect of pulling the soldier beams back into the retained soil (Figure 49). The crosshatched area in Figure 49 represents the change in soldier beam deformations and ground surface movements in response to stressing the anchor. Cantilever-type movements decreased significantly as the result of anchor prestressing, and in the case of Model Test 3, soldier beams were pulled back beyond the initial zero measurement taken prior to excavation. In the model tests, the response of the soldier beams to anchor prestressing was influenced by void closure between the lagging and geotextile fabric. Despite the large soldier beam displacements, ground movements between soldier beams were essentially unchanged by anchor prestressing. Figure 50 shows that the lagging that remained did not move in response to the stressing of the anchors. These measurements are consistent with observed distortions of chalk lines established on the surface of the sand, which showed significant relative displacement of the soldier beams with respect to the lagging and ground.

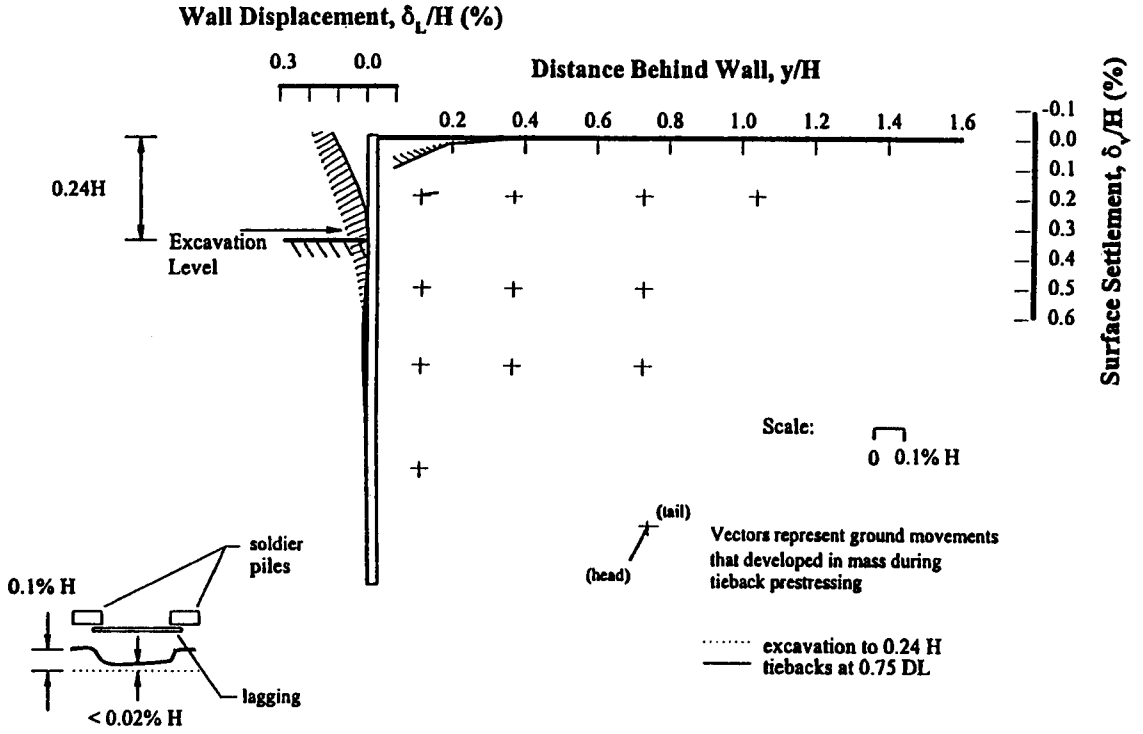

FIGURE 49
Effect of Anchor Stressing on Wall and Ground Movements Behind Soldier Beams

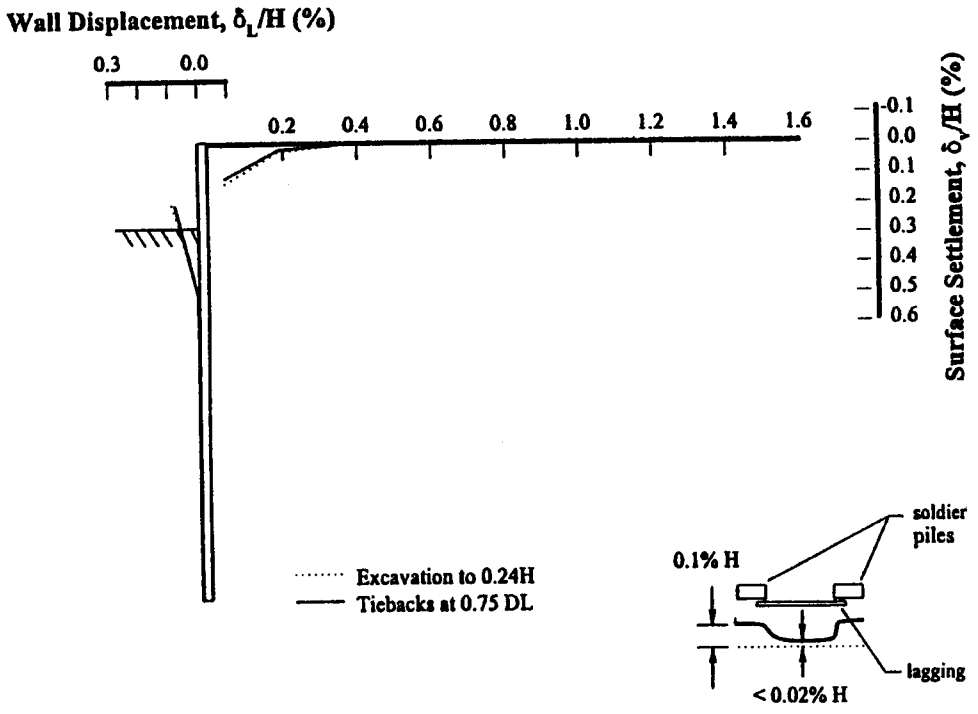

FIGURE 50
Effect of Anchor Stressing on Wall and Ground Movements Between Soldier Beams

3.2.3 Excavation Below the Upper Anchors

Excavation below the upper ground anchors resulted in lateral bulging of the walls, with maximum displacements near the excavation level (Figure 51). Lateral bulging developed with the walls essentially fixed against displacement at the ground anchor level, and additional resistance to movement developed by mobilization of passive resistance along the embedded length of the beams. For intermediate stages of construction, soldier beam embedment was sufficient to develop a point of contraflexure at a depth of about $0.2H$ below the excavation level.

The development of bulging deformations during excavation below a ground anchor is consistent with experience with internally supported walls (O'Rourke, 1974). Maximum bulging deformations in the model tests ranged from about 0.02 to 0.06 percent of H. The significance of bulging deformations in the model tests depended upon wall stiffness and the depth excavated below a support.

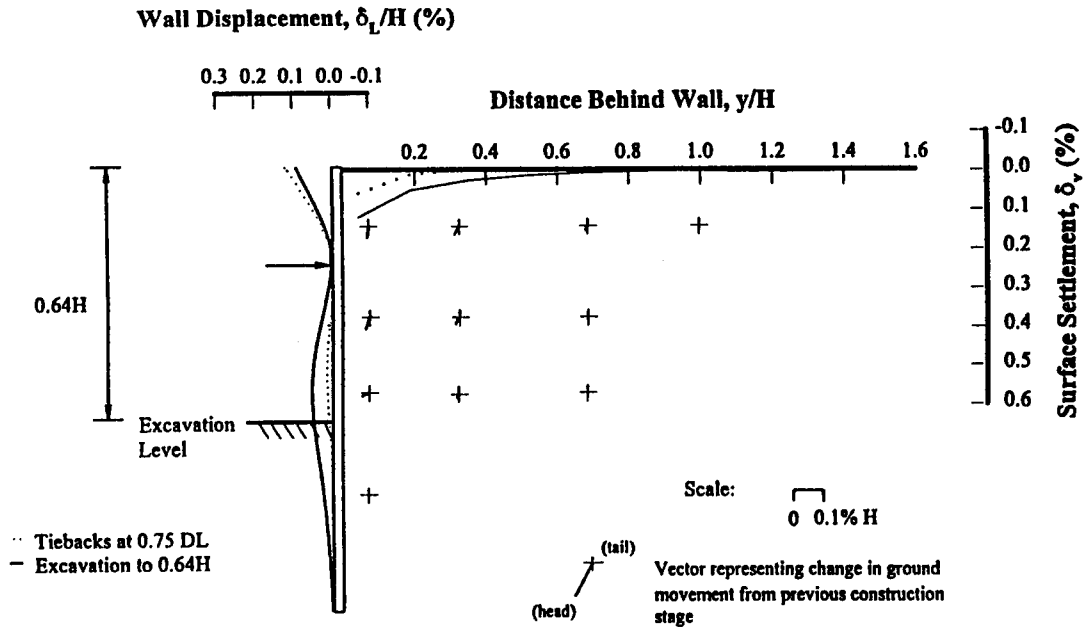

FIGURE 51
Development of Bulging Deformations During Excavation Below the Anchor

3.2.4 Stressing of Lower Ground Anchors

A single level of ground anchors supported Model Tests 1 and 2 at a depth of $0.36H$. Model Tests 3 and 4 were supported by two rows of anchors. Upper anchors were installed at a depth of $0.24H$ and the lower level of ground anchors was installed at a depth of $0.64H$. Stressing the lower anchors had a similar effect on soldier beam deformations as stressing of the upper level of ground anchors. The beams were pulled back into the retained soil, which significantly reduced lateral bulging below the upper ground anchors (Figure 52). Lateral and vertical ground movements between soldier beams were essentially unchanged by stressing of a lower level of ground anchors (Figure 53).

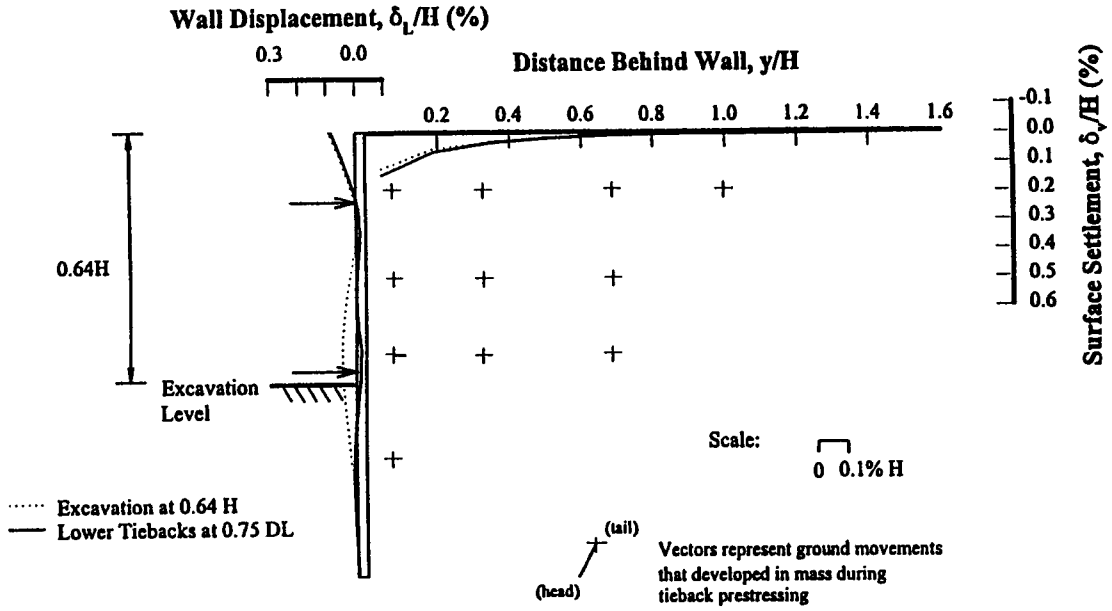

FIGURE 52
Effect of Lower Anchor Stressing on Wall and Ground Movements Behind Soldier Beams

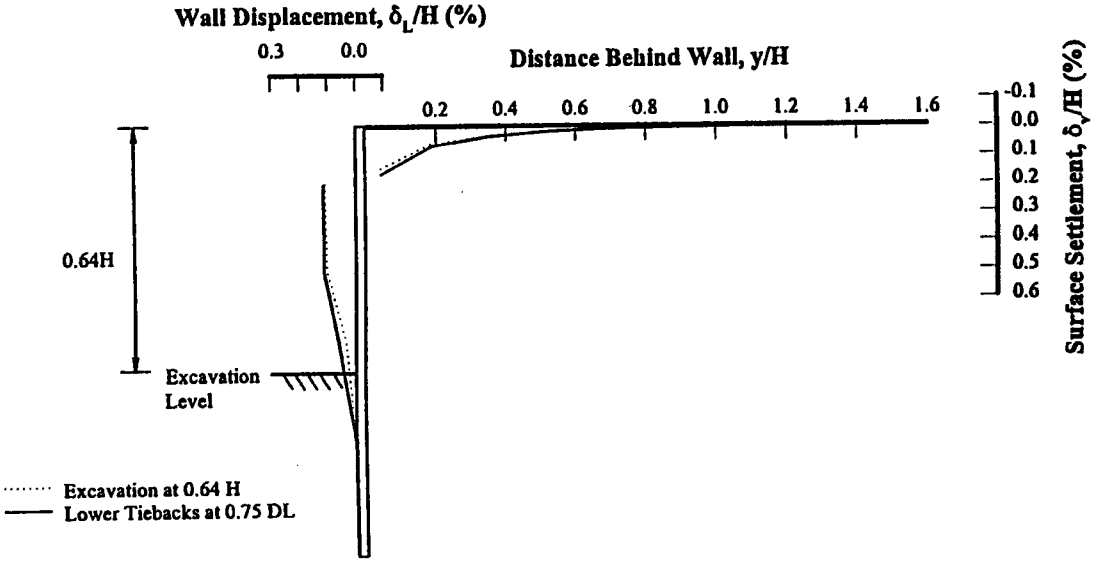

FIGURE 53
Effect of Lower Anchor Stressing on Wall and Ground Movements Between Soldier Beams

3.2.5 End of Construction Conditions

Excavation below the ground anchors resulted in the development of lateral bulging and rotation about the soldier beam toe. The wall in Model Test 4 also translated outward (Figure 54). Wall rotation and translation could be correlated with beam settlements associated with mobilization of end bearing resistance to support vertical loads.

Maximum lateral wall displacements at the end of construction ranged from about 0.05 to 0.26 percent of H, which is within the range of movements typically observed for anchored walls (Clough and O'Rourke, 1990). Maximum lateral movements were observed at the top of the walls, and could be defined by cantilever-type displacements above the upper ground anchor, and outward rotation and translation associated with beam settlements. Table 6 summarizes maximum lateral wall movements for the model tests and the contribution from bending (cantilever-type displacements and lateral bulging) and outward rotation and translation. Observations from the full-scale walls constructed at Texas A&M are shown for comparison. The model test results show that, in addition to bending components of wall deformation, anchored walls also can display a significant component of outward rotation associated with settlement. Lateral translation was observed in the full-scale walls and the two of the model walls. It was not possible to isolate the cause of the translational movements.

Ground surface settlements at the end of construction were maximum at the wall and decreased approximately linearly to a small value at a distance behind the wall of about $1.5H$. The shape of the surface settlement troughs at the end of construction can be represented by Equation 3.1, with coefficient, n, in the range of 2 to 3.5. Note that the shape of the surface settlement trough is consistent with that which developed during excavation to the first level of anchors, but the value of the coefficient, n, changed. Maximum ground surface settlements in the model tests ranged from about 0.18 to 0.61 percent of H. Ground movements in the retained soil can be bounded approximately by the envelope shown in Figure 54.

TABLE 6
Contribution of Bending and Soldier Beam Settlement to Wall Movements for the Model and Texas A&M Walls

WALL	BEAM	MAXIMUM HORIZONTAL DISPLACEMENT, y_{max} (% H)	CANTILEVER BENDING DISPLACEMENT, y_{cant} (% y_{max})	BULGING DISPLACEMENT, y_{bulge} (% y_{max})	ROTATIONAL DISPLACEMENT, y_{rot} (% y_{max})	TRANSLATIONAL DISPLACEMENT, y_{trans} (% y_{max})
TAMU one-tier	15	0.24	54	29	38	8
	16	0.24	50	25	38	12
Model 1 one-tier	4	0.13	36	18	64	0
	5	0.15	33	18	67	0
Model 2 one-tier	4	0.26	95	15	1	4
	5	0.24	98	20	0	3
TAMU two-tier	7	n/a	n/a	n/a	n/a	n/a
	8	0.45	36	11	53	11
Model 3 two-tier	4	0.05	61	35	39	0
	5	0.05	75	33	25	0
Model 4 two-tier	4	0.19	52	29	32	16
	5	0.18	50	32	28	22

Note: Displacements for the model and Texas A&M (TAMU) walls are expressed as a percentage of wall height with the excavation at design grade.

n/a = data not available

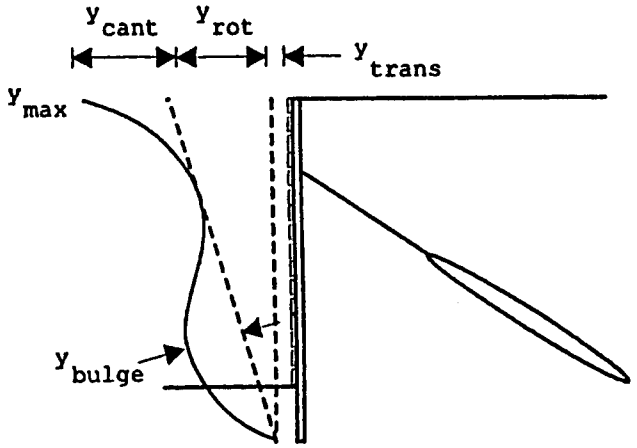

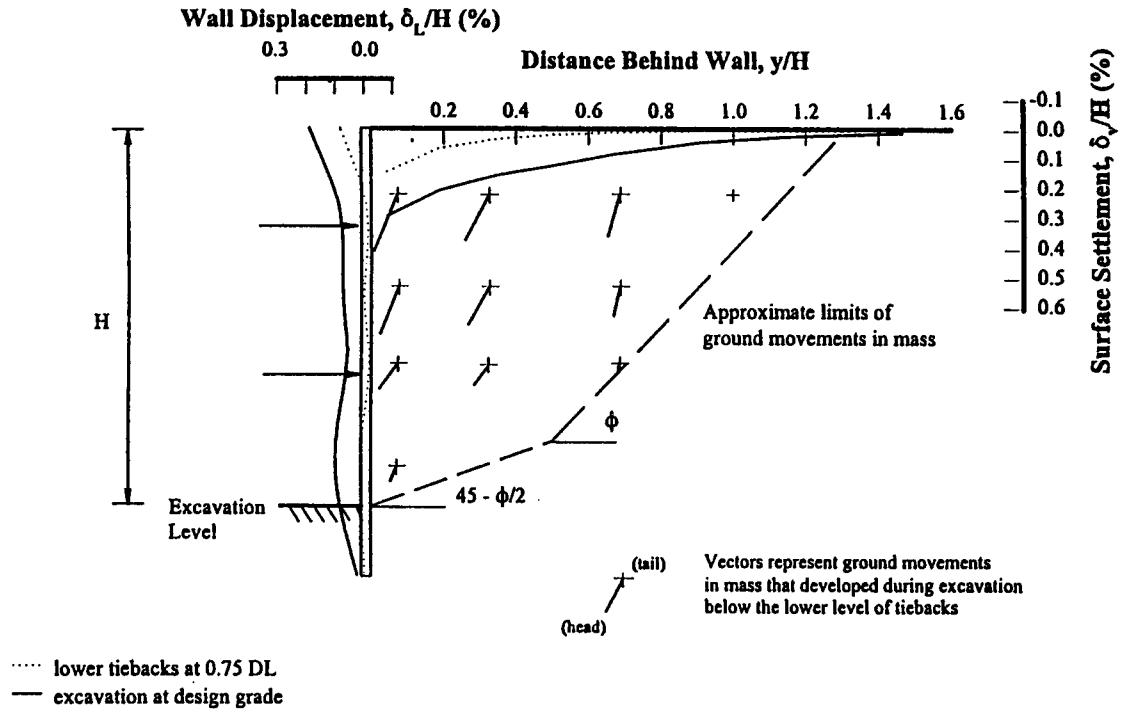

FIGURE 54
Patterns of Wall and Ground Movement with Excavation at Design Grade

3.3 SOURCES OF WALL MOVEMENT

Ground anchor walls develop bending components of deformation, i.e., cantilever-type movements and lateral bulging, similar to internally supported walls. They also may experience components of outward rotation and/or translation about the toe of the wall. Bending deformations for anchored walls normally are less than bending deformations for internally supported walls. Internally supported walls require over-excavation before installation of the support. Limited over-excavation is necessary for anchored walls. The source of outward rotation and translation in the model tests was soldier beam settlement associated with mobilization of end bearing resistance required to support the vertical component of ground anchor force and downdrag. Other possible sources of translation and rotation include: elongation of the ground anchor tendon in response to increased loads, anchor yield or load redistribution along the tendon bond length, and mass movements behind the ground anchors. The significance of various sources of wall movement is discussed in this section using model test observations and available field case studies. Emphasis is placed on the parameters controlling wall movements and their control in design.

3.3.1 Bending

Both cantilever deformations and lateral bulging below a ground anchor are resisted through an interaction of soil and structure defined by bending. The significance of cantilever and bulging deformations in the model tests depended principally on the depth of the cut, H, wall stiffness, EI, and the unsupported span, L. In general, bending deformations increased with increasing depth of cut, increasing length of unsupported span, and decreasing wall stiffness.

A beam-on-elastic foundation analysis was used to provide a framework for organizing the significant variables controlling the bending response of an anchored wall. The walls were represented by a strip of unit width defined by a bending stiffness, EI. The response of the soil was idealized by linear springs, represented by a spring constant, k. Nodal forces were applied to the strip over the length of the unsupported span to simulate the change of in-situ ground stress associated with excavation. It was assumed that the change in stress associated with excavation was proportional to the initial at-rest stress. Displacements at anchor levels were constrained, consistent with model- and full-scale observations.

Results of the beam-on-elastic foundation analysis show that cantilever and bulging deformations can be represented as a function of the relative stiffness of soil to structure (Figures 55 and 56). Cantilever and bulging deformations are normalized with respect to the elastic response of the continuum for the case of no wall and represented as a function of relative stiffness of the soil to structure, defined according to

$$F = \frac{E_s L^3}{EI} \qquad \ldots [3.2]$$

in which E_s represents a secant modulus on the soil's stress-strain curve, EI is the bending stiffness for a unit width of wall, and L is the unsupported span of the wall. (It was assumed that the spring constants used to represent the soil response in the analysis could be related to soil modulus by the width of the loaded area, i.e., $kL = E_s$.) The most significant feature of the theoretical trends is the shape of the curves, which consist of a steep initial segment, followed by a transition to a flat line portion at large values of relative stiffness. For small values of relative stiffness (≤ 1 for cantilever deformations; ≤ 10 for bulging deformations), cantilever and bulging displacements vary with the fourth power of wall span, in accordance with classical beam theory. The most effective way to control bending deformations for walls that are stiff with respect to the soil, therefore, is to reduce the depth of excavation to the first ground anchor level and the spacing between rows of anchors. At large values of relative stiffness (≥ 100 for cantilever deformations; ≥ 500 for bulging deformations), the theoretical solution corresponds to the elastic case for the condition of no wall, i.e., bending deformations depend on the elastic constant of the continuum and width of the loaded area.

Model test observations and field measurements are plotted in Figures 55 and 56 to provide a practical perspective for the theoretical results and to summarize available experience. The elastic constants used to represent the model test and full-scale wall observations were obtained

by back-computation from the deformation response of the walls during ground anchor unloading. Jaky's equation was used to represent the coefficient of at-rest earth pressure for the model sand. At-rest earth pressure coefficients for the full-scale walls were determined with consideration of stress history, in accordance with the observations summarized by Mesri and Hayat (1993). Tables 7 and 8 summarize the assumed elastic constants and earth pressure coefficients used to represent other field cases. In general, the elastic constants are in the range used to predict settlement of shallow foundations in the working stress range. Model test observations show good correlation with the theoretical trends.

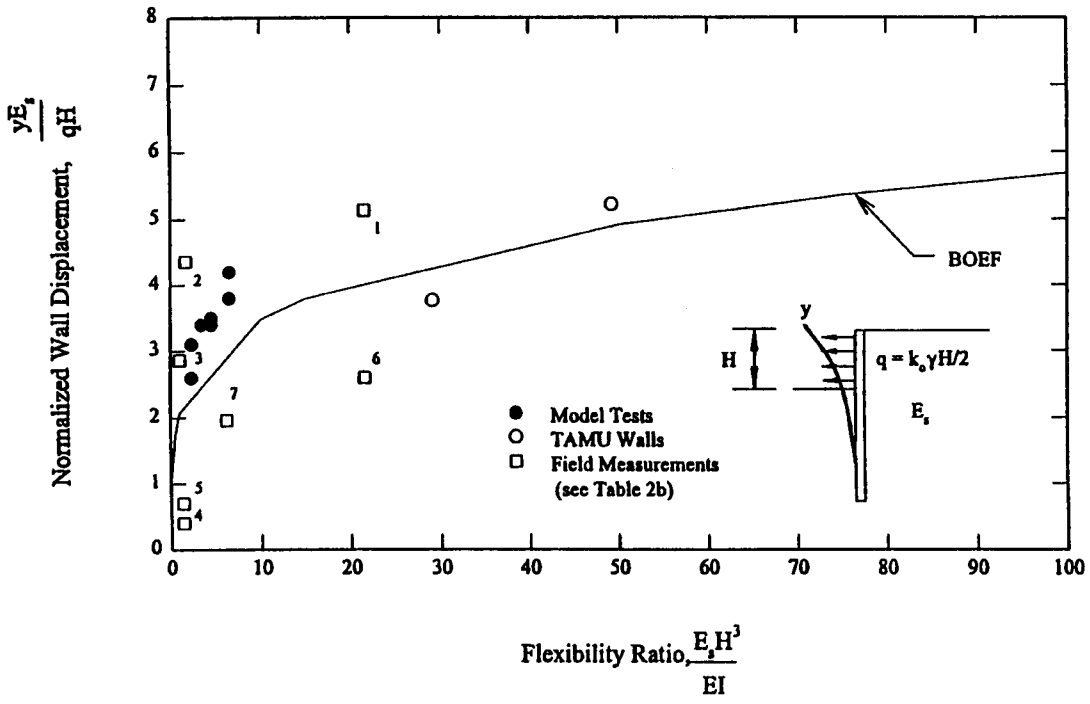

FIGURE 55
Influence of Relative Soil/Wall Stiffness on Cantilever Deformations

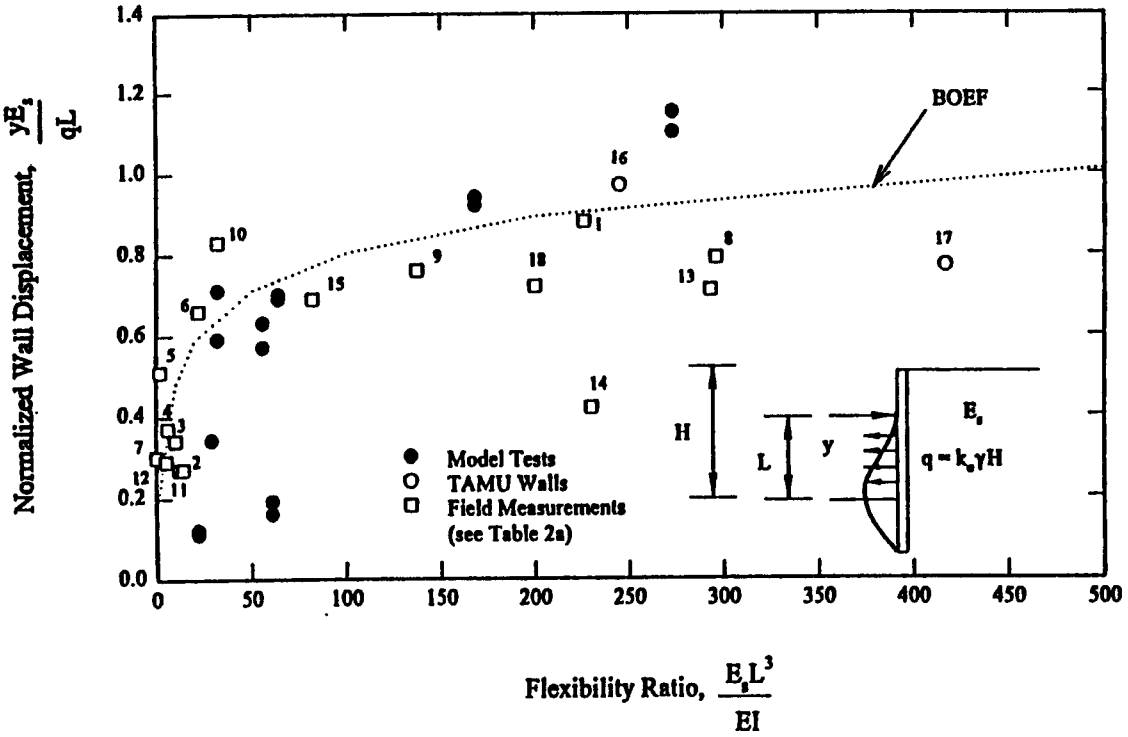

FIGURE 56
Influence of Relative Soil/Wall Stiffness on Lateral Bulging

TABLE 7
Summary of Cantilever Movements Associated with Anchored Wall Construction

NO.	REFERENCE	CANTILEVER DISPLACE-MENTS (in)	SOIL PROPERTIES			WALL CHARACTERISTICS			
			Description	K_o	E_s (psi)	Wall Type	H (ft)	EI (kip-ft^2/ft)	L_{cant} (ft)
1	Littlejohn & MacFarlane (1975) Keybridge House	0.5	gravels, stiff clay	1.0	12000	SL	47	288000	15
2	Johnson, et al. (1977)	0.55	glaciomarine	0.7	5000	SL	31	288000	11
3	Kooistra & Beringen (1984) Slurry Wall	0.71	medium-dense sands	0.5	2000	SL	29.5	633000	13
4	Hansmire et al. (1989) Panel 41	0.08	glacial tills	0.5	10000	SL	39	1.2E06	16
5	Hansmire, et al. (1989) Panel 63	0.14	glacial tills, rock	0.5	10000	SL	52	1.2E06	16
6	Ulrich (1989) Republic Bank Center	0.38	stiff clays, med. sands	1.4	3500	BP	54	183000	14
7	Ulrich (1989) Smith Tower	0.37	stiff clays, med. sands	1.4	3500	BP	50	383000	13
8	Chung & Briaud (1993) Beams 15/16	0.45	loose-med. dense sands	0.5	6000	SP	25	9900	10
9	Chung & Briaud (1993) Beams 7/8	0.4	loose-med. dense sands	0.5	6000	SP	25	3000	8

Notes: 1. SP = soldier beam wall, SL = slurry wall, ShP = sheet pile wall, and BP = bored pile (reinforced concrete shaft) wall.
2. Section properties for slurry and bored pile walls have been computed on the basis of an uncracked section.

TABLE 8
Summary of Bulging Deformations Associated with Anchored Wall Construction

NO.	REFERENCE	LATERAL BULGE (in)	SOIL PROPERTIES			WALL CHARACTERISTICS			
			Description	K_o	E_s (psi)	Wall Type	H (ft)	EI (kip-ft^2/ft)	L_{bulge} (ft)
1	Clough, et al. (1972)	0.75	glacial till outwash	1.3	11000	SP	55	8500	11
2	Littlejohn & MacFarlane (1975) Guildhall Precincts	0.1	gravels	0.5	7000	SL	34	168000	12
3	Littlejohn & MacFarlane (1975) Keybridge House	0.14	gravels, stiff clay	1.0	12000	SL	47	288000	13
4	Johnson, et al. (1977)	0.2	glaciomarine	0.7	5000	SL	31	288000	13
5	Kooistra & Beringen (1984) Slurry Wall	0.66	medium-dense sands	0.5	2000	SL	29.5	633000	17
6	Kooistra & Beringen (1984) Sheet Pile Wall	0.63	medium-dense sands	0.5	2000	ShP	23	59200	17
7	Hata, et al. (1985)	2.3	soft clays	0.5	700	SL	91	2.7E06	12
8	Symons, et al. (1988)	0.34	glacial outwash	0.6	10000		ShP	31	1123
9	H.C. Nutting (1988)	0.12	stiff clays	0.8	15000	SP	26	21200	11
10	Ulrich (1989) Hermann Teaching Hospital	0.39	stiff clays, med. sands	1.2	10000	BP	23	183000	16
11	Ulrich (1989) Republic Bank Center	0.17	stiff clays, med. sands	0.9	10000	BP	54	183000	12
12	Ulrich (1989) Smith Tower	0.24	stiff clays, med. sands	0.9	7000	BP	50	383000	12
13	Caliendo, et al. (1990)	0.95	stiff clays, gravel	0.6	5000	SP	43	38400	25
14	Houghton & Dietz (1990) High Street	0.18	glacial tills	1.0	15000	SP	62	9400	10
15	Houghton & Dietz (1990) Pearl Street	1.25	glaciomarine	1.0	4000	SP	63	9400	11
16	Chung & Briaud (1993) Beams 15/16	0.21	loose-med. dense sands	0.5	7000	SP	25	9900	16
17	Chung & Briaud (1993) Beams 7/8	0.15	loose-med. dense sands	0.5	7000	SP	25	3000	9
18	Anderson, et al. (1994) St. Louis Center	0.28	stiff clays, med. dense silts/sands	0.6	6000	SP	30	9500	13

Notes: 1. SP = soldier beam wall, SL = slurry wall, ShP = sheet pile wall, and BP = bored pile (reinforced concrete shaft) wall.
2. Section properties for slurry and bored pile walls have been computed on the basis of an uncracked section.

3.3.2 Wall Settlement

Wall settlement can negatively affect wall performance. In a case history described by Shannon and Strazer (1970), they observed about 3 in of outward lateral movement of an anchored wall, coincident with large wall settlements, as the excavation approached design grade (Fig-

ure 57). The wall consisted of drilled-in (16-in diameter) soldier beams and lagging, with the beam toe penetrating 6 ft below final grade. End bearing soils consisted of a hard, heavily overconsolidated, slickensided clay. The wall was supported by up to eight levels of ground anchors, inclined downward between 30 and 35°. Design ground anchor loads were about 48 kips/beam, corresponding to a downward vertical component of load of about 190 kips/beam. For reference, the axial capacity of the soldier beam toe estimated using Reese and O'Neill's (1988) recommendations was between 100 and 200 kips depending on the undrained strength assumed for the hard clay. Thus, the computed available axial capacity of the beams was probably marginal ($FS \approx 1.0$) for the anticipated vertical loads. According to Shannon and Strazer (1970), soldier beam bearing conditions were probably exacerbated by a disturbed zone of soil next to an existing railroad tunnel.

Hanna (1968) has described the mechanics of wall response due to settlement based on observed performance of small-scale models. According to Hanna, wall settlement geometrically facilitates outward movement of the wall at the anchor connection, without change in ground anchor loads, assuming a point of rotation at depth behind the wall (Figure 58). The amount of movement, therefore, depends on the wall settlement and the inclination of the ground anchors.

In the model tests, soldier beam settlements became significant as the excavation level approached design grade. Beam settlements developed principally from progressive transfer of axial load to the beam tips, associated with reduced carrying capacity in skin friction above the excavation level, and an increase in the vertical component of force supported by the wall due to downdrag (Figure 59). The tendency for outward rotation of the model walls associated with soldier beam settlements was resisted by mobilization of passive resistance along the beam toe. This produced a wall deformation response that consisted principally of outward rotation about the beam toe. Kinematically, the observed model wall response can be represented by wall movements, consistent with Hanna's observations, and rotation of the wall about the lower ground anchor level (Figure 60).

A geometric relationship between wall rotation and settlement can be computed that depends on the inclination of the ground anchors and the position of the lower ground anchor on the wall (Figure 61). As shown in Figure 61, the observed rotation of the model wall agrees closely with the geometric relationship. Available field data also are represented. Of particular interest are the full-scale wall results described by Weatherby, et al., 1998. They describe the performance of an anchored soldier beam and lagging wall that consisted of both driven and drilled-in soldier beams. The driven beams consisted of 6- and 10-in sections. The drilled-in beams were installed in 18- or 24-in drilled shafts backfilled with either lean mix or structural concrete. During construction, soldier beam settlements varied. At some locations, the drilled-in beams settled twice as much as the driven beams, resulting in lateral wall movements due to beam settlement of up 0.45 percent H (where H represents the depth of the cut at design grade).

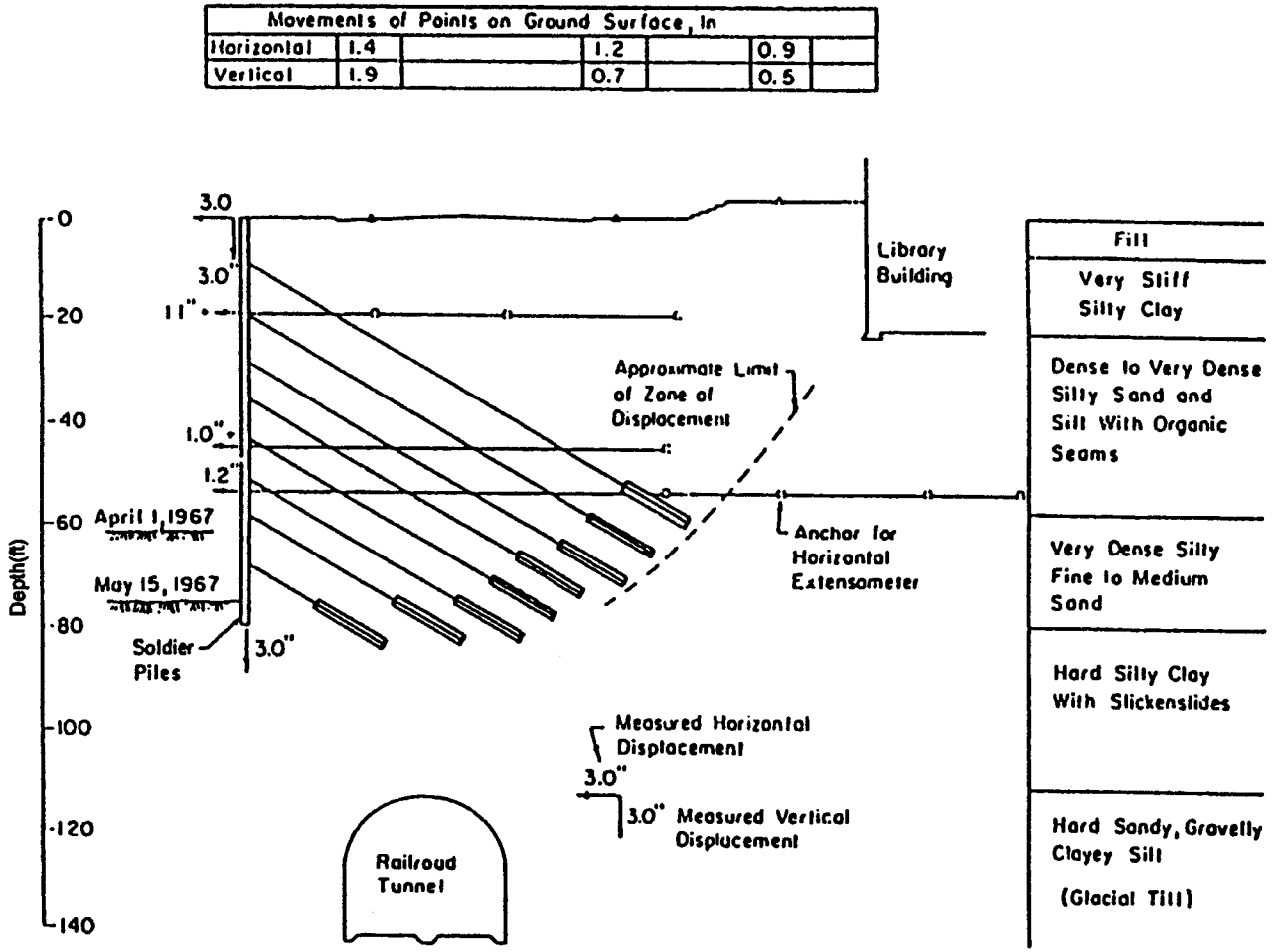

FIGURE 57
Relationship Between Soldier Beam Settlement and Lateral Displacement for an Anchored Wall in Stiff, Fissured Clays and Galcial Tills (Shannon and Strazer, 1970)

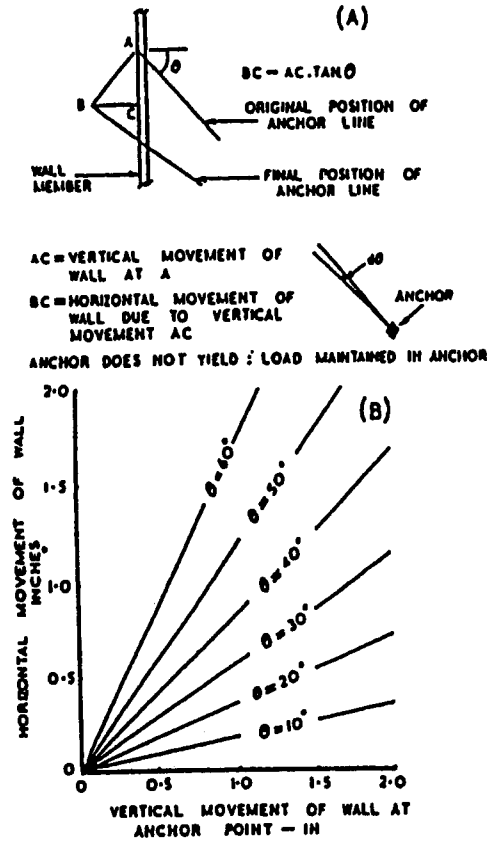

FIGURE 58
Relationship Between Settlement and Wall Movement Observed in Small-scale Model Anchor Tests (Hanna, 1968)

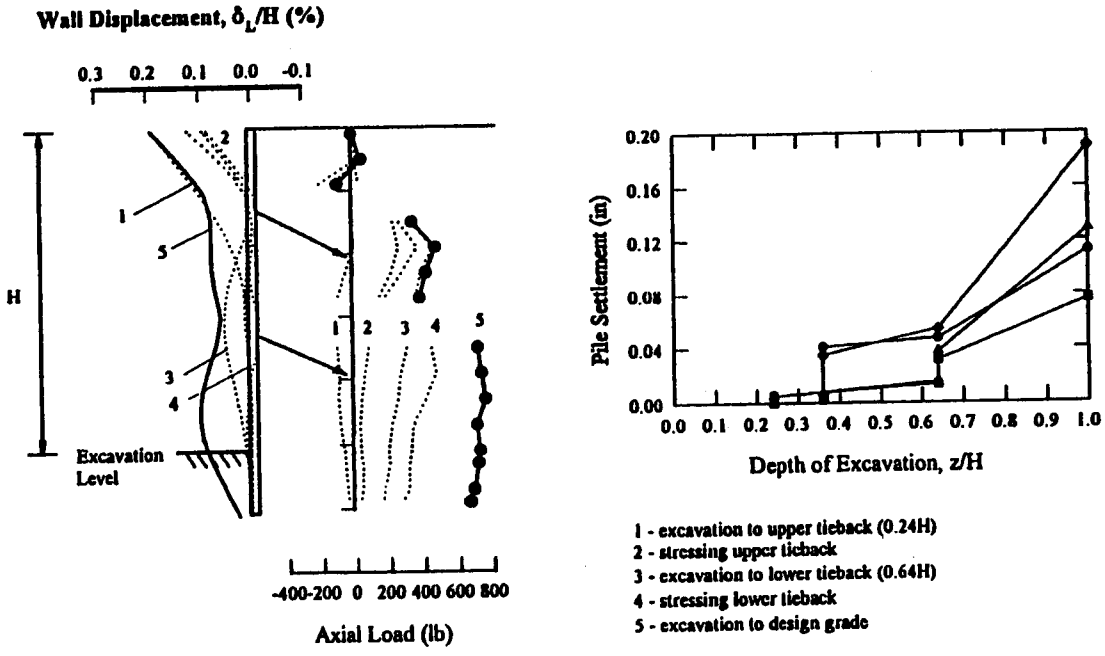

FIGURE 59
Development of Wall Rotation and Soldier Beam Settlements in the Model Tests

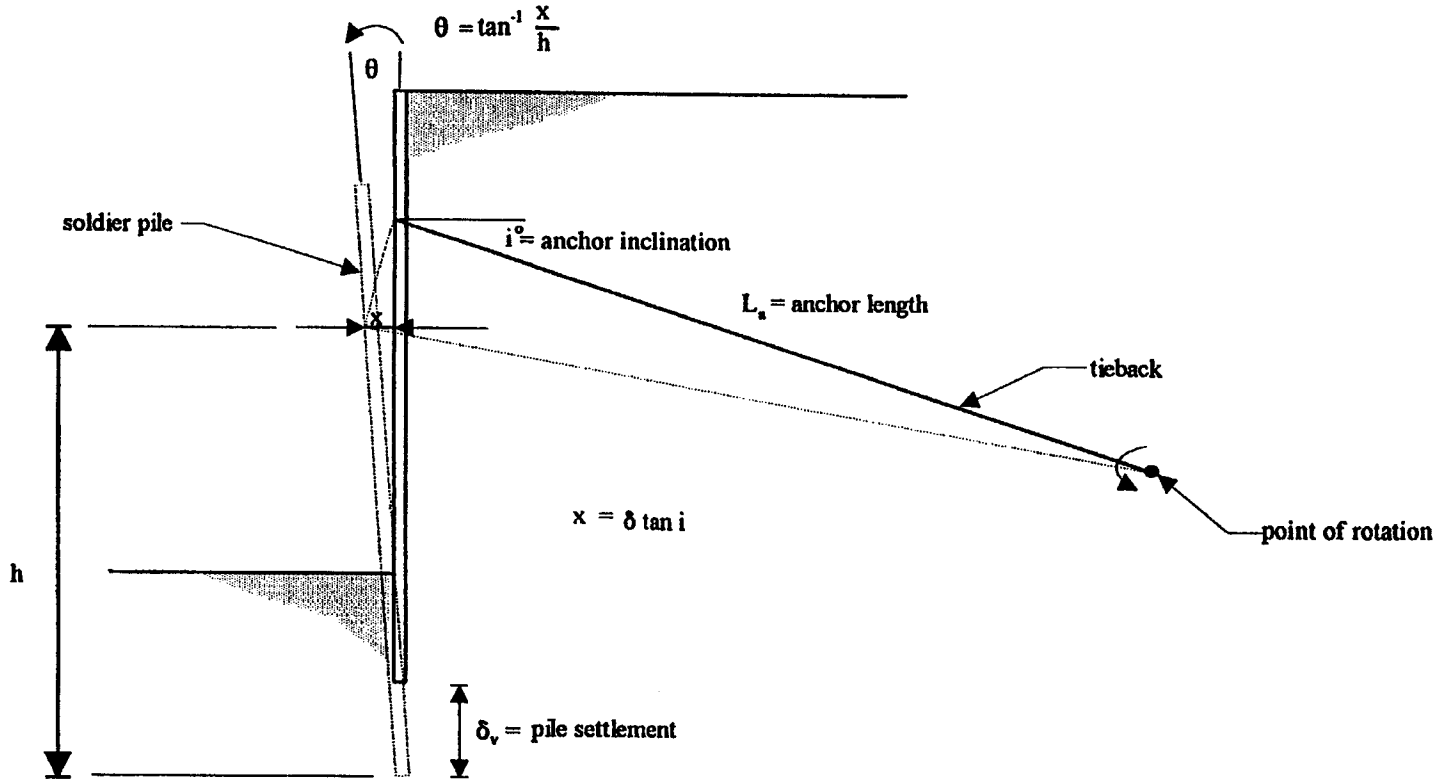

FIGURE 60
Relationship Between Soldier Beam Settlement and Wall Rotation Observed in the Model Tests

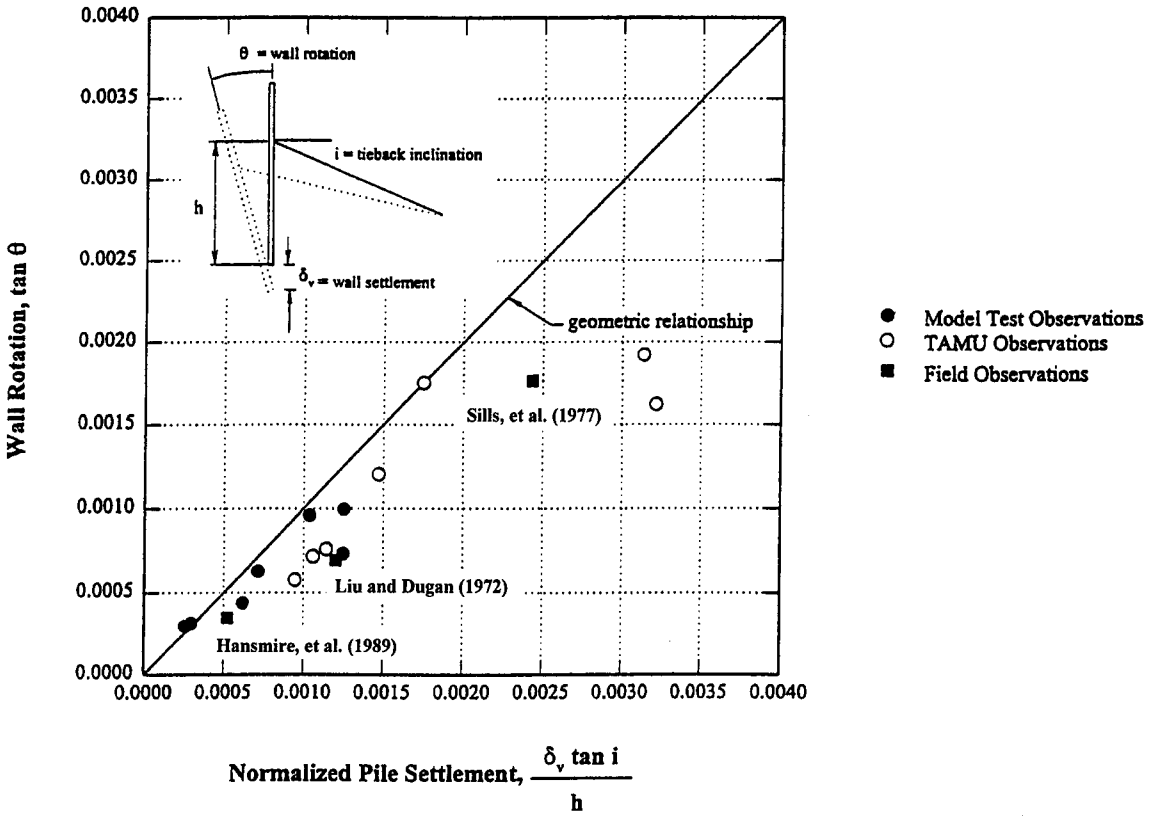

FIGURE 61
Relationship Between Observed and Computed Wall Rotations Resulting from Wall Settlement

3.3.3 Changes in Ground Anchor Loads (Effect of Prestressing)

In current practice, ground anchors are usually prestressed to between 75 and 100 percent of design loads, computed from an earth pressure distribution providing a resultant thrust intermediate to Rankine active and at-rest conditions. Field measurements have generally shown only small changes in ground anchor loads throughout construction. Significant increases in ground anchor forces have been observed where low prestress loads have been used, and the implications for wall performance are illustrated in a case history by Rizzo, et al. (1968). They described the performance of a ground anchor supported soldier beam and lagging wall installed in loose to dense sands. For one section of the cut, ground anchors were prestressed to 50 percent of the Rankine active earth pressure, while for an adjacent section of the wall, ground anchors were prestressed to about 110 percent of the at-rest pressure. Maximum lateral wall movements for the low prestress section of wall were about 0.45 percent H, compared with 0.12 percent H, where higher prestress loads were used.

More recently, Winter (1990) described the performance of a soldier beam and lagging wall supported by ground anchors and installed in stiff fissured clays. A trapezoidal earth pressure distribution with an intensity of $30H$ (H represents the maximum depth of cut) was selected for design. Ground anchors were generally locked-off at 100 percent of their design loads, excluding a test section, where ground anchors were locked-off at 45 percent of their design loads. Figure 62 compares lateral wall movements at the test section with those at wall sections using the higher ground anchor prestress loads. At the wall section constructed using the higher prestress loads, the top of the wall was pulled back into the retained soil, while the lower portion of the wall displayed a characteristic bulge of about 0.5 in (0.05 percent H). At the wall section constructed using the lower prestress loads, bulging is less pronounced, and wall movements consisted principally of outward rotation about the beam toe. Rotation was required to mobilize additional loads in the ground anchors. Ground anchor loads in the section with the lower lock-off loads increased as the wall moved. Anchor forces in the other section of the wall did not change significantly. The maximum lateral movement of the wall at the test section measured about 0.9 in (0.1 percent H). Thus, the consequence of lower lock-off loads was increased wall movements, although in the stiff clays the performance was well within the accepted range of wall deformations.

To provide an additional perspective on the importance of proper anchor lock-off, ground anchors in Model Test 2 were unloaded after achieving design grade. Model Test 2 was supported by a single level of ground anchors at a depth of 27 in, $0.36H$. Loads in each ground anchor were simultaneously reduced in small decrements and the deformation response of the wall and ground was recorded. Load reduction was continued until no further decrease in loads could be achieved, which was assumed to correspond to a limiting stage of stress (FS = 1.0). Figure 63 summarizes the observed response of the wall. Wall and ground movements are normalized with respect to the depth of the cut and plotted as a function of factor of safety (FS), defined as

$$FS = \frac{\tan\phi_{avail}}{\tan\phi_{mob}} \qquad \ldots [3.3]$$

in which ϕ_{avail} represents the available friction angle and ϕ_{mob} represents the mobilized friction angle. The available friction angle was calculated from a trial wedge analysis, assuming that the horizontal component of measured anchor force and passive toe resistance defined the limiting state of lateral stress when the anchor loads could no longer be reduced. Measured axial soldier beam strains were used to determine the vertical component of force imposed on the wall by the soil. The back-computed available friction angle was about 42°. Mobilized friction angles for previous load decrements were calculated in a similar manner.

At design grade, the estimated factor of safety with respect to a limit condition was about 1.8. During the initial stages of unloading (FS = 1.8 to 1.3), wall movement consisted principally of translation associated with mobilization of passive resistance along the embedded length of the wall. Comparatively small increases in wall and ground movements were observed for this stage of unloading. Further reduction in ground anchor loads ($FS \leq 1.3$) resulted in increased

translation and rotation of the wall about the toe. Lateral wall movements and ground surface settlements accelerated as the factor of safety decreased below about 1.3. With respect to the limiting stress condition in the model tests, observations suggest a minimum factor of safety of 1.3 to restrict model wall and ground movements to a range of about 0.1 to 0.3 percent H. A factor of safety of 1.3 is typically used when designing permanent ground anchor walls. Observed performance of anchored walls in the field suggests that a factor of safety of 1.2 to 1.3 is sufficient. The behavior described in Figure 63 indicates that, when the factor of safety is reduced below some threshold value, wall movements will increase significantly. At this time it is uncertain whether the factor of safety for full-scale walls can be lowered below 1.2 and still keep the lateral movements relatively small.

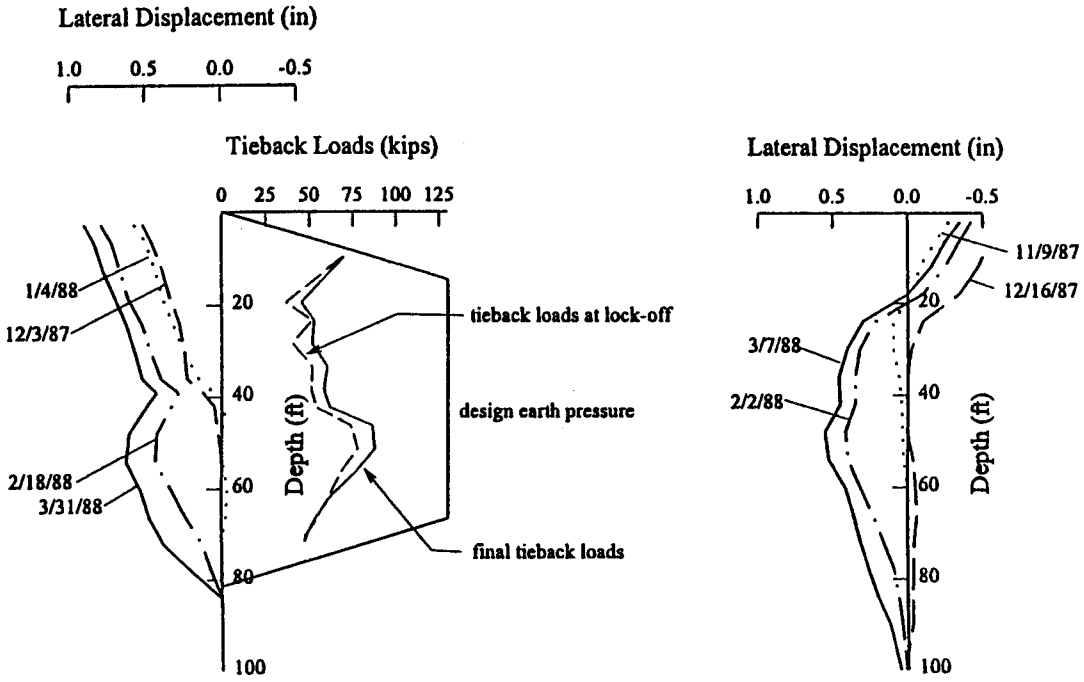

a) 45 percent prestress

b) 100 percent prestress

FIGURE 62
Comparison of Observed Deformations for an Anchored Wall Constructed Using Different Prestress Loads (Winter, 1990)

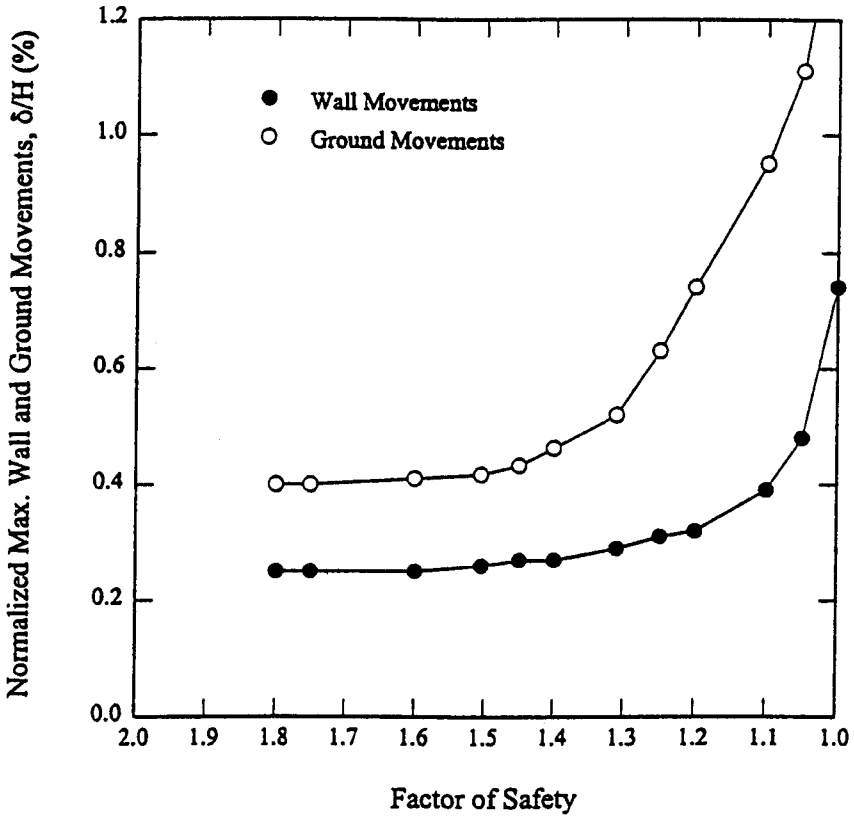

FIGURE 63
Relationship Between Wall and Ground Movements and Anchor Loads During Unloading in Model Test 2

3.3.4 Ground Anchor Yielding or Load Redistribution

Anchors that have not been properly load tested may not be able to develop adequate load-carrying capacity to support the wall or they may fail to hold the lock-off load without significant time dependent movements (creep). If a group of anchors move through the ground, then the wall will translate laterally.

Ground strains that develop behind an anchored wall can result in a redistribution of load along the length of the anchors. These strains represent a potential additional source of wall movement associated with elongation of the ground anchors. The potential for load redistribution, as it contributes to wall movements, depends upon the location of the tendon bond length and the magnitude and extent of the ground strains. Load redistribution movements will be small,

but where wall and surface movements must be kept to the absolute minimum, the tendon bond length should be located outside the zone of ground movements generated by excavation.

The significance of load redistribution is considered in two case histories presented by Shields, et al. (1978) and Caliendo, et al. (1990). Shields, et al.examined load redistribution along pressure-injected ground anchors for two projects, referred to as National Capital Bank and 1800 Massachusetts Avenue. Both walls consisted of soldier beams and lagging supported by a single level of ground anchors and installed in dense sands and stiff clays. At 1800 Massachusetts Avenue, a single level of inclined rakers was used to support the lower third of the wall. Section views showing the relationship between wall and ground anchor geometry for the two projects are shown in Figure 64. Ground anchors were installed by driving a 3-in OD casing to the desired depth, inserting the anchor tendon (1¼-in Dywidag bars) into the casing, and then grouting the tendon bond length at high pressures (150 to 450 psi) as the casing was withdrawn. The unbonded length was not grouted. Resistance-type strain gauges were installed on selected bars at 3-ft intervals along the tendon bonded length.

The load distributions along the anchor length after lock-off, and at several stages through the construction sequence, are shown in Figure 64. The most significant feature of the load transfer curves is the rapid attenuation of load toward the back of the anchor immediately following lock-off, particularly for the anchor at National Capital Bank. With the progress of excavation, the load transfer curves show an increase in load toward the back of the anchors, which becomes more pronounced as the excavations approach design grade. Ground anchor loads for both projects were essentially constant throughout the construction sequence. By integrating the load distribution along the anchor length, it is possible to estimate the additional elongation of the ground anchors associated with load redistribution. For Capital National Bank and 1800 Massachusetts Avenue, the estimated change in ground anchor lengths from lock-off to design grade were 0.041 in (0.012 percent H) and 0.026 in (0.0066 percent H), respectively. Movements of these magnitudes are not significant compared with the normal movements associated with anchored walls. Similar displacements due to load redistribution was reported by Caliendo, et al. for a soldier beam and lagging wall installed in similar soils.

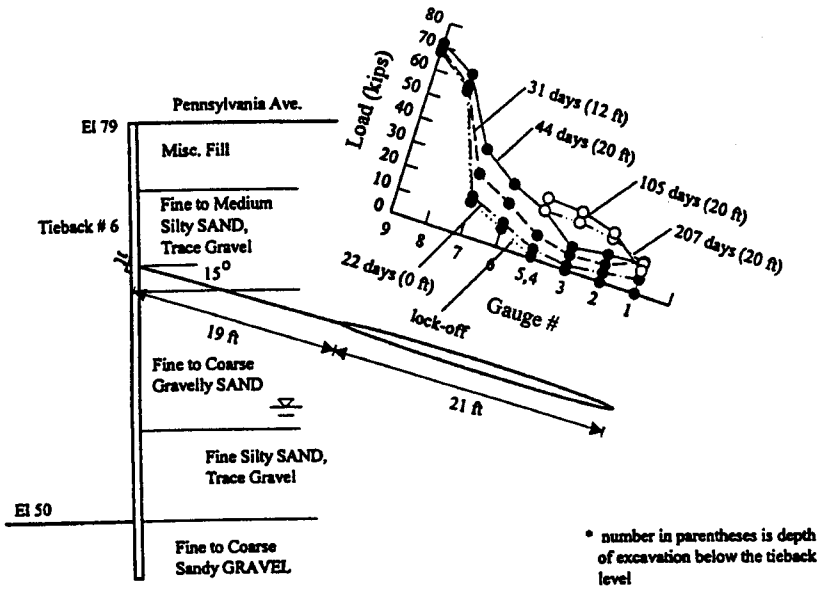

a) National Capital Bank

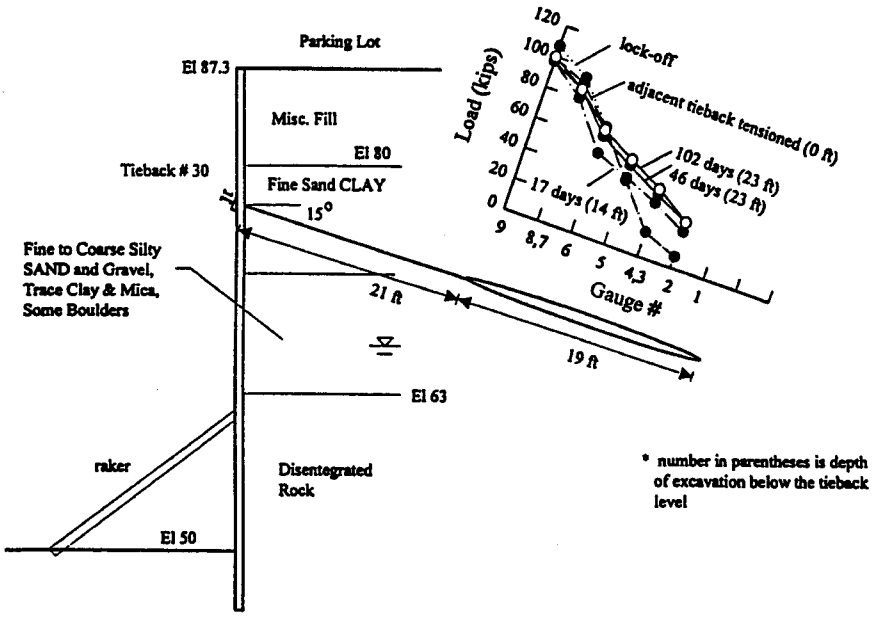

b) 1800 Massachusetts Avenue

FIGURE 64
Load Transfer Characteristics Along Pressure-injected Ground Anchors in Sand (Shields, et al. 1978)

3.3.5 Mass Movements

Ground anchors can provide resistance to ground strains that develop along the tendon bond length, as reflected by a redistribution of load along the anchor length through construction. Ground movements that develop behind the anchors are unrestrained, however, and represent a potential additional source of wall movement. As illustrated in the following case histories, the importance of this component of wall movement depends on the length of the ground anchors, initial stress conditions in the ground, and soil strength and stiffness.

Sills, et al. (1977) described the performance of a ground anchor supported slurry wall installed in stiff, fissured London clay. The wall was about 26 ft high and supported by four levels of ground anchors with a total length of about 52 ft (Figure 65). Lateral wall movements at the end of construction consisted principally of outward translation and rotation about the toe, with a maximum displacement at the top of the wall of about 1 in. Because of the large stiffness of the wall panels and close spacing of ground anchors, bending components of deformation were very small. Wall settlement did develop during excavation below the third level of ground anchors and accounted for about one-half of the maximum lateral movement of the wall. The balance of the observed wall movement was due to development of ground strains behind the ground anchors, at a distance behind the wall of over twice the depth of the cut. Despite use of high prestress loads (note that a zone of volume compression developed between the wall and ground at a distance of about $0.5H$ behind the wall), large lateral movements developed behind the ground anchors. These movements may have resulted from stress relief as the ground relaxed in response to the excavation.

Houghton and Dietz (1990) described the performance of a ground anchor supported soldier beam and lagging scheme for a deep excavation in Boston (55 ft). Section 2.5.3.2 of the report by Weatherby, et al. (1998) describes the lateral movement and axial load behavior of the wall. Performance for two wall sections (High Street and Pearl Street) was reported. Both wall sections were of similar stiffness and supported by six levels of ground anchors (a seventh level of anchors and inclined rakers were added at the Pearl Street section with the excavation near design grade). The ground anchors were located behind a plane passing through the wall at the excavation level and making an angle of about 34° with vertical. A comparison of lateral wall movements for Pearl and High Streets is shown in Figure 66. Wall movements for the Pearl Street section included much greater (up to three times) contributions from bulging below the upper ground anchor and outward rotation about the toe of the wall. Soldier beams for both wall sections were founded in very dense glacial tills, so that the contribution from beam settlement to outward wall rotation was probably small (beam settlement measurements were not made).

As shown in Figure 67, it is possible to develop small lateral movements in stiff clays and dense sands at distances behind the wall of between 0.4 and 0.6 H, which is the region in which the ground anchors along Pearl and High Street were installed. Thus, the small rotational components of movement observed along High Street possibly developed from load redistribution along the tendon bond length and/or small movements behind the anchors.

Along Pearl Street, subsequent geologic studies revealed the presence of a thick glacio-marine deposit, which was not previously known to exist. This material was much weaker than the dense tills found over most of the site. An inclinometer located 33 ft behind the wall showed large lateral movements (Figure 68). This inclinometer was not installed until the excavation was near design grade. As illustrated in Figure 67, ground movements can develop behind an anchored wall for a distance of 1.5 to $2H$. Thus, the length and position of the ground anchors along Pearl Street probably were insufficient to effectively restrain ground movements that developed in the glacio-marine deposit.

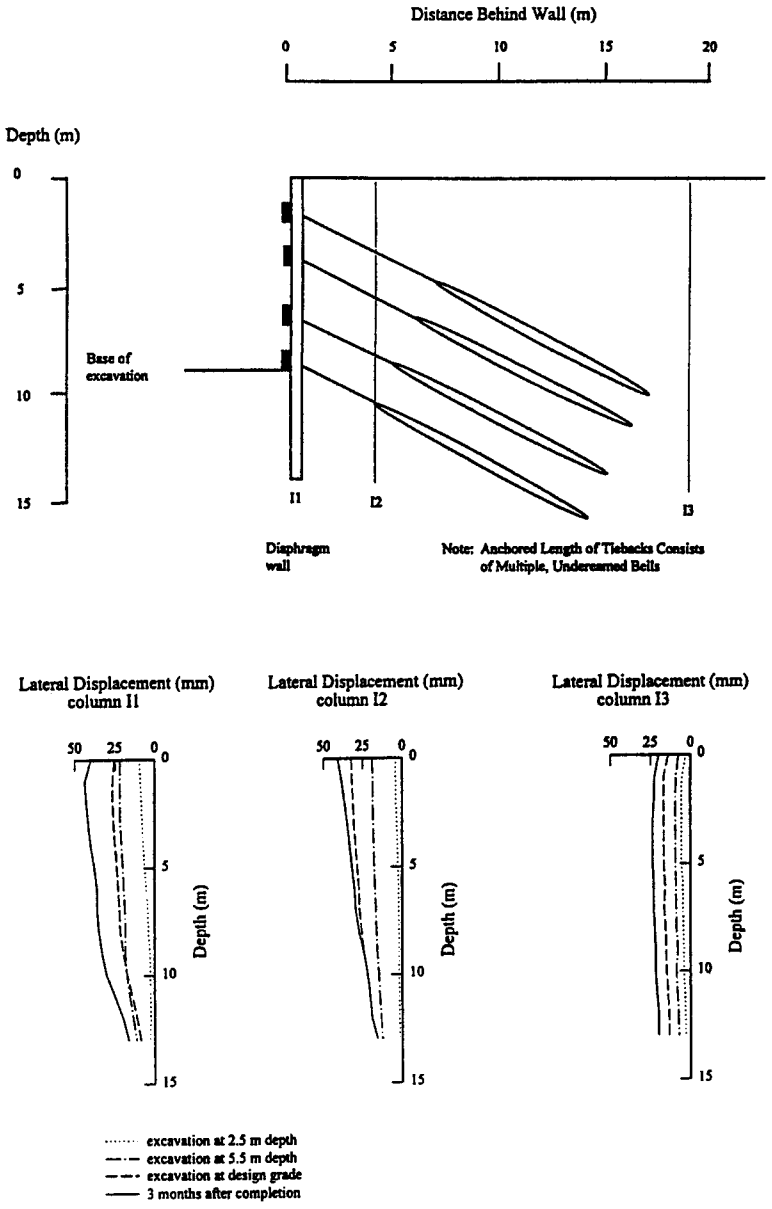

FIGURE 65
Development of Ground Movements Behind Ground Anchors in Stiff London Clay (Sills, et al. 1977)

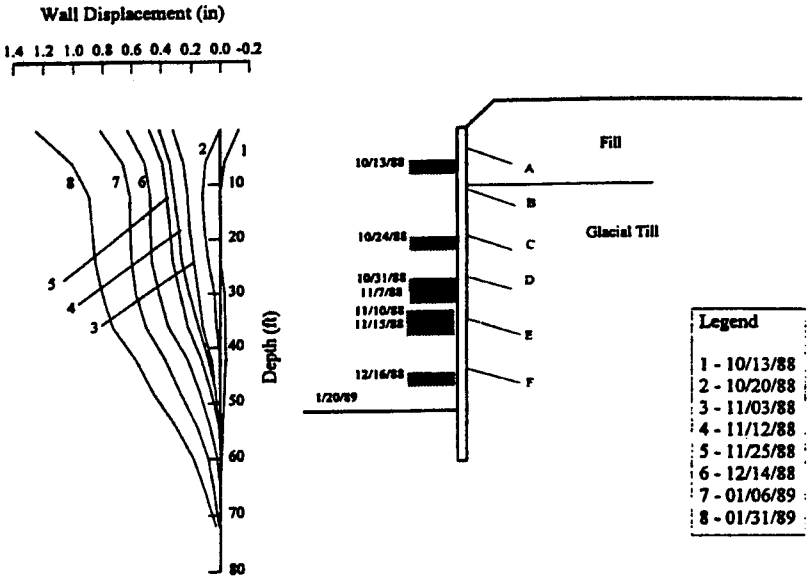

a) High Street

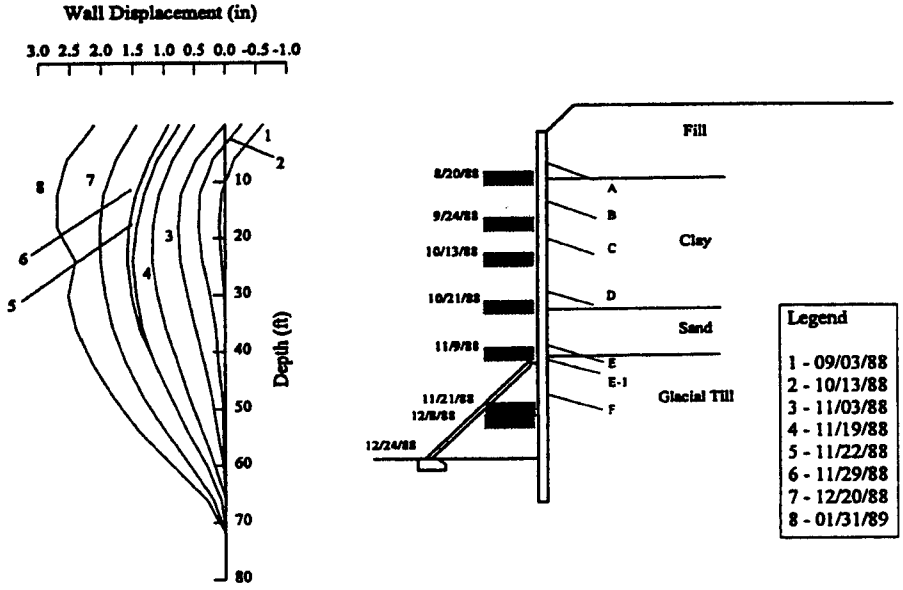

b) Pearl Street

FIGURE 66
Comparison of Wall Movements for a Deep Excavation in Boston
(Houghton and Dietz, 1990)

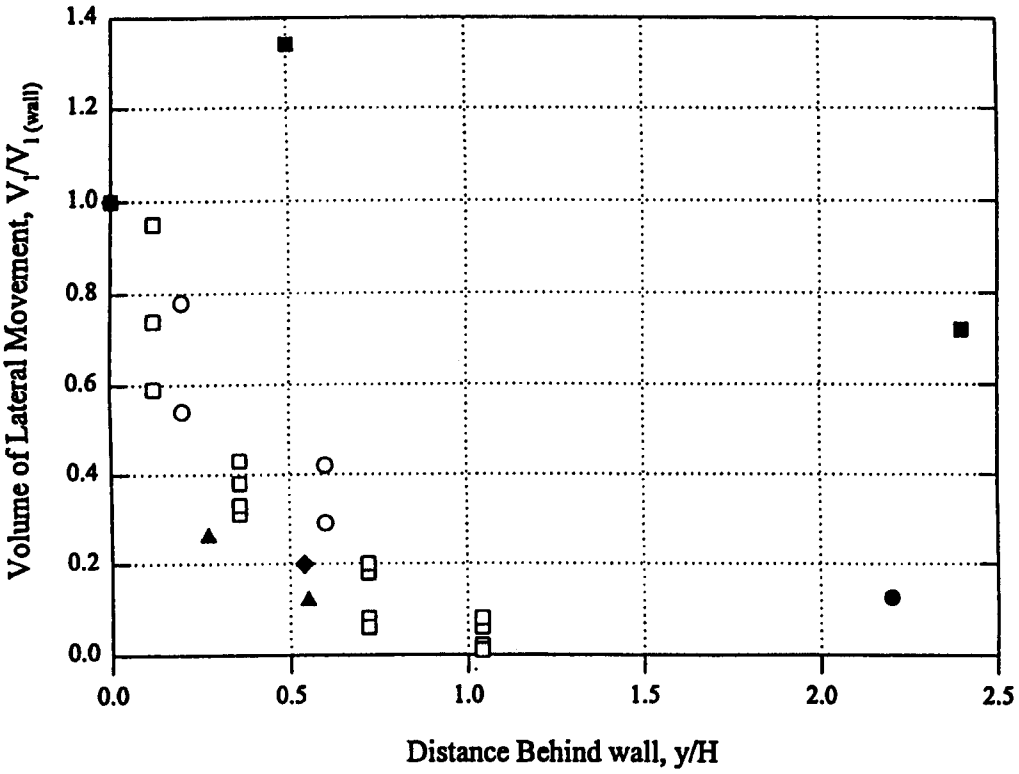

- ● Kooistra and Beringen (1984), medium-dense sands
- ▲ O'Rourke (1975), stiff clays and dense sands
- ◆ Liu and Dugan (1972), Stiff clays and dense sands
- ■ Stills, et al. (1977), stiff clays, high lateral stresses
- □ Model tests
- ○ TAMU walls

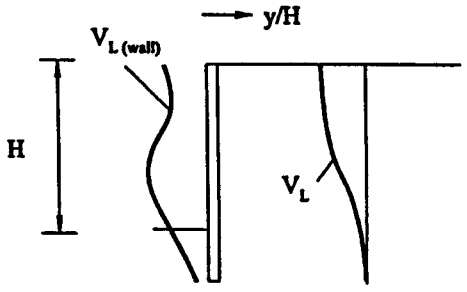

FIGURE 67
Change in Lateral Ground Volumes with Distance Behind an Anchored Wall

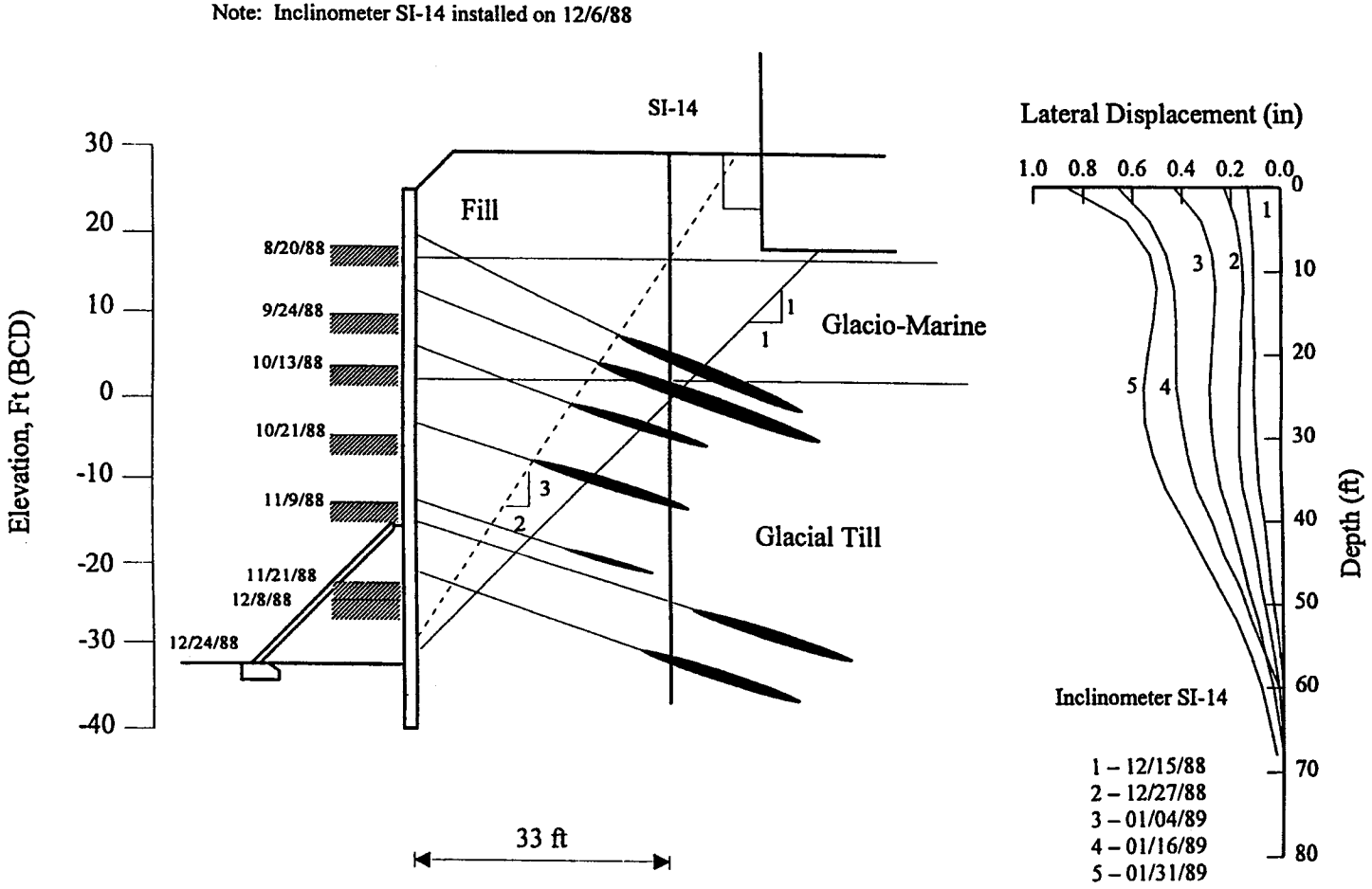

FIGURE 68
Development of Ground Movements in the Anchor Bond Length at Pearl Street
(Houghton and Dietz, 1990)

3.4 SUMMARY

Ground movements develop during anchored wall construction due to installation of wall components, excavation to the first ground anchor level, installation of ground anchors, stressing of ground anchors, and excavation below the ground anchor level. Each stage of construction contributes to the observed pattern of wall and ground movement. Movement associated with installation of the wall and the ground anchors should be small if good construction practices are followed.

In the cantilever stage, each successive increment of excavation results in a non-linear increase in wall and ground movements. These movements can be controlled by reducing the depth to the first ground anchor level. Stressing of the upper level anchors will pull the soldier beams back into the retained soil. Normally, the cantilever displacements of flexible walls will not be significantly reduced as a result of anchor stressing. Even if the beams are pulled back significantly, lateral and vertical ground movements between soldier beams will be essentially unchanged by ground anchor stressing. Excavation below the upper ground anchors results in lateral bulging of the walls, with maximum displacements near the current excavation level. Ground surface settlements at the end of construction were maximum at the wall and decreased to a small value at a distance behind the wall of about $1.5H$.

Ground anchor walls also may include a significant component of outward rotation and translation about the toe of the wall. The sources of outward rotation and translation are:

- Soldier beam settlement associated with mobilization of end bearing resistance required to support the vertical component of ground anchor force.
- Elongation of the anchor tendons associated with a load increase.
- Anchor yielding or load redistribution in the anchorage zone.
- Mass movements behind the ground anchors.

Movements from the last three items in the above list are generally small. Each of these components could contribute significantly to wall movements for specific soil conditions and wall geometry. Soldier beam settlement or the use of triangular earth pressure diagrams are the most common source for wall rotational movements. Effects of beam settlement on outward rotation were illustrated in the model tests and the Texas A&M walls.

CHAPTER 4
DISTRIBUTION OF FORCES

4.1 INTRODUCTION

Anchored wall design assumes that the ground anchors and lateral toe resistance balance the lateral earth load that develops as the excavation proceeds. In current practice, earth pressures are evaluated from experience with internally supported walls, or from classical earth pressure concepts. Apparent earth pressure diagrams (Chapter 2 of *Summary Report of Research on Permanent Ground Anchor Walls*, "Volume I: Current Practice and Limiting Equilibrium" (Long, et al., 1998)), or triangular earth pressures, with resultant thrusts ranging from active Rankine to at-rest conditions are used in design. Simplifying assumptions regarding boundary conditions at the anchors and subgrade are usually made to determine the distribution of forces to the anchors and toe (hinge method). Alternatively, a portion of the design earth pressure envelope is assigned to each ground anchor and the toe of the wall (tributary area method). Depending on the earth pressure envelope used in design and procedures used to evaluate wall equilibrium, a wide range of anchor forces and toe penetration depths can be computed.

In addition to providing equilibrium for lateral forces, the distribution of vertical forces on an anchored wall must be considered. Ground anchors are inclined downward to facilitate construction and locate the bond length in suitable ground. As a result, ground anchor stressing introduces a vertical force to the wall. Furthermore, relative downward movement of the ground with respect to the wall can increase the vertical loads applied to the wall above the vertical component of the ground anchor load (downdrag).

An important part of the model studies concerned measurement of the distribution of lateral and vertical forces associated with ground anchor stressing and excavation. In this chapter, model test observations are used to describe the general mechanics of load development. Other model studies and available field measurements are used to qualify the model test observations. Special emphasis is placed on the significance of mobilized lateral toe resistance and downdrag. Practical guidance is provided for determining the required distribution of forces on an anchored wall.

4.2 LATERAL EARTH PRESSURES

The development of lateral earth pressure during anchored wall construction is discussed in this section of the report, with an emphasis on the significance of the reaction developed below the base of the excavation, and the conditions for which it becomes important. Model test observations are used to illustrate the basic mechanics of lateral thrust development, but are compared with available field measurements so that the model test observations can be extended to practice. The anchor prestressing effect is described and the influence of relative stiffness on the shape of the earth pressure distribution is evaluated. Practical guidance is provided for dis-

tributing the design thrust to the wall and for determining bending stresses, ground anchor forces, and toe penetration requirements.

Lateral earth pressures in the model tests were interpreted from measured bending strains. The procedure consisted of curve fitting, with appropriate boundary conditions, to obtain a twice differentiable function that could be used to calculate lateral earth pressures.

4.2.1 Relationship to Wall Deformations

Lateral earth pressures used in design of anchored walls usually take the form of a triangular or apparent earth pressure diagram, with resultant thrusts ranging from active Rankine to an at-rest state of stress. The implicit assumption made when using a triangular or uniform distribution of pressure is a pattern of deformation consistent with their development. *The Canadian Foundation Manual* (1985), for example, suggests a triangular distribution of pressure for anchored walls that experience a significant component of outward rotation about the toe. When wall deformations can be reduced to bending in the span between anchors, they suggest using apparent earth pressure envelopes consistent with strut load measurements.

The concept of an interrelationship between wall movements and earth pressures has developed from a combination of theoretical and practical experience. Rankine earth pressure theory, for example, defines the state of stress on a vertical plane when every element of soil is on the verge of failure. The limiting state of stress is defined in relationship to a Mohr-Coulomb failure envelope, so that the stress on the vertical plane increases in simple proportion to depth, corresponding to a triangular distribution of earth pressure. The deformation condition required to develop this limiting state of stress consists of outward translation or rotation about the toe. For rigid walls, Terzaghi (1934 and 1941) experimentally found that the top of the wall had to move about 0.05 to 0.1 percent H (where H represents the height of the wall) to develop the limiting state of stress. Some common conceptions concerning the relationship between earth pressures and wall deformations, defined from theory and practice, are summarized in Figure 69.

The relationship between lateral earth pressures and wall movements is delineated in Figures 70 through 74 for relevant construction stages of the model walls. Observations from Test 4 are used as an example.

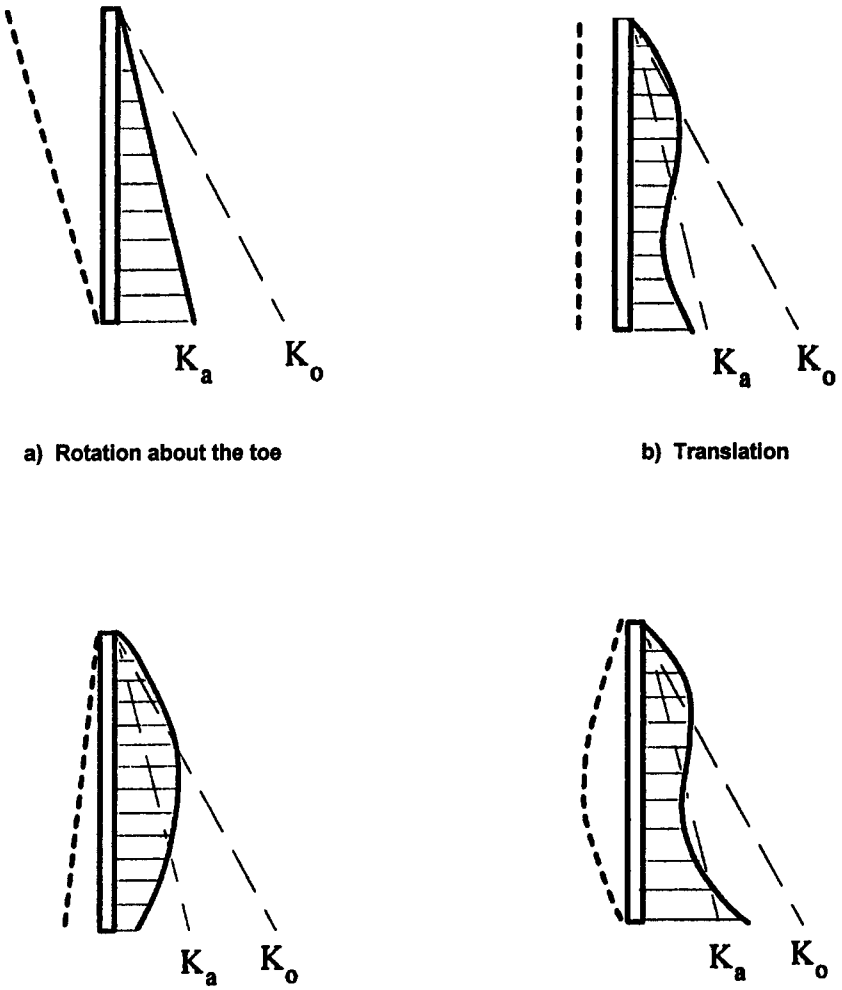

FIGURE 69
Relationship Between Wall Deformations and Lateral Earth Pressures for Rigid and Flexible Structures (after Terzaghi, 1941)

4.2.1.1 Excavation to the First Ground Anchor Level

Excavation to the first anchor level resulted in a pattern of deformation consistent with a flexible cantilever (Figure 70). Model studies of the behavior of flexible cantilever walls by Rowe (1952) suggest an earth pressure distribution that is classically triangular. However, in the model anchored wall studies, the earth pressure interpretation suggests a parabolic distribution of active thrust on the upper part of the walls. The resultant thrust was approximately equal to total force given by a Coulomb trial wedge solution for a ϕ of 44° and mobilized wall friction of $2/3\phi$. The position of the resultant thrust on the wall acted at a distance from the bottom of the cut of between 0.4 and $0.6H$ (where H represents the depth of excavation). The parabolic shape of the earth pressure distribution reflects the sequence of excavation and the installation of lagging between the soldier beam. Each small excavation increment made for installation of the lagging boards caused the ground between the soldier beams to move outward relative to the soldier beams and previously lagged sections of the wall. It appears that during excavation, active thrust was redistributed to stiffer, previously lagged sections of the wall. The construction sequence for anchored soldier beam walls differs from the construction sequence used by Rowe (1952) for his continuous cantilever models. Thus, earth pressures depend upon the magnitude and distribution of wall movements and the sequence of construction.

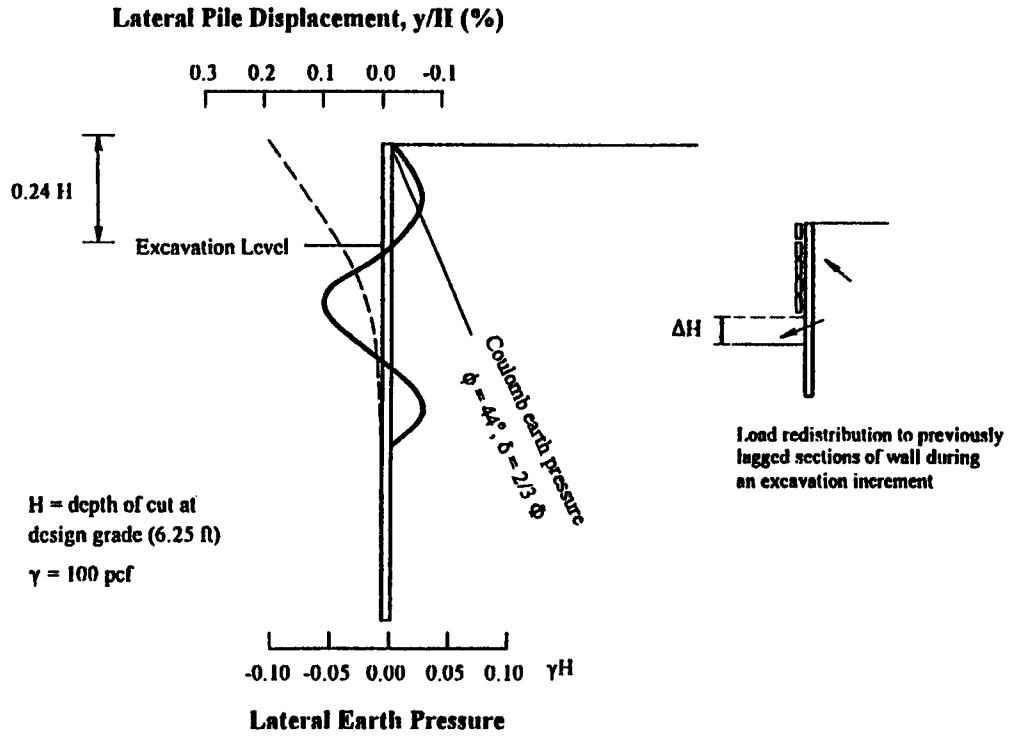

FIGURE 70
Lateral Wall Movements and Earth Pressures with Excavation at First Anchor Level (cantilever stage)

4.2.1.2 Ground Anchor Stressing

Significant changes in lateral earth pressures developed during anchor stressing (Figure 71). Ground anchor stressing pulled the soldier beams and lagging back into the retained soil, resulting in development of passive thrust on the upper part of the wall. The pressure "bulb" was approximately symmetric about the anchor level and greater than the at-rest stress (for $\phi = 44°$) to a depth of about $0.4H$ (where H represents the depth of the cut at design grade). With ground anchor loads at 120 percent of design, the maximum pressure approached the Rankine passive value. Decreasing loads to 75 percent of design resulted in a reduction in pressure, although beam deformations were essentially unrecovered. Although the beams were pulled back into the ground significantly (~ 0.1 percent H) during anchor stressing, the lagging movements were comparatively small (≤ 0.01 percent H). Anchor stressing resulted in significant increases in lateral pressures on the wall, while the overall wall deformations were small compared with other stages of construction.

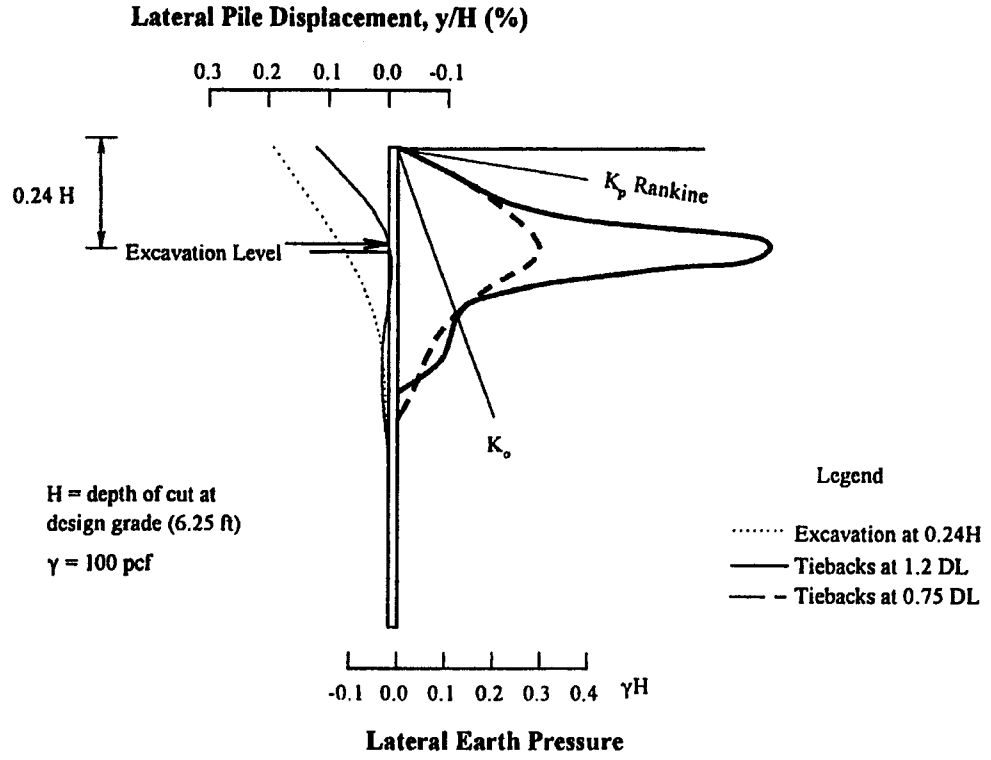

FIGURE 71
Lateral Wall Movements and Earth Pressures During Anchor Stressing

4.2.1.3 Excavation Below a Ground Anchor

Excavation below the upper anchors resulted in lateral bulging of the wall in the span between the anchor and excavation level. Figure 72 shows that outward bulging of the wall resulted in a decrease in pressure in the span and a redistribution of pressure to the anchor and base of the wall. Both the pattern of observed wall deformation and the redistribution of pressure are consistent with field experience with strutted walls (Terzaghi, 1941). Changes in pressure during excavation below an anchor were comparatively small. Therefore, ground anchors are effective in controlling components of wall deformation associated with the tendency for load redistribution.

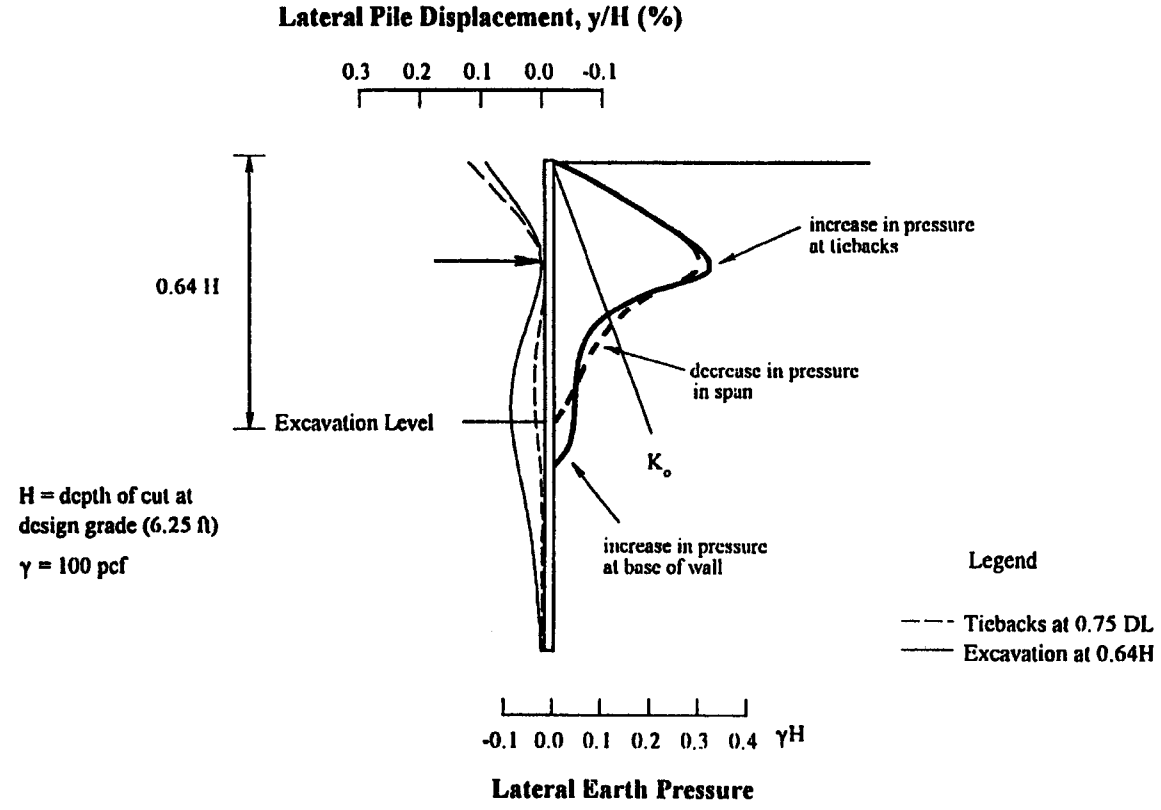

FIGURE 72
Lateral Wall Movements and Earth Pressures with Excavation at Lower Anchor Level

4.2.1.4 End of Construction

Stressing of the lower ground anchors resulted in a similar wall deformation response to that observed during stressing of the upper anchors, and development of a passive pressure bulb close to the support (Figure 73). During excavation below the lower level of anchors, lateral bulging developed in the span between the lower anchors and design grade. Wall deformations also included a significant component of outward rotation associated with beam settlements (Figure 74). According to Terzaghi's (1934) rigid retaining wall experiments in sand, and Rowe's (1952) work with flexible anchored bulkheads, wall rotation was sufficient to develop a triangular distribution of pressure on the wall. However, the lateral earth pressures measured in the model-scale anchored walls retained the characteristic passive pressure bulbs locked-in by ground anchor stressing (Figure 74). Thus, development of rotation during anchored wall construction is not consistent with a triangular distribution of pressure.

Figures 74 and 75 show the relationship between observed lateral earth pressures and the design earth pressure envelope used to design the walls supported by two levels and a single level of ground anchors, respectively. Near the anchors, the design earth pressure envelope represents a good approximation to the observed earth pressures. In general, the observed earth pressures are more pronounced at the anchor levels, but decrease below the design intensity of pressure in the span between supports. One of the most important observations in the model tests was the comparatively small pressure that developed below the lowest level of anchors. This has important implications for the required toe reaction below the base of the excavation. Model test observations were in basic agreement with the earth pressure interpretations developed from measured bending strains for the full-scale wall sections constructed at Texas A&M.

Figure 76 compares the mobilized lateral earth pressures from the model walls with the pressures from the Texas A&M wall. Lateral earth pressures for the model walls and the full-scale walls were similar in shape. Mobilized lateral earth pressures for the one-tier wall were less than the design pressures. Mobilized lateral earth pressures for the two-tier walls were about equal to the design pressures. Lateral earth pressures at the second level of anchors in the two-tier walls reflect the effect of stressing the anchors. The lower lateral earth pressures in the span between the anchor and the bottom of the excavation in the one-tier wall reflect the pressures mobilized to support the ground below the anchors.

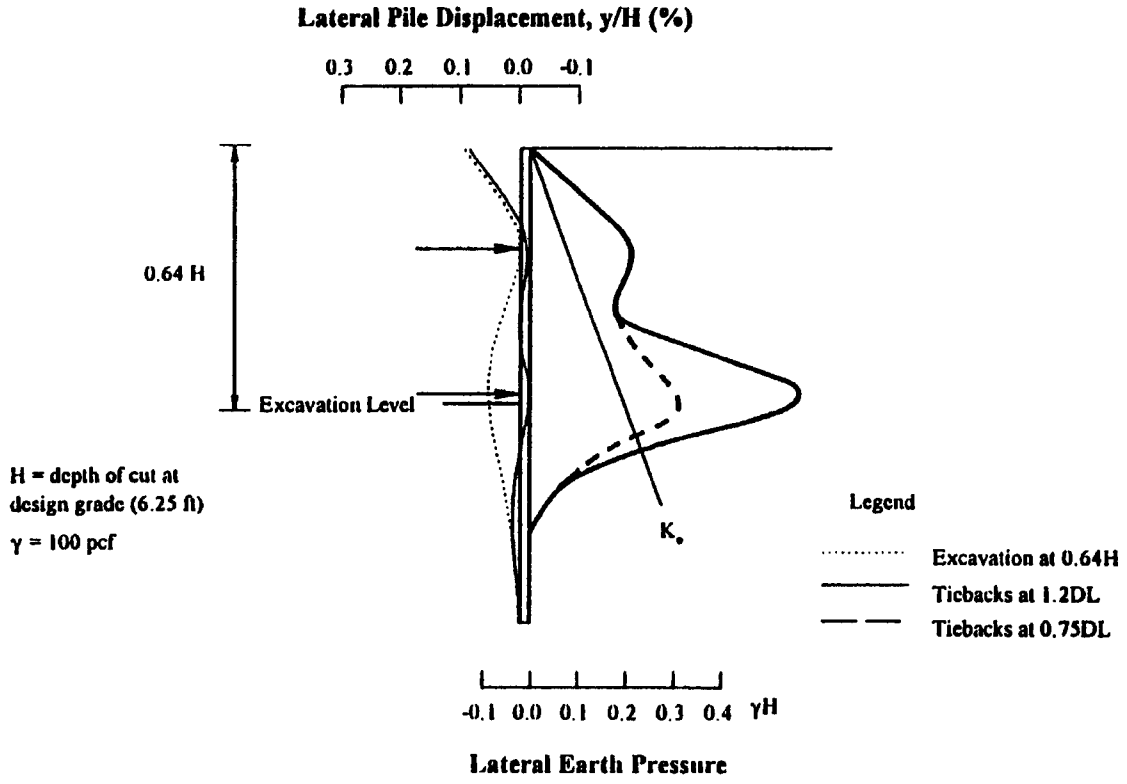

FIGURE 73
Lateral Wall Movements and Earth Pressures During Stressing of a Lower Anchor

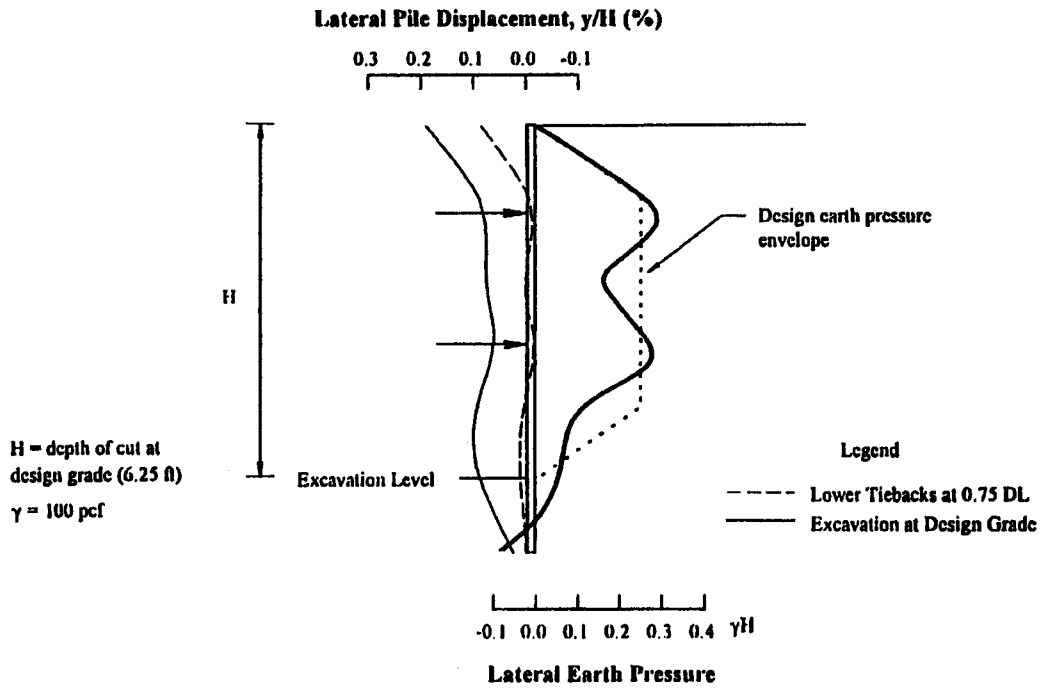

FIGURE 74
Lateral Wall Movements and Earth Pressures with Excavation at Design Grade – Two-tier Wall

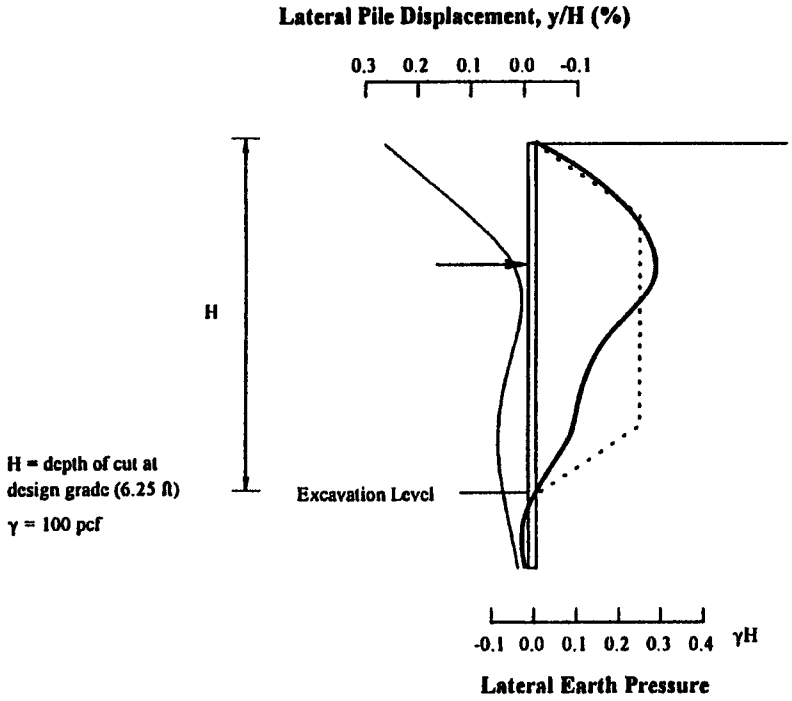

FIGURE 75
Lateral Wall Movements and Earth Pressures with Excavation at Design Grade – One-tier Wall

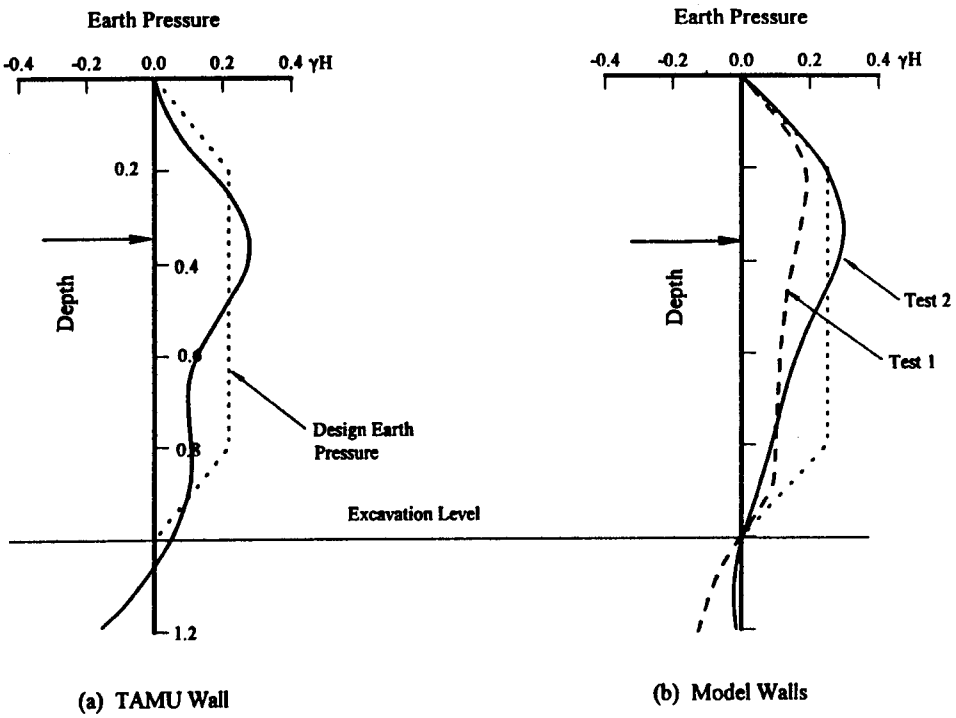

a) One-tier Walls – End of Construction

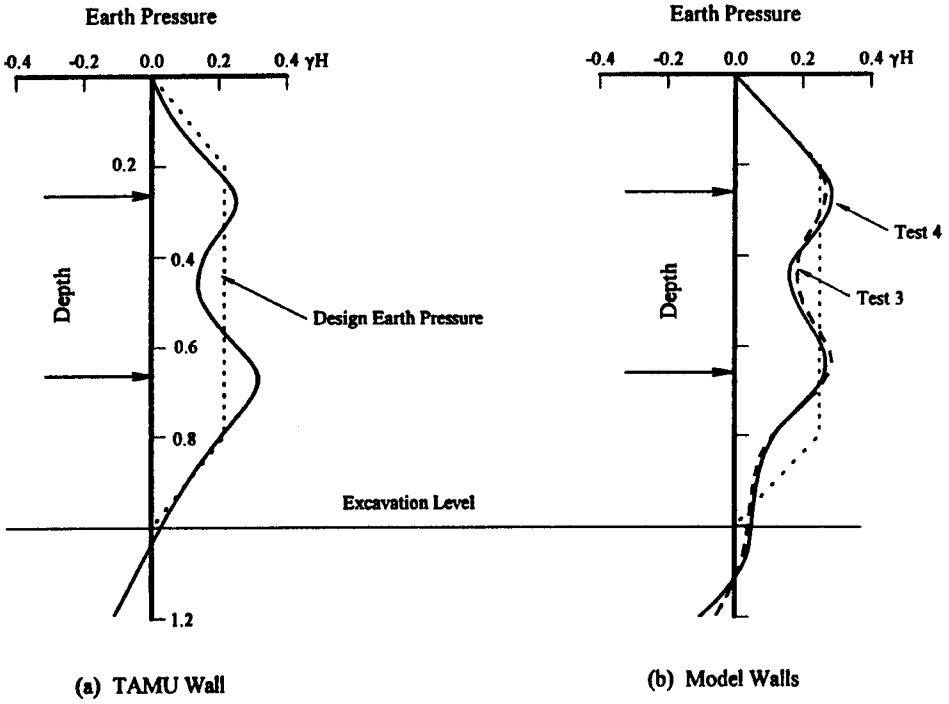

b) Two-tier Walls – End of Construction

FIGURE 76
Comparison of Lateral Earth Pressures on Texas A&M Walls and Model Walls

4.2.2 Ground Anchor Stressing Effects

Anchor stressing is done to balance the expected thrust associated with excavation and to reduce deformations that would develop if the anchors were unstressed. The importance of ground anchor stressing in controlling wall deformations was illustrated in a case history presented by Rizzo, et al. (1968). In the model tests, lateral earth pressures were determined principally by anchor stressing, with only small changes in lateral pressures associated with subsequent excavation. Locking-off the anchors in the model wall at 75 percent of the design load was adequate to control ground movements and prevented anchor load increases. The lock-off load was about 1.2 times the Rankine earth pressure.

In addition to reducing components of wall deformation associated with unstressed anchors, stressing also may be used to control lateral pressures on the lower part of the wall. This has implications for the design of the embedded portion of the soldier beam (toe). Figure 77 shows the distribution of shear and earth pressure at the end of construction for the model walls supported by one and two levels of ground anchors, respectively. The portion of the earth pressure diagram balanced by the horizontal component of anchor force is distinguished from the remaining earth pressure near the base of the wall. The earth pressure on the lower part of the wall is significantly less than the Coulomb pressure with fully mobilized wall friction, and is balanced by mobilized lateral toe resistance and beam tip shear. Even in Test 1, where anchor slippage contributed to a decrease in anchor forces, lateral earth pressures were less than the Coulomb pressures ($K_a = 0.18$) as shown in Figure 78.

Figure 79 summarizes the thrusts at the base of the walls, P_b, not balanced by the horizontal components of anchor force. Also shown in the table is the effective height of retained soil required to yield the observed thrusts, based on a Coulomb trial wedge analysis with $\phi = 40°$ and mobilized wall friction equal to $2/3\phi$. The equivalent heights range from about one-half to two-thirds of the length of the unsupported span below the lowest level of ground anchors. Support for the weight of soil above the effective height is maintained by the anchor load applied above.

The mechanisms by which the ground anchors support the weight of soil above some effective height can be understood by examining ground response during anchor stressing and subsequent excavation. During anchor stressing, the soldier beams are pulled back into the retained soil, resulting in development of a zone of compression. Even as the wall rotates outward as the soldier beam settlements, the zone of compression near the ground anchors is maintained (Figure 80). The development of a zone of compression behind an anchored wall also is consistent with observations by Sills, et al. (1977). They described ground response during construction of an anchored slurry wall in London clay, and observed significant lateral ground strains in the ground anchor bond zone. Despite the movements that developed in the bond zone, the zone of compression established during anchor stressing was maintained throughout construction. Figure 81 shows that the lateral movement near the front of the anchors was greater than lateral movements at the wall throughout the depth of the cut when the excavation

reached design grade. Thus, outward wall translation and rotation from sources other than wall settlement do not relieve the wall pressures developed during ground anchor stressing.

Excavation below an anchor results in lateral extension of the soil outside a "compression zone" developed during ground anchor stressing. The tendency for lateral extension of the soil is resisted by the compression zone. Lateral and vertical loads in the soil "arch" onto the zone of compression and the soil behind the critical failure surface (Figure 82). Arching reduces the vertical load on the wedge of soil supported by the base of the wall (zone 3 in Figure 82), resulting in a lateral load less than the Coulomb value for the full height of the cut.

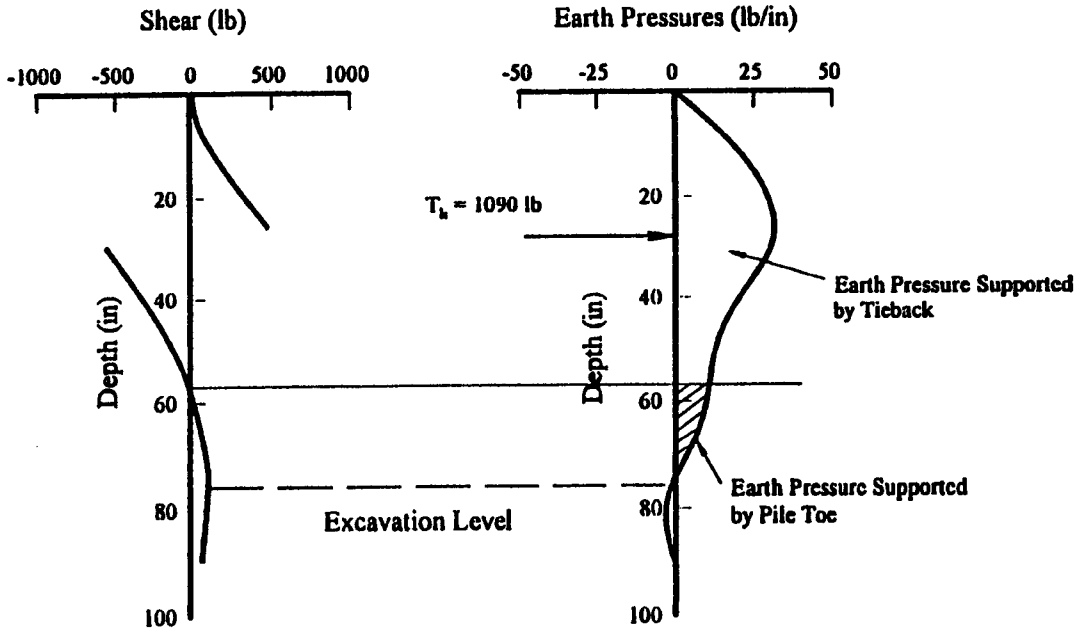

a) Model Test 2, SP4

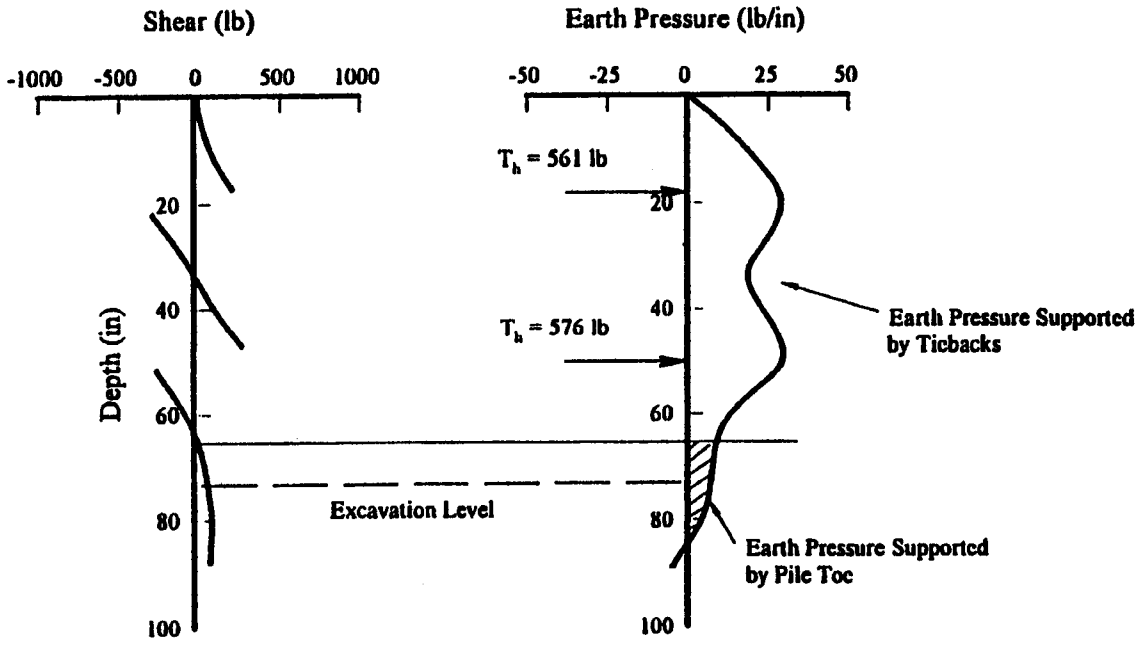

b) Model Test 4, SP4

FIGURE 77
Shear and Earth Pressures in Model Soldier Beams at the End of Construction

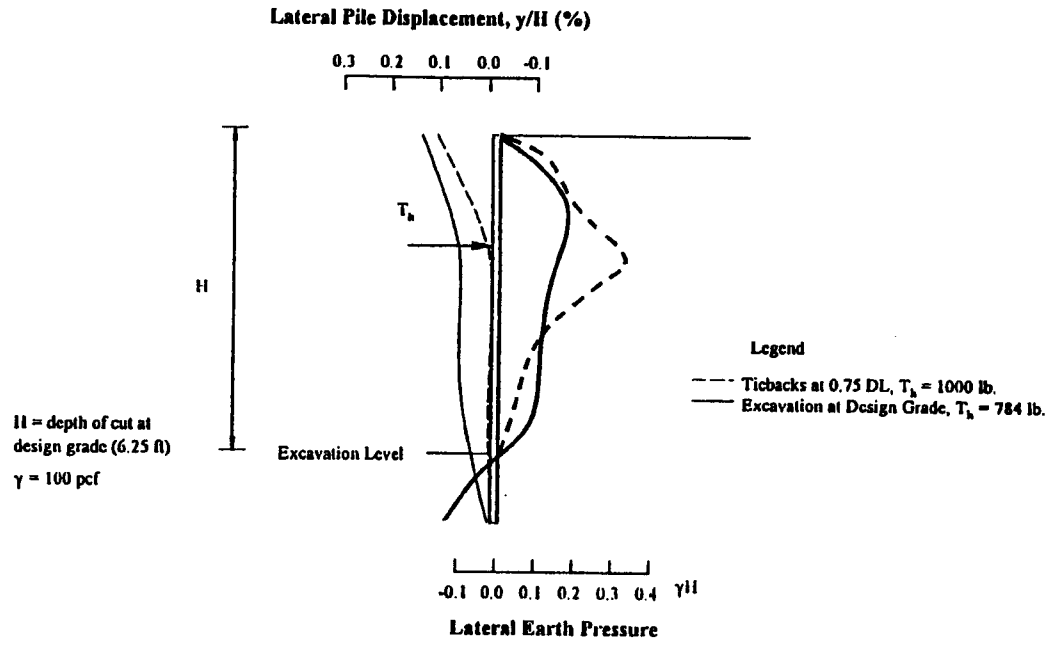

FIGURE 78
Lateral Wall Movements and Earth Pressures at End of Construction – Model Test 1, SP4

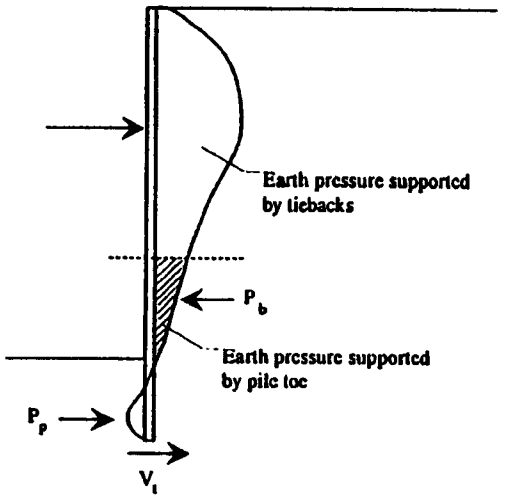

Test	P_b (lb)	H* (ft)
1	150	2.5
2	121	2.2
3	90	1.8
4	104	1.9

H* = height of wedge of soil required to yield the observed thrust near the base of the wall supported by pile toe

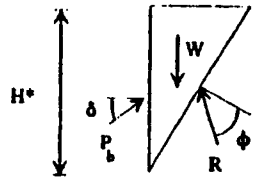

FIGURE 79
Summary of Lateral Earth Pressures at Base of Model Walls Supported by Passive Toe Resistance and Beam Tip Shear

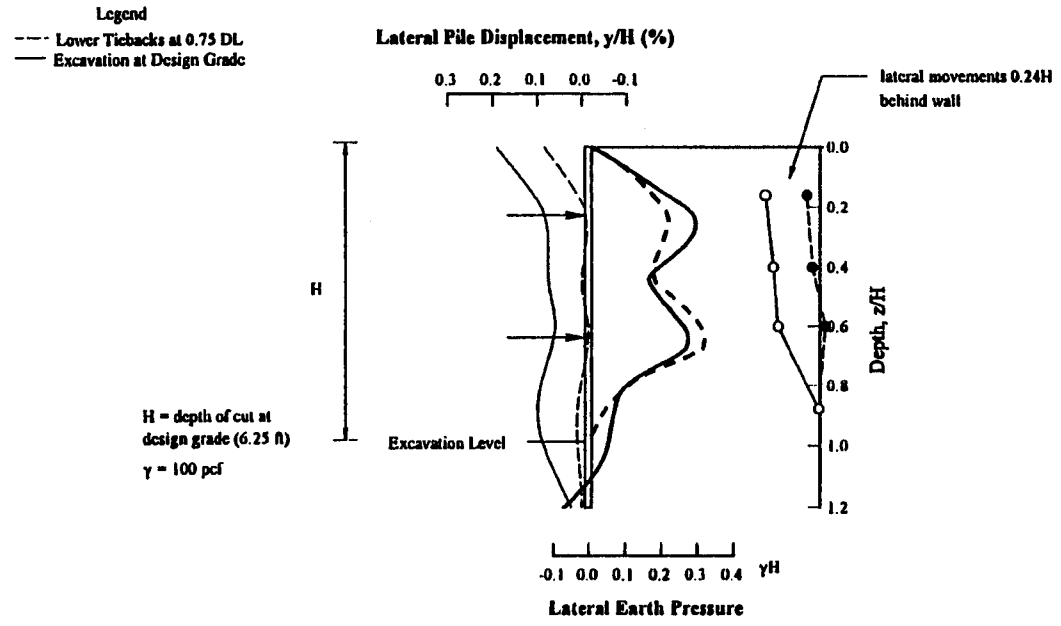

a) Model Test 4, SP4

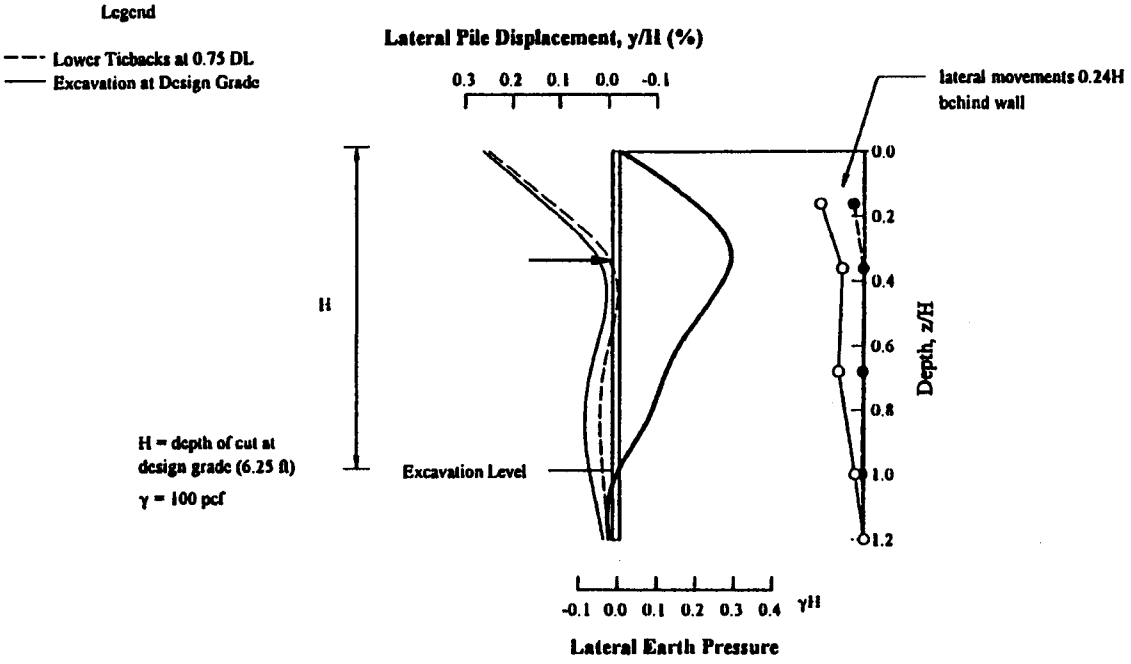

b) Model Test 2, SP4

FIGURE 80
Changes in Lateral Earth Pressures and Ground Movements During Excavation Below Anchor

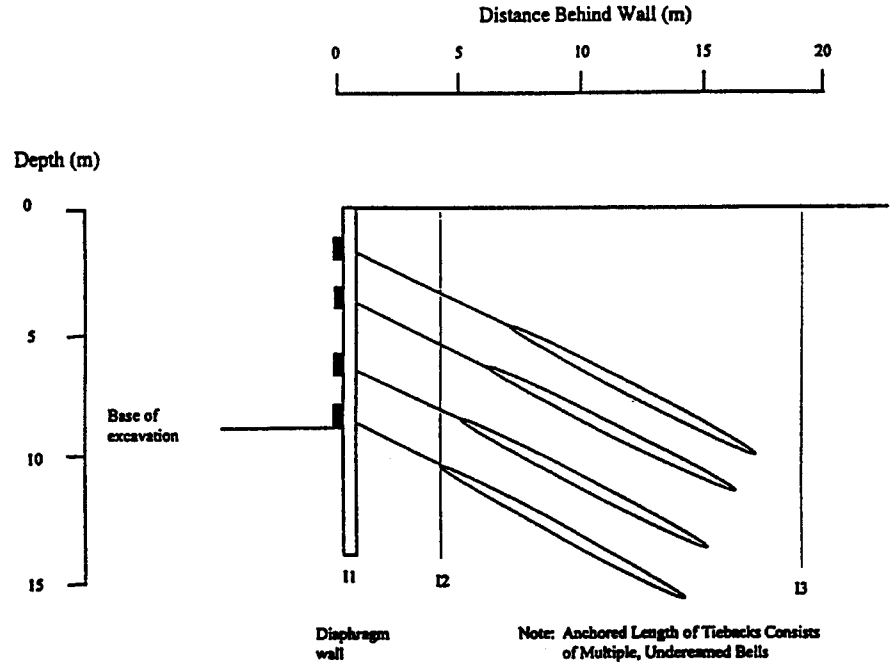

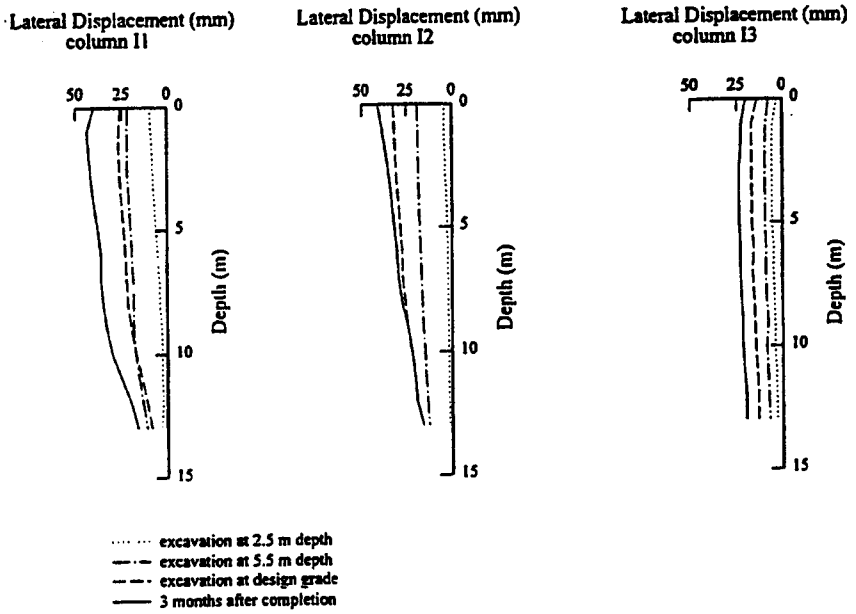

FIGURE 81
Lateral Wall and Ground Movements Behind an Anchored Slurry Wall in London Clay (Sills, et al. 1977)

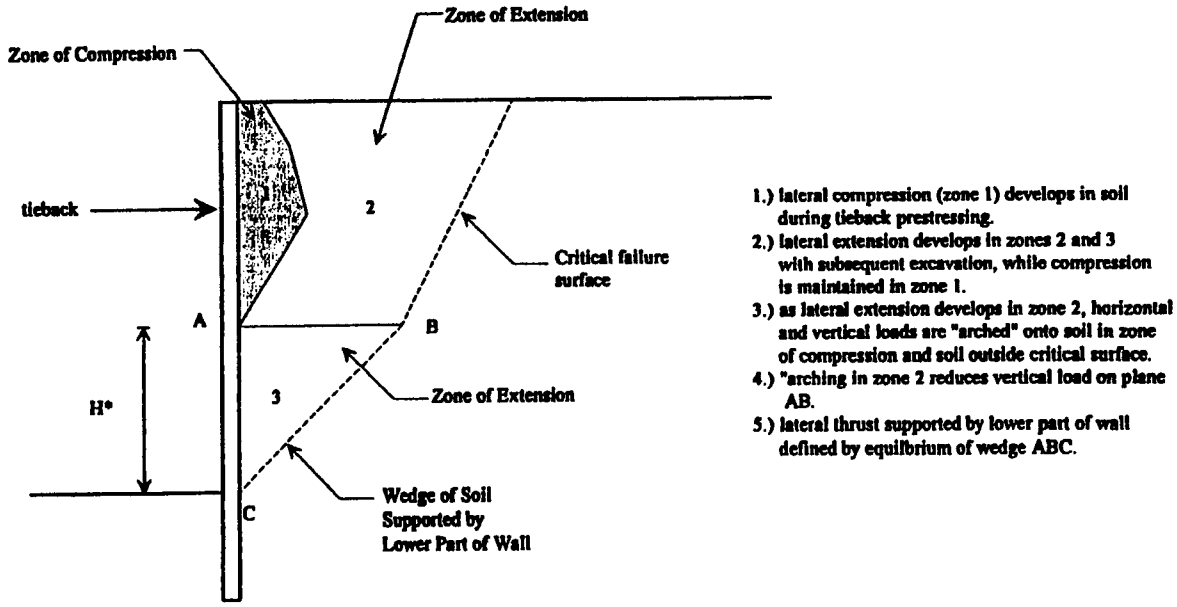

FIGURE 82
Illustration of Anchor Prestressing Effect as it Contributes to Pressures Near the Base of the Wall

4.2.3 Influence of Relative Stiffness

The low pressures near the base of the model anchored walls is consistent with observations made by Terzaghi (1941) for strutted excavations in sands in Berlin (Figure 83). In strutted walls, the low pressures near the bottom of the excavation probably result from a different mechanism of load transfer, compared with anchored walls. For the cases described by Terzaghi (1941), the struts were unstressed, except as a result of driving wedges to facilitate a tight connection between the struts and wales. Subsequent excavation below a strut resulted in lateral bulging of the walls, and load redistribution (arching) to the stiffer components of the system. The potential for load redistribution to the struts or base of the wall is a function, therefore, of the relative stiffness of the struts with respect to the toe. Comparatively small deformations are required to mobilize loads in the struts, so that there is little tendency for development of significant pressures in the toe of the wall.

It is conceivable that the low pressures near the base of the model walls resulted from low lateral toe stiffness. Although small increases in pressure near the base of the wall were observed during excavation below an anchor, these pressures are consistent with a limiting state of stress for the mechanics of ground response associated with ground anchor stressing. As a further

illustration of the influence of relative toe/anchor stiffness in the model tests, consider the changes in lateral pressure associated with unloading of the lower level of anchors in Tests 3 and 4 (Figure 84). Approximately 290 lb/ft of horizontal load was removed from the lower level of anchors in each test, resulting in significant bulging of the walls below the upper anchor. The horizontal component of load in the upper anchors increased between 70 and 100 lb/ft, while the reaction provided by the beam toe increased about 10 lb/ft in Test 3 and 50 lb/ft in Test 4. Thus, the ground anchors tended to attract more load in the model tests.

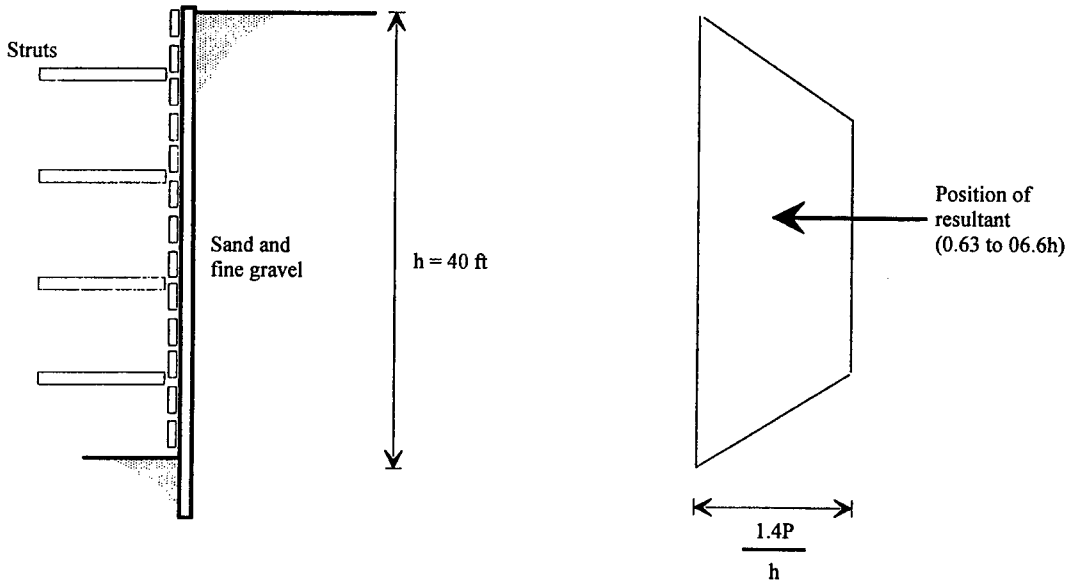

$P = 0.5C_k k_a Wh^2$

h = Depth

W = Weight of critical wedge

k_a = Active earth pressure coefficient for Coulomb conditions

C_k = Factor that depends on state of strain in the critical wedge (see Ohde, 1938)

FIGURE 83
Earth Pressures on a Soldier Beam and Lagging Wall Inferred from Strut Load Measurements (after Terzaghi, 1941)

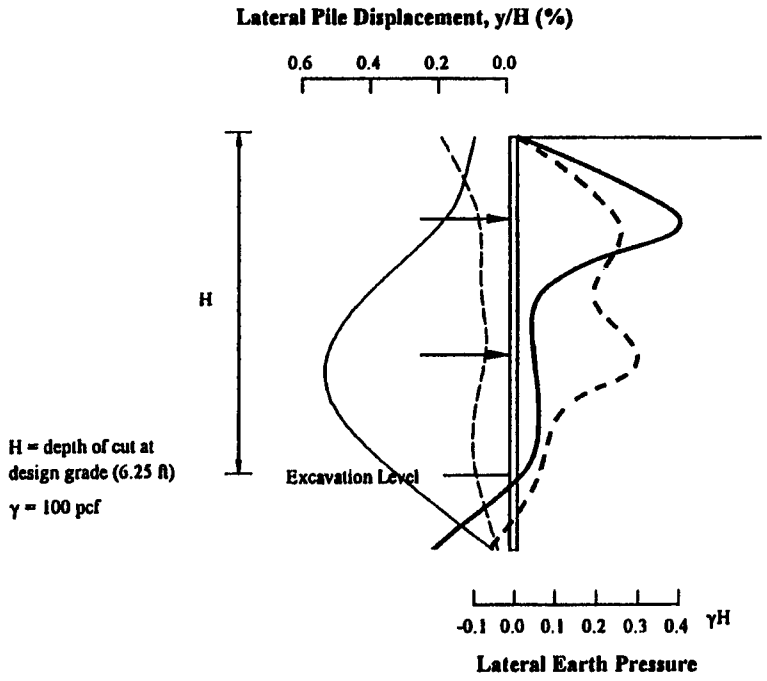

a) Model Test 3, SP4

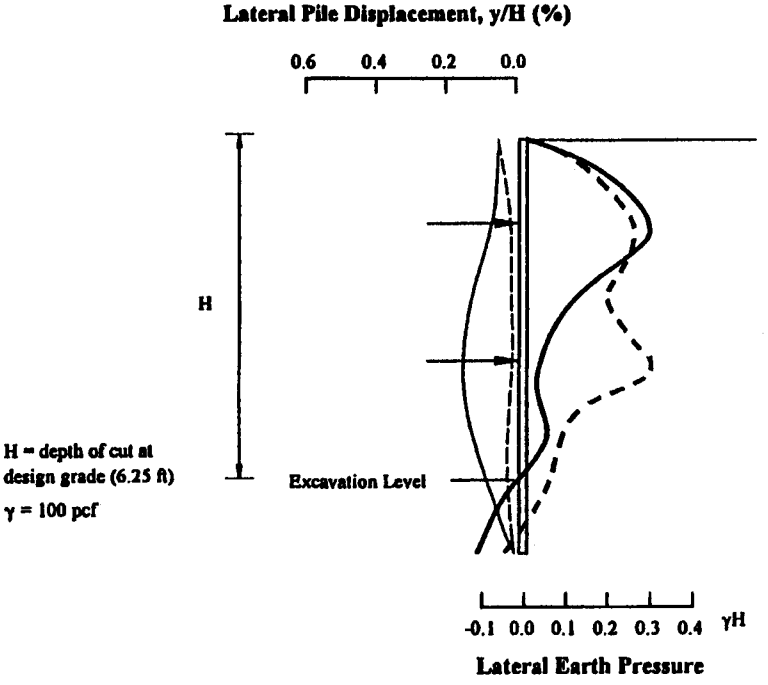

b) Model Test 4, SP4

FIGURE 84
Lateral Wall Movements and Earth Pressures During Unloading of Lower Anchors

4.2.4 Significance of Lateral Toe Resistance

In design of anchored walls, it is assumed that the earth pressure generated by construction is balanced by the ground anchor loads and mobilization of passive resistance along the embedded length of the wall. Toe penetration requirements are determined using force equilibrium or force and moment equilibrium for an assumed design earth pressure distribution. The required reaction below the base of the cut depends primarily on the shape of the design earth pressure and assumed boundary conditions. In general, more conservative toe depths result with a triangular distribution of pressure, compared with apparent earth pressure envelopes developed from strut load measurements.

One of the most significant observations in the model tests was that ground anchor stressing can be used to control the distribution of pressure on the wall. Anchor stressing locks in pressures in the vicinity of anchors, and results in comparatively small pressures near the base of the wall. As a consequence of the small lateral pressures at the base of the walls, mobilized passive toe resistances also were small, compared with computed required reactions. Table 9 summarizes the net toe reaction developed below the bottom of the excavation. Note that the base reactions consisted of passive resistance mobilized along the toe of the wall and beam tip shear.

TABLE 9
Observed Reaction Below the Base of the Excavation at Design Grade

MODEL TEST	SOLDIER BEAM NO.	PASSIVE RESISTANCE (lb)	BEAM TIP SHEAR (lb)	TOTAL LATERAL TOE RESISTANCE (lb)	PERCENT OF COMPUTED TOE REACTION (%)
1	SP4	101	5	106	29
	SP5	120	0	120	33
2	SP4	24	40	64	18
	SP5	32	38	70	19
3	SP4	17	36	53	28
	SP5	35	30	65	34
4	SP4	22	52	74	39
	SP5	68	12	80	42

Development of shear was significant for Model Tests 2 through 4, for which the soldier beams were supported on an enlarged bearing plate (4×6 in). For the axial forces on the soldier beam associated with ground anchor stressing, a mobilized coefficient of friction of between 5 and 10° is sufficient to account for the observed beam tip shear. A significant contribution of shear to the base reaction has also been inferred by Rowe (1952), from his model studies of dredged bulkhead behavior. The observed reaction developed along the toe

of the model soldier beams was typically not more than 40 percent of the computed required reaction.

The model test observations were in basic agreement with the earth pressure interpretations developed from measured bending strains for the anchored soldier beam and lagging walls constructed at Texas A&M. In addition, an experiment conducted by Casagrande (Terzaghi, 1941) for a cut in Boston further supports the model test observations. Wall geometry and soil conditions are shown in Figure 85. The wall consisted of soldier beams and wood lagging supported by two levels of struts. When the excavation was completed, a third level of struts was installed at the bottom of the cut, but they were not stressed. Rather, the soldier beams were cut immediately below the excavation level to observe the load redistribution that occurred due to removal of the lateral resistance provided by the toe. As summarized in Figure 85, small increases in strut loads, corresponding to about 15 percent of the precut loads, developed during cutting of the soldier beams. These observations suggest that mobilized toe resistance provides a small contribution to wall equilibrium.

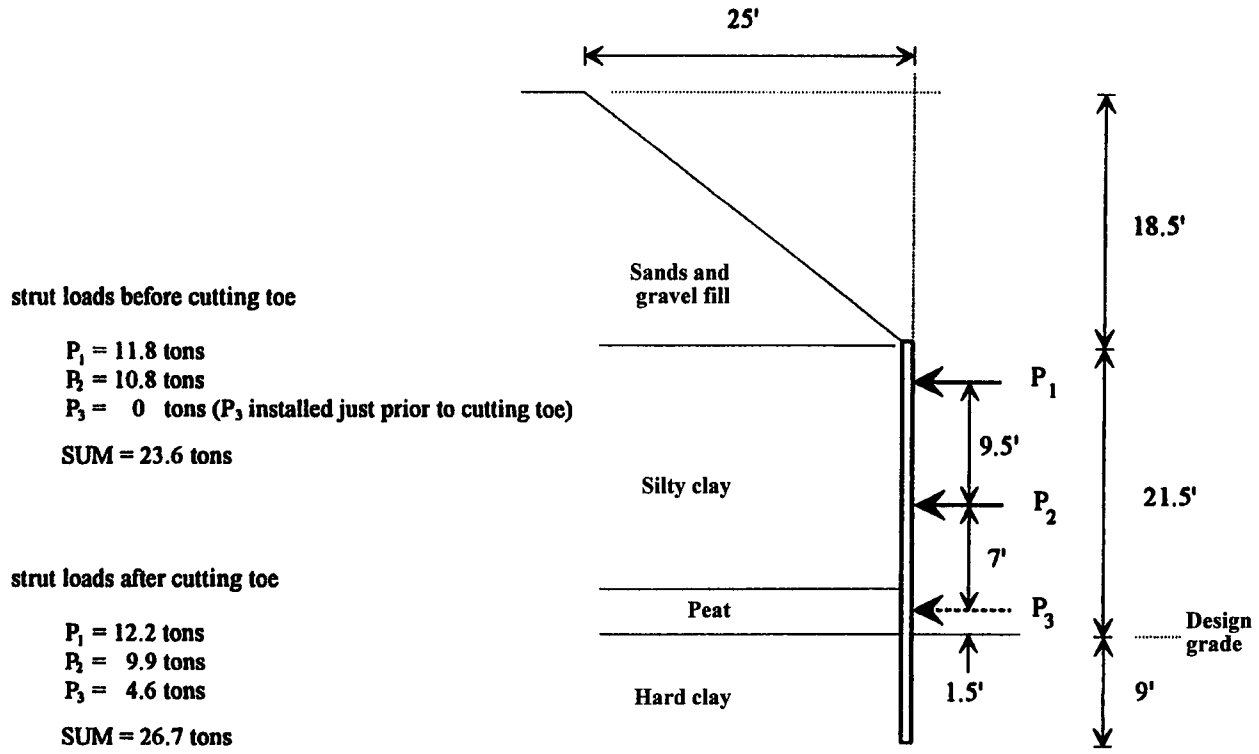

FIGURE 85
Increase in Strut Loads After Cutting of Soldier Beams at the Bottom of an Excavation in Boston (Terzaghi, 1941)

However, there are conditions where the lateral toe reaction can become significant. In Model Test 1, for example, the anchors failed to hold their intended loads. This resulted in a general flattening of the earth pressure near the anchors and increased pressure at the base of the wall (Figure 78). Significant toe resistance also would be expected where low anchor lock-off loads were used, and additional loads in the anchors developed through wall deformations. This condition is analogous to Rowe's (1952) measurements on flexible bulkheads prior to anchor yield (Figure 86).

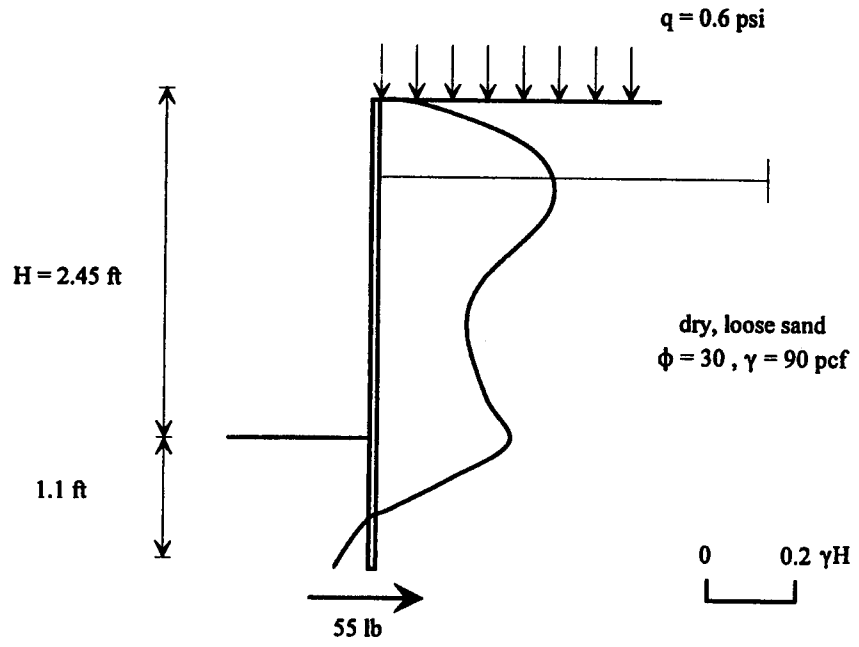

FIGURE 86
Earth Pressure Observations on Flexible Model Bulkheads in Sand (Rowe, 1952)

4.2.5 Practical Considerations

Anchored wall design assumes that the loads in the ground anchors and passive resistance in the toe can be used to balance the thrust associated with excavation. The first step in design, therefore, involves selecting a design earth pressure diagram that can be used to determine the anchor forces, toe penetration depths, and size structural elements of the wall. The total design thrust must be selected with consideration of acceptable levels of wall and ground movement. Model test observations suggest that a factored thrust of 1.3 times the limit value will control wall deformations associated with load increases in the anchors. This assumes that the total thrust is appropriately distributed to the anchors and toe of the wall, and the anchors are prestressed. Experience indicates that the anchor lock-off load should be selected to be be-

tween 75 and 100 percent of the design load determined from an apparent earth pressure diagram.

Model test observations provide insight into the appropriateness of triangular distributions of pressure versus apparent earth pressure diagrams. The tests suggest that wall supported by ground anchors develops earth pressure distributions consistent with apparent earth pressure envelopes developed from strut load measurements. From a practical perspective, use of a uniform or trapezoidal distribution of pressure offers the following advantages over a triangular distribution of pressure:

- Lower design moments and shears.
- Lower pressures at the base of the wall and, therefore, less significant soldier beam toe penetration to satisfy equilibrium of lateral forces.

Even as the model walls underwent significant outward rotation and translation, ground anchor stressing effects were maintained, so that the arguments for use of a triangular distribution of pressure (*Canadian Foundation Manual*, 1985) are inconsistent with model test observations. Furthermore, model test observations show load redistribution to the anchors during excavation below a support. Thus, it is probable, that even if anchor loads were determined using a triangular pressure distribution, load redistribution would produce a nearly uniform distribution of pressure. Load redistribution occurred in the model walls supported by one row of anchors or two rows of anchors. Therefore, conventional apparent earth pressure diagrams should be used to design flexible anchored walls supported by one or more rows of ground anchors. As shown in Figures 87 and 88, a trapezium of earth pressure with intensity of $25H$ gives a reasonable estimate of observed ground anchor forces, toe reactions, and bending moments. If the model walls had been designed to support a rectangular apparent earth pressure diagram, measured anchor loads, toe reactions, and bending moments may have been similar to the values predicted by the rectangular diagram. However, a trapezoidal diagram represents the observed behavior of the wall better than the rectangular diagram. The trapezoidal diagram concentrates the load at the anchors and reduces the load at the ground surface and the bottom of the excavation.

The observations discussed above are appropriate for sands and stiff soils. The presence of soft clays in the soil profile will require additional considerations regarding earth pressures and overall wall stability. For example, consider the case where a weak soil overlies a stiff soil, and the excavation goes through the weak soil and the soldier beams are embedded into the stiff soil. Pressures on the lower portions of the wall would be greater than those observed in the model tests, and the beam toe would develop (and require) greater toe resistances in the stiff soil. In addition, for excavations into deep soft clay deposits with the toe stopping in the soft clay, it is possible that very little toe resistance is developed due to the wall moving with the soil or the development of a deep-seated failure extending beyond the limits of the toe. However, if the wall extends through the soft clay to rock, then significant shear could be developed in the tip of the wall, if the depth to rigid bearing is not too great.

M_{max} = 260 ft-lb/ft, M_{min} = - 84 ft-lb/ft (Test 1)
M_{max} = 245 ft-lb/ft, M_{min} = - 66 ft-lb/ft (Test 2)

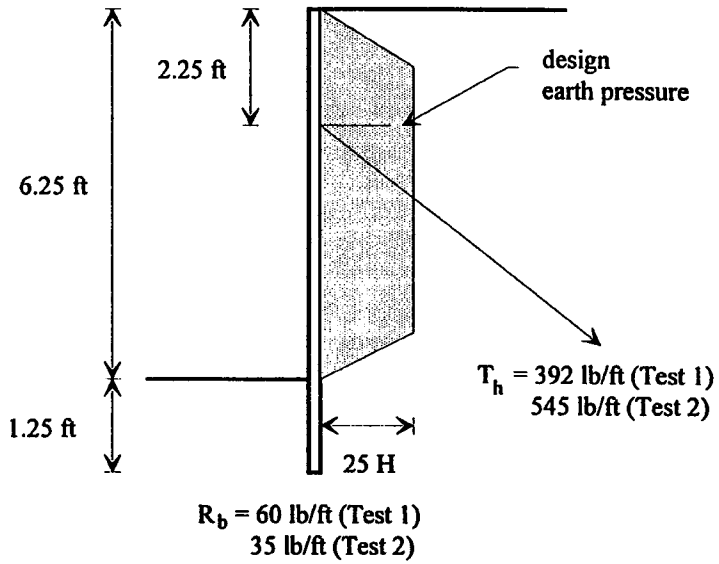

Calculated Forces

1.) Tributary Area Method

T_h = 565 lb/ft R_b = 215 lb/ft M_{max} = 216 ft-lb/ft
M_{min} = -95 ft-lb/ft

2.) Hinge Method

T_h = 609 lb/ft R_b = 171 lb/ft M_{max} = 216 ft-lb/ft
M_{min} = -180 ft-lb/ft

FIGURE 87
Comparison of Calculated and Observed Anchor Forces, Toe Reactions, and Bending Moments for Model Walls with a Single Level of Anchors

M_{max} = 86 ft-lb/ft, M_{min} = - 35 ft-lb/ft (Test 3)
M_{max} = 75 ft-lb/ft, M_{min} = - 33 ft-lb/ft (Test 4)

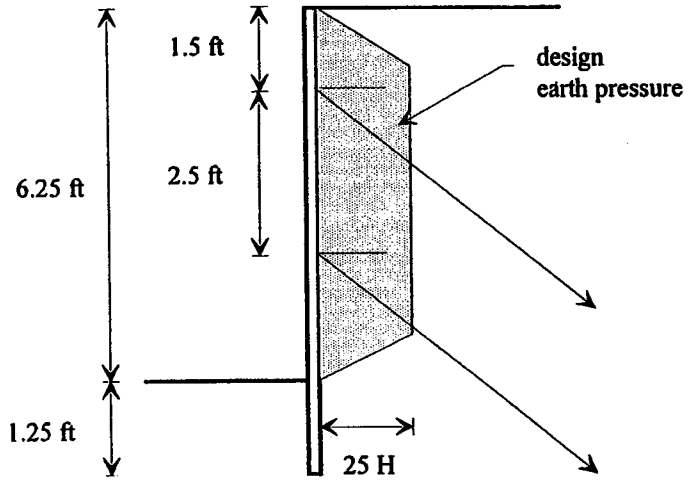

R_b = 33 lb/ft (Test 3)
40 lb/ft (Test 4)

Calculated Forces

1.) Tributary Area Method

T_{h1} = 332 lb/ft R_b = 79 lb/ft M_{max} = 70 ft-lb/ft
T_{h2} = 369 lb/ft M_{min} = -53 ft-lb/ft

2.) Hinge Method

T_{h1} = 350 lb/ft R_b = 96 lb/ft M_{max} = 70 ft-lb/ft
T_{h2} = 333 lb/ft M_{min} = -75 ft-lb/ft

FIGURE 88
Comparison of Calculated and Observed Anchor Forces, Toe Reactions, and Bending Moments for Model Walls with Two Levels of Anchors

4.3 AXIAL LOADS

Ground anchor stressing introduces a vertical component of force in a wall, which ranges from 20 to 50 percent of the lock-off load for typical anchor inclinations. Downward movement of the wall with respect to the retained soil is required to develop support for the vertical component of anchor force. The distribution of axial load along the length of the wall principally depends on the displacements required to mobilize end bearing and skin friction, movements within the supported ground, and the normal stresses on the wall established by ground anchor stressing. Subsequent excavation reduces the ability of the ground to maintain support for the vertical component of anchor force in the zone of significant ground movements. Furthermore, if the excavation causes vertical displacements in the ground (adjacent to the wall) to exceed the vertical settlement of the beam, additional vertical load will be transferred to the wall (downdrag).

The transfer of axial load requires relative vertical displacement between wall and soil. If the wall experiences a greater settlement than the surrounding soil, axial load is transferred from the wall to the soil. On the other hand, if the soil settlement exceeds the wall settlement, load is transferred from the soil to the wall. Model Test 4 is used to illustrate the effect of relative movements on axial load transfer during construction (Figures 12 through 18 and Figure 22).

When the soil next to the wall undergoes less settlement than the wall, then some axial load in the wall is transferred to the soil. These conditions are common for the portion of the wall embedded below the excavation. Upon stressing the first level of anchors in Model Test 4, the axial load in the wall was equal to the vertical component of the anchor force (Figure 13). Because the vertical displacement of the wall is greater than the soil, load transfer occurred from the wall to the surrounding soil. As a result of load transfer from the wall to soil, the axial load decreases with depth.

If the soil adjacent to the wall settles more than the wall, then some of the soil weight will be transferred to the wall (downdrag). As the excavation proceeded below the anchor level in Model Test 4, the retained soil moved out and down relative to the wall (Figure 14). This relative movement caused a partial transfer of soil weight to the wall, resulting in an increase in axial load along a portion of the soldier beam (Figure 15).

Two conditions may result in little axial load transfer: (1) when relative displacements between the soil and beam are very small, or (2) when the interface between wall and soil is weak. The last stage of construction for Model Test 4 illustrates this effect. After the last anchor was locked-off, excavation continued to design grade. Upon completion, the axial load in the wall was approximately equal to the vertical component of the ground anchor load (Figure 22). Very little transfer of axial load was observed along the embedded portion of the beam. Vertical movements of the soldier beam and ground below grade were minor, and as a result, little load was transferred to the soil. The axial load was carried by the soldier beam in end bearing.

Section 2.5.3 of *Summary Report of Research on Permanent Ground Anchor Walls*, "Volume II: Full-scale Wall Tests and a Soil-structure Interaction Model," (Weatherby, et al., 1998) discuses the axial loads applied to anchored walls in more detail and presents four case histories that illustrate the different aspects of axial load behavior. Design guidance is also included in Section 2.5.3.

4.4 SUMMARY

Model-scale anchored wall tests, full-scale tests on anchored walls, and performance of other anchored walls reported in the literature were used to establish the magnitude and character of lateral and vertical forces exerted on anchored walls. Significant aspects of their behavior are summarized below:

- Ground anchor stressing results in significant increases in lateral pressure on the wall with relatively small wall deformations.
- Earth pressure changes during excavation below an anchor were comparatively small. This illustrates the effectiveness of ground anchor stressing in controlling components of wall deformation associated with the tendency for load redistribution.
- Development of rotational and translational movements during anchored wall construction did not result in a triangular distribution of pressure.
- Near the ground anchors, the design earth pressure envelope represents a good approximation of the observed earth pressures. In general, the observed earth pressures are the highest at the anchor levels, and decrease below the design pressure in the span between supports.
- Comparatively small pressures developed below the lowest level of anchors. This has important implications for the required toe reaction below the base of the excavation. Model test observations were in basic agreement with the earth pressure interpretations developed from measured bending strains for the two full-scale wall sections constructed at Texas A&M.
- Lock-off load equal to 75 percent of the design load (about 1.2 times the Rankine earth pressure) were adequate to control movements of the wall. Anchor loads did not increase during construction.
- Earth pressures on the lower part of the wall were significantly less than the Coulomb pressures with fully mobilized wall friction. The earth pressures were balanced by mobilized lateral toe resistance and beam tip shear.
- In general, more conservative toe depths result with a triangular distribution of pressure, compared with apparent earth pressure envelopes developed from strut load measurements.
- Anchor stressing locks in pressures near the ground anchors and results in comparatively small pressures near the base of the wall.

- Reaction developed along the toes of the model soldier beams were typically less than 40 percent of the computed required reaction.
- Trapezoidal apparent earth pressure diagrams are recommended for the design of one-tier and multi-tier walls because of the load redistributions that occur during construction of anchored walls.
- From a practical perspective, use of apparent earth pressure diagrams offers the following advantages over a triangular distribution of pressure: (a) lower design moments and shears and (b) lower pressures at the base of the wall and, therefore, less significant toe penetration to satisfy equilibrium of lateral forces.
- The transfer of axial load requires relative vertical displacement between wall and soil. If the wall experiences a greater settlement than the surrounding soil, axial load is transferred from the wall to the soil. On the other hand, if the soil settlement exceeds the wall settlement, load is transferred from the soil to the wall.

CHAPTER 5
GROUND ANCHOR STUDY

Ten hollow-stem anchors were installed in stiff clay at the U.S. National Site for Geotechnical Experimentation at Texas A&M's Riverside Campus. Six of the ground anchors were instrumented to measure strain in the steel tendon and the anchor grout. Four of the ground anchors were loaded for 70 days to investigate their long-term, load-carrying capacity.

5.1 OBJECTIVES OF THE RESEARCH

The primary focus of the study was to develop an understanding of the behavior of straight-shafted ground anchors installed in stiff cohesive soils. The principal objectives of the research were:

Objective 1 — Study and identify the distribution of strain along the shaft length, and the mechanisms by which load is transferred into the ground. In particular, determine if the section of the grout column above the tendon bond length carries load in compression, and transfers load to the ground.

Objective 2 — Monitor the movements of the grout body during anchor testing to gain increased knowledge of tendon debonding and its effect on load transfer.

Objective 3 — Verify that a short-term creep test can be used to reliably predict long-term, load-carrying capacity of an anchor.

Objective 4 — Determine if the load-displacement-time performance of a ground anchor is load-history dependent. Determine if retesting of a failed ground anchor should be allowed.

5.2 SUBSURFACE CONDITIONS

The test anchors were installed in a very stiff clay associated with the Crockett Shale formation of the Claiborne Group (Kubena, 1989). Over the years, in situ and laboratory tests had been performed to characterize the soil at the site (Briaud, 1991). The data collected from these tests is summarized in Table 10.

TABLE 10 Summary of the Soil Properties at the Anchor Test Site (after Briaud, 1991)

Depth (m)	Description	Plastic Limit (%)	Water Content (%)	Liquid Limit (%)	Total Unit Weight kN/m^3	Undrained Shear Strength (kN/m^2) Compression	Mini Vane	Texas Cone	Pocket Pen.	DDS[1] c' ϕ'	CPT[2] Point kN/m^2	CPT[2] Friction kN/m^2	PMT[3] Limit Press kN/m^2	PMT[3] Modulus kN/m^2	SPT[4] N Blows/0.3m	DMT[5] P0 kN/m^2	DMT[5] P1 kN/m^2
1	Sandy Clay	16	19	35	20.1	95 (UC)		130	115		2000	100	470	6250		260	550
2		18	18	50	20.6	130 (UC) 56 (UU)		90	120	Peak =	1400	115	550	11250	9		
3	Sandy Clay	20.5	20	58.5	20.2	140 (UC) 97 (UU)	150	120	165	$5kN/m^2$, 32°	1900	95	740	11600	11	250	850
4																900	1550
5	Fissured Red Clay	26	30	60	18.7	115 (UC)	140	110	150	Residual =	3000	155	950	22000	16		
6	Gray Clay Sand Seam	24	35	65	18.6	80 (UC)	130	105	140	$0kN/m^2$, 30°					16	250	1950
7						110 (UU)					11500	100				2550	3950
8											5000	200			27		
9	Gray Clay	24	26	72	19.2	209 (UU)			>200	Peak =	6150	240	2400	60000	35	3250	4300
10										$28kN/m^2$, 17°						2830	4200
11											6150	195			31		
12	Gray Clay	20	23	59	19.7	96 (UU)			>200	Residual =	8600	220	3100	120000	44	2600	4400
13						134 (UU)				$10kN/m^2$, 11°							
14											9000	355					
15	Gray Clay	24	25	58	18.7	187 (UU)			>200		8900	360	4600	200000			
16																	
17											10000	350					
18											11000	300					
19																	
20	Gray Clay	23	25	46	21.0	135 (UU)			>200		9400	330	6700	230000			
21											7500	300					
22																	
23	Gray Clay												9100	265000			
24																	
25																	
26																	
27																	
28	Gray Clay												5600	280000			
29																	
30																	
35	Gray Clay												4750	430000			

NOTE: DDS = Drained Direct Shear Test[1] PHT = Pressure Test DHT = Dilatometer Test[3]
CPT = Cone Penetrometer Test[2] SPT = Standard Penetration Test[4]

Two Cone Penetrometer soundings (CPT8 and CPT9), one Preboring Pressuremeter boring (PBPMT2), one Dilatometer boring (DMT), and one Standard Penetration boring (SPT) were made as part of the anchor test program. The locations for the tests are shown in Figure 89, a location plan for the test anchors. Figure 90 shows the SPT Boring Log. Disturbed samples and Shelby Tube samples were collected every 5 ft in the boring. Laboratory tests were conducted to determine unit weight, natural water content, Atterberg limits, and unconsolidated undrained shear strength (UU tests). Tables 11 and 12 summarize the result of the in situ and laboratory test. The Appendix contains the CPT logs, plots of the PBPMT results, and plots of the DMT results.

TABLE 11
Summary of SPT, CPT, and Laboratory Data for the Anchor Test Site (after Briaud, 1991)

DEPTH (ft)	LABORATORY TESTS				ATTERBERG LIMITS			IN SITU TESTS						
	USCS Soil Classification	Unit Weight (pcf)	Moisture Content (%)	s_u (psi)	Liquid Limit (%)	Plastic Limit (%)	Plasticity Index	SPT (blows/ft)	CPT8			CPT9		
									Q_s (tsf)	Q_c (tsf)	F_r (tsf)	Q_s (tsf)	Q_c (tsf)	F_r (tsf)
5	CH	125	23.9	12.5	51	18	33	9	0.8	10	8.0	1.5	18	8.3
10		122	23.6	11.5				11	1.0	18	5.6	0.9	20	8.3
15	CH	129	29.3	18.0	77	27	49	16	1.1	20	5.5	2.0	40	4.5
20		129	29.7	12.2				16	1.5	220	4.7	0.5	10	5.0
25	CL	127	24.2	18.6	43	11	32	27	2.0	50	4.0			
30		122	29.5					35	3.5	60	5.8	1.3	63	2.1
35	CH	119	29.6	18.3	84	34	50	31	2.7	61	4.4	1.2	62	1.9
40		122	27.3	19.7				44	3.4	90	3.8	1.0	82	1.2

TABLE 12
Summary of PMT Data for the Anchor Test Site
(after Briaud, 1991)

DEPTH (ft)	PMT2		
	E_o (ksf)	E_r (ksf)	P_l (ksf)
4	111	167	5.9
9	319	732	16.0
14	333	815	14.9
19	275	1924	34.0
24	632	1595	44.5
34	511	2253	44.0
39	1613	3195	83.0

The soil profile at the site consists of a stiff to very stiff clay from zero to 20 ft, a 1-ft-thick sand layer between 20 and 21 ft, a very stiff to hard clay from 20 to 40 ft, and a very hard clay or clay shale below 40 ft (Briaud, 1991). A small amount of groundwater was present in the sand layer at a depth of 20 ft.

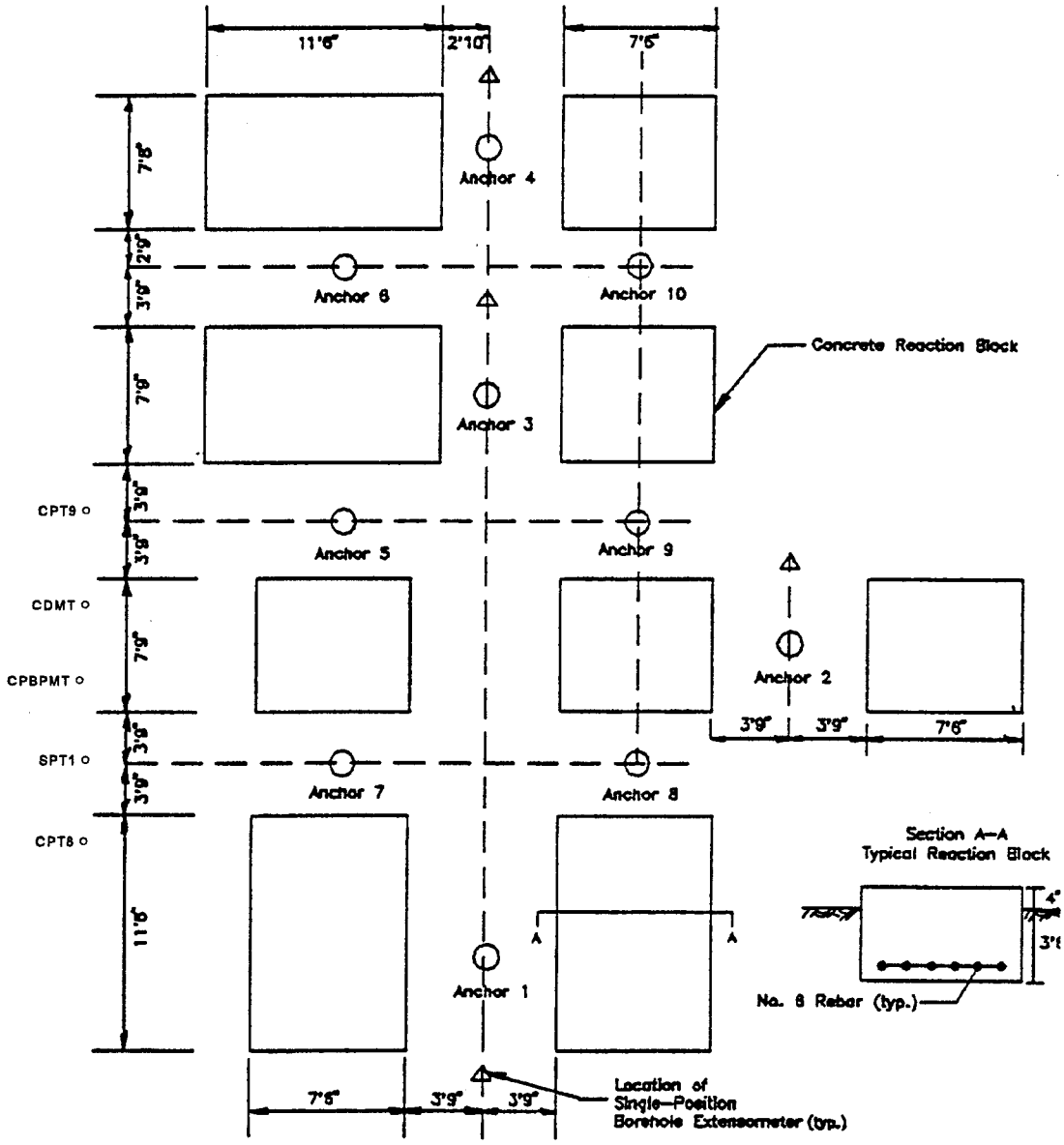

FIGURE 89
Test Anchor Location Plan

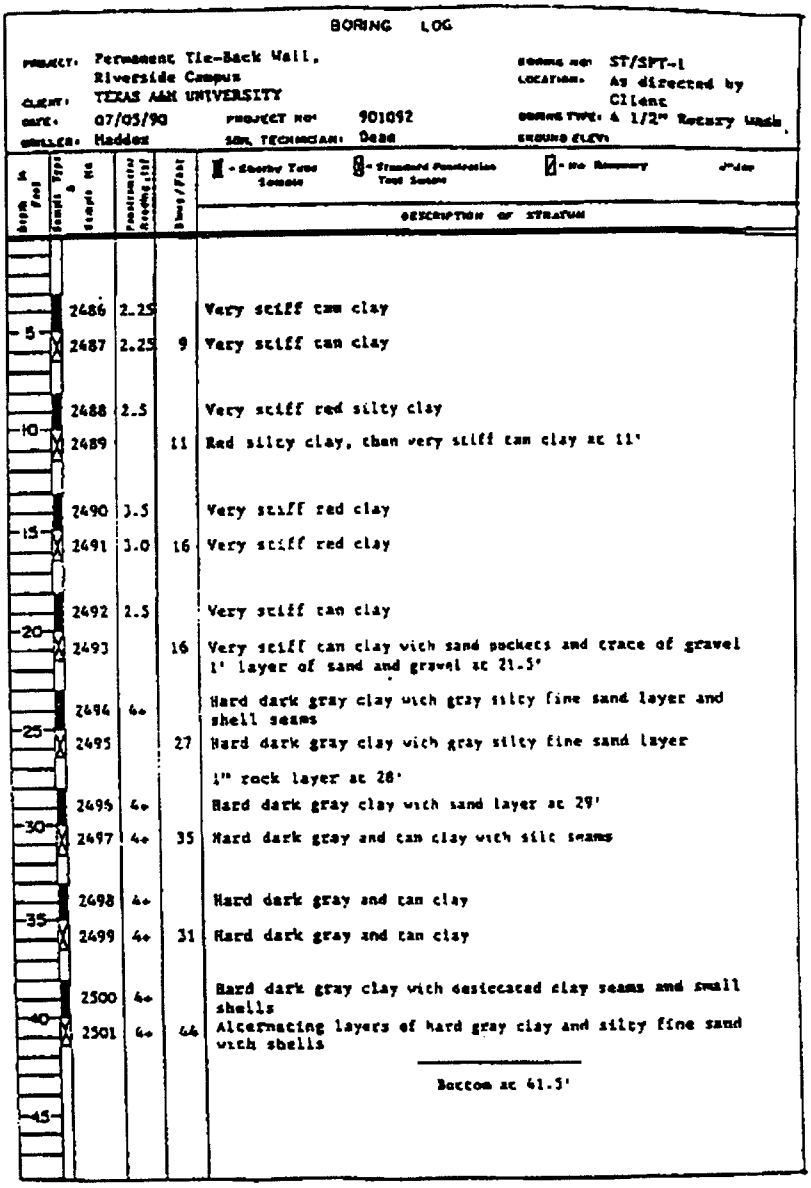

BORING LOG

PROJECT: Permanent Tie-Back Wall, Riverside Campus
CLIENT: TEXAS A&M UNIVERSITY
DATE: 07/05/90
DRILLER: Haddox
PROJECT NO: 901092
SOIL TECHNICIAN: Dean
BORING NO: ST/SPT-1
LOCATION: As directed by Client
BORING TYPE: 4 1/2" Rotary Wash
GROUND ELEV:

S - Shelby Tube Sample
SPT - Standard Penetration Test Sample
NR - No Recovery

Depth in Feet	Sample Type & No.	Penetrometer Reading, tsf	Blows/Foot	DESCRIPTION OF STRATUM
	2486	2.25		Very stiff tan clay
5	2487	2.25	9	Very stiff tan clay
	2488	2.5		Very stiff red silty clay
10	2489		11	Red silty clay, then very stiff tan clay at 11'
	2490	3.5		Very stiff red clay
15	2491	3.0	16	Very stiff red clay
	2492	2.5		Very stiff tan clay
20	2493		16	Very stiff tan clay with sand pockets and trace of gravel 1' layer of sand and gravel at 21.5'
	2494	4+		Hard dark gray clay with gray silty fine sand layer and shell seams
25	2495		27	Hard dark gray clay with gray silty fine sand layer
				1" rock layer at 28'
	2496	4+		Hard dark gray clay with sand layer at 29'
30	2497	4+	35	Hard dark gray and tan clay with silt seams
	2498	4+		Hard dark gray and tan clay
35	2499	4+	31	Hard dark gray and tan clay
	2500	4+		Hard dark gray clay with desiccated clay seams and small shells
40	2501	4+	44	Alternating layers of hard gray clay and silty fine sand with shells
				Bottom at 41.5'
45				

FIGURE 90
Boring Log at the Ground Anchor Test Site

5.3 ANCHOR DESIGN AND CONSTRUCTION

Ten, 12-in-diameter, 45-ft-long, hollow-stem-auger anchors were selected for the test program. Vertical tiedown anchors were installed since a wall was not constructed at the site.

5.3.1 Design

The ground anchors were designed to fail during testing. Originally, a total anchor length of 60 ft was selected. After completing the subsurface investigation, the total ground anchor length was shortened to 45 ft to ensure that the anchors could be failed. The ultimate capacity of the anchor was estimated using Equation 5.1.

$$T_u = \pi\, d_s\, l_a\, \alpha\, s_u \qquad \ldots [5.1]$$

T_u = ultimate capacity of the anchor
d_s = anchor diameter
l_a = anchor length
α = adhesion factor
s_u = undrained shear strength of soil

Using an average undrained shear strength of 2700 psf and an adhesion factor of 0.6, the ultimate load-carrying capacity of the anchors was estimated to be 229 kips. Tendon bond lengths and the grouting procedures were varied to investigate different aspects of load transfer behavior. Table 13 presents the different lengths for Anchors 1 to 10 and Figure 91 describes how these lengths are defined.

TABLE 13
Lengths for Test Anchors

ANCHOR NO.	TOTAL TENDON LENGTH (ft)	DRILLED LENGTH (ft)	TENDON BOND LENGTH (ft)	UNBONDED LENGTH (ft)
1 - 6	51.0	45.0	15.0	36.0
7 - 10	51.0	45.0	30.0	21.0

Anchor tendons were fabricated from seven, 0.6-in-diameter, seven-wire prestressing strands. Each strand had a cross-sectional area of 0.217 in^2. The specified minimum ultimate tensile strength for an individual strand was 58.6 kips. The maximum test load that could be applied to an anchor tendon was 328 kips. Bare strands were bonded to the anchor grout over the tendon bond length. A grease-filled polypropylene sheath was applied over the unbonded length. The sheath served as a bond breaker and allowed the tendon to elongate elastically between the tendon bond length and the stressing head.

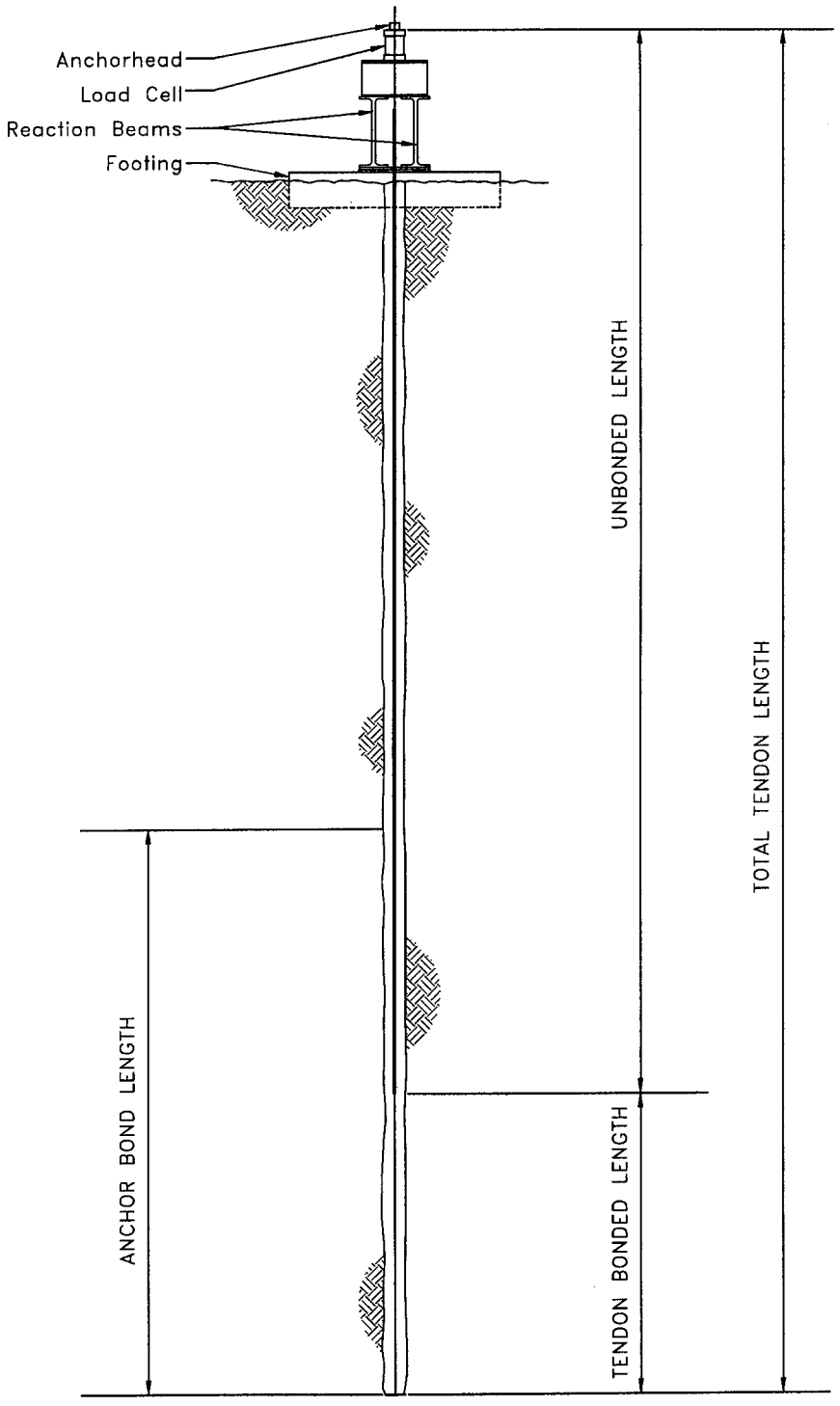

FIGURE 91
Diagram Illustrating Test Anchor Lengths

5.3.2 Construction

A 12-in outside diameter, 4-in inside diameter continuous auger was used to install the anchors. The auger was powered by a hydraulic rotary head capable of developing 12,000 ft-lb of torque. Auger and rotary head were mounted in swing leads that were supported from a crawler crane.

Anchor tendons were manually inserted in the auger, while the leads lay flat on the ground. Then a drill point was fixed to the end of the auger. The cast iron point retained the tendon in the auger while the leads were raised and moved into position, formed part of the cutting head, and sealed the hollow auger stem during drilling.

Anchors were drilled continuously to the 45-ft depth. When the required drilling depth was reached, the auger was slowly extracted while grout was pumped down the stem of the auger. Effective grout pressures of 100 psi were maintained during the grouting of the bottom 35 ft of the anchor. Grout pressures along the upper 10 ft were lower. Auger rotation was kept to a minimum during the extraction of the auger. Grout slump ranged between 6.5 and 10 in, and grout 28-day compressive strengths varied between 3,167–6,700 psi. Theoretical grout volume required to fill the hole was 1.3 yd^3. The estimated actual volume was 1.5 yd^3.

5.3.3 Load Test Frame

All 10 anchors were tested to establish their load-deformation and strain-distribution behavior. A typical test arrangement is shown in Figure 92. A 175-ton hydraulic jack was used to apply the test load to the tendon anchor. Concrete footing provided the reactions for the applied load and pairs of W30×108 reaction beams distributed the test load to the footings. Resting on the reaction beams was a waler fabricated from two C15X33.9 sections. The jack rested upon a bearing plate, and the electrical resistance load cell was set on top of the jack. On each side of the load cell were 9×9×2.5-in bearing plates.

The hydraulic pressure gauge on the pump was used to measure the load applied to the anchor. The pressure gauge was accurate to approximately 1000 lb.

Movements of the ground anchor were measured using a dial indicator capable of measuring to the nearest 0.001 of an inch. The dial indicator was attached to a wooden reference beam, as shown in Figure 92. The reference beam was isolated from the anchor and the reaction system.

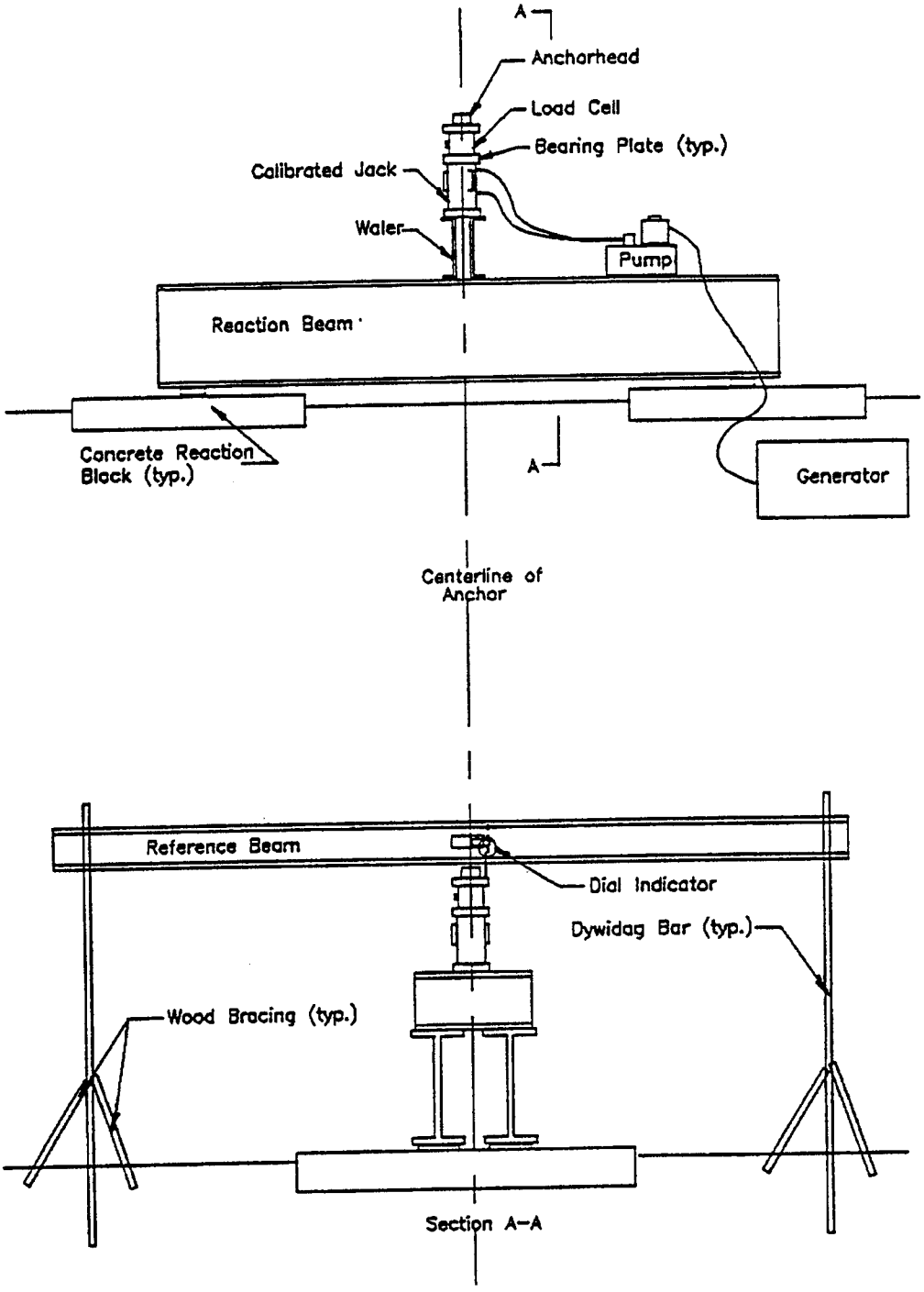

FIGURE 92
Diagram Illustrating the Ground Anchor Load Test Frame

5.4 INSTRUMENTATION

Vibrating wire strain gauges were used to measure the strains within the grout and in the prestressing strain. Electrical resistance load cells were used to monitor load changes during constant load hold periods. The load cells also were used to monitor the load during the 70-day load hold period.

5.4.1 Strain Gauges

Geokon model VCE 4200 vibrating wire embedment gauges were used to measure the strain in the anchor grout. Specially-made Geokon strainmeters were used to measure the strain in the steel tendon. Strain gauges were installed in Anchors 1, 2, 7, 8, 9, and 10. Embedment strain gauges were placed in the grout surrounding the tendon bond length and unbonded length. The strainmeters were attached to the strands in the tendon bond length. Figure 93 shows how the strain gauges were placed. The locations of the strain gauges in each anchor are shown Figure 94. Strainmeter end blocks had to be cushioned so they were free to move with the tendon and not restrained by the anchor grout. Polyurethane foam injected into a mold placed around the end blocks formed the cushion.

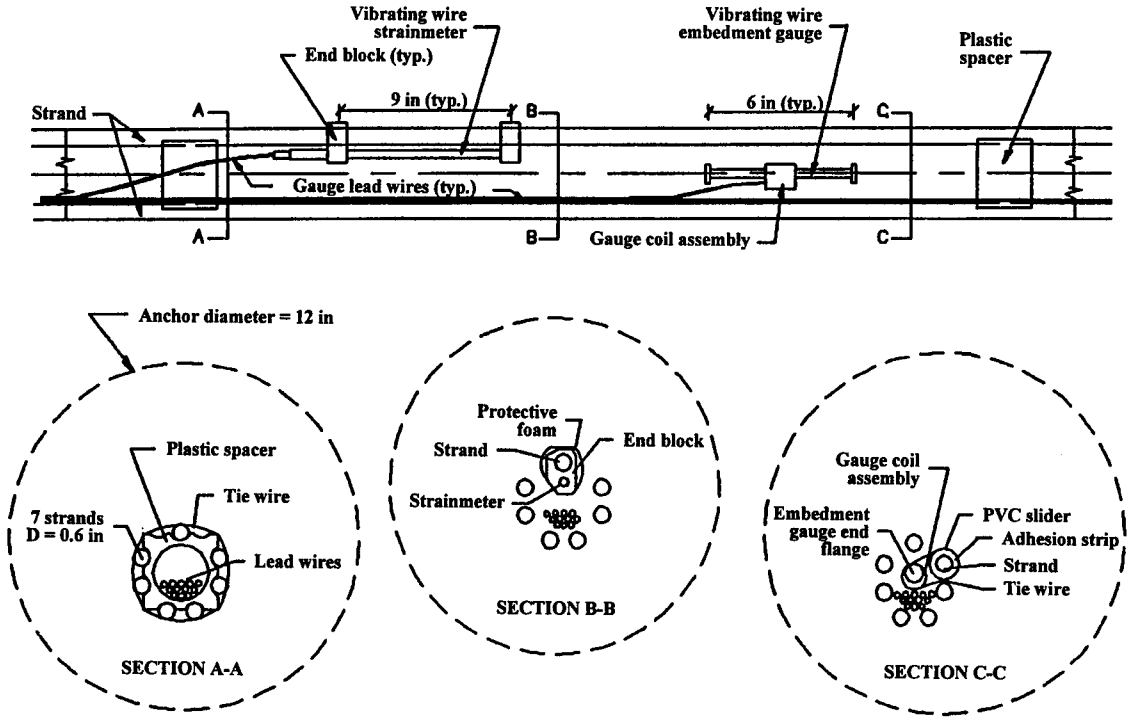

FIGURE 93
Embedment Gauge and Strainmeter Installation for Test Anchors

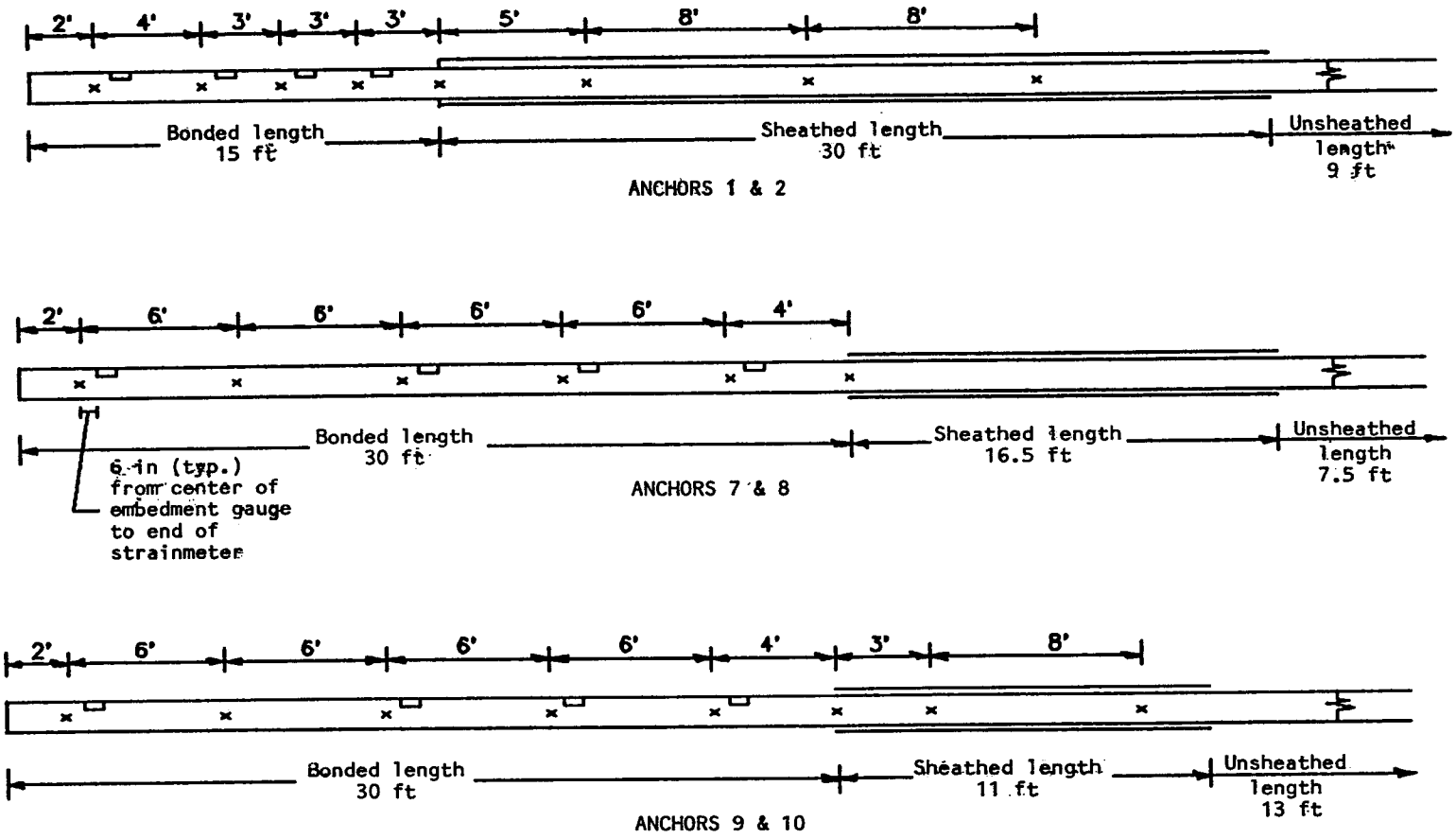

FIGURE 94
Gauge Locations for Instrumented Anchors

5.4.2 Load Cells

Geokon Model 3000-400-4.0 electrical resistance load cells were used to measure anchor load and monitor small changes in load during constant load hold periods. The load cells were also used to monitor the load during the 70-day load hold.

5.4.3 Extensometers

Geokon Model A-3 single-position extensometers were installed to monitor movement of the reaction beams during the 70-day load hold. Reaction movement would cause load changes unrelated to ground anchor movement through the ground. Load changes during the 70-day monitoring period were corrected for reaction movements. Figure 95 shows how the extensometers were installed. A custom-made leveling device was used to measure the movement of the bearing plate with respect to the invar steel extensometer rod anchored below the bottom of the ground anchor. Section 5.5.2.3 describes how the load readings were adjusted for movements of the reaction frame.

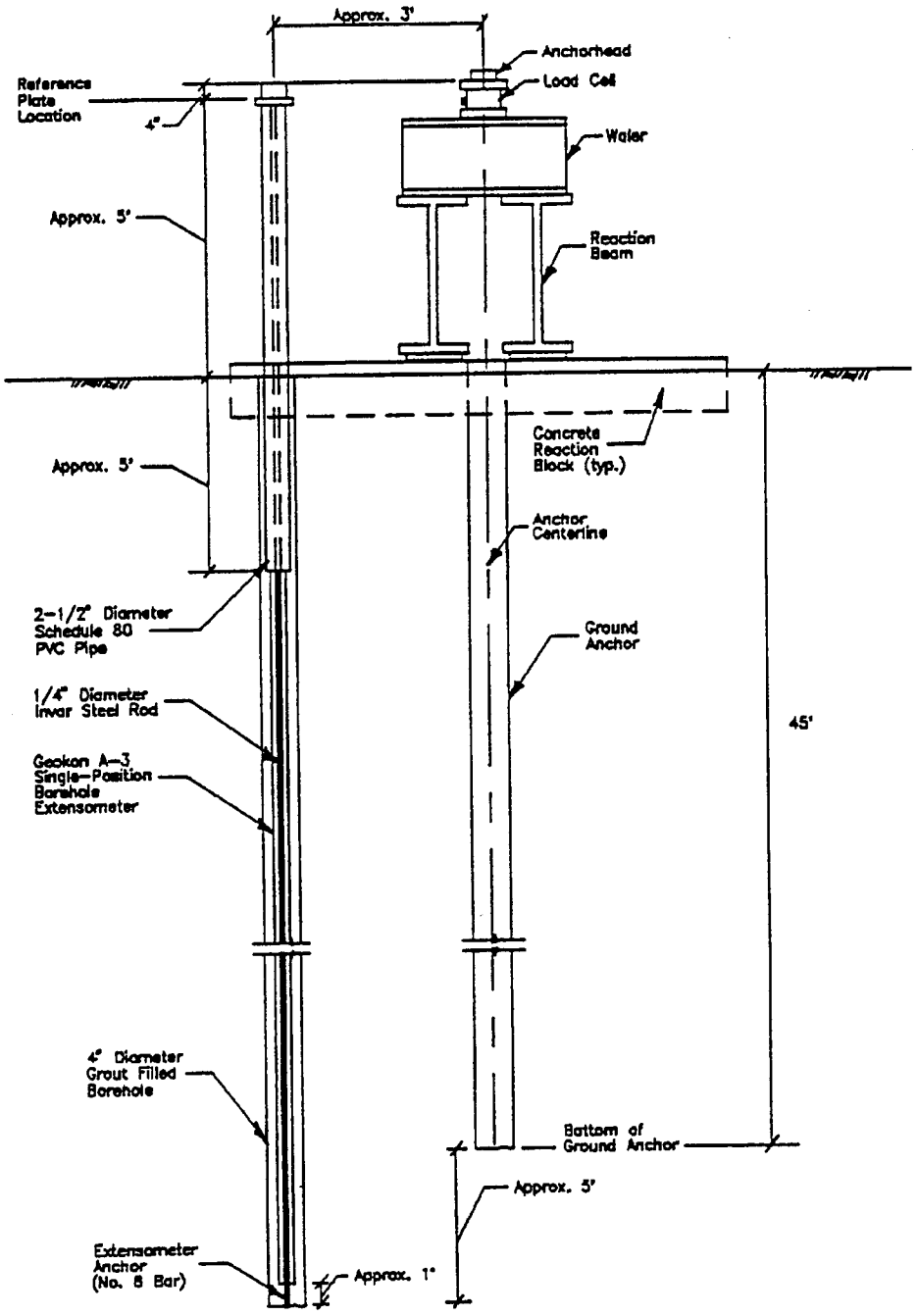

FIGURE 95
Borehole Extensometer Reference for Measuring Movement of the Reaction Beams During the 70-Day Load Hold (not to scale)

5.5 ANCHOR LOAD TESTS

5.5.1 Load Tests Performed

Four types of load tests were conducted during the research: proof, performance, creep, and 70-day load hold tests. Figure 96 shows the loading sequence used for each type of test. The proof, performance, and creep tests were similar to those recommended by AASHTO-ARTBA-AGC's Joint Task Force 27 (1990). Table 14 identifies the tests done on the anchors. During loading, the ultimate capacity of each anchor was estimated by evaluating the time-dependent anchor movements during constant load holds. The objective was to apply a load high enough to cause time-dependent anchor movements without failing the anchor during an initial load test.

TABLE 14
Schedule of Anchor Tests Performed

ANCHOR	TYPE OF TEST							DATE(S) OF TESTS
	PROOF		PERFORMANCE		CREEP		70-DAY LOAD HOLD	
	Initial Loading	Final Loading	Initial Loading	Final Loading	Initial Loading	Final Loading		
1					✓	✓	✓	04/08/91 - 04/10/91 04/19/91 - 07/14/91 07/14/91 - 07/16/91
2					✓	✓	✓	04/10/91 - 04/12/91 04/19/91 - 07/12/91 07/12/91, 07/13/91
3	✓	✓					✓	04/04/91 04/19/91 - 07/10/91 07/10/91
4			✓	✓			✓	04/03/91 04/19/91 - 07/09/91 07/09/91
5	✓	✓						03/26/91 03/26/91
6			✓	✓				03/20/91 03/20/91
7					✓	✓		03/08/91, 03/11/91 03/18/91, 03/19/91
8					✓	✓		03/06/91, 03/07/91 03/07/91
9					✓	✓		03/27/91 03/17/91, 03/28/91
10					✓	✓		03/21/91 03/22/91

Each anchor was retested. The first test is called the initial loading and the second test is designated the final loading. Load increments in the initial and final loadings were generally identical. Retesting was done to detect if the load-movement behavior of the anchors was load-history dependent.

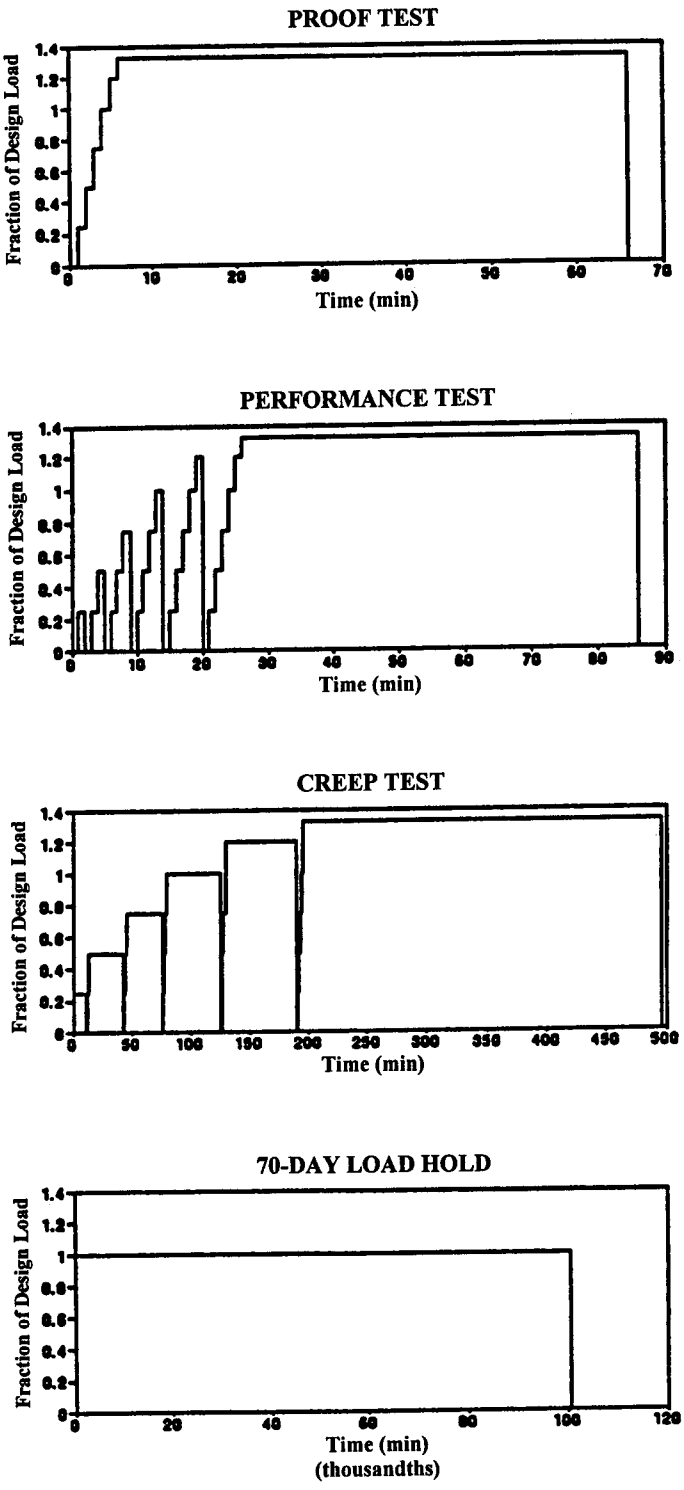

FIGURE 96
Diagram Illustrating the Different Loading Sequences for the Ground Anchor Tests

5.5.2 Ground Anchor Test Results

5.5.2.1 Total, Residual, and Elastic Movements

Figures 97 to 106 contain plots of the total and residual movements versus test loads for the initial and final loadings on Anchors 1 to 10. Test results for the initial loading are represented by the open circles and solid lines. Results for the final loading are represented by the dotted lines and open squares.

Total movements are the measured movements of the anchorhead during testing. During performance and creep tests, the anchors were incrementally loaded and unloaded, as shown in the load sequences in Figure 96. To simplify the presentation of the data, only the total movement at the conclusion of each loading cycle is plotted (Figures 97 to 106).

Residual movements are the non-recoverable movements measured when the anchor load is reduced from a test load to an alignment load. For example, in Figure 106, the movement reading after the load was reduced from 133 kips to the alignment load was 0.250 in. The 0.250-in residual movement was plotted as a function of the 133-kip test load. Residual movements are a measure of an anchor's movement through the ground in response to the test load.

Total movement and residual movement curves for the initial tests show greater movements than the corresponding final loading curves. This behavior illustrates an aspect of time-dependent behavior of ground anchors in fine-grained soils. If the test anchors had been installed in rock or coarse-grained soils, there would not have been as noticeable a difference between the initial and final test curves. The difference between the initial and the final loading were observed in all the anchors no matter how the tendons were bonded to the anchor grout.

Elastic movements of the ground anchor are not shown. They are equal to the total anchor movement minus the residual movement.

5.5.2.2 Creep Movements

Depending on the type of test conducted, different load increments were held constant and creep movements were measured and recorded. Ground anchor creep movements were measured during each load hold. Anchor 6 failed at a relatively low load, and creep movements were taken on Anchor 6. The creep rate in units of inches per log cycle of time for different loads are shown in Figures 97 to 106. Figure 106 shows a typical creep rate plot. The creep rate increases linearly with load until the test load approaches the ultimate capacity of the anchor. As an anchor's ultimate capacity is approached, the creep rate increases and the creep rate curve changes slope.

Ground anchor testing specifications use a creep definition of failure. North American and European standards define a creep failure to occur when the creep rate exceeds 0.08 in per log cycle of time. The creep rate curves for the initial loadings suggest that the established failure criterion is valid for the anchors installed at Texas A&M. When the creep rate exceeded 0.08 in per log cycle, the slope of the creep rate curve changed significantly (Anchors 4, 5, 7, 8, and 10). A creep rate of 0.08 in per log cycle is appropriate for a failure criteria for large-diameter hollow-stem auger-anchors. Anchors that fail the creep criteria had additional load-carrying capacity (Anchors 5, 7, 8, and 10).

Creep rates observed during the initial loading were greater than those observed during the final loading for each anchor. As mentioned earlier, differences between the initial and the final loading resulted from the preloading. Anchor 4 (Figure 100) is of particular interest. During the initial test on Anchor 4, the creep rate at a load of 179 kips was 0.103 in per log cycle of time. This rate exceeded the accepted creep failure rate of 0.08 in per log cycle. When Anchor 4 was retested, the creep rate at a load of 175 kips was 0.029 in per log cycle of time. This rate was well below the failure rate used in specifications. The lower creep rate observed during the final loading of Anchor 4 clearly shows that preloading (load history) affects the creep behavior of a ground anchor. The differences between the initial and the final loading creep rates indicate that the practice of retesting anchors installed in fine-grained soils should be discouraged.

Retesting of regroutable anchors installed in fine-grained soils is a common practice. The above results indicated that retesting of anchors in fine-grained soils may not give a realistic evaluation of an anchor's long-term, load-carrying capacity. For example, if a regroutable anchor carried the maximum test load but failed because its creep rate was too high, then it might behave like Anchor 4 and pass a retest. In this case, retesting would not evaluate the effectiveness of the regrouting. If retesting a regroutable anchor that failed the creep criterion is necessary, then the duration of the load hold should be extended to establish a "virgin" creep rate. Tentatively, it is recommended that the test be extended for 60 min or half a log cycle beyond the original load hold period, whichever is greater.

If a regroutable anchor failed to achieve the maximum test load, it may be regrouted and retested. If regrouting enables the anchor to carry a load 10 percent higher than the original failure load, then preloading effects are believed to be small. Until experience or research suggests otherwise, a creep rate of 0.08 in per log cycle of time can be used for these regroutable anchors.

5.5.2.3 Seventy-day Load Hold Tests

After the initial loading tests were done on Anchors 1 to 4, they were loaded and their load was observed for 70 days (100,800 min). Seventy days was selected, since the time-dependent movement of a ground anchor is believed to vary with the log of time and the movements observed would be 67 percent of the movements observed during 50 years.

The lock-off loads applied to each anchor were selected to be approximately 50 percent of the estimated ultimate capacity for that anchor.

During the 70 days, anchor loads were monitored using electrical resistance load cells. Load changes could result from reaction beam movements, load cell errors, tendon relaxation, temperature-induced strains, time-dependent degradation of the tendon-grout bond, grout creep, and anchor movements. Reaction movements were expected to be large since the soils at the site undergo large-volume changes in response to seasonal moisture changes. Therefore, load readings were corrected for reaction beam movements during the load-hold period. Reaction beams (bearing plate) movements were measured with respect to a single position extensometer anchored below the bottom of the ground anchor (Section 5.4.3). Reaction beam movements between 0.03 and 0.085 in were measured during the observation period. Load changes resulting from movement of the reaction frame were estimated using Equation 5.2

$$T_c = \frac{SAE}{L_e} \qquad \ldots [5.2]$$

where

T_c = load correction (kips)

S = anchorhead bearing plate movement

A = area of steel tendon = 1.519 (in^2)

E = modulus of elasticity of steel tendon = 29,000 (ksi)

L_e = effective elastic length of tendon

The effective elastic lengths for Anchors 1 to 4 were calculated by determining the elastic movements from the load test results and computing the tendon length that would elastically elongate that amount under the applied load. Reaction block movements were estimated to have caused a load reduction of between 3 and 8.5 kips.

Figure 107 is a plot of corrected load loss versus the log of time for the 70-day observation period. Anchor load was normalized by dividing the load by the lock-off load. The load loss data are scattered. Table 15 summarized the load loss percentage for each anchor at the end of the 70-day observation period ($\simeq$100,800 min).

Assuming these load loss rates continue, the maximum load loss after 100 years would be about 12 percent on Anchor 4. This load loss would represent a movement of 0.24 in on a four-strand tendon with an effective elastic length of 30 ft and a design load of 140 kips. The average load loss observed during the 70-day load was 5.6 percent. Creep test data showed that the average creep rate at the lock-off load applied to the four long-term test anchors was 0.01 in/decade. This creep rate corresponded to a load loss of 3.5 percent during the 70-day load hold tests. The load loss observed during the 70-day load hold and

that predicted from the creep test are close considering the potential errors associated with the measurements of the 70-day load loss.

TABLE 15
Seventy-day Load Loss Results for Anchors 1 to 4

ANCHOR NUMBER	LOAD LOSS PERCENTAGE AT CONCLUSION AT 70 DAYS
1	2
2	6.2
3	6.3
4	7.9

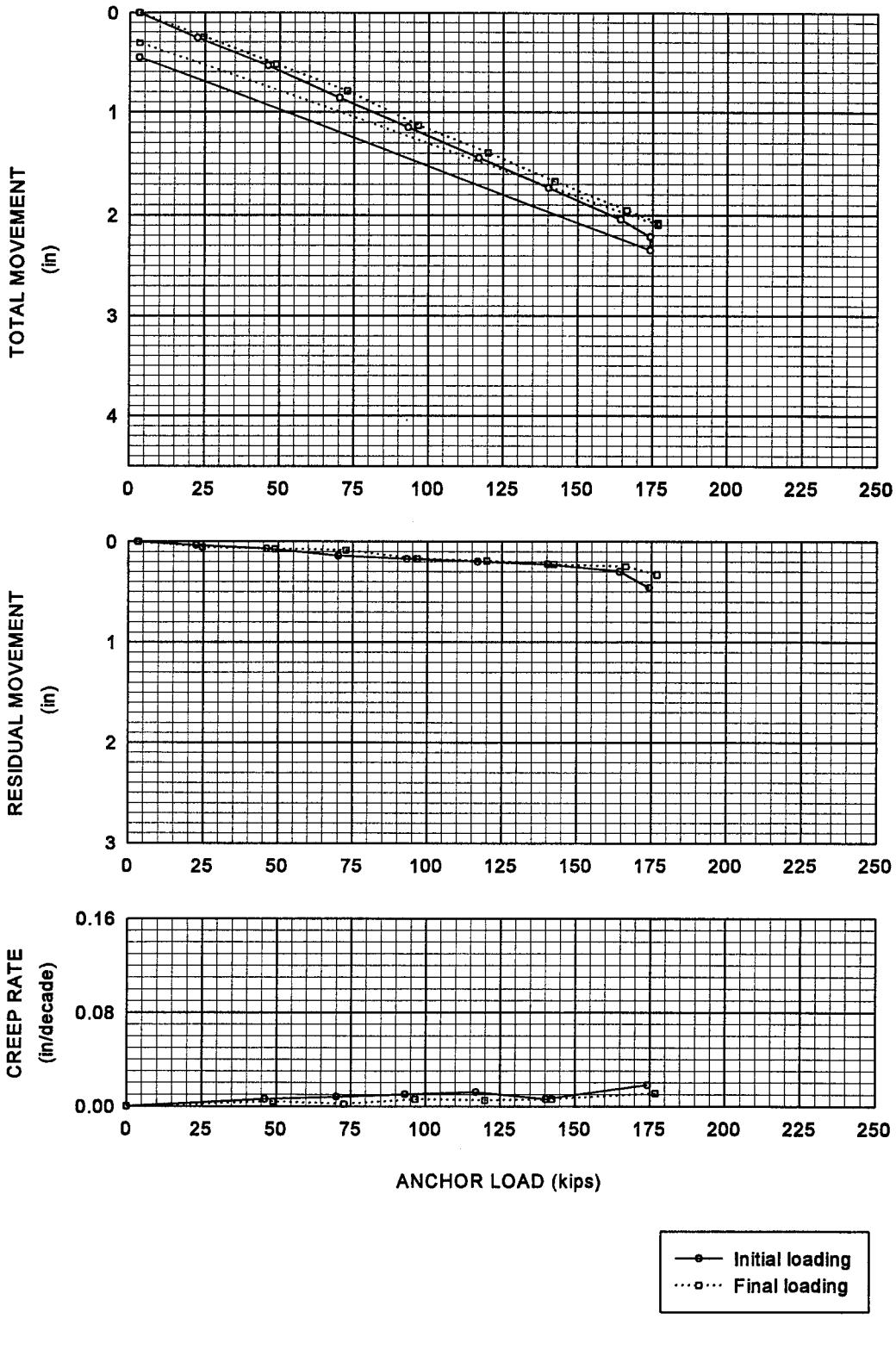

FIGURE 97
Anchor No. 1 Load Test Results

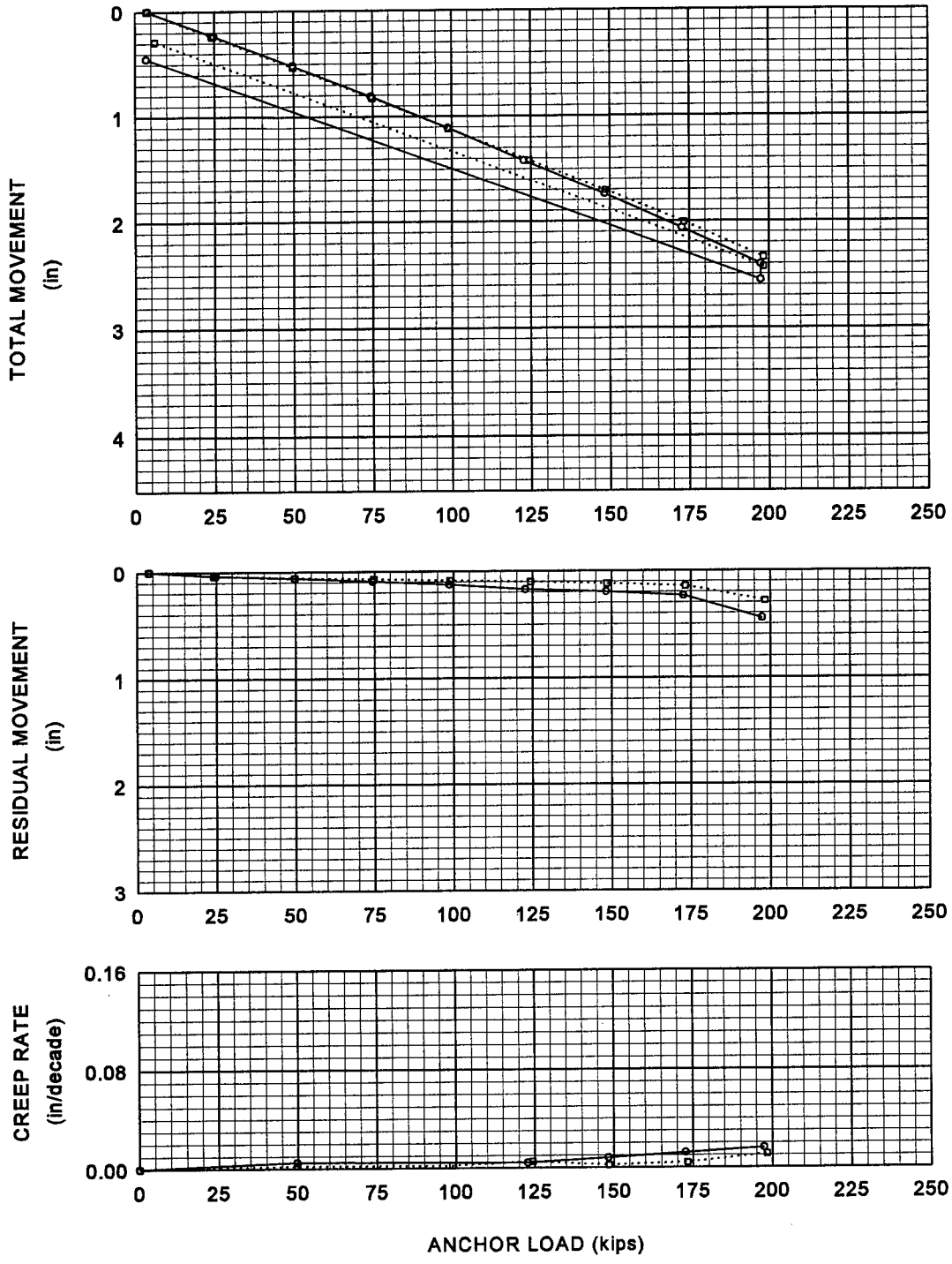

FIGURE 98
Anchor No. 2 Load Test Results

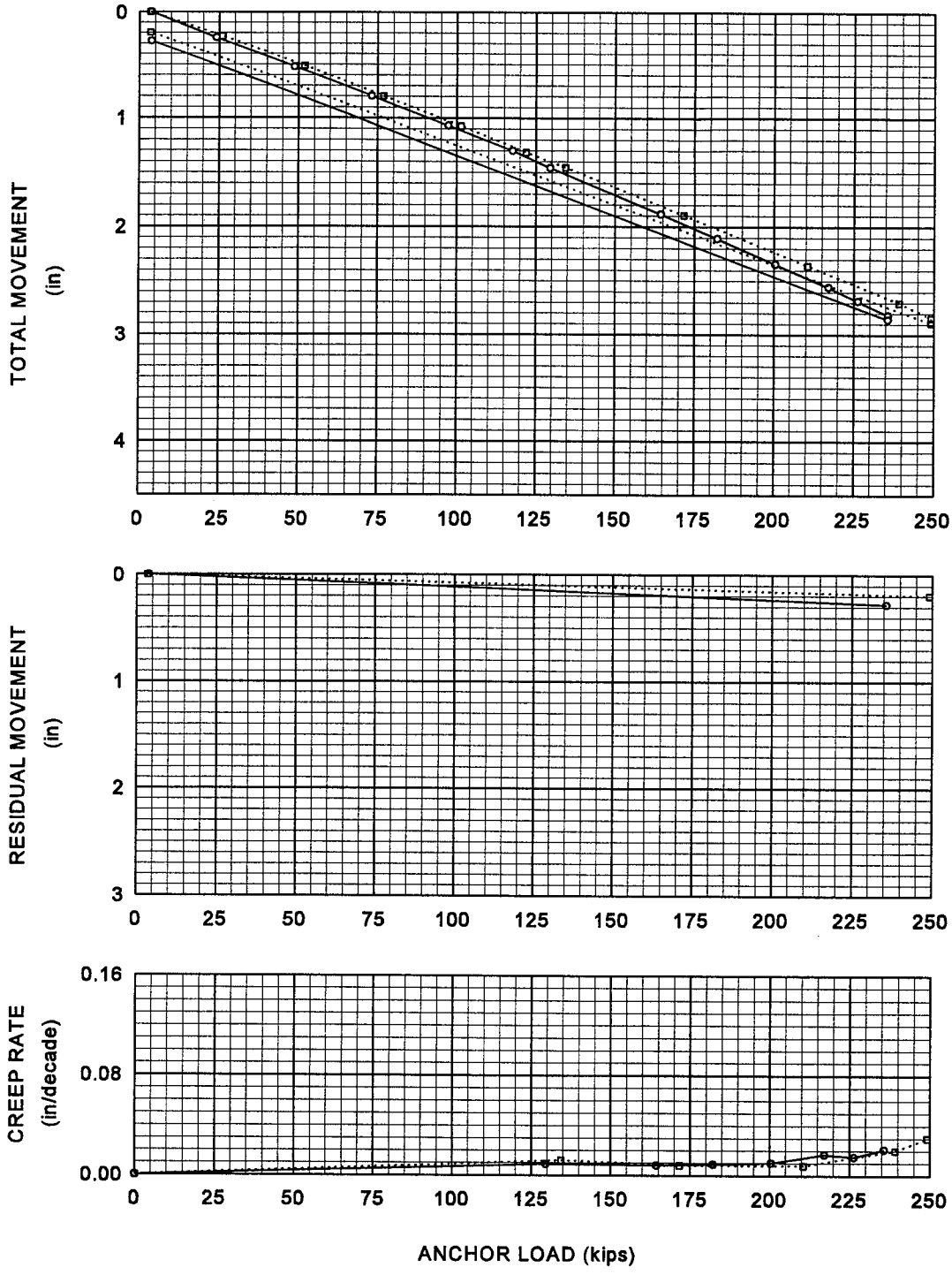

FIGURE 99
Anchor No. 3 Load Test Results

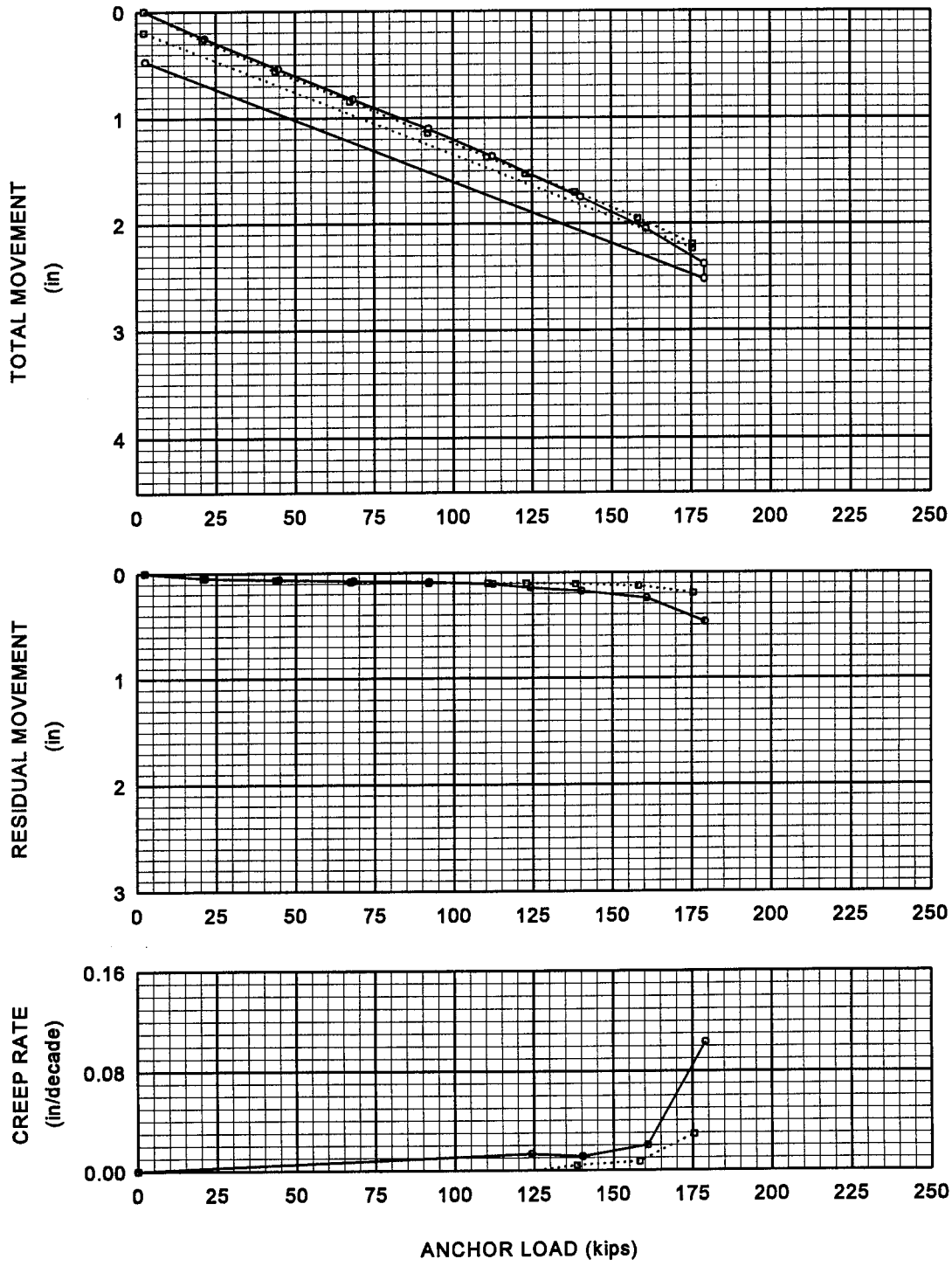

FIGURE 100
Anchor No. 4 Load Test Results

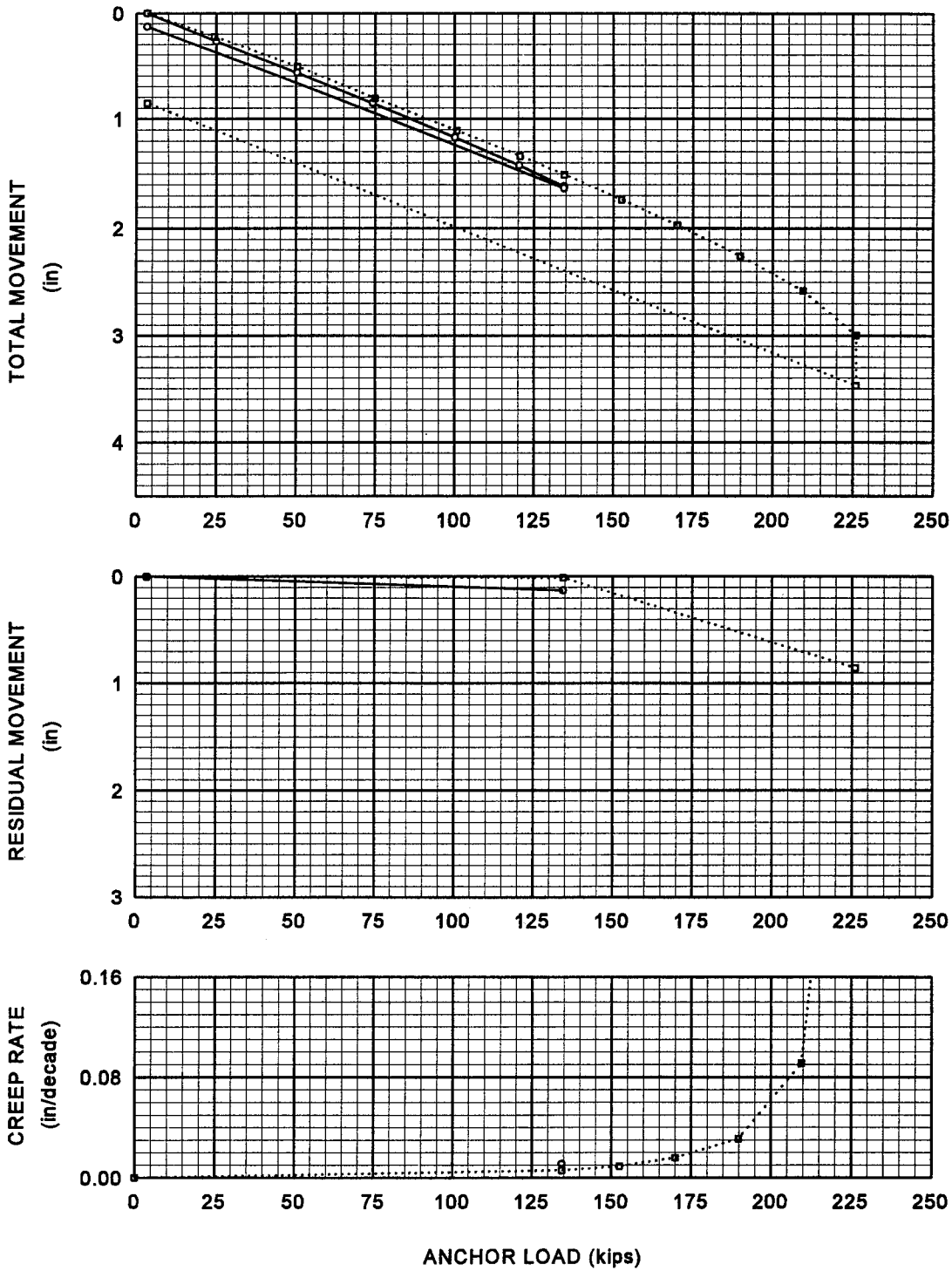

FIGURE 101
Anchor No. 5 Load Test Results

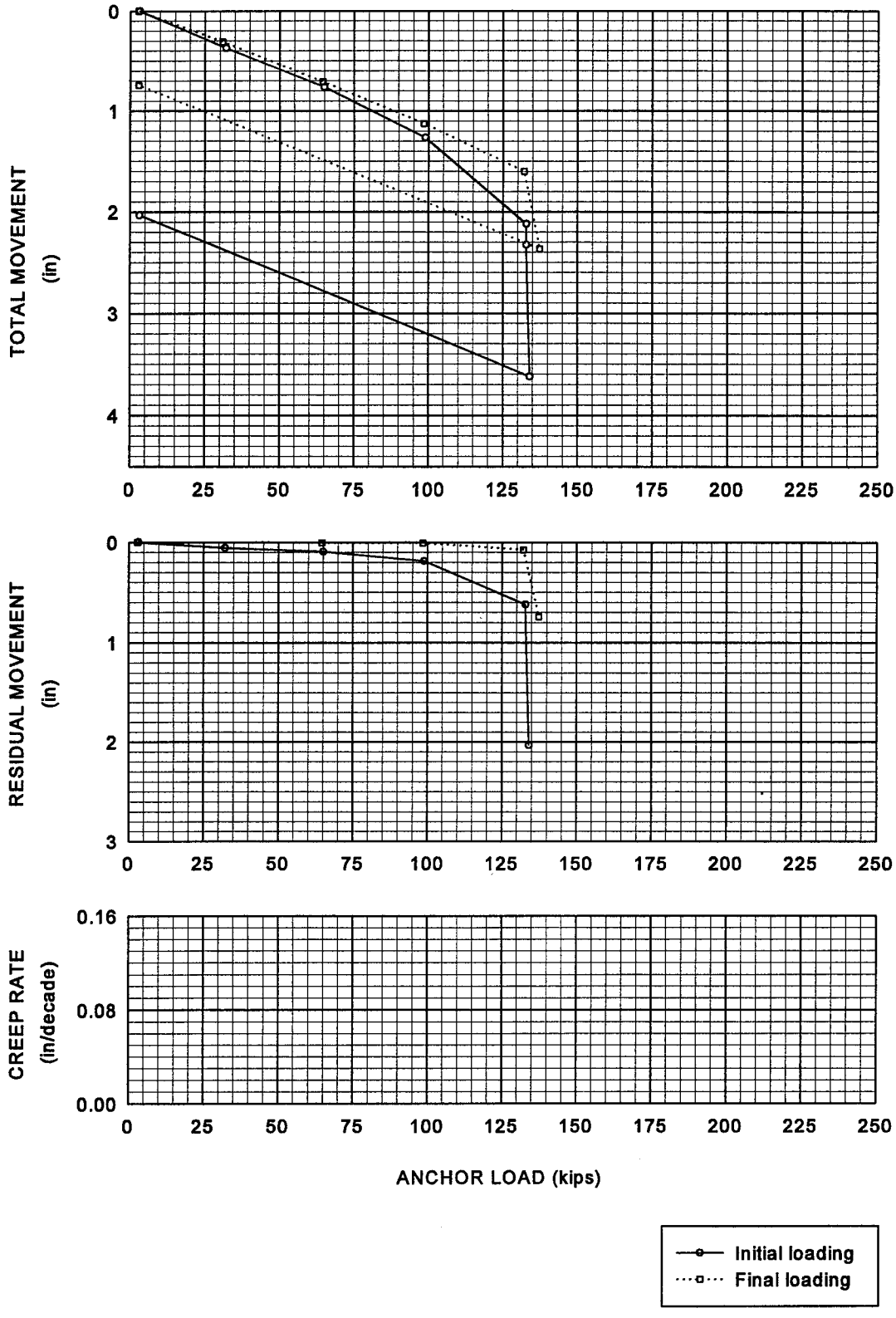

FIGURE 102
Anchor No. 6 Load Test Results

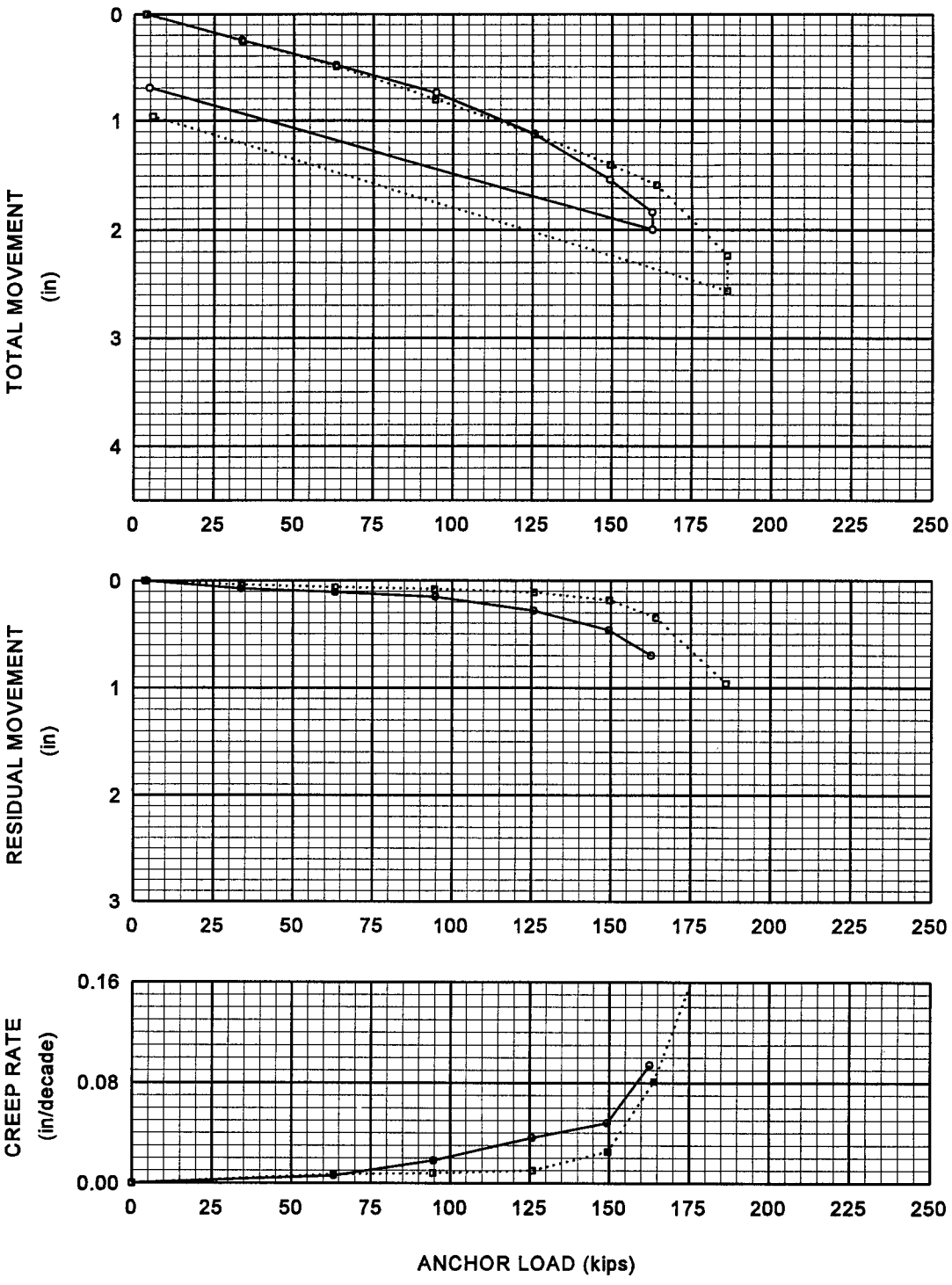

FIGURE 103
Anchor No. 7 Load Test Results

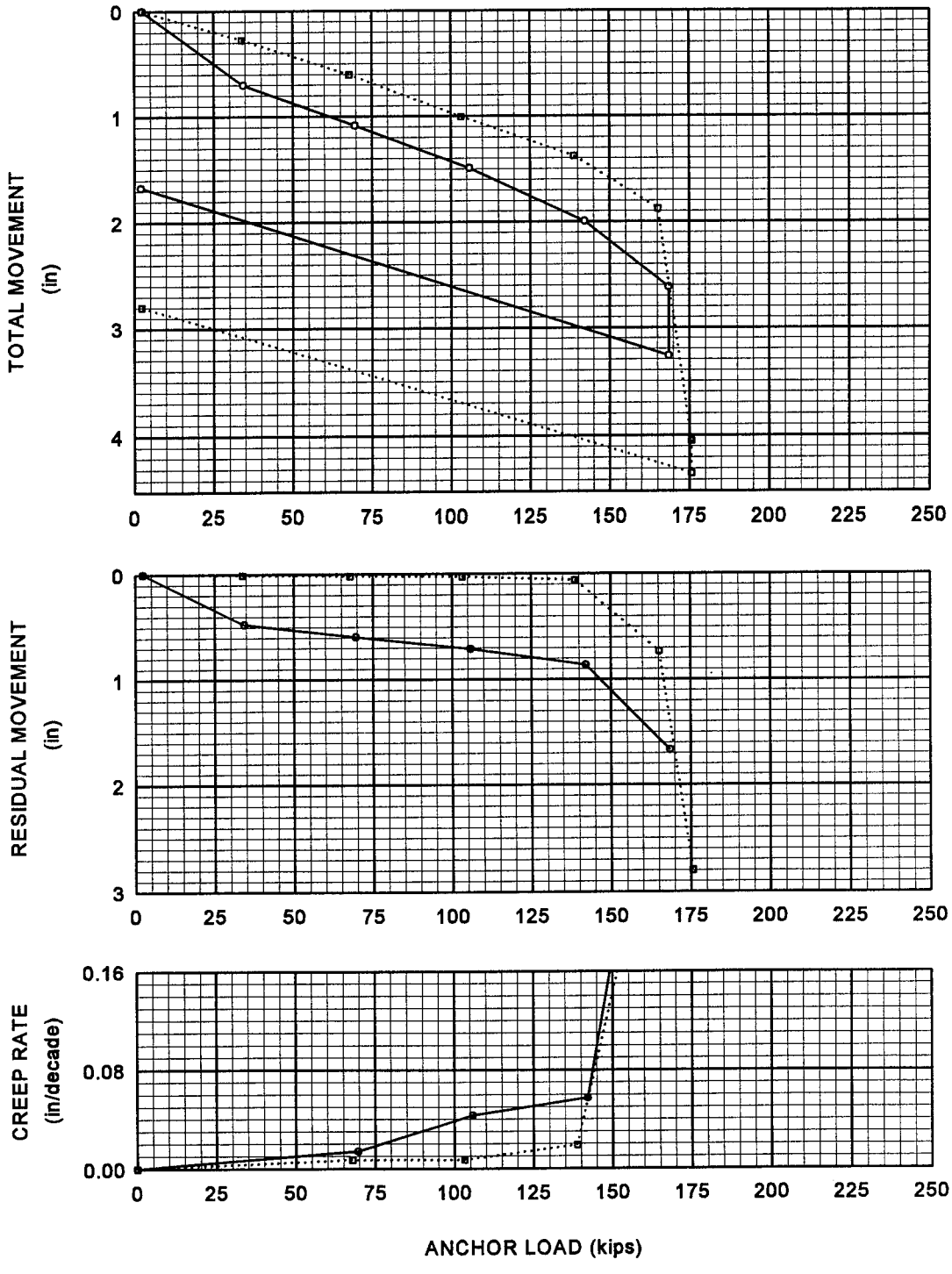

FIGURE 104
Anchor No. 8 Load Test Results

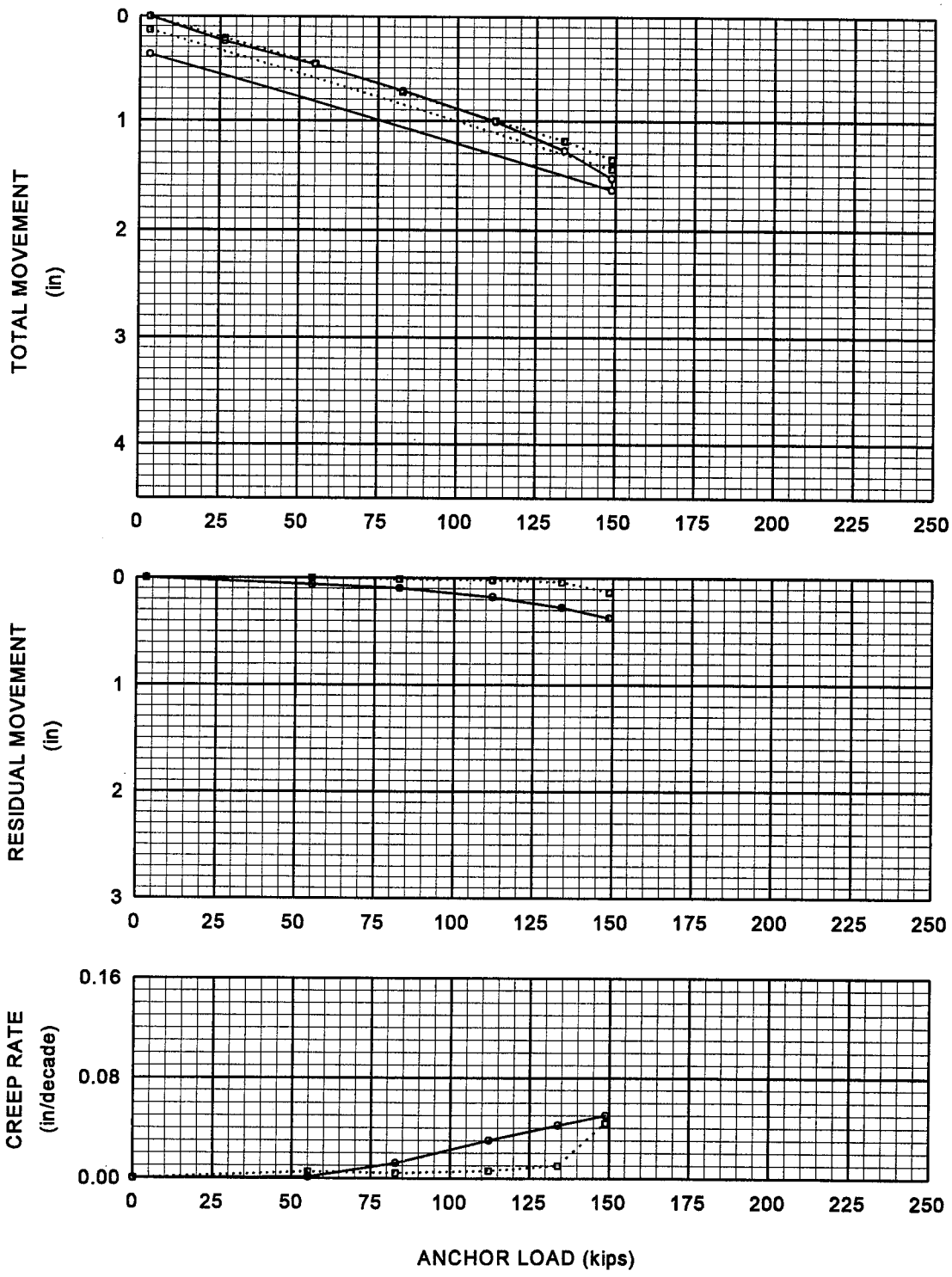

FIGURE 105
Anchor No. 9 Load Test Results

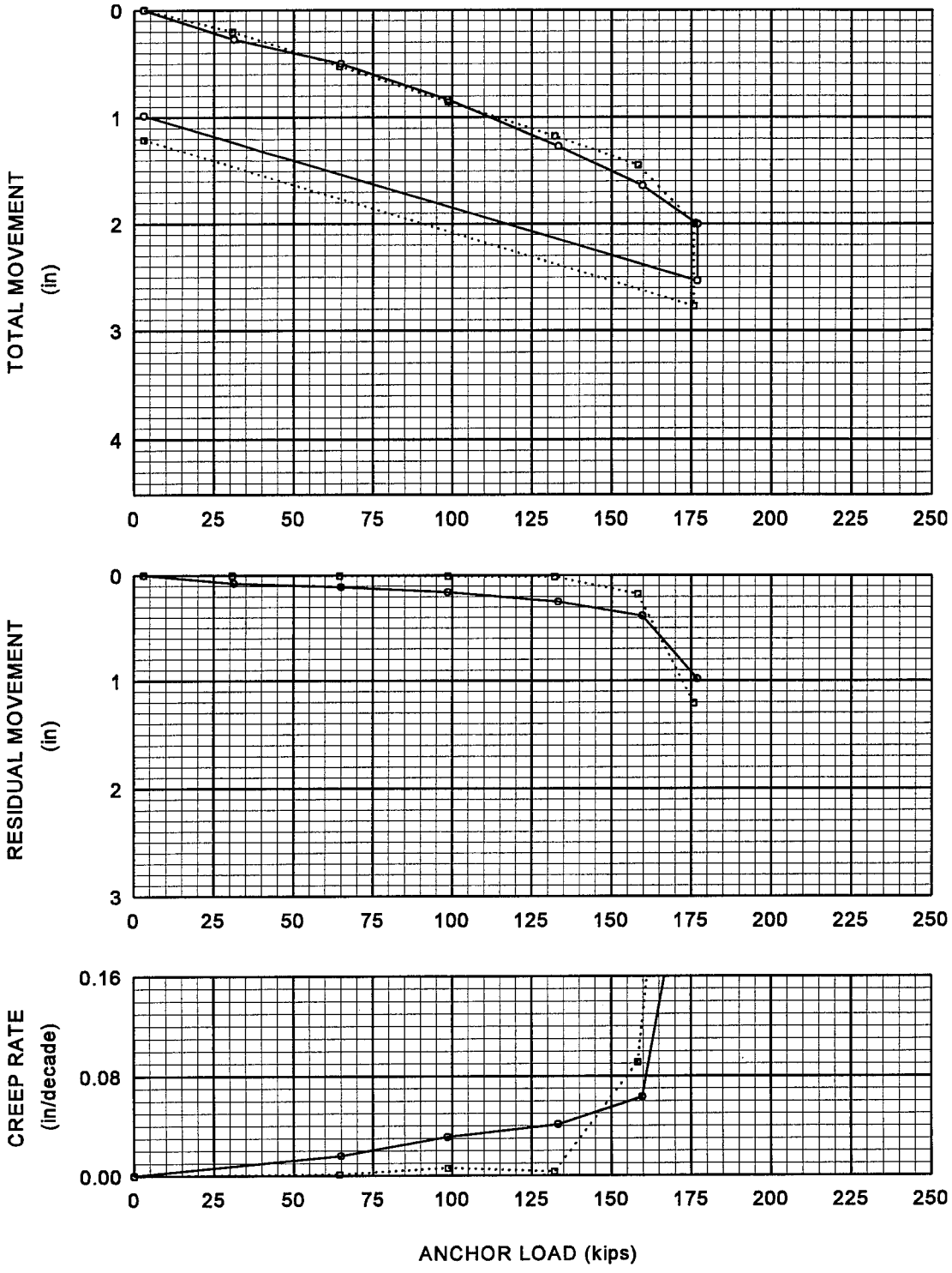

FIGURE 106
Anchor No. 10 Load Test Results

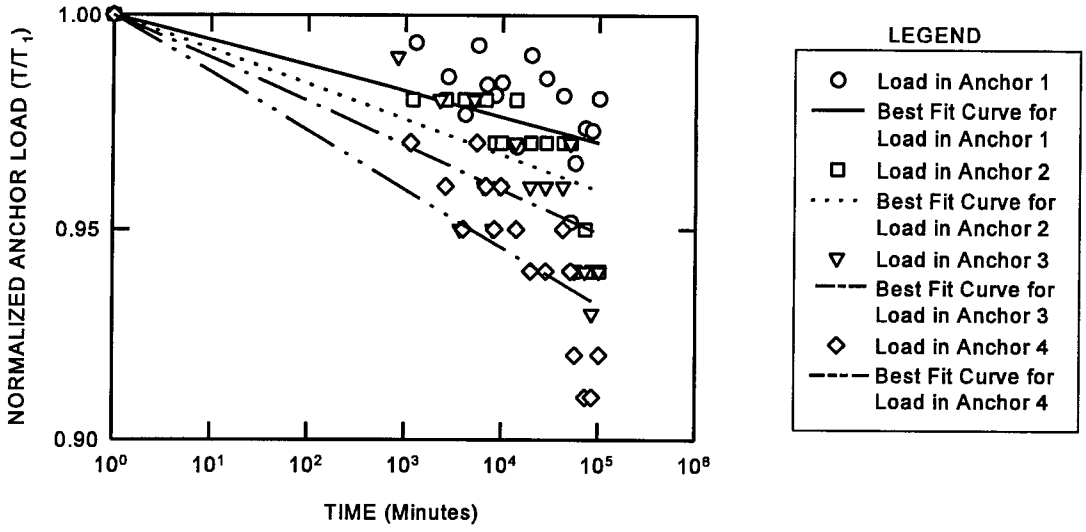

FIGURE 107
Load Loss as a Function of Time – Anchors 1 to 4 (70-day load hold)

5.6 GROUT AND TENDON STRAINS

Six of the anchors were instrumented. Strain gauges positioned in the anchor grout were used to measure strains within the grout body. Strainmeters attached to a prestressing strand were used to measure strain in the anchor tendon. Section 5.4.1 shows the locations of the strain gauges.

Anchors 1, 2, and 7 to 10 were instrumented. Anchors 1 and 2 each had a 15-ft tendon bond length and they were grouted to the surface. Anchors 7 and 8 had a 30-ft tendon bond length. When the auger tip was approximately 15 ft below the surface, grouting for Anchors 7 and 8 was stopped. After extracting the auger, the top of Anchor 7's grout shaft was 6 ft below the ground surface and the top of the grout shaft for Anchor 8 was 8 ft below the ground surface. Anchors 7 and 8 were grouted in this manner in an attempt to duplicate the practice of only grouting the bond length before testing. The grout level was higher than planned because it was not possible to precisely control the grout volume delivered to the auger. Anchors 9 and 10 had 30-ft-long tendon bond lengths and they were grouted to the surface.

Figures 108 to 113 show the strains in the grout and the steel tendon for each of the instrumented anchors. Grout and tendon load are shown on the right y-axis. Grout and tendon strains at the bottom of the tendon bond length are shown to be zero. Tendon strains at the

top of the tendon bond length were not measured and they were assumed to be equal to the strain associated with the applied test load. Large tensile grout strains were observed over much of the tendon bond length. The cracking strain for the grout was estimated to be 100 με (100×10^{-6} in/in). The grout surrounding most of the tendon bond length is assumed to be cracked. Since the measured strains exceed the cracking strain, load in the anchor tendon can be related directly to the measured tensile strains. Load in the anchor grout can be determined where the measured strains are less than a positive 100 με.

5.6.1 Anchors 1 and 2

Figures 108 and 109 show the strains and loads in the grout and tendon for Anchors 1 and 2, respectively. The strain levels in the grout and the steel are approximately the same for the bottom 10 ft of the anchor. Strains exceeded the cracking strain over most of the tendon bond length. As a composite section, the grout and steel tendon can carry 48.9 kips in tension before the grout cracks. When the grout cracks, the axial tensile stiffness of the anchor changes from a composite section to a steel section. The steel section can only carry 4.4 kips at a strain of 100 με. Therefore once the grout cracks, the anchor has to elongate 11 times further to transfer the same load as an uncracked section. Above 10 ft, the grout goes into compression and the tensile strains in the tendon increased rapidly. Where the grout surrounding the bare tendon is in compression, the prestressing steel has debonded from the grout.

Grout embedment strain gauges surrounding the tendon in the unbonded length show that Anchors 1 and 2 behaved differently. The compressive load in the anchor grout for Anchor 1 at 36 ft from the bottom of the anchor was 96.6 kips (55 percent of the full test load), while the load in Anchor 2 at that location was 24.0 kips (12 percent of the full test load). Ludwig and Weatherby (1989) presented the test results for similar instrumented anchors installed in stiff clay till in Seattle. They found that anchors with short tendon bond length, similar to Anchors 1 and 2, transfer less than 15 percent of the applied load up the shaft to a point located twice the tendon bond length from the bottom of the anchor. Anchor 2 had similar behavior to that reported by Ludwig and Weatherby, but the behavior of Anchor 1 cannot be explained.

5.6.2 Anchors 7 and 8

Figures 110 and 111 show that the grout and tendon strains are approximately equal for a significant portion of the 30-ft tendon bond length of Anchors 7 and 8. Large grout strains along the tendon bond length suggest that the grout is cracked to within a few feet of the bottom of the anchor. Strain readings indicate that load was transferred down to near the bottom of the anchor. Compressive grout strains at 30 ft show that the tendon has debonded from the grout at the top of the tendon bond length. The top of the grout for Anchors 7 was 6 ft above the upper end of the tendon bond length. The grout for Anchor 8 was 8 ft above the top of the tendon bond length. About 35 kips was transferred to the grout column over the unbonded length of Anchor 7. Compressive strains at 30 ft for Anchor 8 indicate that more than 200 kips was transferred to the grout column over the unbonded length. The load transferred up

the shaft for Anchor 7 is reasonable but the load transferred up the shaft for anchor 8 is unrealistically high.

5.6.3 Anchors 9 and 10

Anchors 9 and 10 were similar to Anchors 7 and 8, except the grouted shaft extended to the ground surface and the grout surrounding the unbonded length was instrumented (Figures 112 and 113). Grout and tendon strains over the bottom 20 to 25 ft of the anchors are similar. Strains suggest that the grout is cracked along most of the tendon bond length. Near the upper portion of the tendon bond length the grout goes into compression, indicating that the tendon debonded from the grout. Along the unbonded length, the patterns of compressive strains are very different for Anchors 9 and 10. The strains along the unbonded length of Anchor 10 indicate that unrealistically high compressive strains were measured along most of the unbonded length. These high strains could not be explained. Unbonded length strain gauges installed in Anchor 9 appear to have worked satisfactorily. The strain gauge at 30 ft from the back of the anchors indicates that the grout column carried 72 kips of load up the shaft over the unbonded length.

5.6.4 Discussion

Strain and load measurements show that the behavior of large-diameter, hollow-stem-augered anchors is affected by the tendon bond length selected. Anchors 1 to 4 had 15-ft-long tendon bond lengths. Fifteen ft was selected since it was sufficient to bond the tendon to the grout and it forced the load to be transferred to the back of the anchor. Shortening the tendon bond length placed most of the grout column in compression and caused Anchors 1 to 4 to behave differently from Anchors 5 to 10 (tendon bond length was equal to the anchor bond length).

Grout and tendon strains reflect the axial stiffness of an anchor. Large grout and tensile strains indicate that an anchor is more flexible than an anchor with smaller tensile strains. Anchors 1 and 2 were much stiffer than Anchors 7 to 10. Measured grout strains (Figures 108 to 113) and total movement curves (Figures 97 to 106) show that Anchors 1 to 4 were much stiffer than the other anchors. Anchors 1 to 4 as a group developed higher ultimate load-carrying capacities and exhibited lower creep movements than the other anchors.

Stiff "compression" anchors should develop higher ultimate capacities than more flexible anchors. The additional capacity comes from two sources. First, the grout shaft moves less to mobilize load-carrying capacity, enabling the peak grout-soil bond stresses to function over a greater portion of the anchor. Second, most of the grout body is placed in compression. Compression causes the grout body to expand radially, enhancing the grout-soil contact rather than radial contraction associated with tensile stresses within the grout.

Bonding the anchor tendon to the lower portion of the anchor length transfers the anchor load to the end of the anchor, and enables the anchor to develop its capacity well behind the critical failure surface ("no-load zone"). Figure 109 shows that 88 percent of the maximum test load

was developed over the bottom 36 ft of the anchor. On the other hand, Figure 112 shows that about half of the load was transferred to the grout shaft over the unbonded length. Forcing the load to the back of an anchor enables large-diameter anchors to be grouted to the surface and avoid developing significant capacity from the soil supported by the wall (no-load zone). Results indicated that the unbonded length should extend between 15 and 20 ft behind the no-load zone.

When the tendon bond lengths of large-diameter anchors start at the top of the anchor bond zone, then the anchors will develop capacity from the ground that the anchor is intended to support. Anchor testing is not able to detect whether a large-diameter anchor develops capacity within the no-load zone. If the tendon bond length coincides with the anchor bond length, then the current practice of grouting only the bond length before testing should be continued for large-diameter anchors.

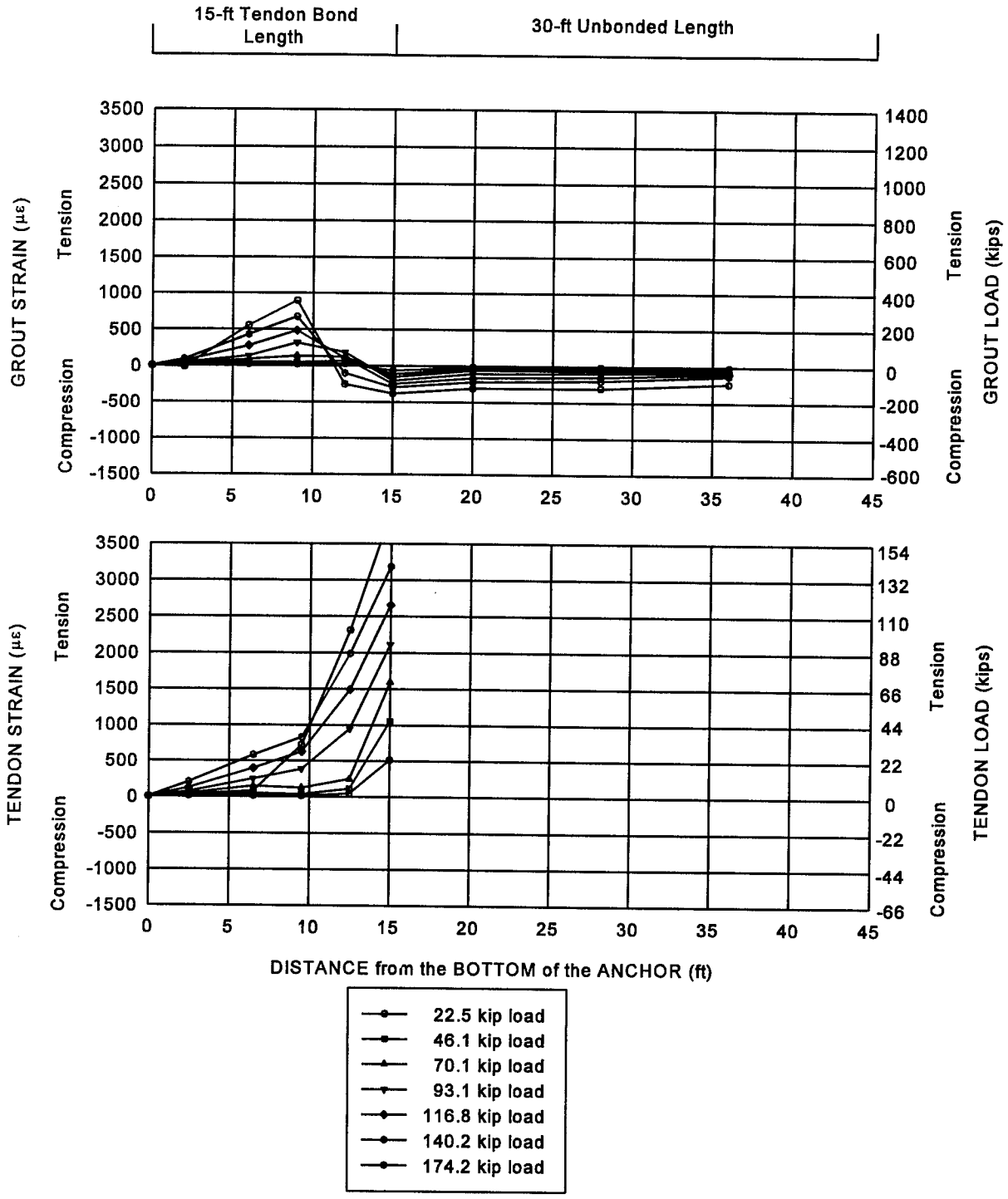

FIGURE 108
Strains in the Grout and Tendon – Anchor No. 1

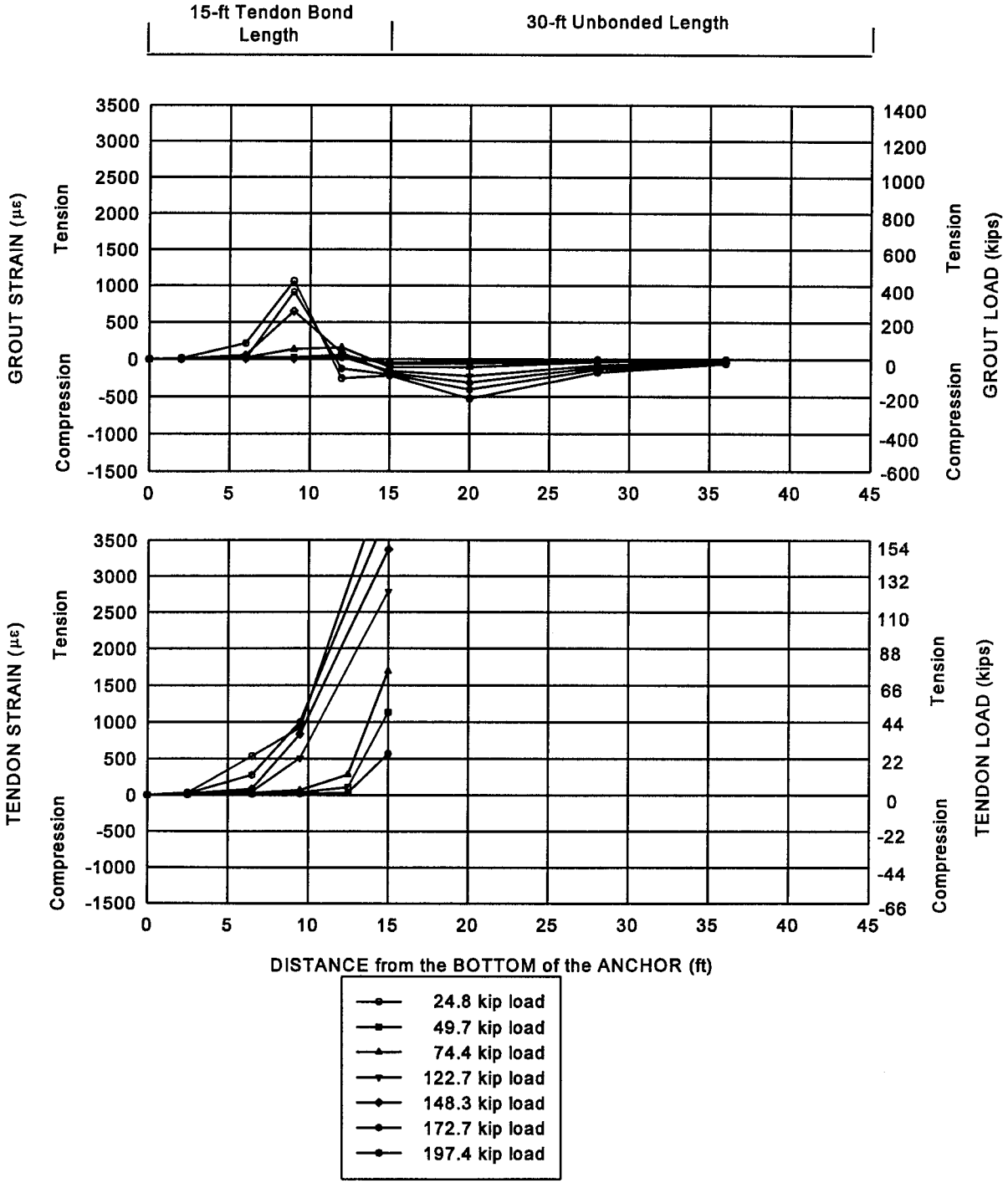

FIGURE 109
Strains in the Grout and Tendon – Anchor No. 2

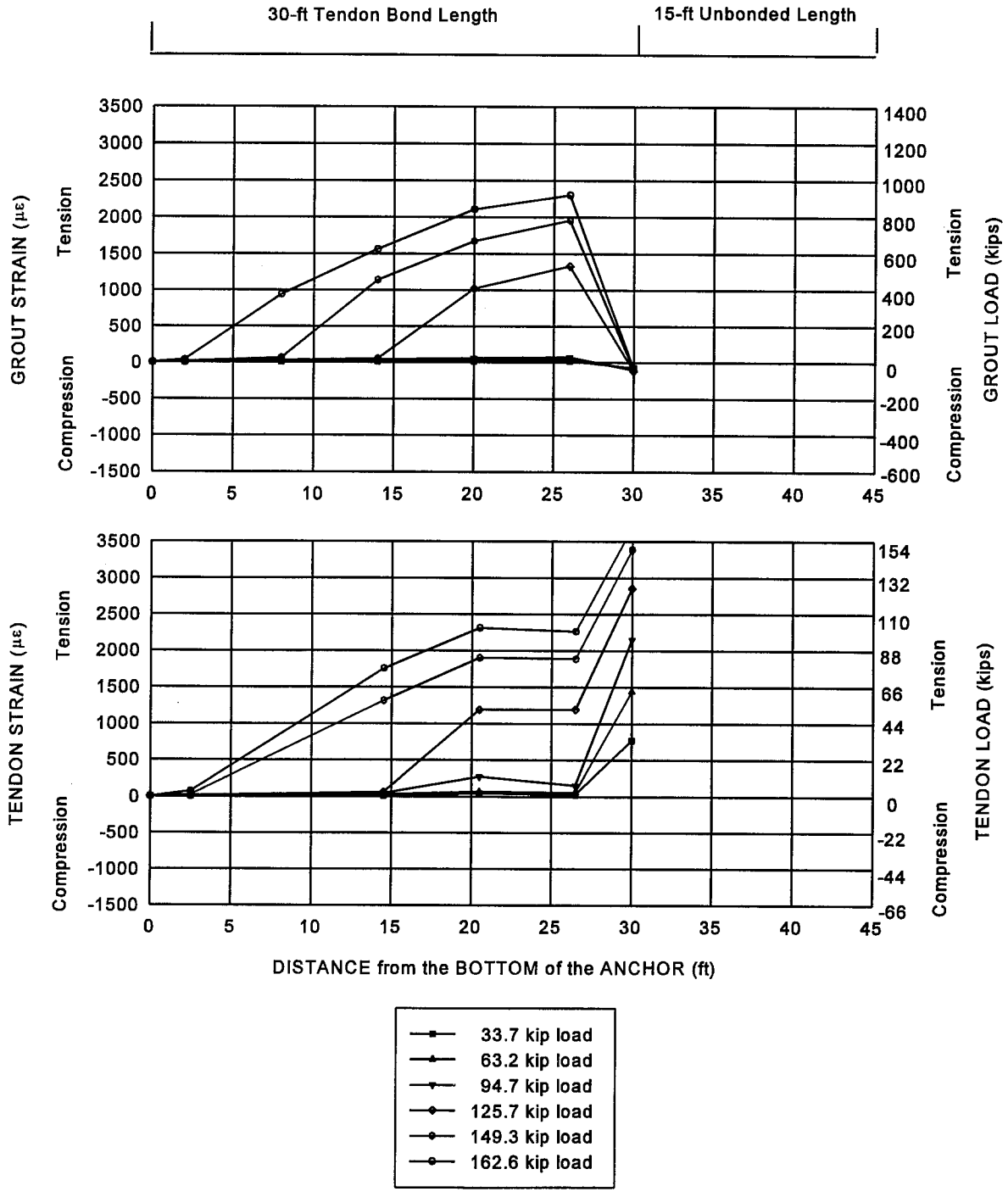

FIGURE 110
Strains in the Grout and Tendon – Anchor No. 7

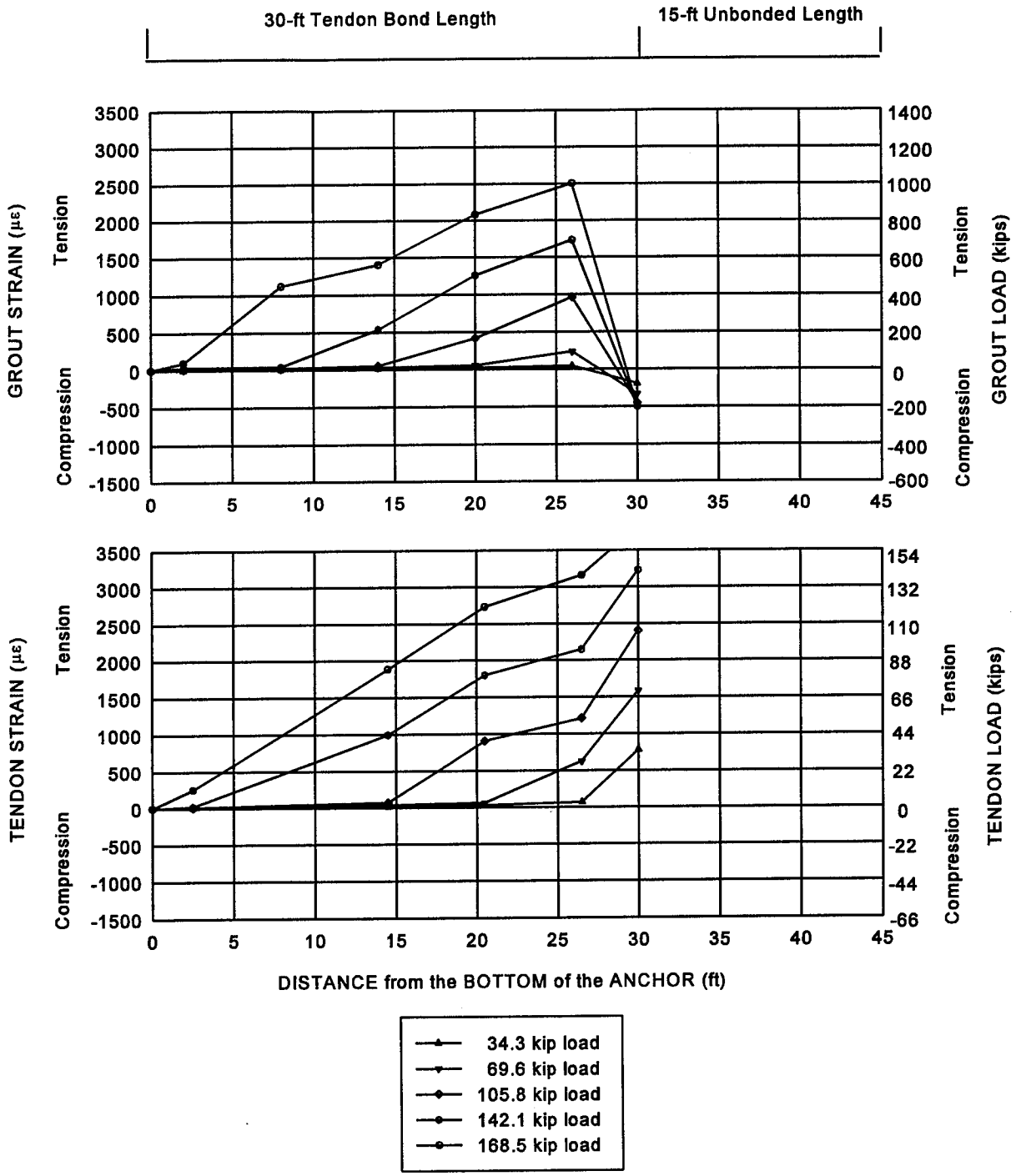

FIGURE 111
Stress in the Grout and Tendon – Anchor No. 8

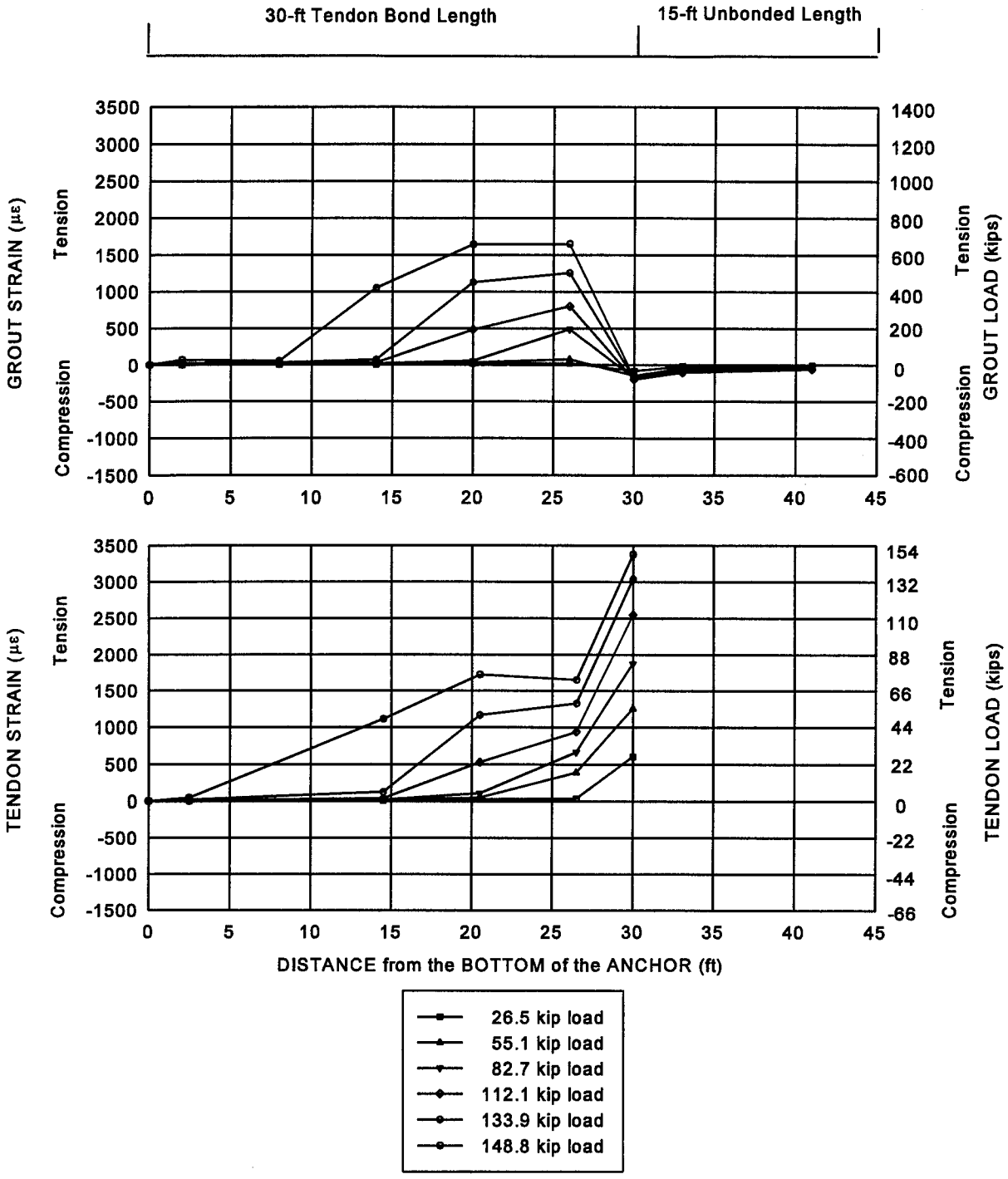

FIGURE 112
Strains in the Grout and Tendon – Anchor No. 9

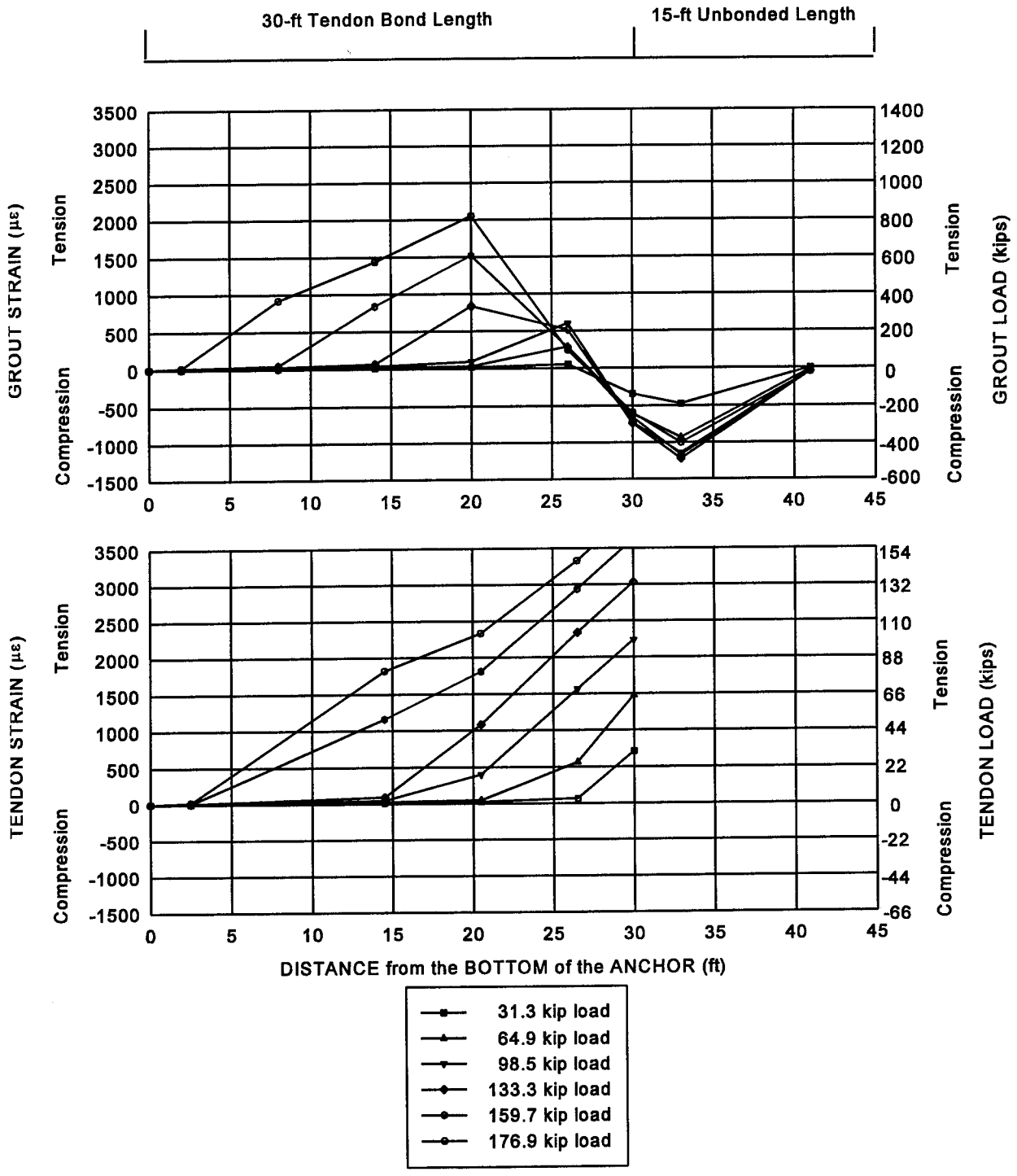

FIGURE 113
Stress in the Grout and Tendon, Anchor No. 10

5.7 CONCLUSIONS AND RECOMMENDATIONS

Ten, 12-in-diameter, hollow-stem-augered tiedown anchors were load tested as part of the ground anchor wall research conducted at Texas A&M. Six of the anchors were instrumented to allow the strains with the grout body and the tendon to be measured. Four of the anchors were loaded and monitored for 70 days. The results of the test program are:

- Large-diameter, hollow-stem-augered anchors develop load-carrying capacity along the grout shaft surrounding the unbonded tendon length.

- Develop a compression anchor by extending the unbonded tendon length to at least the mid-point of the anchor bond length.

- Compression anchors develop their load-carrying capacity from the lower portion of the anchor, and prevent the development of significant load-carrying capacity from the no-load zone.

- Compression anchors can be grouted to the ground surface in one phase.

- Compression anchors are axially stiffer than anchors with tendon bond lengths equal to the anchor bond length.

- Higher grout to soil bond stresses are developed along the grout shafts of stiff anchors than along the shafts of more flexible anchors.

- Stiff anchors develop higher ultimate loads than flexible anchors with the same anchor bond lengths.

- Short-term creep testing satisfactorily evaluated the long-term load-carrying capacity of ground anchors installed in fine-grained soils. Movements and load losses predicted from short-term tests were similar to values measured during the 70-day load holds.

- Anchor acceptance criterion of 0.08 in of creep movement per decade of time is valid for large-diameter, hollow-stem-augered anchors.

- Retesting of anchors installed in fine-grained soils should not be allowed. Preloading during initial testing will affect the test results during retesting. Creep movements will be significantly less during the second test.

- Retesting of regroutable anchors must be carefully done in order to prevent preloading from reducing the creep movements during retesting.

APPENDIX

Figure 114 shows the logs for cone penetrometer soundings CPT8 and CPT9 conducted at the ground anchor site. The plot of preboring pressuremeter boring PBPMT2 at the anchor test site is shown in Figure 115. Figure 116 shows the results of a dilatometer test at the clay site.

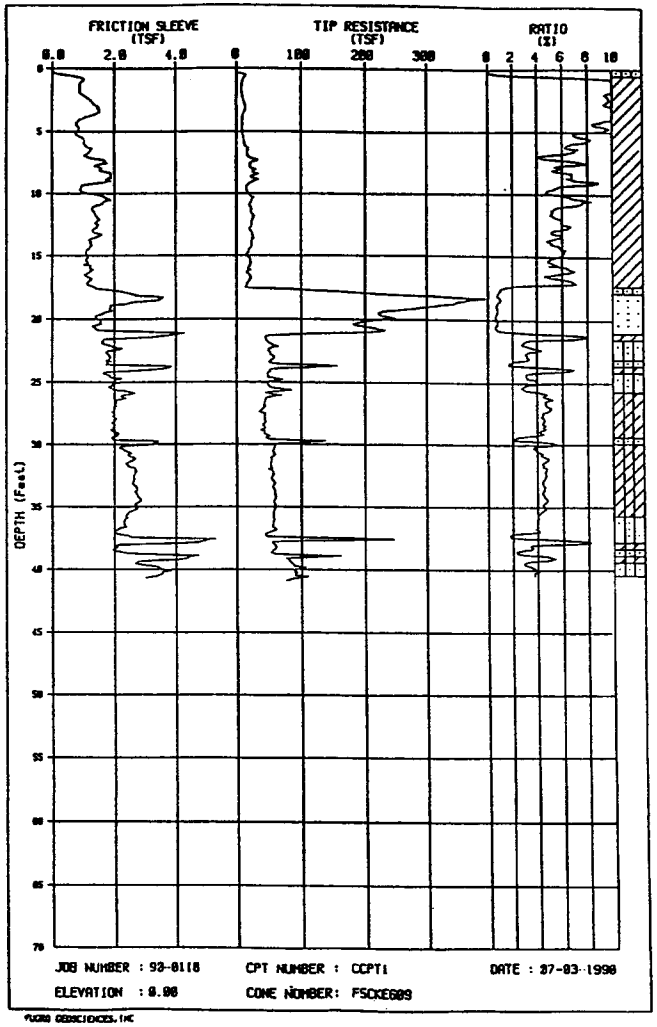

a) CPT 8

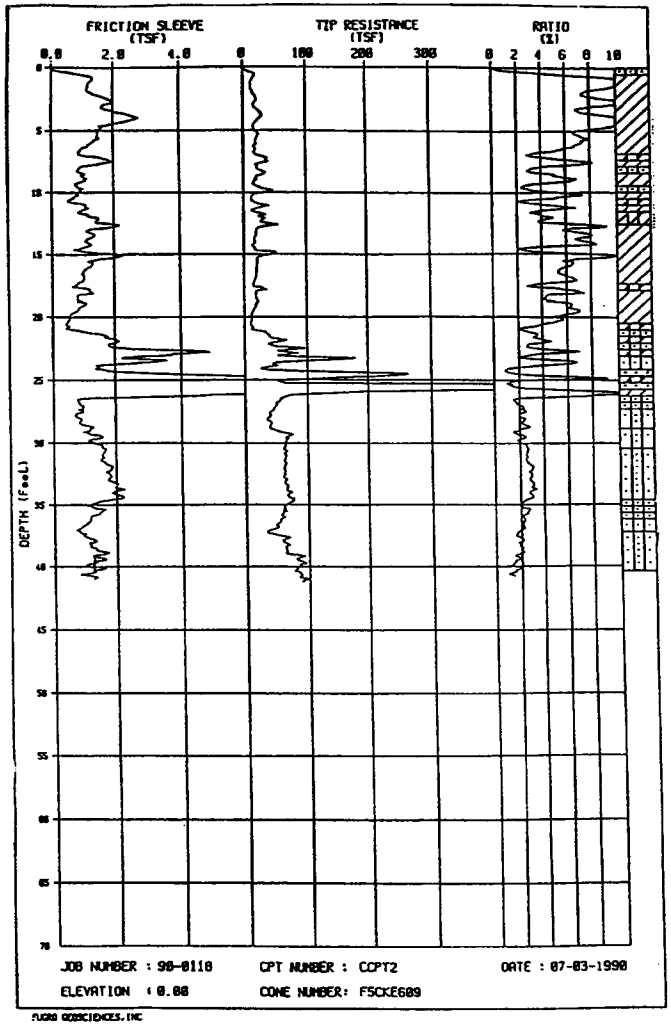

b) CPT9

FIGURE 114
Results of Cone Penetrometer Tests at the Anchor Test Site

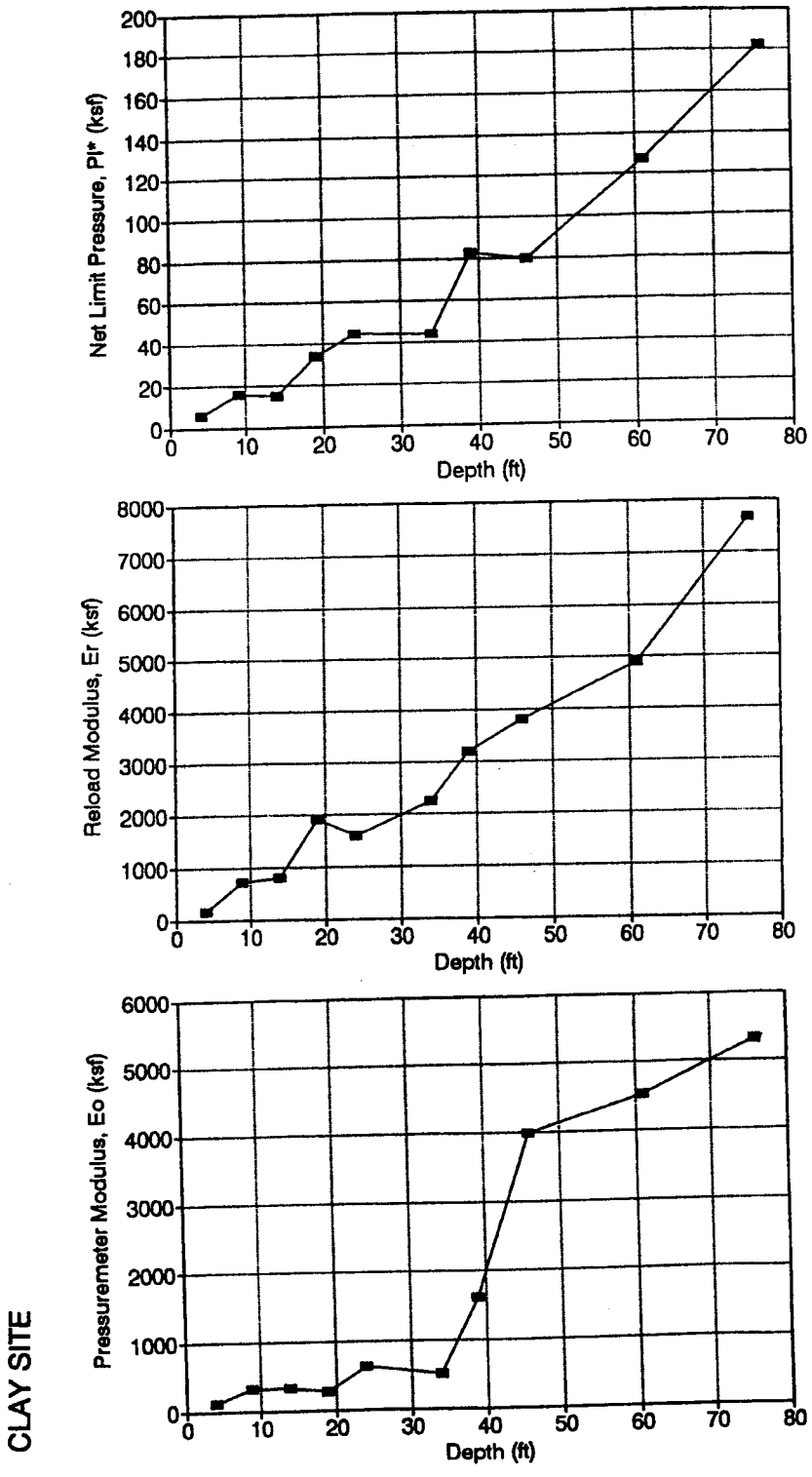

FIGURE 115
Summary of the Preboring Pressuremeter Test at the Anchor Test Site

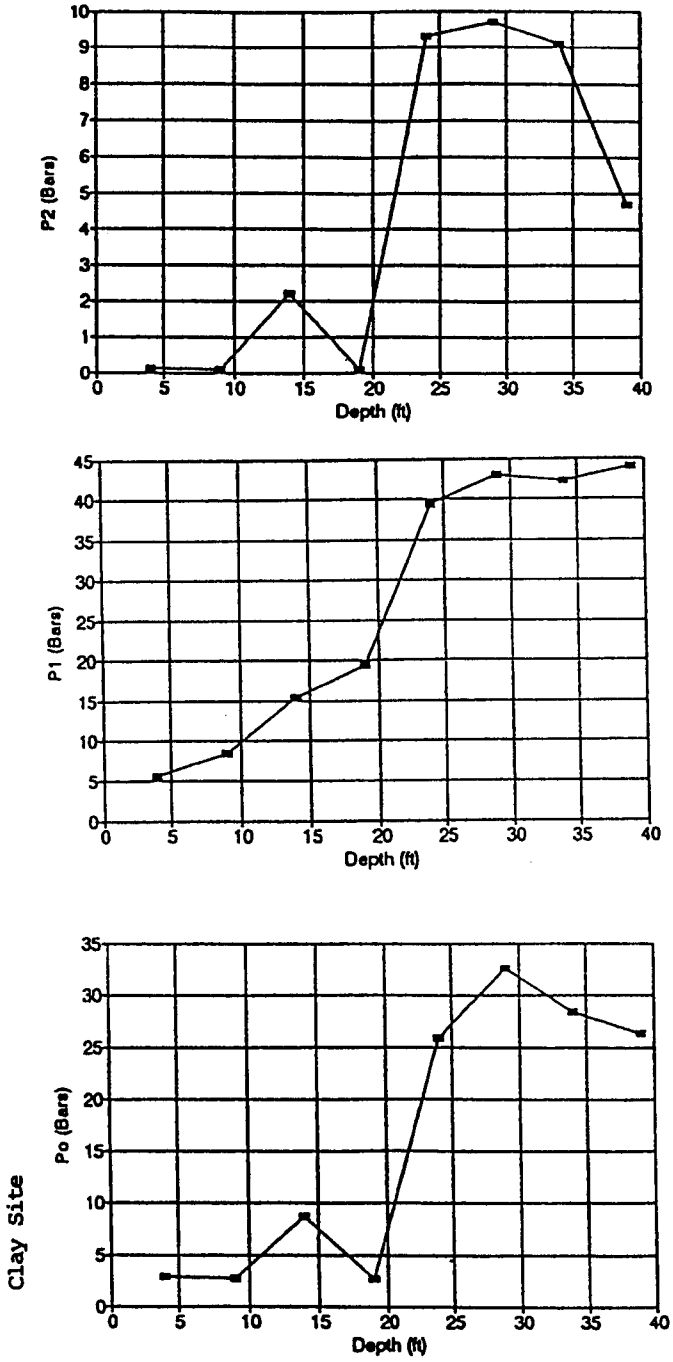

FIGURE 116
Summary of the Dilatometer Test at the Anchor Test Site

REFERENCES

Anderson, T.C., Reinfurt, J., Reitz, P., and Licari, T. (1994). *Temporary Shoring Support Systems in an Urban Environment*, ASCE Annual Convention and Exposition, Atlanta, GA.

Briaud, J.L. (1991). "The Two Texas A&M University Sites for Geotechnical Experimentation: Sand and Clay," *Report to the National Science Foundation*, Texas A&M University, College Station, TX.

Caliendo, J.A., Anderson, L.R., and Gordon, W.J. (1990). "A Field Study of a Tieback Excavation with a Finite Element Analysis," *Proceedings: Design and Performance of Earth Retaining Structures*, ASCE and Cornell University, Geotechnical Special Publication No. 25, pp. 747-763.

Canadian Geotechnical Society (1985). *Canadian Foundation Manual*, 2nd Edition, Vancouver, British Columbia.

Chung, M. and Briaud, J. (1993). *Behavior of a Full-Scale Tieback Wall in Sand*, Geotechnical Engineering, Department of Civil Engineering, Texas A&M University, College Station, TX, 249 pp.

Clough, G.W. and O'Rourke, T.D. (1990). "Construction Induced Movements of In-situ Walls," *Proceedings: Design and Performance of Earth Retaining Structures*, ASCE and Cornell University, Geotechnical Special Publication No. 25, pp. 439-470.

Clough, G.W., Weber, P.R., and Lamont, J. (1972). "Design and Observation of a Tied-Back Wall," *Proceedings: Performance of Earth and Earth-Supported Structures*, Vol. 1, Part 2, Purdue University and ASCE, pp. 1367-1389.

H.C. Nutting Company (1988). *Progress Report: Tied-back Retaining Wall Performance Study*, Demonstration Project No. 68, North Street Grade Separation, Lima, Ohio, Prepared for the Ohio Department of Transportation, May 12.

Hanna, T.H. (1968). "Design and Behavior of Tie-Back Retaining Walls," *Proceedings: 3rd Budapest Conference on Soil Mechanics and Foundation Engineering*, pp. 410-418.

Hansmire, W., Russell, H., Rawnsley, R.P., and Abbott, E.L. (1989). "Field Performance of Structural Slurry Wall," ASCE *Journal of Geotechnical Engineering*, Vol. 115, No. 2, pp. 141-156.

REFERENCES
(continued)

Hata, S., Ohta, H., Yoshida, S., Kitamura, H., and Honda, H. (1985). "A Deep Excavation in Soft Clay: Performance of an Anchored Diaphragm Wall," *Proceedings: 5th International Conference on Numerical Methods in Geomechanics*, Nagoya, pp. 725-730.

Houghton, R.C. and Dietz, D.L. (1990). "Design and Performance of a Deep Excavation and Support System in Boston, Massachusetts," *Proceedings: Design and Performance of Earth Retaining Structures*, ASCE and Cornell University, Geotechnical Special Publication No. 25, pp. 795-816.

Johnson, E.G., Gifford, D.G, and Haley, M.X. (1977). "Behavior of Shallow Footings Near a Diaphragm Wall," ASCE Annual Convention, Session 40 (preprint), *Protection of Structures Adjacent to Braced Excavations,* San Francisco, October 19.

Kooistra, T.J.and Beringen, F. (1984). "Predicted and Observed Lateral Deformations of Anchored Retaining Walls," *International Conference on Case Histories in Geotechnical Engineering*, Vol. I, University of Missouri, Rolla.

Kubena, M.E. (1989). *Tension Capacity of Two Drilled and Grouted Piles*, thesis presented to Texas A&M University, in College Station, Texas, in partial fulfillment of the requirements for the degree of Master of Science.

Littlejohn, G.S. and MacFarlane, I.M. (1975). "A Case History Study of Multi-Tied Diaphragm Walls," *Diaphragm Walls and Anchorages,* Institution of Civil Engineers, pp. 113-221.

Liu, T.K. and Dugan, J.P. (1972). "An Instrumented Tied-Back Deep Excavation," *Proceedings: Performance of Earth and Earth-supported Structures*, ASCE and Purdue University, Vol. 1, Part 2, pp. 1323-1340.

Long, J.H., Weatherby, D.E., and Cording, E. J. (1998). *Summary Report of Research on Permanent Ground Anchor Walls*, "Volume I: Current Practice and Limiting Equilibrium Analyses," Report No. FHWA-RD-98-065, Federal Highway Administration, McLean, VA.

Ludwig, H.P.and Weatherby, D.E.(1989). "Behavior of a Tieback in Cohesive Soil." *Proc., XII International Conference on Soil Mechanical and Foundation Engineering*, Rio De Janeiro, Brazil, 1023-1026.

Mesri, G and Hayat, T.M. (1993). "The Coefficient of Earth Pressure at Rest," *Canadian Geotechnical Journal*, Vol. 30, No. 4, pp. 647-666.

REFERENCES
(continued)

Milligan, G.W.E. (1974). *The Behavior of Rigid and Flexible Retaining Walls in Sand*, Ph.D. Thesis, University of Cambridge.

Mueller, C.G., Long, J.H., Weatherby, D.E., Cording, E.J., Power III, W.F., and Briaud, J.-L. (1998). *Summary Report of Research on Permanent Ground Anchor Walls*, "Volume III: Model-scale Wall Tests and Ground Anchor Tests," Report No. FHWA-RD-98-067, Federal Highway Administration, McLean, VA.

Ohde, J. (1938). Der Theorie des Erdruckes unter besonderer Berucksichtigung der Erddruck Verteilung, Die Boutechnik, Vol. 16, pp. 150-159, 176-180, 241-245, 331-335, 480-487, 570-571, 753-761.

O'Rourke, T.D. (1975). *A Study of Two Braced Excavations in Sands and Interbedded Stiff Clay*, Ph.D. Thesis, University of Illinois, Urbana-Champaign, 255 pp.

O'Rourke, T.D. (1981). "Ground Movements Caused by Braced Excavations," *ASCE, Journal of the Geotechnical Engineering Division,* Vol. 107, No. GT 9, pp. 1159-1177.

O'Rourke, T.D. and Cording, E.J. (1974). *The Observed Performance of Deep Subway Excavation*, Final Report, Project 1B0011, Prepared for the Washington Metropolitan Area Transit Authority, University of Illinois at Urbana-Champaign, September 12, 1974, pp. 101-103.

Reese, L.C. and O'Neill, M.W. (1988). *Drilled Shafted: Construction Procedures and Design Methods,* FHWA Report No. HI-88-042, Washington, DC.

Rizzo, P.C., Ellison, R.D., and Shafer, R.J. (1968). *Prestressed Tieback Walls for Two Deep Excavations in Buffalo, New York*, ASCE Annual Convention, Pittsburgh.

Rowe, P.W. (1952). "Anchored Sheet Pile Walls," *Proceedings of the Institution of Civil Engineers*, Part 1, pp. 27-70.

Shannon, W.L. and Strazer, R.J. (1970). *Tied-Back Excavation Wall for Seattle First National Bank*, ASCE, Civil Engineering, March, pp. 62-64.

Shields, D.R., Schnabel, H., and Weatherby, D.E. (1978). "Load Transfer in Pressure Injected Anchors," *Journal of the Geotechnical Engineering Division*, ASCE, Vol. 104, No. GT9, pp. 1183-1196.

REFERENCES
(continued)

Sills, G.C., Burland, J.B., and Czechowski, M.K. (1977). "Behavior of an Anchored Diaphragm Wall in Stiff Clay," *Proceedings: 9th International Conference on Soil Mechanics and Foundation Engineering*, Vol. 3, pp. 147-154.

Symons, I.F, Little, J.A., and Carder, D.R. (1988). "Ground Movements and Deflections of an Anchored Sheet Pile Wall," *Engineering Geology of Underground Movements*, Engineering Geology Special Publication No. 5, pp. 117-127.

Terzaghi, K. (1934). "Large Retaining-Wall Tests," *Engineering News-Record*, 112, pp. 136-140.

Terzaghi, K. (1941). *General Wedge Theory of Earth Pressure*, Transactions, ASCE, Paper No. 2099, pp. 68-97.

Terzaghi, K. (1943). *Theoretical Soil Mechanics*, John Wiley & Sons, New York, Seventh Printing, 510 pp.

Terzaghi, K., Peck, R.B., and Mesri, G. (1996). *Soil Mechanics in Engineering Practice*, 3rd Edition, John Wiley & Sons, New York.

Ulrich, E.J. (1989). 'Tieback Supported Cuts in Overconsolidated Soils," *Journal of Geotechnical Engineering*, ASCE, Vol. 115, No. 4, pp. 521-545.

Urzua, A. and Weatherby, D. E. (1998). *TB Wall - Anchored Wall Design and Analysis Program for Personal Computers*, Report No. FHWA-RD-98-093, Federal Highway Administration, McLean, VA.

Weatherby, D.E. (1982). *Tiebacks*, Federal Highway Administration Report, FHWA-RD-82-046.

Weatherby, D. E. (1997). *Design Manual for Permanent Ground Anchor Walls*, Report No. FHWA-RD-97-130, Federal Highway Administration, McLean, VA.

Weatherby, D. E. (1998). *Summary Report of Research on Permanent Ground Anchor Walls*, "Volume IV: Conclusions and Recommendations," Report No. FHWA-RD-98-068, Federal Highway Administration, McLean, VA.

Weatherby, D.E., Chung, M., Kim, N.-K., and Briaud, J.-L. (1998). *Summary Report of Research on Permanent Ground Anchor Walls*, "Volume II: Full-scale Wall Tests and a Soil-structure Interaction Model," Report No. FHWA-RD-98-066, Federal Highway Administration, McLean, VA.

REFERENCES
(continued)

Winter, D.G. (1990). "Performance of a Tieback Shoring Wall in Overconsolidated Sand and Clay," *Proceedings: Design and Performance of Earth Retaining Structures*, ASCE and Cornell University, Geotechnical Special Publication No. 25, pp. 764-777.

Wong, K.S. and Broms, B.B. (1989). "Lateral Wall Deflections of Braced Excavations in Clay," ASCE, *Journal of Geotechnical Engineering*, Vol. 115, No. 6, pp.853-870.